Development of cyclodecapeptides from the tyrothricin complex as anticancer peptides

by

Rosalind Jeanette Van Wyk
BSc Honours (Biochemistry)

Dissertation approved for the degree
Magister Scientae (Biochemistry)

in the
Faculty of Science
at the
University of Stellenbosch

Supervisor: Prof. Marina Rautenbach
Department of Biochemistry
University of Stellenbosch

April 2019

Stellenbosch University https://scholar.sun.ac.za

Declaration

By submitting this thesis electronically, I ***Rosalind Jeanette Van Wyk*** declare that the entirety of the work contained therein is my own, original work, that I am the sole author thereof (save to the extent explicitly otherwise stated), that reproduction and publication thereof by Stellenbosch University will not infringe any third party rights and that I have not previously in its entirety or in part submitted it for obtaining any qualification.

Rosalind Jeanette Van Wyk ..... **Name**

14 January 2019 ..... Date

Copyright © 2019 Stellenbosch University

All rights reserved

Stellenbosch University https://scholar.sun.ac.za

Summary

The ability of cancer cells to become simultaneously resistant to various chemotherapeutic agents, a phenomenon known as multidrug resistance, remains the cause that prevents successful treatment of cancer. The tyrocidines and analogues, produced by soil bacterium *Brevibacillus parabrevis*, have been shown to be active anticancer peptides. As with many other anticancer peptides, the tyrocidines are toxic to human red blood cells which limits their use as anticancer agent. Fortunately, many different strategies exist to reduce drug toxicity and improve delivery to target sites such as targeted nanocarriers or liposomal formulations. As little research has been done on the formulation and incorporation of the tyrocidines in nanocarrier systems to target cancer cells, the formulation strategies in the present study were kept simple.

We set out in this basic strategy to formulate selected tyrocidines with three lipid-based molecules, cholesterol sulfate (CS), palmitic acid (C16) and lysophosphatidylcholine (LPC), with subsequent biophysical analyses and determination of biological activity of the peptides alone and in formulation. The spherical constructs formed by the Trcs was a novel discovery. This formation of the spherical structures was hampered or completely disrupted by the formulants suggesting detergent-like effects. Decreased dimers and loss of total signal of ionic species of the C16 and LPC formulations indicated the formation of stable neutral peptide-formulant complexes. On the other hand, CS formulation maintained total ionic species signal suggesting a less stable formulation. Significant blue shifts in the fluorescence spectrums were seen for the CS formulated peptides, indicating pronounced stacking of aromatic rings in a hydrophobic environment. It was clear to us that these formulants have significant effects on the oligomerisation of the peptides, which dictates their antimicrobial activity.

The CS and C16 formulations significantly decreased the haemolytic activity of the peptides which was one of the main goals of this study. We confirmed that all the tyrocidines investigated in this study are highly active against three cancerous cell lines (LNCaP, C4-2B, HT-29) Interestingly, no direct relationship between hydrophobicity or size of the peptides and the activity of the peptides towards cancer and non-cancerous cells were observed, strongly suggesting alternative targets, possibly of internal nature. Selectivity studies revealed a promising lead formulation, TpcC:C16, that has potential as alternative anticancer agent.

Stellenbosch University https://scholar.sun.ac.za

Opsomming

Die vermoë van kankerselle om gelyktydig weerstandig te raak teen verskillende chemoterapeutiese agente, 'n verskynsel bekend as multimedikament-weerstand, is die oorsaak wat suksesvolle kanker behandeling verhoed. Die tirosidiene en analoë, vervaardig deur die grondbakterium *Brevibacillus parabrevis,* is aktiewe antikanker peptiede. Soos baie ander antikanker peptiede, is die tirosidiene toksies teen menslike rooibloedselle, wat hul gebruik as antikanker agente beperk. Gelukkig bestaan daar strategieë om middel-toksisiteit te verlaag en die aflewering by teikenselle te verbeter soos byvoorbeeld nanodraers of liposomale formulasies. Omdat daar min navorsing is oor die formulering en gebruik van tirosidiene in nanodraer sisteme om kankerselle te teiken, was die formuleringstrategieë in die huidige studie eenvoudig gehou.

Ons het in die eenvoudige strategie geselekteerde tirosidiene geformuleer met drie lipied-gebaseerde molekules, cholesterolsulfaat (CS), palmitiensuur (C16) en lisofosfatidielcholien (LPC), gevolg deur biofisiese analises en bepaling van biologiese aktiwiteit van die peptiede alleen en in formulasies. Die sferiese konstrukte wat deur die tirosidiene gevorm is, is 'n nuwe ontdekking. Hierdie vorming van die sferiese konstrukte was verminder of heeltemal ontwrig deur die formulante, wat dui op 'n detergent-agtige effek. Afname in dimere en verlies van totale sein van ioniese spesies in die C16 en LPC formulasies het die vorming van stabiele neutrale peptied-formulant komplekse aangedui. Daarteenoor is die totale sein van ioniese spesies in die CS formulasies behou wat dui op minder stabiele formulasies. Beduidende verskuiwings in die fluoressensie spektra is vir die CS formulasies waargeneem, wat uitgesproke pakking van aromatiese ringe in 'n hidrofobiese omgewing aandui. Dit was duidelik dat die formulante beduidende effekte op die oligomerisasie van die peptiede het, wat hulle antimikrobiese aktiwiteit dikteer.

Die CS en C16 formulasies verlaag hemolitiese aktiwiteit van die peptiede wat een van die hoofdoelwitte van die studie was. Ons het bevestig dat al die bestudeerde tirosidiene hoogs aktief is teen drie kankersellyne (LNCaP, C4-2B en HT-29). Geen direkte verhouding tussen die hidrofobisiteit of grootte van die peptiede en hul aktiwiteit teenoor kankerselle en normale menslike selle kon gevind word nie, wat op alternatiewe teikens dui, waarskynlik intern van natuur. Selektiwiteit studies het 'n belowende voorloper formulasie, TpcC:C16, met potentiaal as alternatiewe antikanker agent, uitgewys.

Stellenbosch University https://scholar.sun.ac.za

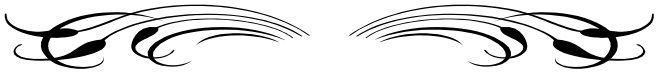

"When you're at the end of your rope, tie a knot and hold on."

Theodore Roosevelt

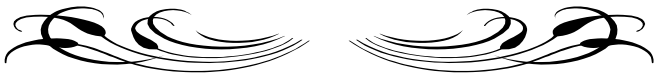

Stellenbosch University https://scholar.sun.ac.za

Acknowledgements

I would like to express my thanks and gratitude to the following persons and institutions:

- My supervisor, Professor Marina Rautenbach for her guidance and support, and for teaching me to never give up and to believe in myself.
- The staff at Central Analytic Facilities (CAF) at the University of Stellenbosch in particular Dr. Marietjie Stander and Mr. Malcolm Taylor.
- Dr. Vikas Kumar and Mr. Jai Singh at the Sophisticated Instrument Centre (SIC) at the Dr. Harisingh Gour University in Sagar, India, as well as Ms. Madelaine Frazenburg at the University of Stellenbosch CAF, for scanning electron microscopy images.
- Students from the group of Dr. Karl Storbeck and Prof. Amanda Swart in the Biochemistry department and Dr. Tanja Davis from the Physiology department (University of Stellenbosch, Stellenbosch, South Africa) for providing cell cultures for activity assay in this study.
- The National Research Foundation and BIOPEP Peptide Fund for their financial support in achieving my MSc.
- The BIOPEP group for their assistance when needed, their friendship and for all the memories, making it hard to say goodbye.
- My family for financially and emotionally supporting me and believing in me and for always being there when times are tough.
- All my friends for their unconditional love and for accepting me exactly as I am.

Stellenbosch University https://scholar.sun.ac.za

Table of Contents

Stellenbosch University https://scholar.sun.ac.za

Stellenbosch University https://scholar.sun.ac.za

Stellenbosch University https://scholar.sun.ac.za

List of Abbreviations and Acronyms

$[2M+2H]^{2+}$	doubly charged dimer
$[M+2H]^{2+}$	doubly charged ion
$[M+H]^{+}$	singly charged molecular ion
5-FU	5 -fluorouracil
ABC	ATP binding cassette
ABC-P	ABC transporter in placenta
ACN	acetonitrile
ACPs	anticancer peptides
AmB	Amphotericin B
AMP(s)	antimicrobial peptide(s)
ATCC	American type culture collection
ATP	adenosine triphosphate
BCRP	breast cancer resistant protein
Br. parabrevis	*Brevibacillus parabrevis*
BSEP	bile salt export protein
C16	palmitic acid
$CaCl_2$	calcium chloride
CAF	Central Analytical Facilities
CCS	collision cross section
CPPs	cell penetrating peptides
CS	cholesterol sulfate
DHFR	dihydrofolate reductase
DMAEMA	dimethylaminoethyl methacrylate
DMPC	dimyristoylphosphatidylcholine
DNA	deoxyribonucleic acid
EGFR	epidermal growth factor receptor
EPR	enhanced permeability and retention
ESI-MS	electrospray ionisation mass spectrometry
EtOH	ethanol
FBS	foetal bovine serum
FCS	foetal calf serum
FdUMP	fluorodeoxyuridine monophosphate
FdUTP	fluorodeoxyuridine triphosphate
FUTP	fluorouridine triphosphate
GFLG	glycylphenylalanylleucylglycine
GS	gramicidin S
HC_{50}	concentration leading to 50 % haemolysis
HEK293	human embryonic kidney
HEPES	hydroxyethylpiperazineethanesulfonic
HGC	hydrophobically modified glycol chitosan cholanic acid
HPLC	high performance liquid chromatography
IARC	International Agency for Research on Cancer
Ibu	ibuprofen
IC_{50}	concentration leading to 50% microbial growth inhibition
IM-MS	ion mobility spectrometry linked to mass spectrometry
IMS	ion mobility spectrometry
LB	Luria Bertani
LC	liquid chromatography
LC_{50}	lethal concentration leading to 50 % proliferation inhibition
LC-MS	liquid chromatography linked mass spectrometry
LNCaP	human prostatic adenocarcinoma
LPC	lysophosphatidylcholine

Stellenbosch University https://scholar.sun.ac.za

m/v	mass per volume
m/z	mass over charge ratio
MDR	multiple drug resistance
MeOH	methanol
mPEG PPF	methoxy PEG polypropylene fumarate
M_r	relative molar mass
MRP1	multidrug resistance associated protein 1
MS	mass spectrometry
MTX	methotrexate
MXR	mitoxantrone resistant gene
O	ornithine
OCC	N-carboxymethyl chitosan
OD	optical density
OQLCS	octadecyl quaternised lysine modified chitosan
Orn	ornithine
P. falciparum	*Plasmodium falciparum*
PAAs	poly-amino acids
PALA	N-(phosphonacetyl) -l-aspertate
PBS	phosphate buffered saline
PEGylated	polyethylene glycol modified
PGB	P-glycoprotein
Phc(s)	phenycidine(s)
PhcA	phenycidine A
Phcs	phenycidines
PoLp	polymeric liposome
Poly-Ala	poly-alanine
PS	phosphatidylserine
PSMA	prostate specific membrane antigen
PTX	Paclitaxel
PVP	poly-N-vinylpyrrolidone
RBC	human reded blood cells
RNA	ribonucleic acid
RP-HPLC	reverse phase high performance liquid chromatography
R_t	retention time of analyte in column chromatography
S. caespitosus	*Streptomyces caespitosus*
SCSA	side chain surface area
SD	standard deviation
SEM	scanning electron microscopy
SPGP	sister of PGP
spp.	species (plural)
TATp	transactivator of transcription protein
Tcn	tyrothricin
TEM	transmission electron microscopy
TFA	trifluoroacetic acid
TFA	trifluoroacetic acid
TfR	transferrin receptor
TGS	tryptone glucose and salts culture medium
TOF	time of flight
Tpc(s)	tryptocidines(s)
TpcA	tryptocidine A
$TpcA_1$	tryptocidine A_1
TpcB	tryptocidine B
$TpcB_1$	tryptocidine B_1
TpcC	tryptocidine C

Stellenbosch University https://scholar.sun.ac.za

$TpcC_1$	tryptocidine C_1
Tpcs	tryptocidines
TrcC	tyrocidine C
Trc C_1	tyrocidine C_1
Trc(s)	tyrocidine(s)
TrcA	tyrocidine A
$TrcA_1$	tyrocidine A_1
TrcB	tyrocidine B
$TrcB_1$	tyrocidine B_1
Trcmix	tyrocidine mixture
Trcs	tyrocidines
TS	thymidylate synthase
TSA	tryptone soy agar
TSB	tryptone soy broth
TWIM-MS	traveling wave ion mobility mass spectrometry
UPLC	ultra performance liquid chromatography
UPLC-MS	ultraperformance liquid chromatography linked mass spectrometry
V. rosea	*Vinca rosea*
v/v	volume per volume
WHO	World Health Organisation

Standard 3-letter and 1 letter abbreviations were used for the natural amino acids, with uppercase 1-letter abbreviations for L-amino acid residues and lower case 1-letter abbreviations for D-amino acid residues in peptide sequences

Stellenbosch University https://scholar.sun.ac.za

Preface

The development of multidrug-resistance (MDR) in cancer has become a worldwide crisis in the healthcare industry. The increasing number of cancer cases can be attributed to increased exposure to risk factors and failure of current cancer treatments. In addition, chemotherapy is non-selective and destroys healthy tissues and cancerous tissues. Consequently, the immune systems of the patients are compromised. Cancer patients with compromised immune systems are therefore at a higher risk to contract an untreatable nosocomial infections. Antibiotics are ineffective in treating such infections due to MDR and the lack of novel antibiotics. Therefore, cancer patients face three problems, i) the failure of chemotherapy due to MDR, ii) side-effects caused by non-selectivity of chemotherapeutics and iii) contraction of an untreatable nosocomial fungal infection. It is of utmost importance to find new anticancer drugs with complementary activity against microbial pathogens that can overcome MDR and the non-selectivity of current cancer therapeutics. Promising alternatives to conventional drugs are antimicrobial peptides (AMPs), specifically the tyrocidines (Trcs) and analogues from the tyrothricin complex. The Trcs show high activity towards bacteria, fungi and cancer, with potentially low accumulation in tissues and minimal risk of resistance development. Although these peptides have the potential as alternative therapeutic drugs, major drawbacks do exist due to their tendency to form oligomers and their non-selective cytotoxicity, specifically their haemolytic activity. The hypothesis that will be tested in this study is if the formulation of tyrocidines in specific biocompatible lipid nanocarriers will modulate the toxicity associated with the peptides by influencing both the biophysical properties of the peptides in solution, as well as masking the toxic moieties without compromising activity. To test the hypothesis a number of aims and objectives were set as described below.

RESEARCH AIMS AND OBJECTIVES

Aim 1: *The production, extraction, purification and characterization of selected tyrocidines and analogues from the tyrothricin complex*.

Objectives:

1. Purification of tyrocidine mixture and individual tyrocidine peptides from *Brevibacillus parabrevis* culture extracts and commercial tyrothricin mixture using semi-preparative high-performance liquid chromatography (HPLC).
2. Development of C_8 HPLC purification method
3. Confirmation of purity and characterization of the individual purified peptides and peptide fractions with electrospray mass spectrometry (ESMS) and ultraperformance liquid chromatography coupled to ESI-MS (UPLC-MS).

   The results from this study are presented in Chapter 2

Stellenbosch University https://scholar.sun.ac.za

Aim 2: *Formulation and biophysical analysis of the purified peptides and peptide formulations*.

Objectives:

1. Preparation of peptide formulations with lipid-based molecules, cholesterol sulphate (CS), palmitic acid (C16) and lysophosphatidylcholine (LPC)
2. Visual analysis of self-assembly/aggregation of peptides and formulations with scanning electron microscopy
3. Analysis of self-assembly/aggregation and stability of peptides and formulations with traveling wave ion mobility mass spectrometry (TWIM-MS) and fluorescence spectroscopy (FS).

The results from this study are presented in Chapter 3

Aim 3: *Characterization of anti-cancer and toxicity of the optimized peptide formulations.*

1. Determination of the toxicity of the peptides and formulations against human erythrocytes and human embryonic kidney (HEK293) cells.
2. Determination of the anticancer activity of the peptides and formulations towards human prostatic adenocarcinoma (LNCaP), human colorectal adenocarcinoma (HT-29) and human prostatic carcinoma (C4-2B) cells of the selected optimized formulations.
3. Determination of selectivity indexes (HC_{50}/IC_{50} and LC_{50}/IC_{50}) of the peptides and formulations from toxicity and activity assays.

   The results from this study are presented in Chapter 4

THESIS CONTENT

The thesis comprises of literature background in Chapter 1 on multidrug resistance, antimicrobial peptides with anticancer activity and current nanodrug delivery strategies for effective drug delivery. The experimental methods, results and discussions are given in Chapters 2-4. As this study reports statistical significances on the biological activity of many different formulations and peptides towards 5 different cell lines, an addendum with summarised statistics is given at the end of Chapter 4. Finally, Chapter 5 summarises conclusion and future studies in the field of tyrocidine formulations.

OUTPUTS OF MSc STUDY

- Van Wyk RJ* (March 2018) Formulation of peptides from the tyrothricin complex, Biochemistry Forum, University of Stellenbosch, Oral presentation
- Van Wyk RJ*, Rautenbach M (2018) Characterization of the anti-cancer activity of formulated and modified tyrocidine peptides, SASBMB 2018 Conference, Potchefstroom, South Africa

Stellenbosch University https://scholar.sun.ac.za

- Van Wyk RJ* (February 2019) Development of cyclodecapeptides from the tyrothricin complex as anti-cancer peptides, Biochemistry Forum, University of Stellenbosch, Oral defence of the MSc thesis
- Van Wyk RJ, Kumar V, Rautenbach M* (2019) The influence of lipid formulants on the self-assembly and toxicity of cyclodecapeptides from tyrothricin, article to be submitted to MBio.

*Presenter/Corresponding author

Stellenbosch University https://scholar.sun.ac.za

Chapter 1
OVERVIEW OF CHEMOTHERAPEUTIC RESISTANCE AND ANTIMICROBIAL PEPTIDES AS ALTERNATIVE ANTICANCER DRUGS

1.1 INTRODUCTION

Cancer is well-known to be one of the leading causes of death worldwide and has been ranked as first or second cause of death at <70 years of age in 91 of 172 countries and third or fourth in an additional 22 countries according to estimates by the world health organisation (WHO)[1]. t is evident that cancer incidence and mortality rates are growing rapidly worldwide with an estimated 18.1 million new cases and 9.6 million deaths in 2018 according to International Agency for Research on Cancer (IARC) [1]. The increasing number of cancer cases and deaths can be attributed to various factors. These factors include aging, size of population and the prevalence of risk factors including behavioural, occupational, environmental risk factors, and which are mostly related to socioeconomic development[1, 2, 3].

Cancer treatment methods may be used alone, in combination or sequentially and depends on health status of the patient, the molecular characteristics of the tumour, location of the tumour, and severity of the disease. Surgical removal of tumours is usually the first line of treatment and is often used in combination with radiotherapy for localised cancers. The most common treatment for metastatic tumours is chemotherapy which consists of a wide range of cytotoxic drugs that are employed to preferentially target proliferating cancer cells [4]. However, chemotherapeutic drugs have very low selectivity and also target normal healthy cells leading to adverse side effects such as hair loss, vomiting and suppression of the immune system in patients [5]. Cancer can reoccur, and this is primarily due to inherent or acquired resistance to the chemotherapeutic drugs used [6]. In many cases the tumours are resistant to a wide

Stellenbosch University https://scholar.sun.ac.za

range of drugs which is known as multiple drug resistance (MDR) [6]. MDR is the major implication in the overall failure of chemotherapy and as a result higher mortality rates are observed [1]. Cancer patients are also at a higher risk of contracting nosocomial fungal infections due to their compromised immune systems caused by invasive surgery and chemotherapy [7, 8]. This chapter presents a brief overview of mechanism of action of conventional cytotoxic agents used for cancer treatment and how resistance develops towards these agents. The use of antimicrobial peptides as alternative chemotherapeutic agents and the formulation of AMPs to improve delivery, stability and toxicity of the peptides are broadly also discussed.

1.2 BROAD OVERVIEW OF CONVENTIONAL CYTOTOXIC DRUGS AND THEIR MECHANISM OF ACTIONS

Chemotherapy is the most widely used treatment for various types of cancer, especially for metastatic tumours [9]. Chemotherapy consists of a diverse group of cytotoxic agents that acts by targeting various biosynthetic processes involved in the proliferation of cancer cells. These cytotoxic agents can be classified according to their target sites and mode of actions [4]. The groups include the antimetabolites, alkylating agents, anthracyclines, camptothecins and analogues, epipodophyllotoxins and mitotic spindle poisons (Vinca alkaloids and taxanes)[4, 10-13] .

The antimetabolites consist of antifolates and pyrimidine and purine antagonists which results in the disruption of DNA and RNA synthesis [11]. Examples of antimetabolites are methotrexate (MTX), 5-fluorouracil (5-FU) and N-(phosphonacetyl)-L-aspartate (PALA)[14-16]. MTX is an antifolate which inhibits dihydrofolate reductase (DHFR), an enzyme involved in the metabolism of folates [15, 16] . Inhibition of DHFR results in reduced folate synthesis which are co-factors that are essential for the synthesis of both pyrimidine and purine [15, 16]. The analogue of uracil, 5-FU, is converted to active

Stellenbosch University https://scholar.sun.ac.za

metabolites, fluorodeoxyuridine monophosphate (FdUMP), fluorodeoxyuridine triphosphate (FdUTP) and fluorouridine triphosphate (FUTP), intracellularly [14]. These fluoronucleotides are then mis-incorporated into RNA and DNA. Furthermore, 5-FU also inhibits thymidylate synthase (TS) which is involved in nucleotide synthesis [14]. PALA inhibits aspartate transcarbamylase, the enzyme that catalyses the second reaction of pyrimidine nucleotide synthesis [16]. The antimetabolite antitumor drugs all interact with enzymes involved in the synthesis of nucleotides which are essential building blocks for DNA and RNA [16].

The alkylating agents exerts antitumor activity by binding to DNA, which leads to cross-linking between DNA strands, causing disruptions of the normal processes of transcription and replication. Examples of alkylating agents are the antibiotic, mitomycin C [17], isolated from *Streptomyces caespitosus* and the platinum coordination complex *cis*-diamminedichloroplatinum (II), cisplatin [18, 19]. Alkylation and cross-linking of DNA is also a mechanism of action of the anthracycline antibiotics doxorubicin [20] and daunorubicin [21]. However, the anthracyclines have various additional mechanisms of action including intercalation into DNA, damage of DNA via free radical formation and inhibition of DNA topoisomerase II [21]. The camptothecins and analogues and epipodophyllotoxins inhibit topoisomerase I [22, 23] and poisons topoisomerase II [24], respectively. The inhibition of topoisomerase I by camptothecins and analogues (example topotecan) leads to formation of DNA single-strand breaks thereby inhibiting DNA replication and synthesis [22, 23]. Whereas, epipodophyllotoxins such as etoposide poisons rather than inhibits the topoisomerase II, leading to single-strand and double-strand breaks in DNA which ultimately cause cell apoptosis [24, 25].

The last major group of cytotoxic agents are the mitotic spindle poisons which includes the Vinca alkaloids and taxanes which influences polymerisation dynamics of

Stellenbosch University https://scholar.sun.ac.za

microtubules leading to mitotic blocking [11, 26]. The Vinca alkaloids are derived from the periwinkle plant *Vinca rosea* and include antitumor drugs, vinblastine and vincristine. The taxanes are also derived from plants, however, are semisynthetic and include paclitaxel and docetaxel [26, 27]. At high drug concentrations, the Vinca alkaloids inhibit microtubule polymerisation whereas the taxanes stimulate and stabilise microtubule polymerisation. The mechanisms of action of the Vinca alkaloids and taxanes are the same at low drug concentration with the suppression of microtubule dynamics resulting in mitosis disruption at metaphase/anaphase transition [26].

1.3 MULTIDRUG RESISTANCE DEVELOPMENT IN CANCERS

Although there is a diverse group of cytotoxic agents available for the treatment of cancer, their effectiveness has been limited due to resistance development of cancer tumours [28]. Tumours may be intrinsically resistant to chemotherapeutic drugs or may acquire resistance to the initial chemotherapeutic agent after treatment and often show cross-resistance to other unrelated drugs [6]. The ability of tumours to become resistant to multiple drugs is known as multidrug-resistance (MDR), a phenomenon preventing successful treatment of cancers [6, 9, 28]. The mechanisms of MDR and how it develops remains complex and is not fully understood, however two general MDR mechanisms include i) reduced accumulation of the cytotoxic drugs in the tumour cells due to decreased drug influx or increased drug efflux and ii) genetic and epigenetic alteration in the tumour cells leading to activated detoxifying systems and blocking of apoptotic pathways which affects tumour sensitivity towards drugs (Figure 1.1)[9, 28].

Stellenbosch University https://scholar.sun.ac.za

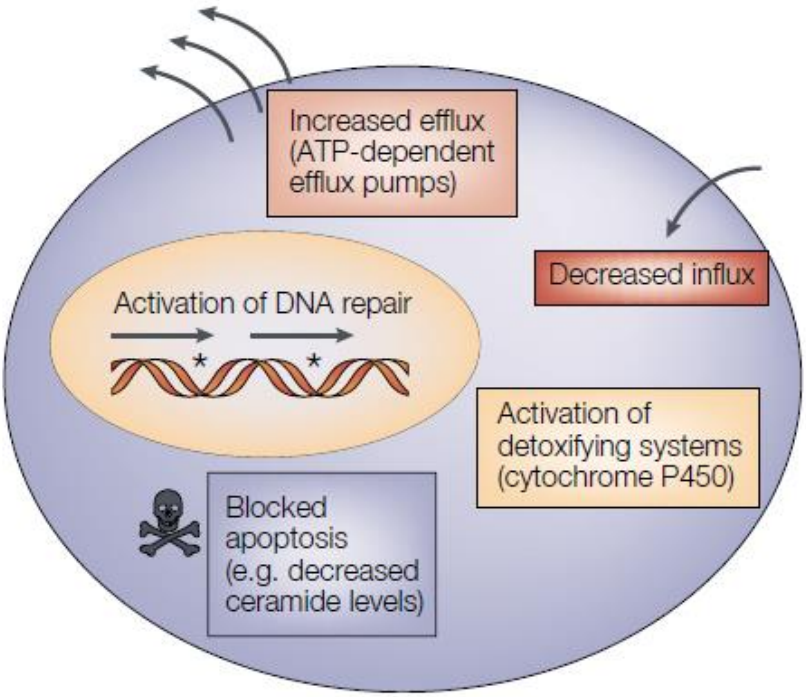

Figure 1.1 Schematic depiction of general mechanisms involved in MDR [9]. One mechanism is the increased activity of efflux pumps such with overexpression of the ATP dependent transporters observed. Additionally, reduced influx of drugs that enter the cells via endocytosis or via intracellular carriers. Activation of detoxifying systems, such as cytochrome P450 mixed function oxidases, results in drug resistance in the cases where drug accumulation is not influenced. Alteration in the DNA repair mechanisms which results in repairment of DNA damage caused by cytotoxic drugs is another mechanism of drug resistance. Lastly, disruption of apoptotic signalling pathways in cells with mutant/non-functional p53 or decreased ceramide levels is also implicated in multidrug resistance[9]. Figure reproduced from [9]

1.3.1 ATP-dependent efflux pumps as major MDR systems

The family of ATP-binding cassette (ABC) transporters are a group ATP-dependent efflux pumps that share sequence and structural homology[29]. The ABC transporter genes are divided into seven sub-families (ABCA-ABCG) according to sequence homology and domain organisation [29]. A total of 48 human ABC transporter genes have been identified [29] and 11 of these transporters are implicated in MDR (Table 1.1) [9]. The basis of the mechanism of action by which all these ABC transporters causes resistance is by overexpression of these ATP-dependent pumps in various tumours leading to efficient removal of cytotoxic drugs.

Stellenbosch University https://scholar.sun.ac.za

Overexpression of P-glycoprotein (PGP) in MDR cells is one of the best characterised ABC-transporter associated with MDR in terms of biochemical and genetic aspects [30, 31]. PGP is encoded by the ABCB1 gene (also known as MDR1 gene) [32, 33] and consists of 12 transmembrane regions [34] that bind various hydrophobic drugs such as Vinca alkaloids and anthracyclines [31] (Table 1.1). Subsequent ATPase activity stimulation induces conformational change that transfers the drugs to the outer leaflet of the membrane or to the extracellular space [35]. Another well-researched ABC transporter implicated in MDR is the multidrug-resistance-associated protein 1 (MRP1) also known as ABBC1 [36]. The structure of MRP1 is similar to that of PGP, however has amino-terminal extension composed of five membrane-spanning domains [36]. The mechanism of MRP1 is based on the ATP-dependent transport of glutathione/glucuronate conjugates of chemotherapeutic drugs [37, 38] as well as the cotransport of unmodified drugs, such as vincristine, with glutathione to extracellular space [39]. An additional five members of the ABCC (ABCC2-ABCC6 or MPR2-MRP6) subfamily have been identified and characterised [40] of which the majority have been implicated in MDR of tumours (MPR2-MPR5), with specificity towards various chemotherapeutic drugs (refer to Table 1.1) [9, 40]. Some chemotherapeutic drugs are poor substrates for PGP and MPR1 with cancer cells resistant to the drug, mitoxantrone, expressing genes encoding distant members of the ABC transporter family. These distant members are known as ABCG2 or by their common name MXR (mitoxantrone-resistant gene) [41], BCRP (breast cancer resistant protein)[42] or ABC-P (ABC-transporter in placenta) [43]. The substrate specificity of these ABCG2 transporters is broadened by acquired mutation of the MXR/BCRP/ABC-P genes [44, 45].

Stellenbosch University https://scholar.sun.ac.za

Table 1.1 Summary of ABC transporters implicated in MDR and their chemotherapeutic substrates. Table adapted from [9].

Common name	Systemic name	Tissue	Chemotherapeutic substrates	Non-chemotherapeutic substrates	References
PGP/MDR1	ABCB1	Intestine, liver, kidney, placenta, blood-brain barrier	doxorubicin, daunorubicin, vincristine, vinblastine, actinomycin-d, paclitaxel, docetaxel, etoposide, teniposide, bisantrene, homoharringtonine	Neutral and cationic organic compounds, many commonly used drugs	31
MDR2/3	ABCB4	Liver	paclitaxel, vinblastine	Phosphatidylcholine, few hydrophobic drugs	46-49
MRP1	ABCC1	All tissues	doxorubicin, epirubicin, etoposide, vincristine, methotrexate	Glutathione and other conjugates, organic anions, leukotriene C4	36-40
MRP2	ABCC2	Intestine, liver, kidney	methotrexate, etoposide, doxorubicin, cisplatin, vincristine, mitoxantrone	Similar to MRP1, non-bile salt organic anions	40, 50-53
MRP3	ABCC3	Intestine, liver, kidney, pancreas, adrenal glands	etoposide, teniposide, methotrexate, cisplatin, vincristine, doxorubicin	Glucuronate and glutathione conjugates, bile salts	54, 55
MRP4	ABCC4	Intestine, pancreas, lung, ovary, prostate, testis	methotrexate, thiopurines	Nucleotide analogues, organic anions	56, 57
MRP5	ABCC5	Most tissues	6-mercaptopurine 6-thioguanine	Nucleotide analogues, cyclic nucleotides, organic anions	58, 59
MXR BCRP ABC-P	ABCG2	Placenta, liver, intestine, breast	doxorubicin, daunorubicin, mitoxantrone, topotecan, sn-38	Prazosin	41-45, 60
BSEP SPGP	ABCB11	Liver	paclitaxel	Bile salts	61-65
ABCA2	ABCA2	Brain, monocytes	estramustine	Steroid derivative, Lipids	29, 66, 67

Stellenbosch University https://scholar.sun.ac.za

Other ABC transporters implicated in MDR include BSEP (bile salt export protein) which was originally named SPGP (sister of PGP)[61], the phosphatidylcholine flippase MDR2 (also known as MDR3) [46, 47, 68] which is closely related to MDR1/PGP and steroid transporter ABCA2 [29, 66, 67] (refer to Table 1.1).

Although the over-expression of ABC transporters in cancers has a major detrimental effect on chemoterapeutic drug potency and is leading to treatment failures, these proteins can be potential targets for blocking agents that could have synergistic actions with chemotherapeutic drugs. The over-expression of ABC transporters in cancers could be beneficial for selectively targeting cancers with peptides, ligands and antibodies. These membrane-bound proteins would also be very sensitive to membrane-active compounds such as the antimicrobial peptides (AMPs) which will be discussed in the next section.

1.4 ANTIMICROBIAL PEPTIDES AS ALTERNATIVE CHEMOTHERAPEUTIC AGENTS FOR THE TREATMENT OF CANCER

It is of utmost importance to find new anticancer drugs that can overcome MDR and the non-selectivity of current cancer therapeutics, in particular the negative influence of chemotherapeutic drugs on the immune system[8]. Novel drugs to target MDR cancers without compromising the immune system, is an important consideration in anticancer drug development. Promising alternatives to conventional chemotherapeutic drugs are the AMPs. AMPs have received much attention as alternative antibiotics due to their potent activity against a broad spectrum of microbes including bacteria [69], viruses [70], fungi [71], as well as cancer [72, 73, 74]. This group of peptides also has high selectivity, potentially low toxicity, low accumulation in tissues and low risk of resistance development [74]. AMPs form part of the innate immune systems of various living multicellular organisms [75], as well as defence molecules of

Stellenbosch University https://scholar.sun.ac.za

bacteria and consist of a wide range of structurally diverse peptides[73, 74]. Regardless of their structural diversity all AMPs have an amphipathic nature which underlies their interaction with target cells and mechanism of action [71, 76]. Most AMPs selectively target the anionic membranes of bacterial and fungal cells, inserts into the membrane, destabilizes the membrane and essentially induces cell death [77]. The cell membranes of prokaryotes and eukaryotes differ in their composition and arrangement of lipids and sterols. Prokaryotic membranes have significant amounts of anionic phospholipids on the membrane outer leaflet [78], whereas eukaryotic membranes consist of zwitterionic phospholipids on the outer leaflet leading to a predominately neutral cell surface[79]. Healthy eukaryotic cells are also protected against AMPs by membrane-stabilizing cholesterol [76, 80]. Cancer cells on the other hand display a quite different cell surface due to their rapid proliferation [81, 82]. Cancer cells alter their membrane composition by increasing expression of anionic molecules such as phosphatidylserine (PS)[83], O-glycosylated mucins[84], saililated gangliosides[85] and heparan sulfates [86] which results in an overall negative membrane charge. An additional difference between tumour cells and healthy mammalian cells is the elevated amount of microvilli on the surface of tumour cells [87] which increases the surface area of the cancer cells allowing increased amount of AMPs to interact [88]. Therefore AMPs with anticancer properties have been extensively researched and although it is thought that AMPs have will selective activity for tumour cells, development of such AMPs, so-called anticancer peptides (ACPs) for clinical application has been slow. Activity towards tumours cannot be predicted according to the structures of ACPs as of yet, and are regarded as unique chemotherapeutic agents with various modes of actions[81, 89]. The ACPs can be categorised into the ACPs with membranolytic activity and ACPs with non-membranolytic activity towards cancers

Stellenbosch University https://scholar.sun.ac.za

cells. The ACPs with membranolytic activity include the magainins [90], melittin [91, 92], cecropin [93] and the beetle defensin D-peptides A, B, C and D [94] (refer to Table 1.2 for a summary and references). Initial evidence of membranolytic activity was discovered in a study done by Cruciani *et al.* [90] on magainin 2 that showed cytolytic activity towards hematopoietic and solid tumour cell lines. Other studies showed that the membranolytic activity of these ACPs can be achieved via the accumulation on the cell membrane surface in a carpet-like manner (carpet model)[95] or accumulate via hydrophobic interaction and forming transmembrane channels or pores (toroidal pore or barrel-stave model) [96]. In these models the end result is membrane permeabilization and cell lysis. Alternatively, apoptosis can be induced by the permeation and swelling of the mitochondria resulting in release of cytochrome C [97]. Release of cytochrome C induces Apaf-1 oligomerisation, caspase 9 activation and conversion of pro-caspase 3 to caspase 3 [98]. Buforin IIb, a histone-H2A derived peptide has been shown to kill cancer cells by mitochondrial dependent-apoptosis pathway [85]. The mitochondrial-dependent apoptosis pathway is also associated with upregulation of molecules in the death receptor pathway as in the case for tachyplesin [99]. ACPs with non-membranolytic activity has also been described such as the insect derived, alloferon 1 and 2 peptides which have immunomodulatory properties [100]. Refer to Table 1.2 for examples of some of the major ACPs and their anticancer activities.

Similarly to the major ACPs in Table 1.2 below, a group of other antimicrobial peptides, the tyrocidines, possess activity against various cancer cell lines [101]. This has sparked an interest in these peptides by our group to develop the tyrocidines into future anticancer agents which was the main focus of the present study.

Stellenbosch University https://scholar.sun.ac.za

Table 1.2 Selected major ACPs, their primary structures and their anticancer activities.

Anticancer peptide	Primary sequence	Anticancer activity	Reference
Melittin	GIGAVLKVLTTGLPALISWIKRKRQQ	Membranolytic, phospholipase A2 activator	91, 92
Tachyplesin	KWCFRVCYRGICYRRCR	Activation of complement C1q, induction of cancer cell differentiation	99, 102
Cecropin B	KWKVFKKIEKMGRNIRNGIVKAGPAIAVLGEAKAL	Membranolytic	93
Magainin 2	GIGKFLHSAKKFGKAFVGEIMNS	Membranolytic	90
Buforin IIb	RAGLQFPVGRLLRRLLRRLLR	Mitochondria-dependent apoptosis, caspase 9 activation	85
D-peptide A D-peptide B D-peptide C D-peptide D	RLYLRIGRR RLRLRIGRR ALYLAIRRR RLLLRIGRR	Membranolytic	94
Alloferon 1 Alloferon 2	HGVSGHGOHGVHG GVSGHGQHGVHG	Immunomodulatory	100

1.5 OVERVIEW OF TYROCIDINES AND ANALOGUES

The tyrocidines and analogues, a group of antimicrobial peptides (AMPs), were first discovered by Dubos in 1939 from the extracts of a cultured soil bacillus as part of a complex known as tyrothricin [103]. The tyrothricin complex, produced during the late logarithmic growth phase of *Brevibacillus parabrevis*, consists of the basic cyclodecapeptides known as the tyrocidines and the neutral linear gramicidins [104-107]. The tyrocidines were discovered 10 years after the antibiotic penicillin, however was the first antibiotic used in medical industry in the form of topical [108-110] and oral drugs (throat lozenges) [111], as their haemolytic toxicity limited their application [112].

1.5.1 Primary and secondary structure

The primary structure of Trcs and analogues consists of a conserved sequence (cyclo[D-Phe^{1}-L-Pro^{2}-L-X^{3}-D-X^{4}-L-Asn^{5}-L-Gln^{6}-L-X^{7}-L-Val^{8}-L-X^{9}-L-Leu^{10}]). Variations (depicted by X) generally occur at position three, four, seven and nine (Figure 1.2).

Stellenbosch University https://scholar.sun.ac.za

Substitution of position seven with tyrosine (Tyr), phenylalanine (Phe) or tryptophan (Trp) gives rise to the Trcs, and the analogues phenycidines (Phcs) and tryptocidines (Tpcs), respectively. Whereas, substitution of three and four (Phe and Trp), and nine (ornithine, Orn, and lysine, Lys) give rise to the A/A_1, B/B'/B_1/B_1' and C/C_1 analogues [107, 113, 114]. In total 28 different Trcs and analogues have been characterised by Tang *et al.* [113] with 24 accounted for by amino acid variability mentioned above. The tyrocidine A, A_1, B, B_1, C, C_1 analogues are detected in highest abundance and are considered as the six major Trcs present in the cyclodecapeptide mixture [113, 115].

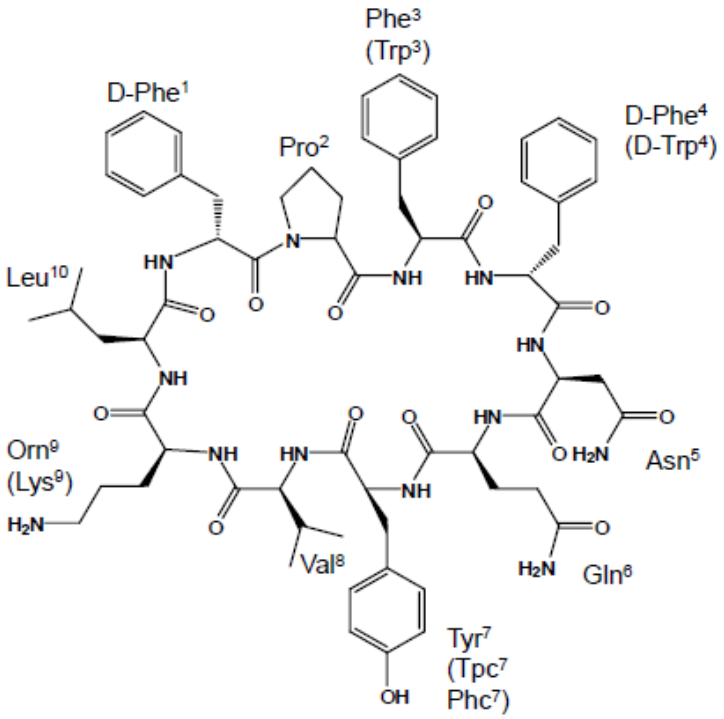

Figure 1. 2 The primary structure of Tyrocidine A. The amino acids are given by their three letter abbreviations with ornithine represented by Orn. The amino acids that are variable at certain positions are shown in brackets. Amino acid at position seven can be substituted by phenylalanine or tryptophan to produce the phenycidines and tryptocidines, respectively. Figure adapted from Tang *et al*. [113].

The secondary structure of Trc A and TrcC adopts the conformation of a two-stranded antiparallel B-sheet with a type II B-turn, formed by Leu^{10}, Phe^{1}, Pro^{2}, Phe^{3}, and a distorted type I β-turn, formed by Asn^{5}, Gln^{6}, Tyr^{7}, Val^{8}, at either end of the structure

Stellenbosch University https://scholar.sun.ac.za

[116-121]. The secondary structures are stabilised by four intramolecular hydrogen bonds, three formed between the amide and carbonyl groups of the backbone and the fourth hydrogen bond located between the backbone amide of Val[8] and side chain amide of Asn[5]. Further stabilisation of the secondary structure is achieved via hydrophobic interactions between amino acid side chains of Phe[4], Val[8] and Leu[10] [121]. The L-Trp[4]/L-Phe[4] and L-Orn[9] residue are located on the same face of the monomeric β-sheet structures [120] (Figure 1.3). The tyrocidines have been shown to have low amphipathicity in monomeric form as the polar and non-polar residues are not separated into hydrophobic and hydrophilic faces [120]. Although variation in the amino acid sequence of the primary structure of the Trcs, the secondary structure of the different tyrocidines are proposed to be conserved [122] (Figure 1.3).

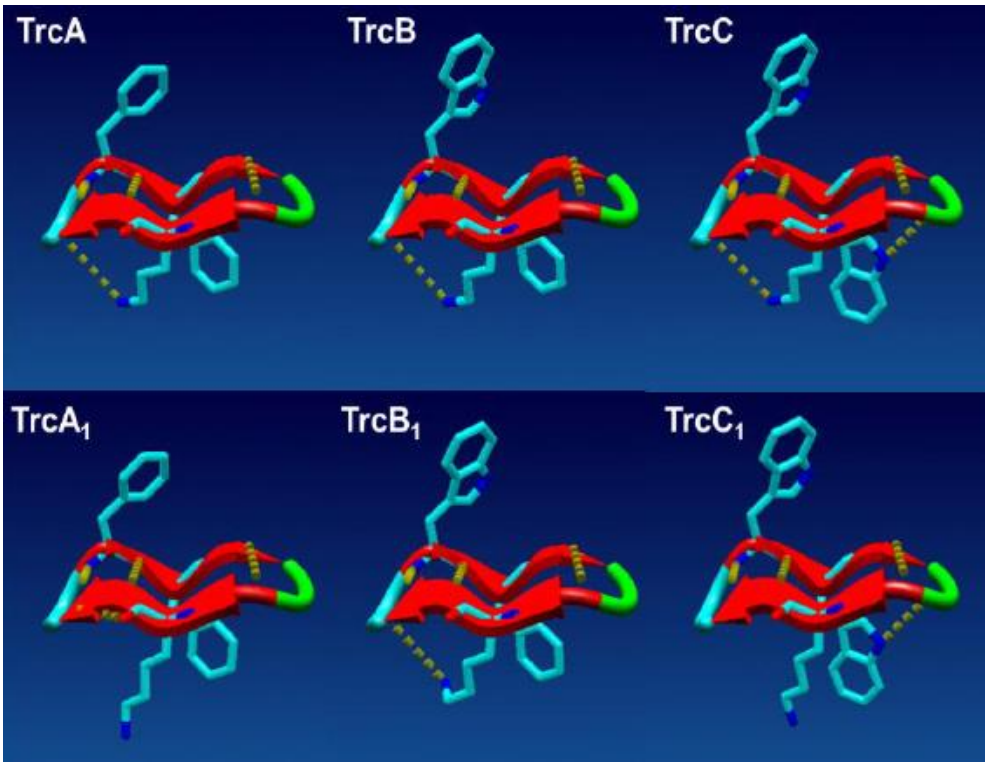

Figure 1.3 The secondary structures of the six major tyrocidines created from TrcC and TrcA models of Munyuki *et al*.[120]. The two stranded antiparallel B-sheet structure connected by the type I and type II B turns are shown. The side chains of the variable amino acids of the aromatic dipeptide unit (L-X[3]-L-X[4]), L-Lys[9]/Orn[9] and the intramolecular hydrogen bonds are also shown. Figures reproduced with permission (M. Rautenbach, unpublished data)

Stellenbosch University https://scholar.sun.ac.za

Homodimers of Trc A [120, 121] and TrcC [120] lead to highly amphipathic structures which are formed by strong association of the β-sheets of two monomers in an edge to edge fashion[120, 121] (creating a continuous four-stranded antiparallel β -sheet) or by stacking on top of each other[120]. Similar to the monomer stabilisation, stabilisation of dimer formed edge to edge is achieved by hydrogen bonds between the backbones of the amino acid residues of two monomers [120, 121]. Whereas, dimers formed by stacking on top of each other are stabilised by hydrophobic interactions [120]. The possibility of the tyrocidines to form dimers via various orientations indicates that the cyclodecapeptides can form larger oligomers[120]. Loll *et al.* [121] elucidated the dimeric structure of Trc A by means of X-ray crystallography (Figure 1.4). The dimers are formed by two monomers that strongly associate into highly amphipathic structures consisting of four β-strands in a continuous antiparallel β-sheet stabilised by backbone-backbone hydrogen bonds and hydrophobic interaction between side chain of Val[8] and Leu[10] from two monomers. The four stranded antiparallel β-sheet of the dimer forms a significant curvature, with the side chains of hydrophobic amino acids on the convex face and the side chain of polar L-Orn[9] residue on the concave face. The backbone carbonyl groups of D-Phe[1], Asn[5] and Gln[6] point outward from concave face with the side chain of Gln[6] (extending equatorially from dimer) well position to orientate toward the concave side of the dimer, giving the concave face a polar character.

1.5.2 Mechanism of action

The tyrocidines have been shown to interact with the lipids in the lipid-bilayer of the cell membrane [123] leading to disruption and permeabilization of the bilayer [124] which ultimately results in cell lysis and death [125]. The increased amphipathicity of the tyrocidines observed when in dimeric form [120, 121] and the low amphipathicity

Stellenbosch University https://scholar.sun.ac.za

associated with the monomeric conformation [120] of the tyrocidines suggests that the dimers are the active moieties of these cyclodecapeptides.

In a model developed by Loll *et al.* [121] the hydrophobic convex face of the highly curved dimer structure inserts into lipid bilayer of membranes and the hydrophilic concave face orientated towards the extracellular space (aqueous environment). Furthermore, the D-Phe^4 extending from the centre of the convex face, is proposed to be buried in the lipid bilayer while side chain of Tyr^7 directed towards the concave face of the dimer and is therefore exposed to aqueous environment [121].

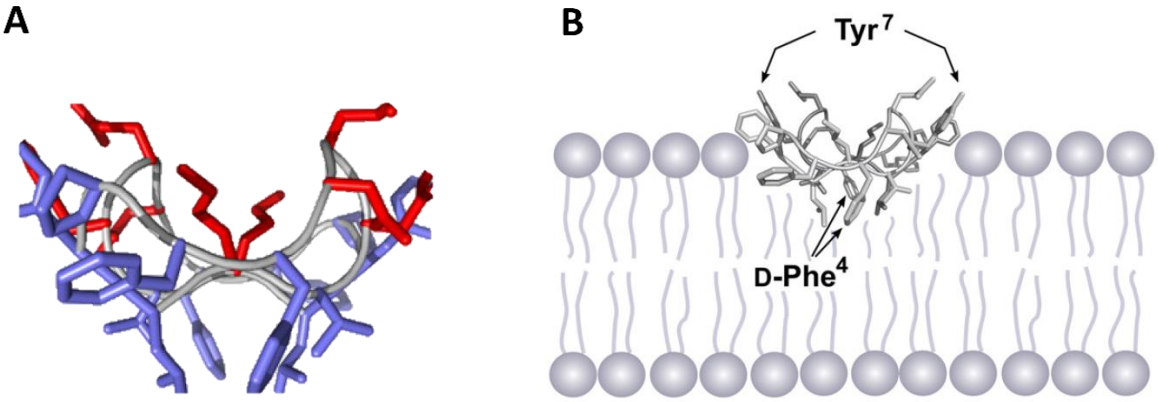

Figure 1.4 The dimer structure of Trc A showing A) the highly curved amphipathic structure formed by two monomers with hydrophobic side chains at convex face (shown in blue) and hydrophilic side chains at concave face (shown in red) and B) the mechanism of dimer interaction with lipid bilayer of membranes with the convex face and D-Phe^4 inserting into the membrane while Tyr^7 and concave face orientated towards exterior of the membrane. The figures were reproduced from Loll *et al*. [121]

The tyrocidines have been shown to oligomerise into higher order structures which are believed to form pore-like structures that are similar to the homologous Gramicidin S (GS) [107,126, 127, 128, 129, 130]. TrcA and TrcC were shown to form defined ion-conducting pores that do not have a major influence on phospholipid head-group orientation[131].

Alternative targets and mechanisms of actions have been proposed other than the lytic activity on the cell membrane, [101, 132, 133, 134] which includes the food vacuole morphology [134] and cell cycle regulation [101] of the malaria parasite *Plasmodium*

Stellenbosch University https://scholar.sun.ac.za

falciparum, as well as the disruption of glucose metabolism in Gram-positive bacteria[135, 136]. The tyrocidines have also been proposed to target DNA resulting in disruption of normal transcription and replication processes [123] after the observation that the Trcs binds to the DNA and inhibits transcription in the producer organism *in vitro* [137-140]. Wenzel *et al*. [131] observed the loss of peripheral membrane proteins and an influence on intracellular proteins, as well as clustering of fluid regions in the *Bacillus subtillis* cell membrane upon exposure to the Trcs. These non-lytic mechanisms would still depend on initial membrane interaction in order to possibly translocate into cells or be internalised by cells. Although many mechanisms of action for the Trcs have been proposed, the exact mode(s) the Trcs elicit their activity towards various microbes, including cancer cells, varies and remains to be fully elucidated for each cell type. However, their multiple mechanisms of action, various targets and the large library of Trcs analogues reduces the risk of resistance development, making these cyclodecapeptides promising compounds for development of alternative chemotherapeutic drugs.

1.6 DRUG FORMULATION AND TARGETING OF CANCERS

Although AMPs, such as the tyrocidines, have potential as alternative chemotherapeutic drugs, major drawbacks do exist due to their chemical and physical instability, tendency to form aggregates, enzymatic degradation, short circulating half-life, rapid elimination and in some of the more potent ACPs, their toxicity [141]. The poor pharmacokinetic profiles of chemotherapeutic drugs and their associated toxicity led to extensive research in the development of drug delivery systems [142].

Covalent and non-covalent formulations of AMPs can be designed to actively and passively target the cancer cells by exploiting the tumour environment, a concept that dates back to 1960 when Ehrlich first described the “magic bullet”[143]. However, “active

Stellenbosch University https://scholar.sun.ac.za

targeting" happens after "passive targeting" and therefore cannot be separated [144]. Differences in the tumour vasculature and pH compared to normal tissues are the major characters taken into consideration when designing nano-formulations and nanocarriers for drug delivery systems. For active targeting, different ligands can be coupled to the AMP (or drug) or incorporated at the surface of nanocarriers (covalently or non-covalently) to target receptors/enzymes overexpressed in the targeted cancer cells [145]. For passive targeting, nanocarrier and nano-formulations can be used with the so-called enhanced permeability and retention (EPR) effect that traps larger particles around the more permeable tumour sites[146, 147]. Figure 1.5 shows the basis of active and passive targeting of tumours.

For the nano-formulation of AMPs (or ACPs) it is hypothesised that the nano-formulation will protect the peptide from degradation and mask its toxic activity, but if toxic peptides in nano-particles are released in the vicinity of tumour they will lyse cancer cells displaying a more positive cell membrane [149]. Necrosis of the cancer cells will elicit an acute sterile inflammation [150] that could promote removal of cancerous cells. The released AMPs would also be degraded leaving a low general toxicity footprint on the heathy tissue.

1.6.1 Active targeting of cancers

Targeting ligands generally used in nanocarrier design includes small molecules, peptides, carbohydrates, proteins and antibodies [151]. Receptors that can be targeted in cancer therapeutics include the prostate specific membrane antigen (PSMA) overexpressed in prostate cancer[152], the folate receptors overexpressed in 40% of human cancers[153], the transferrin receptor (TfR)[154], CD44 receptor and epidermal growth factor receptor (EGFR) overexpressed various cancer cells[155, 156], as well as the overexpressed ABC transporters in certain cancer cells[9].

Stellenbosch University https://scholar.sun.ac.za

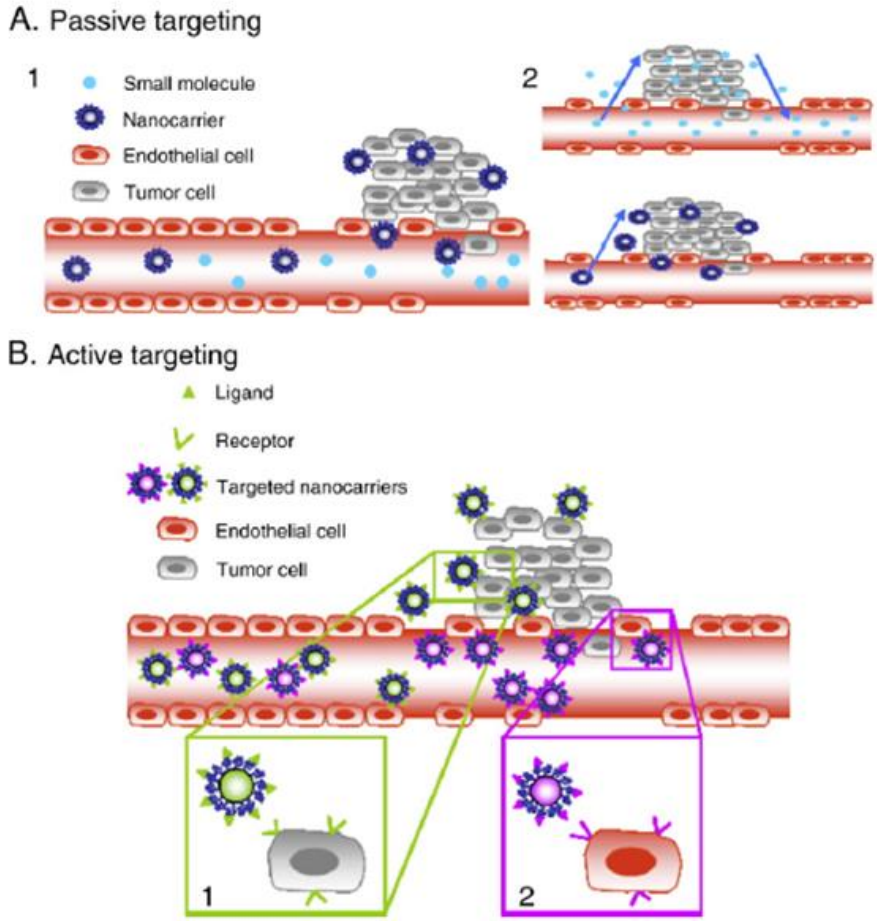

Figure 1.5 Schematic showing A. passive and B. active targeting of tumour cells. A. (1) The nanocarriers reach the tumour cells via leaky vasculature. (2) Schematic signifying the importance of size for the accumulation of nanocarriers in the tumour due to larger size compared to smaller drugs that can diffuse back into the tumour blood vessel. B. Targeted nanocarrier that actively target receptors overexpressed or expressed by (1) cancer cells or (2) angiogenic endothelial cells. Figure reproduced from [148]

The PSMA is also known as folate hydrolase and catalyses the hydrolytic cleavage of α- or γ-linked glutamates from small molecules and peptides[152]. Therefore poly-glutamate or poly-glutamate folates can be used as targeting ligands in the design of anti-prostate cancer drugs [152]. Folic acid (Vitamin B9), transferrin, hyaluronan and EGF can be used as ligand for targeting of folate receptors[153], TfRs [154], CD44s[157] and EGFRs[155], respectively. Antibodies were the first class of ligands used to decorate micelles for targeted delivery to tumour cells and are so efficient due to high affinity for their targets. Antibodies, used as ligand used to target cancer cells, include anti-CD3 Ab[158], anti-HER2 (Herceptin)[159], anti-CD20 Mab (Rituximab)[160] to name a few. Refer

Stellenbosch University https://scholar.sun.ac.za

to a comprehensive review by Nicolas *et al.* [145] for other ligands used in nanocarrier drug delivery systems. Enzymatic degradation of the ligand upon ligand/receptor interaction leads to the disruption of the nanocarrier and could subsequently release the drug or ACP at the target site [151-161]. Incorporation of acid-labile bonds (ester, hydrazine, imine etc.) between the ligands and nanocarrier can also be used to achieve pH triggered release of drugs with the bond being disrupted as it enters the acidic environment of cancer tumours [162].

1.6.2 Passive targeting of cancers

Passive targeting can be achieved via the enhanced permeability and retention (EPR) effect [146147]. Tumour and metastatic cancer cell in tissues lead to increased permeability of the environment around the cancer due to angiogenesis and low level chronic inflammation[146, 147]. The EPR effect is achieved by significantly increasing the circulation time of a drug by incorporating it in a nanocarrier thereby maximizing the opportunity for the drug to reach the more permeable target site, without dilution in the healthy tissues which the nano-drug cannot enter due to its size [163].

Polymer-type nanocarriers

Poly(ethylene glycol) modified (PEGylated) nanocarriers have received much attention due to their biocompatibility and prolonged circulation time. In 2007, amphiphilic poly(lactic-acid)-*block*-poly(ethylene glycol) (PLA-*b*-PEG) nanocarriers loaded with Paclitaxel were brought to the market [151] and more recently PEG amide conjugates of the membrane active an toxic amphotericin B were shown to cure mice suffering from candidiasis [164]. Popular amphiphilic (co)polymers currently investigated in the field of drug delivery are PLA-b-PEG, poly(glycolic acid)-*b*-PEG (PGA-*b*-PEG), poly(lactide-co-glycolide)-*b*-PEG (PLGA-*b*-PEG), poly(ε-caprolactone)-*b*-PEG (PCL-*b*-PEG) and poly(valero lactone)-*b*-PEG (PVL-*b*-PEG). The core of the nanocarrier is

Stellenbosch University https://scholar.sun.ac.za

formed by the hydrophobic polymer(PLA, PGA, PLGA, PCL and PVL) and the shell by the hydrophilic PEG polymer [151]. Lipids, poly-amino acids (PAAs) and carbohydrates can also be conjugated to PEG to form polymeric liposomes, combining the benefits of both liposomes and polymeric nanocarriers. Studies on the antibacterial activity of PEGylated AMPs (nisin-PEG[165], PEG-CaLL[166] and BacE-PEG[167]) revealed decreased activity for all of the PEG-conjugates compared to their parent AMP alone indicating that even though PEGylation can improve biocompatibility and prevent their degradation by enzymes, the risk of compromising their activity exists. However, all the PEGylated AMPs mentioned are hydrophilic and therefor PEGylation of hydrophobic peptides may prove to be beneficial considering their increased solubility by PEG [168].

A cyclodecapeptide mixture of the tyrocidines has been used to construct a peptide-polymer conjugate with activity towards malaria[169]. The tyrocidines alone possesses antimalarial activity but selective need to be improved. The tyocidines were conjugated to biocompatible and pH-labile linker on poly(N-vinylpyrrolidone) (PVP). The Trc-PVP construct formed nanoparticles due to the self-assembly of the tyrocidines and these nanoparticles were decorated with a targeting peptide ligand which targets the red blood cells infected with the malaria parasite.

Carbohydrate-type nano-formulations and carriers

An ideal carbohydrate for design of targeted nanocarriers is cyclodextrin which forms a circular ring consisting of glucose monomers [170]. The hydroxyl groups are exposed to the exterior and the glycosidic oxygen and non-exchangeable hydrogen atoms orientated inwards Therefor a hydrophobic cavity is formed by cyclodextrins that is ideal to sequester hydrophobic drugs. The hydroxyl groups on the exterior can easily be modified to functionalize the structure with ligands or other small molecules. Bellocq

Stellenbosch University https://scholar.sun.ac.za

et al. [171] synthesized a polymer based cyclodextrin nanoparticle comprised of three parts i) a linear cyclodextrin polycation used to condensate nucleic acids into the nanoparticle, ii) a Tf-PEG-adamantane (Tf-PEG-AD) conjugate for targeted delivery and iii) AD-PEG for stabilization of the nanoparticle. The cyclodextrin-based particle formulation with 0.05% Tf-PEG-AD increased the transfection of K562 cancer cells 4-fold, indicating retention of high receptor binding affinity and TfR mediated internalization [171]. The carbohydrate, chitosan is also extensively employed in targeted drug delivery due to the easily modifiable amino groups in the backbone. Chitosan modified nanocarriers include trimethylated chitosan, N-octyl-O, N-carboxymethyl chitosan (OCC), hydrophobically modified glycol chitosan-cholanic acid (HGC) and octadecyl-quaternised lysine modified chitosan (OQLCS) [151]. Interestingly, chitosan itself has activity against fungi, including and interacts with the anionic phospholipids present on fungi cell membranes thereby disrupting the cell membrane[172]. Wang *et al*. [173]developed a polymeric liposome (PoLp) consisting of cholesterol and OQLCS conjugated to FA or PEG. The OQLCS-FA and OQLCS-PEG functions as targeting and protection moieties, respectively. In the acidic environment of cancer cells, OQLCS bonds unfold and slowly releases drugs at the target site. It was also shown that the FA-PEG coated OQLCS PoLp's are taken up by MCF-7 cancer cells, which may be attributed to the positive charge of the nanocarrier and folate receptor-mediated endocytosis [173]. This endocytic pathway has limits due to the inability of the nanocarrier to escape the endosomal vesicle. Subsequently, the endosomal entrapped drug and nanocarrier enters lysosomal vesicles followed by enzymatic degradation. Examples of AMP-chitosan conjugates include the chitosan-pexiganan conjugate[174] and anoplin-chitosan conjugates[175] The successful novel synthesis of chitosan-pexiganan (a magainin AMP analogue) was reported by Batista *et al.*[174] as

Stellenbosch University https://scholar.sun.ac.za

potential treatment of infected wounds, however no activity assays were performed. In addition, a study of the antimicrobial activity of the anoplin-chitosan conjugate revealed lower MIC toward *Escherichia coli* compared to the free anoplin which is a promising result for AMP-chitosan conjugates as future drug delivery systems [175].

Lipid nano-formulations and carriers

Encapsulation of AMPs and ACPs in liposomes and micelles has been proven to be a successful way of delivering these peptides to target cells [176]. Due to their amphiphilic nature, both hydrophobic and hydrophilic peptides can be delivered via these lipid-nanocarriers [177]. Their ability to reduce toxicity and increase circulating half-life of the AMPs makes them very attractive to medical industry[176]. Examples of AMPs that have been formulated with these carriers include nisin [178, 179], polymyxin B [180] and LL-37 [181]. Many chemotherapeutic drugs have also been formulated with liposomes for improved delivery and reduced toxicity of the drug. Refer to Table 1.3 for summary of FDA approved liposome formulations combined with different drugs. Amphotericin B, a rather toxic membrane-active antifungal drug, is also used as liposomal formulation (AmBisome, and Albecet) for the treatment of fungal infections with reduced toxicity [184]. How the toxicity of Amphotericin B was reduced without compromising its membrane active mode of action can be used as guide to formulate toxic ACPs and AMPs.

Peptides as nanocarrier ligands

To improve the intracellular uptake of nanocarriers by target cells, cell penetrating peptides (CPPs), many of which are also AMPs, have been investigated largely for their enhancement of cellular entry by different mechanisms. Examples of CPPs include transactivator of transcription protein (TATp), penetratin, polyarginines and lysine containing transportan and Pep-1 [182]. It was shown by Torchilin *et al*. [183] that

Stellenbosch University https://scholar.sun.ac.za

liposomes conjugated with TAT along with protection moiety, PEG, abolishes the liposome internalization ability. This can be attribute to the steric hindrance created by PEG that prevents direct contact of the CPP with the target cell surface[183]. Formulation of drugs with liposomes conjugated to TAT alone results in improved internalization but off target attack of cells due to non-selectivity of CPPs.

Table 1.3 Summary of FDA approved liposomal drug therapies with nano-formulation advantages and year approved. (Adapted from Bobo *et al.* [184])

Name	Material description	Advantages	Indications	Year approved
DaunoXome® (Galen)	Liposomal Daunorubicin	Increased delivery to tumour site; lower systemic toxicity	Karposi's Sarcoma	1996
DepoCyt© (Sigma-Tau)	Liposomal Cytarabine	Increased delivery to tumour site; lower systemic toxicity	Meningitis Lymphomatous	1996
Marqibo® (Onco TCS)	Liposomal Vincristine	Increased delivery to tumour site; lower systemic toxicity	Acute Lymphoblastic Leukemia	2012
Onivyde® (Merrimack)	Liposomal Irinotecan	Increased delivery to tumour site; lower systemic toxicity	Pancreatic cancer	2015
AmBisome® (Gilead Sciences)	Liposomal Amphotericin B	Reduced nephrotoxicity	Fungal and protozoal infections	1997
Visudyne® (Bausch and Lomb)	Liposomal Morphine sulfate Liposomal Verteporfin	Extended release and increased delivery to site of diseased vessels; photosensitive release	Analgesia (post-operative) Macular degeneration, wet age-related Myopia; ocular Histoplasmosis	2004 2000
Doxil®/Caelyx™ (Janssen)	Liposomal doxorubicin	Improved delivery to site of disease; decrease in systemic toxicity of free drug	Karposi's Sarcoma Ovarian cancer Multiple myeloma	1995 2005 2008
Abelcet® (Sigma-tau)	Liposomal Amphotericin B lipid complex	Reduced toxicity	Fungal infections	1995
Curosurf®/Poractant alpha (Chiesei farmaceutici)	Liposome-proteins SP-B and SP-C	Increased delivery for smaller volume, reduced toxicity	pulmonary surfactant for Respiratory Distress Syndrome	1999

Stellenbosch University https://scholar.sun.ac.za

Fortunately, the steric hindrance of PEG can be overcome by use of “smart” pH-sensitive PEG blocks as protection and shielding moieties instead [185]. Kale *et al*.[185] developed TATp-liposomes coated with acid labile PEG moieties to function as CPP shielding. The acid labile bond between the liposome and the PEG enables the removal of PEG when the PL enters the acidified environment at the surface of cancer cells. Subsequently, the TATp is exposed, induces internalization and overcomes endosomal entrapment of the drug [185].

Considering the membranolytic activity of various AMPs, there is potential that such peptides can be used as both a CCP ligand and as an ACP in anticancer drug conjugates which gives AMPs multifunctionality in terms of its uses in drug delivery systems.

Prodrug nano-formulations

The universal term used for drugs that have been chemically modified to improve their pharmacological properties are known as “prodrugs”. This method uses derivatives of the drug which are temporarily inactive and become activated by enzymatic or non-enzymatic conversion when the drug reaches its target site [186]. Extensive research has gone into micellular prodrug approaches as targeted drug delivery systems for various diseases including cancer. In micellular prodrug systems the drug is covalently linked to either diblock copolymers or phospholipids via a chemically labile bond. For instance, Seetharaman *et al*. [187]introduced N,N’-dimethylaminoethyl methacrylate (DMAEMA) as a pH-responsive cross linker between the drug, ibuprofen (Ibu), and diblock copolymer consisting of methoxy-PEG-polypropylene fumarate (mPEG-PPF). The pH-sensitive Ibu-mPEG-PPF micellular prodrug showed controlled release of Ibu as the acidity of solution increases. Transmission electron microscopy

Stellenbosch University https://scholar.sun.ac.za

(TEM) analysis confirmed that the protonation (at acidic pH) of DMAEMA crosslinker results in micelle swelling, disassembly and ultimately drug release [188]. In a different prodrug study, an enzyme-sensitive glycylphenylalanylleucylglycine (GFLG) tetrapeptide was used as a linker between anticancer drug, paclitaxel (PTX), and PEGylated peptide dendrimer [189]. The GFLG oligopeptide is degraded upon internalization by cathepsin B, a lysosomal cysteine protease overexpressed in breast cancer cells. Subsequently, PTX is released in the cytoplasm of the cancer cells [189]. The functional groups of AMPs, for instance the amino group of Lys and the Tyr hydroxyl group of the tyrocidines, present sites for covalent linkage of pH-sensitive or enzyme sensitive cross linkers to produce AMP-prodrugs which can then be incorporated into liposomal/micellar, PVP or PEG diblock copolymer nanocarriers. Klumperman *et al.* [169] used this strategy of pH-dependent release of the Trcs from a PVP-nanocarrier to target the red blood cell stage of the malaria parasite. Due to the anaerobic metabolism of the parasite leading to lower pH in the infected red blood cell and in the food vacuole, the tyrocidines were hypothesised to be release as a toxic bolus eradicating the intracellular parasite[169].

1.7 Formulation of the tyrocidines and analogues

The cyclodecapeptides, tyrocidines and analogues, have four functional groups (amino group of Lys, amide groups of Asn and Gln, and hydroxyl group of Tyr) as possible sites of covalent conjugation of various ligands such as PEG, carbohydrates, lipids and other peptides (CPPs or cross linkers). However, as little research has been done regarding Trcs as ACPs and the fact that the solution behaviour of the Trcs is quite complex, the exploratory formulation of these peptides was kept basic. The fact that so many AMPs, similar to tyrocidines, have been incorporated into lipid formulations with associated reduced toxicity and improved delivery, micellular non-

Stellenbosch University https://scholar.sun.ac.za

covalent formulations were chosen as strategy to reduce toxicity and improve delivery of the tyrocidines in the present study. In this we followed some of the formulations used for detoxifying amphotericin B for the Trcs and analogues in this study. The lipids chosen for formulation were cholesterol sulfate (CS), an anionic sterol, palmitic acid (C16) a saturated fatty acid (anionic), and lyso-phosphatidylcholine (LPC), a neutral lipid and derivative of phosphatidylcholine with one fatty acyl group, as the third formulant.

1.8 REFERENCES

(1) Bray, F., Ferlay, J., Soerjomataram, I., Siegel, R. L., Torre, L. A., and Jemal, A. (2018) Global cancer statistics 2018: GLOBOCON estimates of incidence and mortality worldwide for 36 cancers in 185 coutries. *A Cancer J. Clin. 68*, 394–424.

(2) Clapp, R. W., Jacobs, M. M., and Loechler, E. L. (2008) Environmental and occupational causes of cancer new evidence, 2005-2007. *Rev. Environ. Health 23*, 1–37.

(3) Danaei, G., Vander Hoorn, S., Lopez, A. D., Murray, C. J., and Ezzati, M. (2005) Causes of cancer in the world: comparative risk assessment of nine behavioural and environmental risk factors. *Lancet 366*, 1784–1793.

(4) Luo, J., Solimini, N. L., and Elledge, S. J. (2009) Principles of cancer therapy: oncogene and non-oncogene addiction. *Cell 136*, 823–837.

(5) Coates, A., Abraham, S., Kaye, S. B., Sowerbutts, T., Frewin, C., Fox, R. M., and Tattersall, M. H. N. (1983) On the receiving end-patient perception of the side-effects of cancer chemotherapy. *Eur. J. Cancer Clin. Oncol. 19*, 203–208.

(6) Dean, M., Fojo, T., and Bates, S. (2005) Tumour stem cells and drug resistance. *Nat. Rev. Cancer 5*, 275–284.

(7) Luqmani, Y. A. (2005) Mechanisms of drug resistance in cancer chemotherapy. *Med. Princ. Pract. 14*, 35–48.

(8) Jarvis, W. R. (1995) Epidemiology of nosocomial fungal infections, with emphasis on candida species. *Clin. Infect. Dis. 20*, 1526–1530.

(9) Gottesman, M. M., Fojo, T., and Bates, S. E. (2002) Multidrug resistance in cancer: role of ATP–dependent transporters. *Nat. Rev. Cancer 2*, 48–58.

(10) Smorenburg, C. H., Sparreboom, A., Bontenbal, M., and Verweij, J. (2001) Combination chemotherapy of the taxanes and antimetabolites: Its use and limitations. *Eur. J. Cancer 37*, 2310–2323.

(11) Johnson, I. S., Armstrong, J. G., Gorman, M., and Burnett, J. P. (1963) The Vinca alkaloids: A new class of oncolytic agents. *Cancer Res. 23*, 1390–1427.

(12) Booser, D. J., and Hortobagyi, G. N. (1994) Anthracycline antibiotics in cancer Therapy. *Drugs 47*, 223–258.

Stellenbosch University https://scholar.sun.ac.za

(13) Malhotra, V., and Perry, M. C. (2003) Classical chemotherapy. *Cancer Biol. Ther. 2*, S1–S4.

(14) Longley, D. B., Harkin, D. P., and Johnston, P. G. (2003) 5-Fluorouracil: Mechanisms of action and clinical strategies. *Nat. Rev. Cancer 3*, 330–338.

(15) Zhao, R., and Goldman, I. D. (2003) Resistance to antifolates. *Oncogene 22*, 7431–7457.

(16) Kinsella, A. R., Smith, D., and Pickard, M. (1997) Resistance to chemotherapeutic antimetabolites: A function of salvage pathway involvement and cellular response to DNA damage. *Br. J. Cancer 75*, 935–945.

(17) Jaap Verweij, and Pinedo, H. M. (1990) Mitomycin C: mechanism of action, usefulness and limitations. *Anticancer. Drugs 1*, 5–13.

(18) Fuertes Castilla, J., Alonso, C., Perez, J.M., M. A. (2003) Cisplatin biochemical mechanism of action: from cytotoxicity to induction of cell death through interconnections between apoptotic and necrotic pathways. *Curr. Med. Chem. 10*, 257–266.

(19) Siddik, Z. H. (2003) Cisplatin: Mode of cytotoxic action and molecular basis of resistance. *Oncogene 22*, 7265–7279.

(20) Tacar, O., Sriamornsak, P., and Dass, C. R. (2013) Doxorubicin: An update on anticancer molecular action, toxicity and novel drug delivery systems. *J. Pharm. Pharmacol. 65*, 157–170.

(21) Gewirtz, D. A. (1999) A critical evaluation of the mechanisms of action proposed for the antitumor effects of the anthracycline antibiotics adriamycin and daunorubicin. *Biochem. Pharmacol. 57*, 727–741.

(22) Hsiang, Y.-H., Hertzber, R., Hecht, S., and Liu, L. F. (1985) Camptothecin induces protein-linked DNA breaks via mammalian DNA topoisomerase I. *J. Biol. Chem. 260*, 14873–14878.

(23) Slichenmyer, W. J., Rowinsky, E. K., Donehower, R. C., and Kaufmann, S. H. (1993) The current status of camptothecin analogues as antitumor agents. *J. Natl. Cancer Inst. 85*, 271–291.

(24) Ross, W., Rowe, T., Glisson, B., Yalowich, J., and Liu, L. (1984) Role of topoisomerase II in mediating epipodophyllotoxin-induced DNA Cleavage. *Cancer Res. 44*, 5857–5860.

(25) Hande, K. R. (1998) Etoposide: four decades of development of a topoisomerase II inhibitor. *Eur. J. Cancer 34*, 1514–1521.

(26) Jordan, M. (2002) Mechanism of action of antitumor drugs that interact with microtubules and tubulin. *Curr. Med. Chem. Agents 2*, 1–17.

(27) Rowinsky, E. K., Cazenave, L. A., and Donehower, R. C. (1990) Taxol: A novel investigational antimicrotibule agent. *J. Natl. Cancer Inst. 82*, 1247–1259.

(28) Ozben, T. (2006) Mechanisms and strategies to overcome multiple drug resistance in cancer. *FEBS Lett. 580*, 2903–2909.

(29) Dean, M., Rzhetsky, A., and Allikmets, R. (2001) The human ATP-binding cassette (ABC) transporter superfamily. *J. Lipid Res. 42*, 1007–1017.

(30) Bradley, G., Juranka, P. F. ., and Ling, V. (1988) Mechanism of multidrug

Stellenbosch University https://scholar.sun.ac.za

resistance. *Biochim. Biophys. Actaiochemica 948*, 87–128.

(31) Ambudkar, S. V., Dey, S., Hrycyna, C. A., Ramachandra, M., Pastan, I., and Gottesman, M. M. (1999) Biochemical, cellular, and pharmacological aspects of the multidrug transporter. *Annu. Rev. Pharmacol. Toxicol. 39*, 361–398.

(32) Juliano, R. L., and Ling, V. (1976) A surface glycoprotein modulating drug permeability in Chinese hamster ovary cell mutants. *Biochim. Biophys. Acta 455*, 152–162.

(33) Ueda, K., Cardarelli, C., Gottesman, M. M., and Pastan, I. (1987) Expression of a full-length cDNA for the human “MDR1” gene confers resistance to colchicine, doxorubicin, and vinblastine. *Proc. Natl. Acad. Sci. 84*, 3004–3008.

(34) Chen, C., Chin, J. E., Ueda, K., Clark, D. P., Pastan, I., Gottesman, M. M., and Roninson, Igor B. (1986) Internal duplication and homology with bacterial transport proteins in the *mdr*1 (P-glycoprotein) gene from multidrug-resistant human cells. *Cell 47*, 381–389.

(35) Ramachandra, M., Ambudkar, S. V., Chen, D., Hrycyna, C. A., Dey, S., Gottesman, M. M., and Pastan, I. (1998) Human P-glycoprotein exhibits reduced affinity for substrates during a catalytic transition state. *Biochemistry 37*, 5010–5019.

(36) Cole, S. P. C., Bhardwaj, G., Gerlach, J. H., Mackie, J. E., Grant, C. E., Almquist, K. C., Stewart, A. J., Kurz, E. U., Duncan, A. M. V., and Deeley, R. G. (1992) Overexpression of a transporter gene in a multidrug-resistant human lung cancer cell line. *Science (80-.). 258*, 1650–1654.

(37) Jedlitschky, G., Leier, I., Buchholz, U., Barnouin, K., Kurz, G., and Keppler, D. (1996) Transport of glutathione, glucuronate, and sulfate conjugates by the MRP gene-encoded conjugate export pump. *Cancer Res. 56*, 988–994.

(38) Muller, M., Meijer, C., Zaman, G. J., Borst, P., Scheper, R. J., Mulder, N. H., de Vries, E. G., and Jansen, P. L. (1994) Overexpression of the gene encoding the multidrug resistance-associated protein results in increased ATP-dependent glutathione S-conjugate transport. *Proc. Natl. Acad. Sci. 91*, 13033–13037.

(39) Loe, D. W., Deeley, R. G., and Cole, S. P. C. (1998) Characterization of vincristine transport by the Mr 190,000 multidrug resistance protein (MRP): evidence for cotransport with reduced glutathione. *Cancer Res. 58*, 5130–5136.

(40) Borst, P., Evers, R., Kool, M., and Wijnholds, J. (2000) A family of drug transporters : the multidrug resistance-associated proteins. *Jounal Natl. Cancer Inst. 92*, 1295–1302.

(41) Miyake, K., Mickley, L., Litman, T., Zhan, Z., Robey, R., Cristensen, B., Brangi, M., Greenberger, L., Dean, M., Fojo, T., and Bates, S. E. (1999) Molecular cloning of cDNAs which are highly overexpressed in mitoxantrone-resistant cells: demonstration of homology to ABC transport genes. *Cancer Res. 59*, 8–13.

(42) Doyle, L. A., Yang, W., Abruzzo, L. V, Krogmann, T., Gao, Y., Rishi, A. K., and Ross, D. D. (1998) A multidrug resistance transporter from human MCF-7 breast cancer cells. *Proceeding Natl. Acad. Sci. USA 95*, 15665–15670.

(43) Allikmets, R., Schriml, L. M., Hutchinson, A., Romano-Spica, V., and Dean, M. (1998) A human placenta-specific ATP-binding cassette gene (ABCP) on chromosome 4q22 that is involved in multidrug resistance. *Cancer Res. 58*, 5337–

Stellenbosch University https://scholar.sun.ac.za

5339.

(44) Honjo, Y., Hrycyna, C. A., Yan, Q., Medina-pe, W. Y., Robey, R. W., Laar, A. Van De, Litman, T., Dean, M., and Bates, S. E. (2001) Acquired mutations in the *MXR / BCRP / ABCP* gene alter substrate specificity in MXR/BCRP/ABCP-overexspessing cells. *Cancer Res. 61*, 6635–6639.

(45) Komatani, H., Kotani, H., Hara, Y., Nakagawa, R., Matsumoto, M., Arakawa, H., and Nishimura, S. (2001) Identification of breast cancer resistant protein/mitoxantrone resistance/placenta-specific, ATP-binding cassette transporter as a transporter of NB-506 and J-107088, topoisomerase I inhibitors with an indolocarbazole structure. *Cancer Res. 61*, 2827–2832.

(46) Smit, J. J. M., Groen, K., Mel, C. A. A. M., Ottenhoff, R., Roan, M. A. Van, Valk, M. A. Van Der, Diseases, L., Centre, A. M., Schinkel, A. H., Elferink, R. P. J. O., Groen, A. K., Wagenaar, E., van Deemter, L., Mol, C. A. A. M., Ottenhoff, R., van der Lugt, N. M. T., van Roon, M. A., van der Valk, M. A., Offerhaus, G. J. A., Berns, A. J. M., and Borst, P. (1993) Homozygous disruption of the murine MDR2 P-glycoprotein gene leads to a complete absence of phospholipid from bile and to liver disease. *Cell 75*, 451–462.

(47) Borst, P., Zelcer, N., and Van Helvoort, A. (2000) ABC transporters in lipid transport. *Biochim. Biophys. Acta 1486*, 128–144.

(48) Ruetz, S., and Gros, P. (1994) Phosphatidylcholine translocase: A physiological role for the *mdr2* gene. *Cell 77*, 1071–1081.

(49) de Vree, J. M. L., Jacquemin, E., Sturm, E., Cresteil, D., Bosma, P. J., Aten, J., Deleuze, J.-F., Desrochers, M., Burdelski, M., Bernard, O., Elferink, R. P. J. O., and Hadchouel, M. (1998) Mutations in the *MDR3* gene cause progressive familial intrahepatic cholestasis. *Proc. Natl. Acad. Sci. 95*, 282–287.

(50) Paulusma, C. C., Bosma, P. J., Zaman, G. J. R., Bakker, C. T. M., Otter, M., Scheffer, G. L., Scheper, R. J., Borst, P., Oude, R. P. J., Paulusma, C. C., Bosma, P. J., Zaman, G. J. R., Bakker, C. T. M., Otter, M., Scheffer, G. L., Scheper, R. J., Borst, P., and Elferink, R. P. J. O. (1996) Congenital jaundice in rats with a mutation in a multidrug resistance-associated protein gene. *Science (80-.). 271*, 1126–1128.

(51) Ito, K., Suzuki, H., Hirohashi, T., Kume, K., Shimizu, T., and Sugiyama, Y. (1997) Molecular cloning of canalicular multispecific organic anion transporter defective in EHBR. *Am. J. Physiol. 272*, G16–G22.

(52) Kartenbeck, J., Leuschner, U., Mayer, R., and Keppler, D. (1996) Absence of the canalicular isoform of the *MRP* gene - encoded conjugate export pump from the hepatocytes in Dubin-Johnson syndrome. *Hepatology 23*, 1061–1066.

(53) Paulusma, C. C., Kool, M., Bosma, P. J., Scheffer, G. L., Borg, F. Ter, Scheper, R. J., Tytgat, G. N. J., Borst, P., Baas, F., and Oude Elferink, R. P. J. (1997) A mutation in the human canalicular multispecific organic anion transporter gene causes the Dubin-Johnson syndrome. *Hepatology 25*, 1539–1542.

(54) Kool, M., Van der Linde, M., and De Haas, M. (1999) MPR3, an organic anion transporter able to transport anti-cancer drugs. *Proceeding Natl. Acad. Sci. USA 96*, 6914–6919.

(55) Belinsky, M. G., and Kruh, G. D. (1999) MOAT-E (ARA) is a full-length MRP/cMOAT subfamily transporter expressed in kidney and liver. *Br. J. Cancer 80*,

Stellenbosch University https://scholar.sun.ac.za

1342–1349.

(56) Chen, Z.-S., Lee, K., and Kruh, G. D. . (2001) Transport of cyclic nucleotides and estradiol 17- β - D -glucuronide by multidrug resistance protein 4 : resistance to 6-mercaptopurine and 6-thioguanine. *J. Biol. Chem. 276*, 33747–33754.

(57) Schuetz, J. D., Connelly, M. C., Sun, D., Paibir, S. G., Flynn, P. M., Srinivas, R. V., Kumar, A., and Fridland, A. (1999) MRP4: A previously unidentified factor in resistance to nucleoside-based antiviral drugs. *Nat. Med. 5*, 1048–1051.

(58) Wijnholds, J., Mol, C. A. A. M., van Deemter, L., Haas, M. de, Scheffer, G. L., Baas, F., Beijnen, J. H., Scheper, R. J., Hatse, S., Clercq, E. De, Balzarini, J., and Borst, P. (2000) Multidrug-resistance protein 5 is a multispecific organic anion transporter able to transport nucleotide analogs. *Proceeding Natl. Acad. Sci. USA 97*, 7476–7481.

(59) Jedlitschky, G., Burchell, B., and Keppler, D. (2000) The multidrug resistance protein 5 functions as an ATP-dependent export pump for cyclic nucleotides. *J. Biol. Chem. 275*, 30069–30074.

(60) Maliepaard, M., Scheffer, G. L., Faneyte, I. F., Van Gastelen, M. A., Pijnenborg, A. C. L. M., Schinkel, A. H., Van de Vijver, M. J., Scheper, R. J., and Schellens, J. H. M. (2001) Subcellular localization and distribution of the breast resistance protein transporter in normal human tissues. *Cancer Res. 61*, 3458–3464.

(61) Childs, S., Yeh, R. L., Hui, D., and Ling, V. (1998) Taxol resistance mediated by transfection of the liver-specific sister gene of P-glycoprotein. *Cancer Res. 58*, 4160–4167.

(62) Gerloff, T., Stieger, B., Hagenbuch, B., Madon, J., Landmann, L., Roth, J., Hofmann, A. F., and Meier, P. J. (1998) The sister of P-glycoprotein represents the canalicular bile salt export pump of mammalian liver. *J. Biol. Chem. 273*, 10046–10050.

(63) Lecureur, V., Sun, D., Hargrove, P., Schuetz, E. G., Kim, R. B., Lan, L. B., and Schuetz, J. D. (2000) Cloning and expression of murine sister of P-glycoprotein reveals a more discriminating transporter than *MDR1*/P-glycoprotein. *Mol Pharmacol 57*, 24–35.

(64) Jacquemin, E. (1999) Cholestatic liver disease progressive familial intrahepatic cholestasis. *J. Gastroenterol. Hepatol. 14*, 594–599.

(65) Wang, R., Salem, M., Yousef, I. M., Tuchweber, B., Lam, P., Childs, S. J., Helgason, C. D., Ackerley, C., Phillips, M. J., and Ling, V. (2001) Targeted inactivation of sister of P-glycoprotein gene (*spgp*) in mice results in nonprogressive but persistent intrahepatic cholestasis. *Proc. Natl. Acad. Sci. 98*, 2011–2016.

(66) Laing, N. M., Belinsky, M. G., Kruh, G. D., Bell, D. W., Boyd, J. T., Barone, L., Testa, J. R., and Tew, K. D. (1998) Amplification of the ATP-binding cassette 2 transporter gene is functionally linked with enhanced efflux of estramustine in ovarian carcinoma cells. *Cancer Res. 58*, 1332–1337.

(67) Vulevic, B., Chen, Z., Boyd, J. T., Davis, W., Walsh, E. S., Belinsky, M. G., and Tew, K. D. (2001) Cloning and characterization of human adenosine 5’ -triphosphate-binding cassette, Sub-family A, transporter 2 (*ABCA2*). *Cancer Res. 61*, 3339–3347.

(68) Zhou, Y., Gottesman, M., and Pastan, I. (1999) Studies of human MDR1-MDR2

Stellenbosch University https://scholar.sun.ac.za

chimeras demonstrate the functional exchangeability of a major transmembrane segment of the multidrug transporter and phosphatidylcholine flippase. *Mol. Cell. Biol. 19*, 1450–1459.

(69) Friedrich, C. L., Moyles, D., Beveridge, T. J., and Hancock, R. E. (2000) Antibacterial action of structurally diverse cationic peptides on gram-positive bacteria. *Antimicrob. Agents Chemother. 44*, 2086–92.

(70) Carriel-Gomes, M. C., Kratz, J. M., Barracco, M. A., Bachére, E., Barardi, C. R. M., and Simões, C. M. O. (2007) In vitro antiviral activity of antimicrobial peptides against herpes simplex virus 1, adenovirus, and rotavirus. *Mem. Inst. Oswaldo Cruz 102*, 469–472.

(71) Rautenbach, M., Troskie, A. M., and Vosloo, J. A. (2016) Antifungal peptides: To be or not to be membrane active. *Biochimie 130*, 132–145.

(72) Bhutia, S. K., and Maiti, T. K. (2008) Targeting tumors with peptides from natural sources. *Trends Biotechnol. 26*, 210–217.

(73) Papo, N., and Shai, Y. (2005) Host defense peptides as new weapons in cancer treatment. *Cell. Mol. Life Sci. 62*, 784–790.

(74) Jenssen, H., Hamill, P., and Hancock, R. E. W. (2006) Peptide antimicrobial agents. *Clin. Microbiol. Rev. 19*, 491–511.

(75) Lai, Y., and Gallo, R. L. (2009) AMPed up immunity: how antimicrobial peptides have multiple roles in immune defense. *Trends Immunol. 30*, 131–141.

(76) Zasloff, M. (2002) Antimicrobial peptides of multicellular organisms. *Nature 24*, 389–395.

(77) Nguyen, L. T., Haney, E. F., and Vogel, H. J. (2011) The expanding scope of antimicrobial peptide structures and their modes of action. *Trends Biotechnol. 29*, 464–472.

(78) Simons, K., and Sampaio, J. L. (2011) Membrane organization and lipid rafts. *Cold Spring Harb. Perspect Biol 3*, 1–17.

(79) Hoskin, D. W., and Ramamoorthy, A. (2008) Studies on anticancer activities of antimicrobial peptides. *Biochim. Biophys. Acta 1778*, 357–375.

(80) Matsuzaki, K. (1999) Why and how are peptide-lipid interactions utilized for self-defense? Magainins and tachyplesins as archetypes. *Biochim. Biophys. Acta 1462*, 1–10.

(81) Schweizer, F. (2009) Cationic amphiphilic peptides with cancer-selective toxicity. *Eur. J. Pharmacol. 625*, 190–194.

(82) Stafford, J. H., and Thorpe, P. E. (2011) Increased exposure of phosphatidylethanolamine on the surface of tumor vascular endothelium. *Neoplasia 13*, 299–309.

(83) Utsugi, T., Schroit, A. J., Connor, J., Bucana, C. D., and Fidler, I. J. (1991) Elevated expression of phosphatidylserine in the outer membrane leaflet of human tumor cells and recognition by activated human blood monocytes. *Cancer Res. 51*, 3062–3066.

(84) Yoon, W. H., Park, H. D., Lim, K., and Hwang, B. D. (1996) Effect of O-glycosylated mucin on invasion and metastasis of HM7 human colon cancer cells.

Stellenbosch University https://scholar.sun.ac.za

Biochem. Biophys. Res. Commun. 222, 694–699.

(85) Lee, H. S., Park, C. B., Kim, J. M., Jang, S. A., Park, I. Y., Kim, M. S., Cho, J. H., and Kim, S. C. (2008) Mechanism of anticancer activity of buforin IIb, a histone H2A-derived peptide. *Cancer Lett. 271*, 47–55.

(86) Kleeff, J., Ishiwata, T., Kumbasar, A., Friess, H., Büchler, M. W., Lander, A. D., and Korc, M. (1998) The cell-surface heparan sulfate proteoglycan glypican-1 regulates growth factor action in pancreatic carcinoma cells and is overexpressed in human pancreatic cancer. *J. Clin. Invest. 102*, 1662–1673.

(87) Zwaal, R. F. A., and Schroit, A. J. (1997) Pathophysiologic implications of membrane phospholipid asymmetry in blood cells. *J. Am. Soc. Hematol. 89*, 1121–1132.

(88) Chan, S. C., Hui, L., and Chen, H. M. (1998) Enhancement of the cytolytic effect of anti-bacterial cecropin by the microvilli of cancer cells. *Anticancer Res. 18*, 4467–4474.

(89) Gaspar, D., Salomé Veiga, A., and Castanho, M. A. R. B. (2013) From antimicrobial to anticancer peptides. A review. *Front. Microbiol. 4*, 1–16.

(90) Cruciani, ricardo a., Barker, jeffery l., Zaslofft, M., Chen, H. -chi., and Colamonici, O. (1991) Antibiotic magainins exert cytolytic activity against transformed cell lines through channel formation. *Proc. Natl. Acad. Sci. 88*, 3792–3796.

(91) Hristova, K., Dempsey, C. E., and White, S. H. (2001) Structure, location, and lipid perturbations of melittin at the membrane interface. *Biophys. J. 80*, 801–811.

(92) Sharma, S. (1993) Melittin-induced hyperactivation of phospholipase A2 activity and calcium influx in ras-transformed cells. *Oncogene 4*, 939–947.

(93) Hung, S. C., Wang, W., Chan, S. I., and Chen, H. M. (1999) Membrane lysis by the antibacterial peptides cecropins B1 and B3: A spin-label electron spin resonance study on phospholipid bilayers. *Biophys. J. 77*, 3120–3133.

(94) Iwasaki, T., Ishibashi, J., Tanaka, H., Sato, M., Asaoka, A., Taylor, D. M., and Yamakawa, M. (2009) Selective cancer cell cytotoxicity of enantiomeric 9-mer peptides derived from beetle defensins depends on negatively charged phosphatidylserine on the cell surface. *Peptides 30*, 660–668.

(95) Oren, Z., and Shai, Y. (1998) Mode of action of linear ampiphatic alpha-helical antimicrobial peptides. *Biopolymers 47*, 451–463.

(96) Shai, Y. (1999) Mechanism of the binding, insertion and destabilization of phospholipid bilayer membranes by α-helical antimicrobial and cell non-selective membrane-lytic peptides. *Biochim. Biophys. Acta 1462*, 55–70.

(97) Mai, J. C., Mi, Z., Kim, S., Ng, B., and Robbins, P. D. (2001) A proapoptotic peptide for the treatment of solid tumors. *Cancer Res. 61*, 7709–7712.

(98) Cory, S., and Adams, J. M. (1998) Matters of life and death: Programmed cell death at cold spring harbor. *Biochim. Biophys. Acta - Rev. Cancer 1377*, R25–R44.

(99) Chen, J., Xu, X. M., Underhill, C. B., Yang, S., Wang, L., Chen, Y., Hong, S., Creswell, K., and Zhang, L. (2005) Tachyplesin activates the classic complement pathway to kill tumor cells. *Cancer Res. 65*, 4614–4622.

(100) Chernysh, S., Kim, S. I., Bekker, G., Pleskachl, V. A., Filatova, N. A., Anikin, V.

Stellenbosch University https://scholar.sun.ac.za

B., Platonov, V. G., and Bulet, P. (2002) Antiviral and antitumor peptides from insects. *Proceeding Natl. Acad. Sci. USA 99*, 12628–12632.

(101) Rautenbach, M., Vlok, N. M., Stander, M., and Hoppe, H. C. (2007) Inhibition of malaria parasite blood stages by tyrocidines, membrane-active cyclic peptide antibiotics from *Bacillus brevis*. *Biochim. Biophys. Acta - Biomembr. 1768*, 1488–1497.

(102) Ouyang, G. L., Li, Q. F., Peng, X. X., Liu, Q. R., and Hong, S. G. (2002) Effects of tachyplesin on proliferation and differentiation of human hepatocellular carcinoma SMMC-7721 cells. *World J. Gastroenterol. 8*, 1053–1058.

(103) Dubos, R. J. (1939) Bactericidal effect of an extract of a soil Bacillus on Gram positive cocci. *Exp. Biol. Med. 70*, 3–4.

(104) Dubos, R. J., and Hotchkiss, R. D. (1941) The production of bactericidal substances by aerobic sporulating Bacilli. *J. Exp. Med. 141*, 155–162.

(105) Dubos, R., and Cattaneo, C. (1939) Studies on a bactericidal agent extracted from a soil Bacillus: III Preparation and activity of a protein-free fraction. *J. Exp. Med. 70*, 249–256.

(106) Fujikawa, K., Suzuki, T., and Kurahashi, K. (1968) Biosynthesis of tyrocidine by a cell-free enzyme system of Bacillus brevis ATCC 8185. I. Preparation of partially purified enzyme system and its properties. *BBA Sect. Nucleic Acids Protein Synth. 161*, 232–246.

(107) Spathelf, B. M. (2010) Qualitative structure-actvity relationships of the major tyrocidines, cyclic decapeptides from *Bacillus aneurinolyticus*. PhD Thesis, Department of Biochemistry, University of Stellenbosch, http://scholar.sun.ac.za/handle/10019.1/4001. Stellenbosch.

(108) Henderson, J. (1946) The status of tyrothricin as an antibiotic agent for topical application. *J. Am. Pharm. Assoc. 35*, 141–147.

(109) Wigger-Alberti, W., Stauss-Grabo, M., Grigo, K., Atiye, S., Williams, R., and Korting, H. C. (2012) Efficacy of a tyrothricin-containing wound gel in an abrasive wound model for superficial wounds. *Skin Pharmacol. Physiol. 26*, 52–56.

(110) Rankin, L. M. (1944) The use of tyrothricin in the treatment of ulcers of the skin. *Am. J. Surg. 65*, 391–392.

(111) Kagan, G., Huddlestone, L., and Wolstencroft, P. (1982) Two lozenges containing benzocaine assessed in the relief of sore throat. *J. Int. Med. Res. 10*, 443–446.

(112) Dimick, K. P. (1951) Hemolytic action of gramicidin and tyrocidin. *Exp. Biol. Med. 78*, 782–784.

(113) Tang, X. J., Thibault, P., and Boyd, R. K. (1992) Characterisation of the tyrocidine and gramicidin fractions of the tyrothricin complex from *Bacillus brevis* using liquid chromatography and mass spectrometry. *Int. J. Mass Spectrom. Ion Process. 122*, 153–179.

(114) Marques, M. A., Citron, D. M., and Wang, C. C. (2007) Development of Tyrocidine A analogues with improved antibacterial activity. *Bioorganic Med. Chem. 15*, 6667–6677.

(115) Troskie, A. M. (2014) Tyrocidines , cyclic decapeptides produced by soil *bacilli* , as potent inhibitors of fungal pathogens. Stellenbosch.

Stellenbosch University https://scholar.sun.ac.za

(116) Gibbons, W. A., Beyer, C. F., Dadok, J., Sprecher, R. F., and Wyssbrod, H. R. (1975) Studies of individual amino acid aesidues of the decapeptide Tyrocidine A by proton double-resonance difference spectroscopy in the correlation mode. *Biochemistry 14*, 420–429.

(117) Kuo, M., and Gibbons, W. A. (1979) Total assignments, including four aromatic residues, and sequence confirmation of the decapeptide tyrocidine A using difference double resonance. Qualitative nuclear overhauser effect criteria for beta turn and antiparallel beta-pleated sheet conformation. *J. Biol. Chem. 254*, 6278–6287.

(118) Kuo, M. C., and Gibbons, W. A. (1979) Determination of individual side-chain conformations, tertiary conformations, and molecular topography of Tyrocidine A from scalar coupling constants and chemical shifts. *Biochemistry 18*, 5855–5867.

(119) Kuo, M. C., and Gibbons, W. A. (1980) Nuclear overhauser effect and cross-relaxation rate determinations of dihedral and transannular interproton distances in the decapeptide tyrocidine A. *Biophys. J. 32*, 807–836.

(120) Munyuki, G., Jackson, G. E., Venter, G. A., Kövér, K. E., Szilágyi, L., Rautenbach, M., Spathelf, B. M., Bhattacharya, B., and Van Der Spoel, D. (2013) β-sheet structures and dimer models of the two major tyrocidines, antimicrobial peptides from *Bacillus aneurinolyticus* . *Biochemistry 52*, 7798–7806.

(121) Loll, P. J., Upton, E. C., Nahoum, V., Economou, N. J., and Cocklin, S. (2014) The high resolution structure of tyrocidine A reveals an amphipathic dimer. *Biochim. Biophys. Acta - Biomembr. 1838*, 1199–1207.

(122) Laiken, S., Printz, M., and Craig, L. C. (1969) Circular dichroism of the tyrocidines and gramicidin S-A. *J. Biol. Chem. 244*, 4454–4457.

(123) Aranda, F. J., and de Kruijff, B. (1988) Interrelationships between tyrocidine and gramicidin A′ in their interaction with phospholipids in model membranes. *Biochim. Biophys. Acta 937*, 195–203.

(124) Goodall, M. C. (1970) Structural effects in the action of antibiotics on the ion permeability of lipid bilayers. *Biochim. Biophys. Acta 203*, 28–33.

(125) Dubos, R. J. (1939) Studies on a bactericidal agent extracted from a soil Bacillus: I. Preparation of the agent. Its acticity in vitro. *J. Exp. Med. 70*, 1–10.

(126) Llamas-Saiz, A. L., Grotenbreg, G. M., Overhand, M., and Van Raaij, M. J. (2007) Double-stranded helical twisted β-sheet channels in crystals of gramicidin S grown in the presence of trifluoroacetic and hydrochloric acids. *Acta Crystallogr. Sect. D Biol. Crystallogr. 63*, 401–407.

(127) Eyéghé-bickong, H. A. (2011) Role of surfactin from *Bacillus subtilis* in protection against antimicrobial peptides produced by Bacillus species.PhD Thesis, Department of Biochemistry, University of Stellenbosch, http://hdl.handle.net/10019.1/6773

(128) Breshow, R., and Chipman, D. (1965) The use of the tyrocidines for the study of conformation and aggregation behavior. *J. Am. Chem. Soc. 87*, 4196–4198.

(129) Ruttenberg, M. A., King, T. P., and Craig, L. C. (1966) The Chemistry of tyrocidine. VII. Studies on association behaviour and implications regarding conformation. *Biochemistry 5*, 2857–2864.

Stellenbosch University https://scholar.sun.ac.za

(130) Williams, R. C., Yphantis, D. A., and Craig, L. C. (1972) Noncovalent association of tyrocidine B. *Biochemistry 11*, 70–77.

(131) Wenzel, M., Rautenbach, M., Vosloo, J. A., Siersma, T., Aisenbrey, C. H. M., Zaitseva, E., Laubscher, W. E., van Rensburg, W., Behrends, J. C., Bechinger, B., and Hamoen, L. W. (2018) The multifaceted antibacterial mechanisms of the pioneering peptide antibiotics tyrocidine and gramicidin S. *MBio 9*, 1–20.

(132) Spathelf, B. M., and Rautenbach, M. (2009) Anti-listerial activity and structure-activity relationships of the six major tyrocidines, cyclic decapeptides from *Bacillus aneurinolyticus*. *Bioorganic Med. Chem. 17*, 5541–5548.

(133) Troskie, A. M., de Beer, A., Vosloo, J. A., Jacobs, K., and Rautenbach, M. (2014) Inhibition of agronomically relevant fungal phytopathogens by tyrocidines, cyclic antimicrobial peptides isolated from Bacillus aneurinolyticus. *Microbiology 160*, 2089–2101.

(134) Leussa, A. N.-N. (2014) Characterisation of small cyclic peptides with antimalarial and antilisterial activity. PhD Thesis, Department of Biochemistry, University of Stellenbosch, http://hdl.handle.net/10019.1/86161.

(135) Dubos, R. J., and Hotchkiss, R. D. (1941) The production of bactericidal substances by aerobic sporulating bacilli. *J. Exp. Med. 73*, 629–640.

(136) Dubos, R. J., Hotchkiss, R. D., and Coburn, A. F. (1942) The effect of gramicidin and tyrocididne on bacterial metabolism. *J. Biol. Chem. 146*, 421–426.

(137) Schazschneider, B., Ristow, H., and Kleinkauf, H. (1974) Interaction between the antibiotic tyrocidine and DNA in vitro. *Nature 249*, 757–759.

(138) Bohg, A., and Ristow, H. (1987) Tyrocidine-induced modulation of the DNA conformation in *Bacillus brevis*. *Eur. J. Biochem. 170*, 253–258.

(139) Ristow, H. (1986) DNA-supercoiling is affected *in vitro* by the peptide antibiotics tyrocidine and gramicidin. *Eur. J. Biochem. 160*, 587–591.

(140) Danders, W., Marahiel, M. A., Krause, M., Kosui, N., Kato, T., Izumiya, N., and Kleinkauf, H. (1982) Antibacterial action of gramicidin S and tyrocidines in relation to active transport, *in vitro* transcription, and spore outgrowth. *Antimicrob. Agents Chemother. 22*, 785–790.

(141) Hancock, R. E. W., and Sahl, H. G. (2006) Antimicrobial and host-defense peptides as new anti-infective therapeutic strategies. *Nat. Biotechnol. 24*, 1551–1557.

(142) Shi, J., Kantoff, P. W., Wooster, R., and Farokhzad, O. C. (2017) Cancer nanomedicine: Progress, challenges and opportunities. *Nat. Rev. Cancer 17*, 20–37.

(143) Ehrlich, P. (1960) The Collected Papers of Paul Ehrlich 3.

(144) Bae, Y. H. (2009) Drug targeting and tumor heterogeneity. *J. Control. Release 133*, 2–3.

(145) Nicolas, J., Mura, S., Brambilla, D., MacKiewicz, N., and Couvreur, P. (2013) Design, functionalization strategies and biomedical applications of targeted biodegradable/biocompatible polymer-based nanocarriers for drug delivery. *Chem. Soc. Rev. 42*, 1147–1235.

(146) Maeda, H., and Matsumura, Y. (1986) A new concept for macromolecular therapeutics in cancer chemotherapy: mechanism of tumoritropic accumulation of

Stellenbosch University https://scholar.sun.ac.za

proteins and the antitumor agent smancs. *Cancer Res. 46*, 6387–6392.

(147) Maeda, H., Bharate, G. Y., and Daruwalla, J. (2009) Polymeric drugs for efficient tumor-targeted drug delivery based on EPR-effect. *Eur. J. Pharm. Biopharm. 71*, 409–419.

(148) Danhier, F., Feron, O., and Préat, V. (2010) To exploit the tumor microenvironment: Passive and active tumor targeting of nanocarriers for anti-cancer drug delivery. *J. Control. Release 148*, 135–146.

(149) Renukuntla1, J., Vadlapudi, A. D., Patel, A., Boddu, S. H., and Mitra, A. K. (2013) Approaches for enhancing oral bioavailability of peptides and proteins. *Int. J. Pharm. 447*, 75–93.

(150) Grivennikov, S. I., Greten, F. R., and Karin, M. (2010) Immunity, Inflammation, and Cancer. *Cell 140*, 883–899.

(151) Nicolas, J., Mura, S., Brambilla, D., Mackiewicz, N., and Couvreur, P. (2013) Design, functionalization strategies and biomedical applications of targeted biodegradable/biocompatible polymer-based nanocarriers for drug delivery. *Chem. Soc. Rev. 42*, 1147–235.

(152) Davis, M. I., Bennett, M. J., Thomas, L. M., and Bjorkman, P. J. (2005) Crystal structure of prostate-specific membrane antigen, a tumor marker and peptidase. *Proc. Natl. Acad. Sci. 102*, 5981–5986.

(153) Low, P. S., and Kularatne, S. A. (2009) Folate-targeted therapeutic and imaging agents for cancer. *Curr. Opin. Chem. Biol. 13*, 256–262.

(154) Daniels, T. R., Delgado, T., Helguera, G., and Penichet, M. L. (2006) The transferrin receptor part II: Targeted delivery of therapeutic agents into cancer cells. *Clin. Immunol. 121*, 159–176.

(155) Scaltriti, M., and Baselga, J. (2006) The epidermal growth factor receptor pathway: A model for targeted therapy. *Clin. Cancer Res. 12*, 5268–5273.

(156) Lurje, G., and Lenz, H. J. (2009) EGFR signaling and drug discovery. *Oncology 77*, 400–410.

(157) Misra, S., Heldin, P., Hascall, V. C., Karamanos, N. K., Skandalis, S. S., Markwald, R. R., and Ghatak, S. (2011) Hyaluronan-CD44 interactions as potential targets for cancer therapy. *FEBS J. 278*, 1429–1443.

(158) Buschle, M., Cotten, M., Kirlappos, H., Mechtler, K., Schaffner, G., Zauner, W., Birnstiel, M. l., and Wagner, E. (1995) Receptor-mediated gene transfer into human T lymphocytes via binding of DNA/CD3 antibody particles to the CD3 T cell receptor complex. *Hum. Gene Ther. 6*, 753–761.

(159) Nahta, R., and Esteva, F. J. (2006) Herceptin: Mechanisms of action and resistance. *Cancer Lett. 232*, 123–138.

(160) Levato, L., and Molica, S. (2018) Rituximab in the management of acute lymphoblastic leukemia. *Expert Opin. Biol. Ther. 18*, 221–226.

(161) Danhier, F., Feron, O., and Préat, V. (2010) To exploit the tumor microenvironment: Passive and active tumor targeting of nanocarriers for anti-cancer drug delivery. *J. Control. Release 148*, 135–146.

(162) Liu, J., Huang, Y., Kumar, A., Tan, A., Jin, S., Mozhi, A., and Liang, X. J. (2014)

Stellenbosch University https://scholar.sun.ac.za

PH-Sensitive nano-systems for drug delivery in cancer therapy. *Biotechnol. Adv. 32*, 693–710.

(163) Iyer, A. K., Khaled, G., Fang, J., and Maeda, H. (2006) Exploiting the enhanced permeability and retention effect for tumor targeting. *Drug Discov. Today 11*, 812–818.

(164) Halperin, A., Shadkchan, Y., Pisarevsky, E., Szpilman, A. M., Sandovsky, H., Osherov, N., and Benhar, I. (2016) Novel water-soluble Amphotericin B-PEG conjugates with low toxicity and potent in vivo efficacy. *J. Med. Chem. 59*, 1197–1206.

(165) Guiotto, A., Pozzobon, M., Canevari, M., Manganelli, R., Scarin, M., and Veronese, F. M. (2003) PEGylation of the antimicrobial peptide nisin A: problems and perspectives. *Farmaco 58*, 45–50.

(166) Morris, C. J., Beck, K., Fox, M. A., Ulaeto, D., Clark, G. C., and Gumbleton, M. (2012) Pegylation of antimicrobial peptides maintains the active peptide conformation, model membrane interactions, and antimicrobial activity while improving lung tissue biocompatibility following airway delivery. *Antimicrob. Agents Chemother. 56*, 3298–3308.

(167) Benincasa, M., Zahariev, S., Pelillo, C., Milan, A., Gennaro, R., and Scocchi, M. (2015) PEGylation of the peptide Bac7(1-35) reduces renal clearance while retaining antibacterial activity and bacterial cell penetration capacity. *Eur. J. Med. Chem. 95*, 210–219.

(168) Fosgerau, K., and Hoffmann, T. (2014) Peptide therapeutics: Current status and future directions. *Drug Discov. Today 20*, 122–128.

(169) Klumperman, L., Reader, P. W., and Rautenbach, M. (2017) Conjugate for malaria.

(170) Duchene, D., Ponchel, G., and Wouessidjewe, D. (1999) Cyclodextrins in targeting: Application to nanoparticles. *Adv. Drug Deliv. Rev. 36*, 29–40.

(171) Bellocq, N. C., Pun, S. H., Jensen, G. S., and Davis, M. E. (2003) Transferrin-containing, cyclodextrin polymer-based particles for tumor-targeted gene delivery. *Bioconjug. Chem. 14*, 1122–1132.

(172) El Ghaouth, A., Arul, J., Asselin, A., and Benhamou, N. (1992) Antifungal activity of chitosan on post-harvest pathogens: induction of morphological and cytological alterations in *Rhizopus stolonifer*. *Mycol. Res. 96*, 769–779.

(173) Wang, H., Zhao, P., Liang, X., Gong, X., Song, T., Niu, R., and Chang, J. (2010) Folate-PEG coated cationic modified chitosan - Cholesterol liposomes for tumor-targeted drug delivery. *Biomaterials 31*, 4129–4138.

(174) Batista, M. K. S., Gallemí, M., Adeva, A., Gomes, C. A. R., and Gomes, P. (2009) Facile regioselective synthesis of a novel chitosan-pexiganan conjugate with potential interest for the treatment of infected skin lesions. *Synth. Commun. 39*, 1228–1240.

(175) Sahariah, P., Sørensen, K. K., Hjálmarsdóttir, M. A., Sigurjónsson, Ó. E., Jensen, K. J., Másson, M., and Thygesen, M. B. (2015) Antimicrobial peptide shows enhanced activity and reduced toxicity upon grafting to chitosan polymers. *Chem. Commun. 51*, 11611–11614.

(176) Çağdaş, M., Sezer, A. D., and Bucak, S. (2014) Liposomes as potential drug carrier systems for drug delivery. *Appl. Nanotechnol. Drug Deliv.* 1–50.

(177) Alavi, M., Karimi, N., and Safaei, M. (2017) Application of various types of

Stellenbosch University https://scholar.sun.ac.za

liposomes in drug delivery systems. *Adv. Pharm. Bull. 7*, 3–9.

(178) Benech, R. O., Kheadr, E. E., Lacroix, C., and Fliss, I. (2002) Antibacterial activities of nisin Z encapsulated in liposomes or produced in situ by mixed culture during Cheddar cheese ripening. *Appl. Environ. Microbiol. 68*, 5607–5619.

(179) Were, L. M., Bruce, B., Davidson, p. michael, and Weiss, J. (2004) Encapsulation of nisin and lysozyme in liposomes enhances efficacy against *Listeria monocytogenes*. *J. Food Prot. 67*, 922–927.

(180) Alipour, M., Halwani, M., Omri, A., and Suntres, Z. E. (2008) Antimicrobial effectiveness of liposomal polymyxin B against resistant Gram-negative bacterial strains. *Int. J. Pharm. 355*, 293–298.

(181) Ron-Doitch, S., Sawodny, B., Kühbacher, A., David, M. M. N., Samanta, A., Phopase, J., Burger-Kentischer, A., Griffith, M., Golomb, G., and Rupp, S. (2016) Reduced cytotoxicity and enhanced bioactivity of cationic antimicrobial peptides liposomes in cell cultures and 3D epidermis model against HSV. *J. Control. Release 229*, 163–171.

(182) Koren, E., and Torchilin, V. P. (2012) Cell-penetrating peptides: Breaking through to the other side. *Trends Mol. Med. 18*, 385–393.

(183) Torchilin, V. P., Rammohan, R., Weissig, V., and Levchenko, T. S. (2001) TAT peptide on the surface of liposomes affords their efficient intracellular delivery even at low temperature and in the presence of metabolic inhibitors. *Proc. Natl. Acad. Sci. U. S. A. 98*, 8786–8791.

(184) Bobo, D., Robinson, K. J., Islam, J., Thurecht, K. J., and Corrie, S. R. (2016) Nanoparticle-based medicines: A review of FDA-approved materials and clinical trials to date. *Pharm. Res. 33*, 2373–2387.

(185) Kale, A. A., and Torchilin, V. P. (2007) Enhanced transfection of tumor cells in vivo using “Smart” pH-sensitive TAT-modified pegylated liposomes. *J. Drug Target. 15*, 538–545.

(186) Han, H. K., and Amidon, G. L. (2000) Targeted prodrug design to optimize drug delivery. *AAPS PharmSci 2*, E6.

(187) Seetharaman, G., Kallar, A. R., Vijayan, V. M., Muthu, J., and Selvam, S. (2017) Design, preparation and characterization of pH-responsive prodrug micelles with hydrolyzable anhydride linkages for controlled drug delivery. *J. Colloid Interface Sci. 492*, 61–72.

(188) Seetharaman, G., Kallar, A. R., Vijayan, V. M., Muthu, J., and Selvam, S. (2017) Design, preparation and characterization of pH-responsive prodrug micelles with hydrolyzable anhydride linkages for controlled drug delivery. *J. Colloid Interface Sci. 492*, 61–72.

(189) Li, N., Cai, H., Jiang, L., Hu, J., Bains, A., Hu, J., Gong, Q., Luo, K., and Gu, Z. (2017) Enzyme-sensitive and amphiphilic PEGylated dendrimer-paclitaxel prodrug-based nanoparticles for enhanced stability and anticancer efficacy. *ACS Appl. Mater. Interfaces 9*, 6865–6877.

Stellenbosch University https://scholar.sun.ac.za

Chapter 2
THE PRODUCTION, PURIFICATION AND CHARACTERISATION OF THE TYROCIDINES AND ANALOGUES

2.1 INTRODUCTION

The phenomenon of multi-drug resistance (MDR) has been described in fungi, viruses, Gram-positive- and Gram-negative bacteria [1-2]. The rise of MDR greatly decreases the efficacy of current treatments against bacterial and fungal infections. Not only do we see this rise of MDR in bacteria and fungi, but also in one of the most fatal diseases around the world, known as cancer. In addition, the immune systems of cancer patients are compromised due to the non-selective nature of chemotherapeutic drugs subsequently increasing the risk of cancer patients contracting dangerous pathogenic infections [3]. Therefore, the discovery of alternative bactericidal and chemotherapeutic agents which limits resistance development and minimises damage to healthy tissue is critical. A group of peptides, known as antimicrobial peptides (AMPs), have received a great deal of attention in this regard. AMPs are generally cationic and exhibit broad spectrum of activity towards fungi, bacteria and cancer cells [4,5]. It has been shown by various studies that the cationic nature of AMPs promotes electrostatic interaction between the peptides and the negatively charged cell membranes/membrane patches of target cells, while their amphipathicity leads to disruption of the cell membrane function, increased permeability and cell lysis [6-7]. Various membranolytic mechanisms of actions have been proposed for AMPs such as the carpet model [8], barrel stave model [9], toroidal-pore model [7,10,11] and detergent type membrane lytic mechanism [12]. The rapid membranolytic activity of AMPs decreases the potential of resistance development

Stellenbosch University https://scholar.sun.ac.za

towards these peptides which make them a very attractive alternative to conventional antibacterial and anticancer drugs [13,14].

In the present study the biophysical and biological activity of a group of AMPs, known as the tyrocidines, will be investigated. The tyrocidines are produced by soil bacterium *Brevibacillus parabrevis,* as part of the tyrothricin complex which consists of the cationic cyclodecapeptides, known as the tyrocidines, and the neutral linear pentadecapeptides, known as the gramicidins [15]. The tyrocidines were first discovered in 1939 by Dubos [16] and later 19 related cyclodecapeptides in tyrothricin (Table 2.1) were identified and characterised by Tang *et al.* [17]. The primary structure of these cyclodecapeptides is conserved with variations generally at residues three and four (aromatic dipeptide unit), residue seven and residue nine. The tyrocidine analogues are formed by substitution of position seven with tyrosine (Tyr), while substitution with phenylalanine (Phe) or tryptophan (Trp) give rise to the phenycidines (Phcs) and tryptocidines (Tpcs), respectively [17-18].

Due to the highly conserved primary structure of the tyrocidines and analogues, the isolation of single peptides from the crude peptide extracts becomes a tedious and difficult task [17]. Our group (BIOPEP™ Peptide Group) have developed a large-scale method to produce and extract the complex mixture of tyrocidines and analogues. The method involves the supplementation of the culture broth of *Br. parabrevis* with specific amino acids to enrich the produced peptide complex with specific peptides of interest [19]. To investigate the biophysical and biological activity of the peptides of interest, purities of 90 % or higher are required, as determined by ultraperformance liquid chromatography (UPLC) linked to high resolution electrospray ionisation mass spectrometry (ESI-MS) (abbreviated as UPLC-MS). To obtain such high chemical purity, reverse-phase high performance liquid chromatography (RP-HPLC) is

Stellenbosch University https://scholar.sun.ac.za

generally utilised in peptide purification as it is an efficient technique to separate and purify peptides according to their physiochemical properties.

Table 2.1 Summary of the tyrocidines and analogues present in tyrothricin extract from *Br. parabrevis*.

Identity	Abbr.[a]	Sequence[b]	Theoretical monoisotopic M_r[c]
Tyrocidine A analogues (Ff)			
Phenycidine A[d]	PhcA or FA	Cyclo-(fP**Ff**NQFVOL)	1253.6597
Phenycidine A_1[d]	$PhcA_1$ or FA_1	Cyclo-(fP**Ff**NQFVKL)	1267.6753
Tyrocidine A	TrcA or YA	Cyclo-(fP**Ff**NQYVOL)	1269.6546
Tyrocidine A_1	$TrcA_1$ or YA_1	Cyclo-(fP**Ff**NQYVKL)	1283.6703
Tryptocidine A	TpcA or WA	Cyclo-(fP**Ff**NQWVOL)	1292.6706
Tryptocidine A_1	$TpcA_1$ or WA_1	Cyclo-(fP**Ff**NQWVKL)	1306.6862
Tyrocidine B analogues (Wf)			
Tyrocidine B/B'	TrcB/B' or YB/B'	Cyclo-(fP(**Wf**/Fw)NQYVOL)	1308.6655
Tyrocidine B_1/B_1'	$TrcB_1$/B_1'or YB_1/B_1'	Cyclo-(fP(**Wf**/Fw)NQYVKL)	1322.6812
Tryptocidine B/B'[d]	TpcB/B' or WB/B'	Cyclo-(fP(**Wf**/Fw)NQWVOL)	1331.6815
Tryptocidine B_1[d]/B_1'[d]	$TpcB_1$/B_1' or WB_1/B_1'	Cyclo-(fP(**Wf**/Fw)NQWVKL)	1345.6971
Tyrocidine C analogues (Ww)			
Tyrocidine C	TrcC or YC	Cyclo-(fP**Ww**NQYVOL)	1347.6764
Tyrocidine C_1	$TrcC_1$ or YC_1	Cyclo-(fP**Ww**NQYVKL)	1361.6921
Tryptocidine C	TpcC or WC	Cyclo-(fP**Ww**NQWVOL)	1370.6924
Tryptocidine C_1[d]	$TpcC_1$ or WC_1	Cyclo-(fP**Ww**NQWVKL)	1384.7080

[a] Abbreviations refer to the amino acid residue at position seven i.e. phenylalanine (Phc/F, tyrosine (Trc/Y) and tryptophan (Tpc/W).
[b] One letter abbreviations representing the amino acids sequences as used by Tang *et al*. [17] with O representing Ornithine and lower case letters representing the D-amino acids.
[c] Theoretical monoisotopic M_r calculated as the sum of the molecular masses of amino acid residues of each peptide.
[d] Low amounts detected

The hydrophobicity of the peptides is exploited during RP-HPLC, allowing separation based on the interaction of the peptides with the hydrophobic stationary and hydrophilic mobile phase of the system. Eyéghé-Bickong [20] optimised a C_{18} HPLC method for the purification of the tyrocidines and their analogues which involved the investigation of the influence of the solvent composition, gradient profile and column temperature on the resolution of the RP-HPLC. Optimal resolution was achieved with a non-linear gradient, column temperature set at 35 °C and solvent A and B consisting of 0.1 % (*v/v*) trifluoroacetic acid (TFA) in water and 10 % solvent A in 100 % acetonitrile (ACN) (*v/v*), respectively [20]. Although an optimised method has been developed, the isolation of single peptides remains a daunting task due to minimal

Stellenbosch University https://scholar.sun.ac.za

structural and chemical differences [17], as well as their tendency to form homo- and hetero-oligomeric structures [21, 22].

After purification with semi-preparative RP-HPLC, the peptide identity and purity must be determined by UPLC-MS, a powerful analytical technique in which high resolution and sensitivity are combined. ESI-MS is an analytical technique in which high accuracy molar mass of a compound (e.g. a peptide) can be determined. After the identification of the peptide identity and integrity with ESI-MS, the chemical purity can be determined with UPLC-MS from the resolved peaks in the resultant positive ion chromatogram [22, 23].

The aim of the study was to produce, extract and purify selected peptides from the tyrothricin complex extracted from bacterial producer cultures. The peptides that were selected to purify and characterise in the present project were TrcA, TrcB, TrcC and TpcC. The TrcA, TrcB and TpcC is usually extracted and purified from amino acid supplemented culture broths of *Br. parabrevis*. Whereas, high purity TrcC is usually more easily obtained from commercially available tyrothricin complex. The commercially available tyrothricin was originally obtained from Sigma-Aldrich (SteinHeim, Germany), but this product has been discontinued. Therefore, it would be ideal if TrcC can also be extracted and purified from supplemented *Br. parabrevis* culture broth, thereby ensuring cost and time effective future purification of TrcA, TrcB and TrcC. The purification of selected peptides by the C_{18} HPLC method of Eyéghé-Bickong [20] and the optimisation of a C_8 RP-HPLC method is described in this chapter. The C_8 RP-HPLC method is a potential alternative method for the purification of the tyrocidines and analogues, including TrcC from the crude peptide extracts of supplemented *Br. parabrevis* culture broths.

Stellenbosch University https://scholar.sun.ac.za

2.2 RESEARCH MATERIALS

The producer strain, *Br. parabrevis* ATCC 8185, used for tyrothricin complex production from which the single tyrocidine peptides were purified, was obtained from the American Type Culture Collections (Manassas, VA, USA). The tryptic soy broth (TSB), agar, D-glucose, tryptone, monopotassium phosphate (KH_2PO_4), magnesium sulphate ($MgSO_4$), calcium chloride ($CaCl_2$), ferric sulphate ($FeSO_4$), manganese sulphate ($MnSO_4$), sodium chloride (NaCl), ethanol (EtOH), diethyl ether and acetone were supplied by Merck (Darmstadt, Germany). Sigma-Aldrich (St Louis, USA) supplied methanol (MeOH), trifluoroacetic acid (TFA, >98%), potassium chloride (KCl), phosphorous pentoxide and commercial tyrothricin extract. Activated carbon and the L- amino acids (L-tryptophan and L-phenylalanine) were purchased from Lurgi (Frankfurt, Germany) and Sigma-Aldrich (SteinHeim, Germany), respectively. Mixed cellulose syringe filters (0.22 µm) were purchased from Merck-Millipore (Massachusetts, USA). Becton Dickson Labware (Lincoln Park, USA) and Lasec (Cape Town, South Africa) supplied Falcon® tubes and petri dishes, respectively. The acetonitrile (ACN, HPLC-grade, far UV cut-off) was purchased from Romil Ltd (Cambridge, United Kingdom). Analytical grade water was prepared by filtering water from a reverse osmosis plant through a Millipore-Q® water purification system (Milford, USA). The Nova-Pak HR C_{18} RP-HPLC semi-preparative column (6 µm particle size, 300 mm x 7.8 mm), C_{18} Nova-Pak® analytical RP-HPLC column (5 µm particle size, 150 mm x 3.9 mm) and Acquity HSS T3 (2.1 × 150 mm; 1.8 µm particle size) UPLC column were purchased from Waters (Milford, USA). The Spherisorb® C_8 column (5 µm particle size, 250 mm X 3.2 mm) was purchased from PhaseSep Pty Ltd (Victoria, Australia).

Stellenbosch University https://scholar.sun.ac.za

2.3 METHODS

2.3.1 Production of the tyrocidines and analogues.

The producer strain (*Br. parabrevis* ATCC 8185) was streaked out on TSB agar plates (30 g/L TSB and 1.5 % agar) using standard sterile techniques and incubated for 24 hours at 37 °C. Subsequently, overnight cultures were prepared by inoculating 20 mL of TSB with a single colony from the pre-culture agar plates followed by incubation for 24 hours at 37 °C on a shaker set at 150 rpm. Culture media were supplemented with 10 mM Trp or 20 mM Phe and peptide production by *Br. parabrevis* proceeded as described by Vosloo *et al*.[19], except that incubation at 37 °C proceeded for 13 days.

2.3.2 Extraction of the tyrocidines and analogues

The extraction methodologies that were used to isolate the individual peptides were developed by the BIOPEP Peptide Group (Stellenbosch, South Africa) and are protected under a non-disclosure agreement. In brief, the supplemented *Br. parabrevis* cultures were subjected to acidification steps and centrifuged at 10 621 *xg* for 10 minutes to obtain wet biomass. Subsequently, culture pellets were subjected to extraction and precipitation steps to obtain crude peptide extracts. This optimised method to produce crude extracts containing 40-85 % (*m/m*) peptide is protected under a non-disclosure agreement with BIOPEP^{TM}, Stellenbosch University. The linear gramicidins were removed by several washing steps with diethyl ether: acetone (1:1 *v/v*) with intermittent centrifugation (5 minutes at 3030 *xg*) steps. The crude peptide extracts were dried under N_2 gas flow, resuspended in 50 % ACN in water, transferred to pyrolised and analytically weighed 20 mL vials followed by lyophilisation. Commercial tyrothricin was also subjected to a few organic

Stellenbosch University https://scholar.sun.ac.za

extraction steps with diethyl ether: acetone (1:1 *v/v*) and centrifuged intermittently for 5 minutes at 3030 *xg* to remove linear gramicidins and to purify tyrocidine mixture (Trcmix).

2.3.3 Semi-preparative HPLC purification of the tyrocidines and analogues

Tyrocidines were purified from Trcmix (extracted from commercial tyrothricin) and the crude peptide extracts from supplemented *Br. parabrevis* culture broths. The crude peptide extracts and purified Trcmix were made up to a concentration of 10 mg/mL and 5 mg/mL, respectively, in 50% ACN in water and subjected to semi-preparative RP-HPLC purification as previously described by Eyéghé-Bickong [20] and Rautenbach *et al*. [24] . Volumes of 100 µL were injected onto a Nova-Pak HR C_{18} semi-preparative HPLC column. The HPLC system consisted of a Waters 6000A pump, Waters 510 pump and a Waters 440 absorbance detector (set at 254 nm) and was controlled by Millenium32 software (Waters, Milford, USA). A non-linear gradient (Table 2.2) at a flow rate of 3 mL/min and column temperature set at 35 °C was used to achieve elution with solvent A consisting of 0.1 % (*v/v*) TFA in water and solvent B of 10 % A in 100 % ACN (*v/v*). The fractions collected were transferred to weighed and pyrolised 20 mL vials, lyophilised and stored at room temperature until characterization with UPLC-MS analysis.

Table 2.2 The non-linear gradient program used for the semi-preparative HPLC purification of the tyrocidines and analogues

Minutes	% Eluent A	% Eluent B	Curve*
0.00	50	50	-
0.50	50	50	6
23.0	20	80	5
24.0	0	100	6
26.0	0	100	6
30.0	50	50	6
35.0	50	50	6

*6 depicts linear and 5 a non-linear concave curve (Waters™)

Stellenbosch University https://scholar.sun.ac.za

2.3.4 Characterisation of crude peptide extracts and single purified peptides with ESI-MS and UPLC-MS analysis

Peptide samples were resuspended in 50% ACN in water to concentrations 1000 µg/mL (for crude peptide extracts) and 250 µg/mL (for pure peptides samples/HPLC fractions). The samples were subsequently centrifuged at 10 621 *xg* for 10 min to remove any particulate material. Volumes of 2 µL (for direct MS analysis) and 3 µL (UPLC separation) of the samples were injected into the UPLC-MS system. The system consisted of a Waters Acquity UPLC® and a Waters Synapt G2 quadrupole time-of-flight (TOF) mass spectrometer and a photo diode array detector. UPLC separation was achieved with a Waters Acquity UPLC® HSS T3 column (2.1 × 150 mm; 1.8 µm particle size) and a minimum and maximum column temperature of 45 °C and 60 °C, respectively. Elution of peptides was achieved with a linear gradient program (Table 2.3) set at a flow rate of 0.3 mL/min with solvent A and B consisting of 1 % formic acid (*v/v*) in water and 100 % ACN containing 1 % formic acid (*v/v*), respectively. For the analysis of the crude peptide extracts and HPLC fractions, a Z-spray electrospray ionization source in the positive mode was used and data acquisition achieved by scanning the mass/charge (*m/z*) ratio range of 300 to 2000. Waters MassLynx V4.1 software (Milford, USA) was used for analysis and characterisation of all samples.

Table 2.3 The linear gradient program used during UPLC-MS analysis of the crude peptide extracts and the respective purified tyrocidines and analogues

Minutes	% Eluent A	% Eluent B	Curve*
0.00	0	0	6
0.50	100	0	6
1.00	70	30	6
10.0	40	60	6
15.0	20	80	6
15.1	0	0	6
18.0	100	0	6

*6 depicts linear curve (Waters™)

Stellenbosch University https://scholar.sun.ac.za

2.3.5 The optimisation of a C_8 HPLC method for the purification of the tyrocidines from crude peptide extract

Trcmix was dissolved in 50 % ACN in water to a concentration of 2 mg/mL. The sample solution was centrifuged at 10 621 *xg* for 10 minutes to remove any particulate material. A volume of 80 µL (160 µg) of sample solution was injected onto a C_{18} Nova-Pak® analytical RP-HPLC column (5 µm particle size, 150 mm x 3.9 mm) and a Spherisorb® C_8 RP-HPLC column (5 µm particle size, 250 mm X 3.2 mm). Three different HPLC non-linear gradient programs (Table 2.4-2.6, program A-C) were tested with protocol A being the analytical C_{18} HPLC linear gradient program optimised by Eyéghé-Bickong [20] which is the general program used for the purification of tyrocidines and analogues by our group. Program A was also tested at different temperatures (25 °C and 35 °C). The C_8 HPLC program D (Table 2.7) is a combination of program B and C. The resolution (R_s) was the HPLC parameter used to compare the separation of peaks achieved with the different HPLC programs, columns and temperatures. The resolution (R_s) is the quantitative measure of the separation of two peaks (n and n+1) in terms of their retention times (t_R) and average peak widths at the base (W_b) and was calculated by using Equation 2.1 [25].

$$Rs = \frac{2(t_{R(n+1)} - t_{R(n)})}{W_{b(n)} + W_{b(n+1)}} \quad 2.1$$

The partially purified Phe supplemented crude peptide extract (160 µg) was subjected to the optimised C_8 HPLC using program D and fractions manually collected to validate this purification method. Fractions were transferred to pyrolised analytically weighed vials and analysed with ESI-MS and UPLC-MS as described above (Section 2.3.4).

Stellenbosch University https://scholar.sun.ac.za

Table 2.4 The C_8 HPLC gradient program A

Minutes	Flow mL/min	% Eluent A	% Eluent B	Curve
0.00	1.0	50	50	-
0.50	1.0	50	50	6
23.0	1.0	20	80	5
24.0	1.0	0	100	6
26.0	1.0	0	100	6
30.0	1.0	50	50	6
35.0	1.0	50	50	6

Table 2.5 The C_8 HPLC gradient program B

Minutes	Flow mL/min	% Eluent A	% Eluent B	Curve
0.00	1.0	40	60	-
0.50	1.0	40	60	6
23.0	1.0	20	80	5
24.0	1.0	0	100	6
26.0	1.0	0	100	6
30.0	1.0	50	50	6
35.0	1.0	50	50	6

Table 2.6 The C_8 HPLC gradient program C

Minutes	Flow mL/min	% Eluent A	% Eluent B	Curve
0.00	1.5	50	50	-
0.50	1.5	50	50	6
23.0	1.5	20	80	5
24.0	1.5	0	100	6
26.0	1.5	0	100	6
30.0	1.5	50	50	6
35.0	1.5	50	50	6

Table 2.7 The optimised C_8 HPLC program D

Minutes	Flow mL/min	% Eluent A	% Eluent B	Curve
0.00	1.5	40	60	-
0.50	1.5	40	60	6
23.0	1.5	20	80	5
24.0	1.5	0	100	6
26.0	1.5	0	100	6
30.0	1.5	50	50	6
35.0	1.5	50	50	6

Stellenbosch University https://scholar.sun.ac.za

2.4 RESULTS AND DISCUSSION

2.4.1 The purification of tyrocidines from the culture broth of Br. parabrevis.

The tyrothricin complex, produced by the soil bacterium *Br. parabrevis*, consists of a basic fraction containing cyclic decapeptides known as the tyrocidines and a neutral fraction containing linear peptides known as the gramicidins [16,17]. Removal of the linear gramicidins provides a complex mixture of tyrocidines and analogues that differ from one another with only one or two amino acid residues. The highly conserved structure of the tyrocidines and analogues make the purification of single peptides a tedious and difficult task [17]. To simplify the purification process of the peptides, the culture medium of *Br. parabrevis* ATCC 8185 was supplemented with Phe and Trp as described by Vosloo *et al.* [19] to produce increased amounts of TrcA and TpcC, respectively. After 13 days of incubation the supplemented cultures were subjected to various extraction and precipitation steps to obtain a crude extract with >50% peptide per dry weight. UPLC-MS analysis of the Phe supplemented crude peptide extract revealed that TrcA (R_t = 10.84) and TrcB (R_t = 9.72) are the peptides contributing to the two major peaks (Figure 2.1 A). Furthermore, it is evident from the ESI-MS spectra that all six major tyrocidines, TrcA (1269.6403), $TrcA_1$ (1283.6618), TrcB (1308.6541), $TrcB_1$ (1322.6652), TrcC (1347.6731) and $TrcC_1$ (1361.6806) are present in the extract (Figure 2.1 C and E). The largest signal intensities are seen for TrcA and TrcB thereby confirming that higher amounts were produced and extracted for these peptides. Some of the tyrocidine analogues, such as PhcA (1253.6557), TpcA (1292.6604) and TpcB (1331.6662) are also present in smaller amounts indicated by lower signal intensities.

Stellenbosch University https://scholar.sun.ac.za

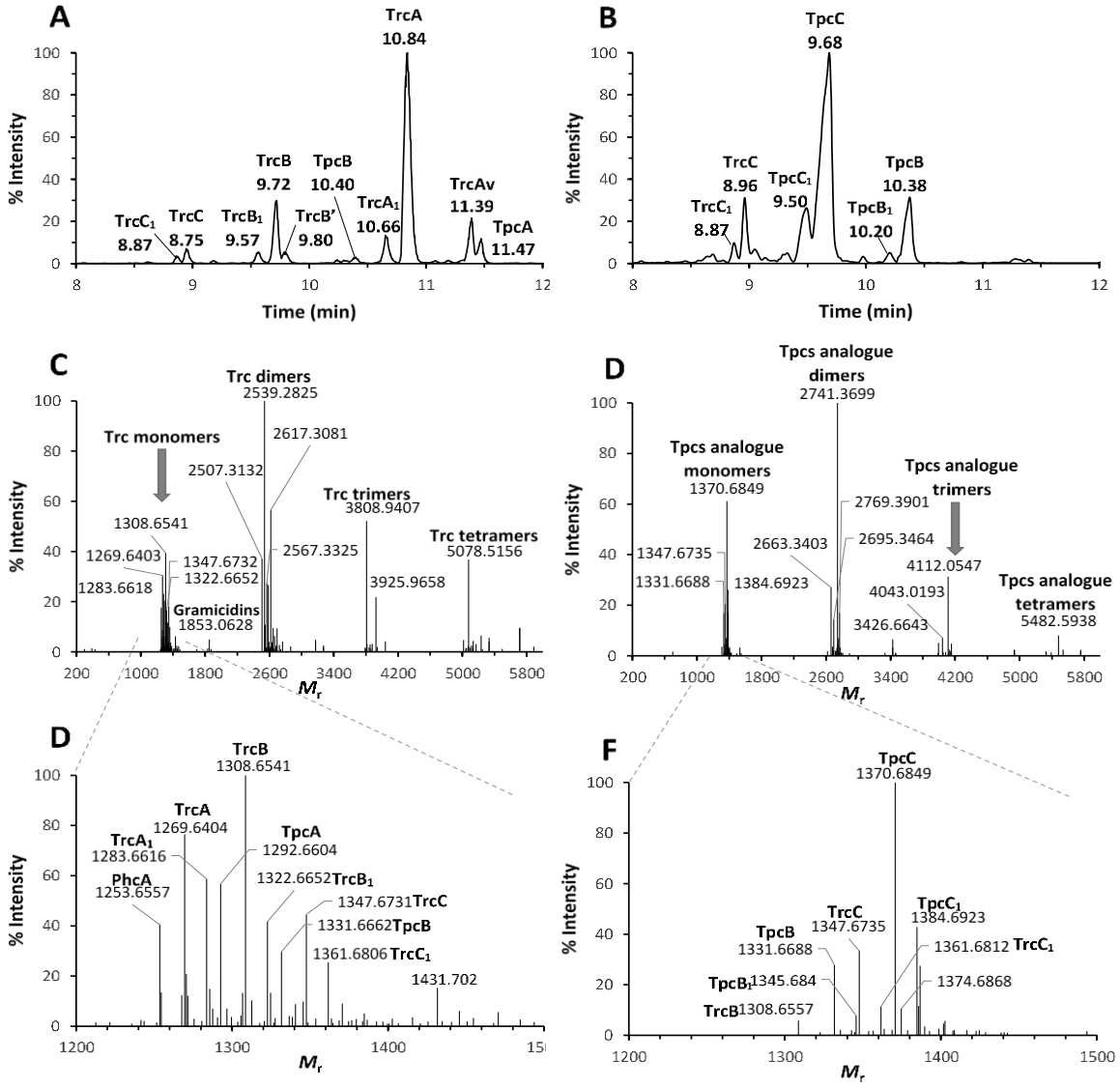

Figure 2.1 The UPLC-MS and ESI-MS analysis of the Phe and Trp supplemented crude peptide extracts. The UPLC chromatograms of A) the Phe supplemented and B) Trp supplemented crude peptide extract shows the peptide retention times above their representative peaks in minutes. The ESI-MS spectra of C) Phe supplemented and D) Trp supplemented crude extracts after MaxEnt 3 analysis over m/z 200-6000 range shows the monomeric to tetrameric species of the tyrocidines. E) The enlarged ESI-MS spectrum of the monomeric peptides present in the Phe supplemented extract. F) The enlarged ESI-MS spectrum of the monomeric peptides present in the Trp supplemented extract.

The tendency of these tyrocidines peptides to oligomerise is evident, with formation of dimers, trimers and tetramers clearly shown in the ESI-MS spectrum (Figure 2.1 C). The UPLC-MS analysis of the Trp supplemented crude peptide extract revealed one major peak, consisting of TpcC (R_t = 9.68), and two minor peaks, consisting of TrcC (R_t = 8.96) and TpcB (R_t= 10.38) (Figure 2.1 B). The ESI-MS spectra indicated

Stellenbosch University https://scholar.sun.ac.za

and confirmed that TpcC (1370.6849) was the analogue produced and extracted in the largest amounts (Figure 2.1 D and F).

The supplementation of the *Br. parabrevis* culture broth with Trp and Phe both resulted in increased production of the peptides and analogues of interests, thereby simplifying the purification methodology. After partial purification of the tyrocidine peptides and analogues, both supplemented crude peptide extracts were subjected to semi-preparative RP-HPLC and several fractions were collected subsequently. In the case of the Phe supplemented crude peptide extract, a total of five fractions were collected between 8 and 19 minutes (Figure 2.2).

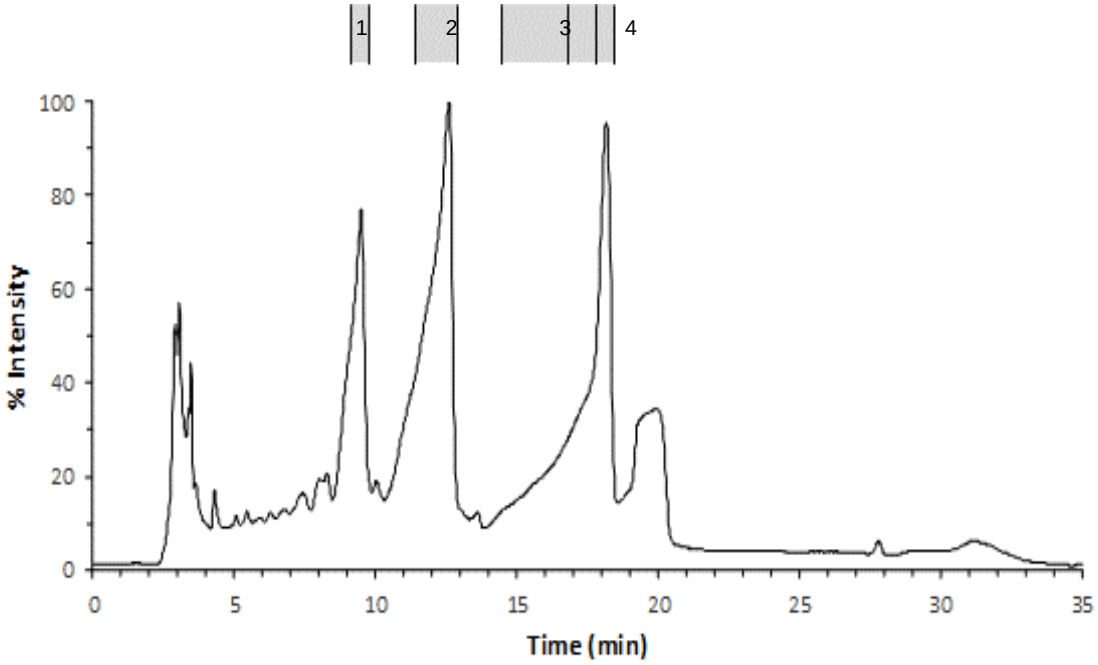

Figure 2.2 The semi-preparative RP-HPLC chromatogram of the Phe supplemented crude peptide extract. The five fractions that were collected between 8 and 19 minutes are shown above the chromatogram.

The peptide composition of each collected fraction was determined by ESI-MS and are summarised in Table 2.8. The tendency of the peptides to form sodium (Na^+) and potassium (K^+) adducts are observable from the ESI-MS analysis with TrcA (fraction 3-5) and TrcB (fraction 2) forming both cation adducts.

Stellenbosch University https://scholar.sun.ac.za

Table 2.8 Summary of the peptide composition of each fraction collected during RP-HPLC of the Phe supplemented crude peptide extract. The enlarged ESI-MS spectrum of each fraction is shown, indicating the monoisotopic M_r for each peptide.

HPLC Fraction	Peptide identity	Experimental M_r[a] (Theoretical M_r[b], ppm error)	Enlarged ESI-MS Spectrum
1	TrcC	1347.6734 (1347.6764, -2.2)	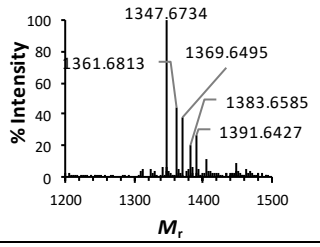
2	TrcB	1308.6541 (1308.6655, -8.7)	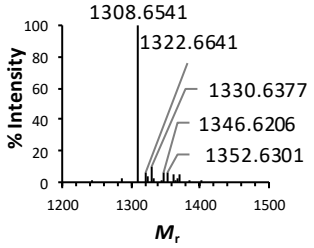
	$TrcB_1$	1322.6641 (1322.6812, -12.9)	
	TrcB Na^+ adduct	1330.6377 (1330.6477, -7.5)	
	TrcB K^+ adduct	1346.6206 (1346.6252, 3,4)	
3	TrcA	1269.6445 (1269.6546,-8.0)	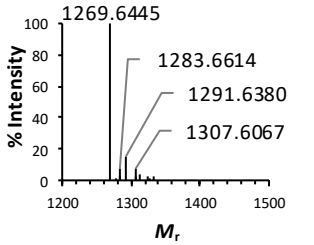
	$TrcA_1$	1283.6614 (1283.6703,-6.9)	
	TrcA Na^+ adduct	1291.6380 (1291.6368, 0.9)	
	TrcA K^+ adduct	1307.6067 (1307.6143, -5.8)	
4	TrcA	1269.6401 (1269.6546, -11.4)	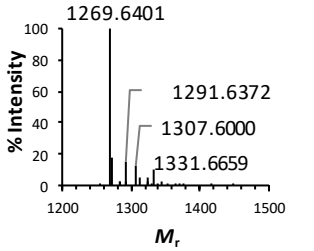
	TrcA Na adduct	1291.6372 (1291.6368, 0.3)	
	TrcA K^+ adduct	1307.6000 (1307.6143, -11.0)	
	TpcB	1331.6659 (1331.6815, -11.7)	
5	TrcA	1269.6438 (1269.6546, -8.5)	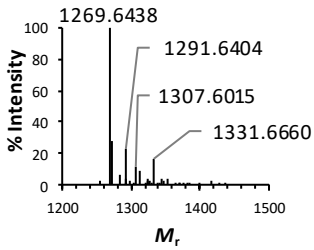
	TrcA Na^+ adduct	1291.6404 (1291.6368, 2.8)	
	TrcA K^+ adduct	1307.6015 (1307.6143, - 9.8)	
	TpcB	1331.6660 (1331.6815, -11.6)	

[a] Monoisotopic M_r as determined from the individual ESI-MS spectra.
[b] Theoretical monoisotopic M*r* calculated as the sum of the molecular weights of amino acid residues of each peptide.

From the initial ESI-MS analysis (Table 2.8) it was obvious that fraction two and three had the highest purity of peptide and were subsequently subjected to UPLC-

Stellenbosch University https://scholar.sun.ac.za

MS. The UPLC-MS analysis revealed that fraction three contained >90 % pure TrcA ($TrcA_1$ contamination) and fraction two contained >90 % pure TrcB (TpcC contamination) (Figure 2.3 A-B, Figure 2.4 A-B).

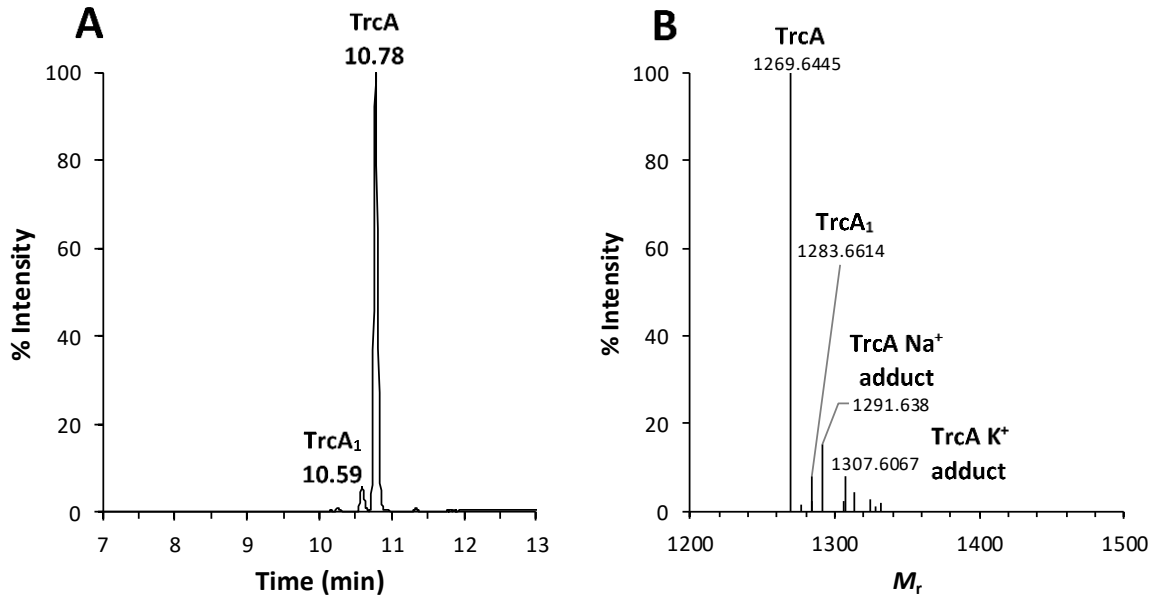

Figure 2.3 The UPLC and ESI-MS analysis of purified TrcA (93.7 % pure). A) The UPLC chromatogram of purified TrcA (250 µg/mL) showing the retention time in min and $TrcA_1$ peptide contamination. B) The ESI-MS spectrum of purified TrcA showing the M_r of the monomeric species and $TrcA_1$ contamination present in the fraction. The presence of the Na^+ and K^+ adducts in the fraction are also shown.

A second preparation of pure TrcB was achieved in a similar manner and the UPLC-MS analysis is shown in Figure 2.4 C-D. The analytical weight of the pure TrcA (93.7 % pure) was 8.96 mg, whereas the analytical weights for the two TrcB preparations (94.0 % pure and 95.8 % pure) were and 4.51 mg and 0.90 mg, respectively.

In a similar manner, the Trp supplemented crude peptide extract was subjected to semi-preparative RP-HPLC. A total of six fractions were collected between 11 and 16 minutes (Figure 2.5). The peptide composition of each collected fraction was determined by ESI-MS and are summarised in Table 2.9.

Stellenbosch University https://scholar.sun.ac.za

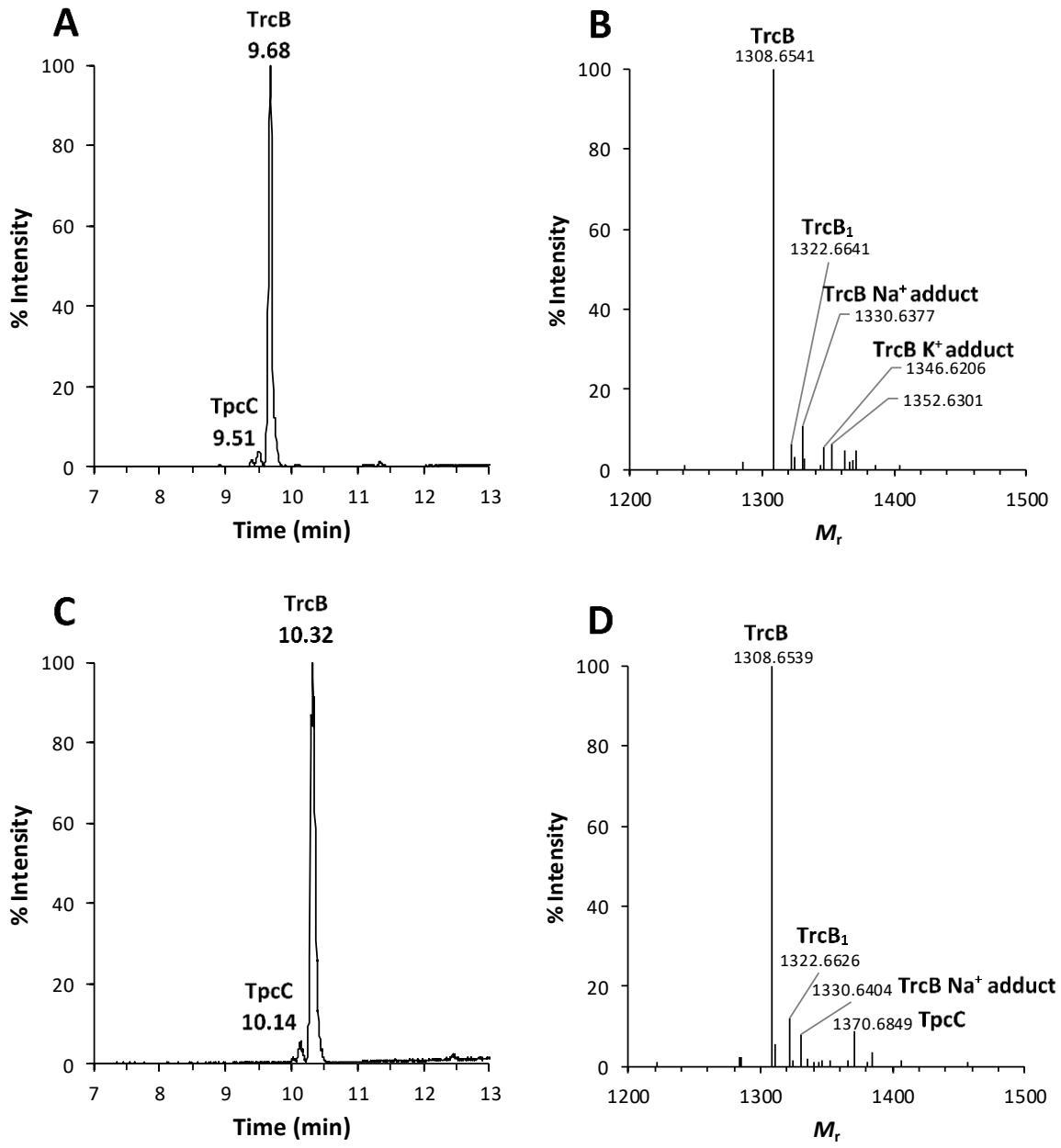

Figure 2.4 The UPLC and ESI-MS analysis of purified two preparations of pure TrcB A) The UPLC chromatogram of the first preparation of purified TrcB (94.0 % pure) (250 µg/mL) showing the retention time in minutes B) The ESI-MS spectrum of the first preparation of purified TrcB showing the M_r of the monomeric species and $TrcB_1$ contamination present in the fraction. C) The UPLC chromatogram of the second preparation of purified TrcB (95.8 % pure) (250 µg/mL) showing the retention time in minutes. The retention time of TrcB differs slightly from the first preparation because a new UPLC column was used. D) The ESI-MS spectrum of the second preparation of purified TrcB showing the M_r of the monomeric species and $TrcB_1$ and TpcC contamination present in the fraction.

Stellenbosch University https://scholar.sun.ac.za

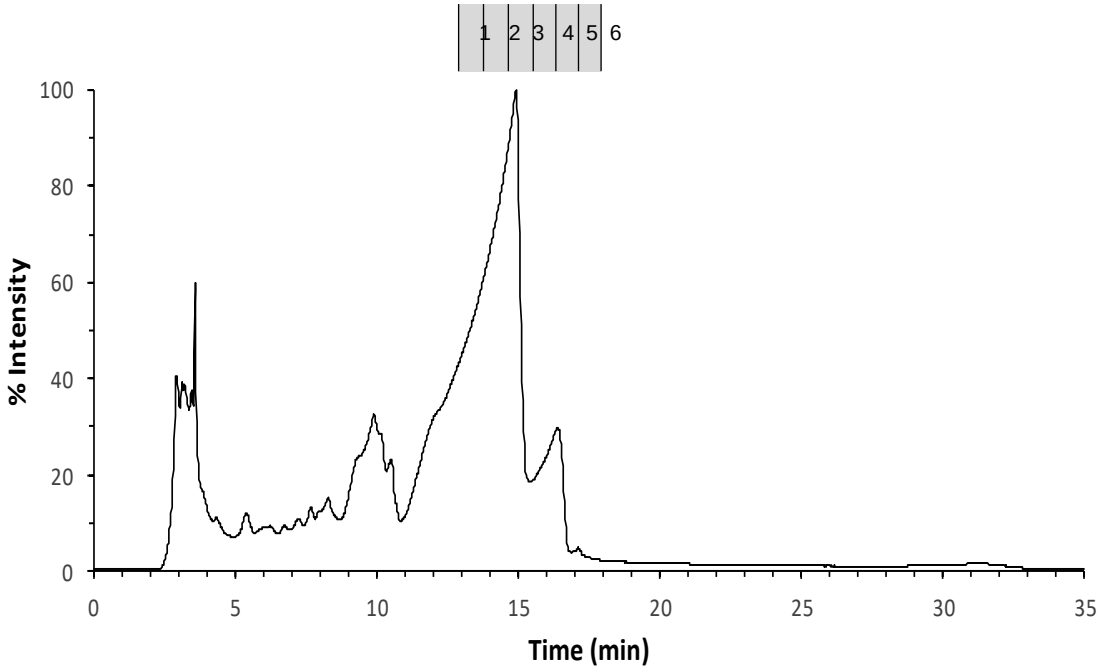

Figure 2.5 The semi-preparative RP-HPLC chromatogram of the Trp supplemented crude peptide extract. The six fractions that were collected between 11 and 16 minutes are shown above the chromatogram.

Similar to the tyrocidines, the TpcC analogues also have the tendency to form Na^+ and K^+ adducts with the presence of Na^+ adducts being more prevalent than the K^+ adducts. From the initial ESI-MS analysis (Table 2.9) it was evident that fraction three to five had the highest purity of peptide and were subsequently subjected to UPLC-MS. The UPLC-MS analysis (data not shown) confirmed that fraction three to five contained TpcC with purities of > 90 %, therefore these fractions were pooled together. The purity of the pooled TpcC fractions was determined as 94.5 % pure with contamination due to $TpcC_1$ (Figure 2.7 A-B). A second TpcC preparation was achieved in a similar manner and UPLC-MS analysis is shown in Figure2.7 C-D. The purity of the second TpcC preparation was determined as 93.1 %. The analytical weight of the two preparations of pure TpcC (94.5 % pure and 93.1 % pure) was determined as 5.54 mg and 5.78 mg, respectively.

Stellenbosch University https://scholar.sun.ac.za

Table 2.9 Summary of the peptide composition of each fraction collected during RP-HPLC of the Trp supplemented crude peptide extract. The enlarged ESI-MS spectrum of each fraction is shown, indicating the monoisotopic M_r for each peptide.

HPLC Fraction	Peptide identity	Experimental M_r[a] (Theoretical M_r[b], ppm error)	Enlarged ESI-MS Spectrum
1	TpcC	1370. 6849 (1370. 6924, -5.5)	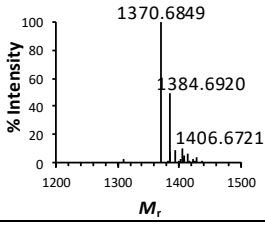
	$TpcC_1$	1384.6920 (1384.7080, -11.6)	
	$TpcC_1$ Na Adduct	1406.6721 (1406.6902, -12.9)	
2	TpcC	1370.6849 (1370.6924, -5.5)	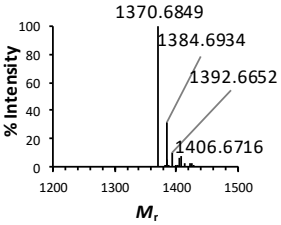
	TpcC Na^+ adduct	1392.6652 (1392,6746, -6.7)	
	$TpcC_1$	1384.6934 (1384.7080, -10.5)	
	$TpcC_1$ Na^+ Adduct	1406.6716 (1406.6902, -13.2)	
3	TpcC	1370.6849 (1370.6924, -5.5)	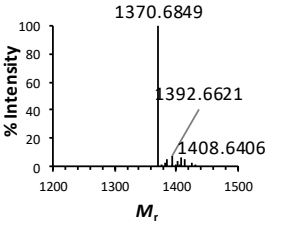
	TpcC Na^+ adduct	1392.6621 (1392.6746, -9.0)	
	TpcC K^+ adduct	1408.6406 (1408.6521, -8.2)	
4	TpcC	1370.6849 (1370.6924, -5.5)	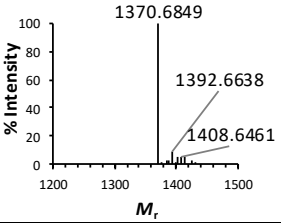
	TpcC Na^+ adduct	1392.6638 (1392.6746, -7.8)	
	TpcC K^+ adduct	1408.6461 (1408.6521, -4.3)	
5	TpcC	1370.6849 (1370.6924, -5.5)	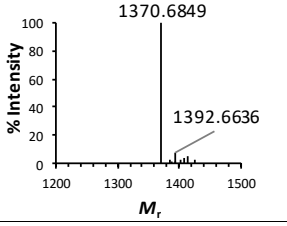
	TpcC Na^+ adduct	1392.6638 (1392.6746, -7.8)	
6	TpcB	1331.6662 (1331.6815, -11.5)	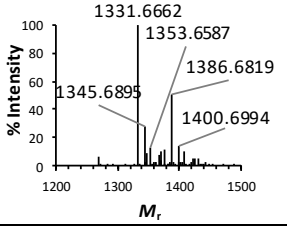
	TpcB Na^+ adduct	1353.6587 (1353.6637, -3.7)	
	$TpcB_1$	1345.6895 (1345.6971, -5.6)	

[a] Monoisotopic M_r as seen in ESI-MS spectrum.
[b] Theoretical monoisotopic M_r calculated as sum of the molecular weights of amino acid residues of each peptide.

Stellenbosch University https://scholar.sun.ac.za

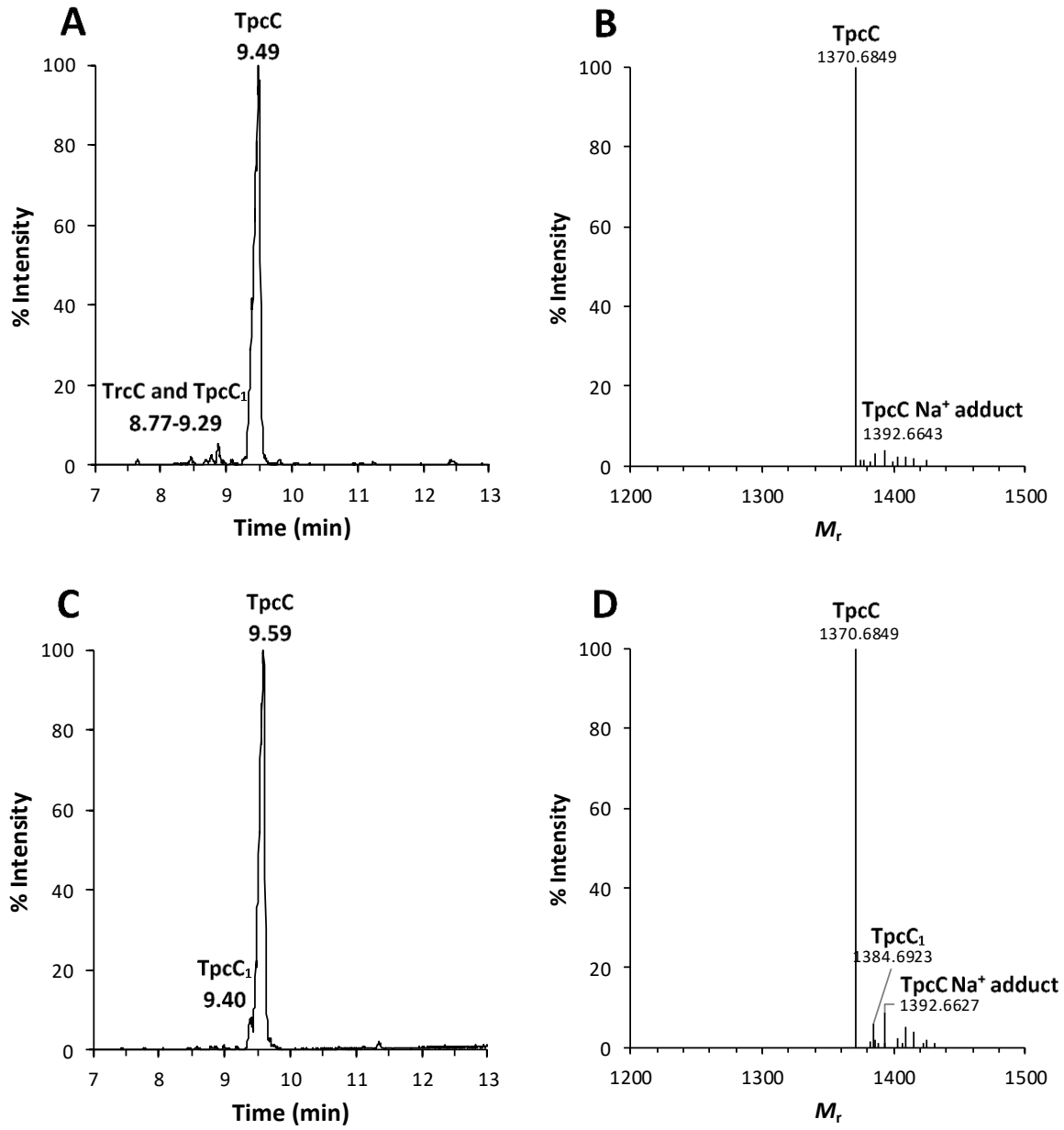

Figure 2.6 The UPLC and ESI-MS analysis of two preparations of pure TpcC. A) The UPLC chromatogram of the first preparation of purified TpcC (94.5 % pure) (250 µg/mL) showing the retention time in minutes and TrcC and $TpcC_1$ peptide contamination. B) The ESI-MS spectrum of the first preparation of purified TpcC showing the M_r of the monomeric species present in the pooled fraction. C) The UPLC chromatogram of the second preparation of purified TpcC (93.1 % pure) (250 µg/mL) showing the retention time in minutes and $TpcC_1$ contamination. The retention time of TpcC differs slightly from the first preparation because a new UPLC column was used. D) The ESI-MS spectrum of the second preparation of purified TpcC showing the M_r of the monomeric species present in the pooled fraction.

2.4.2 The purification of tyrocidine mix and TrcC from commercial tyrothricin

Commercial tyrothricin complex was used to purify Trcmix and TrcC. The commercial tyrothricin complex was subjected to organic extraction with diethyl ether

Stellenbosch University https://scholar.sun.ac.za

and acetone to remove the linear gramicidins. The masses of linear gramicidins range from 1882.0862 to 1896.1018. UPLC-ESI-MS was used to analyse the extracted Trcmix and revealed that the six major tyrocidines (TrcA, $TrcA_1$, TrcB, $TrcB_1$, TrcC and $TrcC_1$) and their tryptocidine (TpcA, $TpcA_1$, $TpcB_1$, TpcC and $TpcC_1$) and phenicidine (PhcA, $PhcA_1$ and PhcC) analogues were present and that the linear gramicidins were successfully removed (Figure 2.7 A-B).

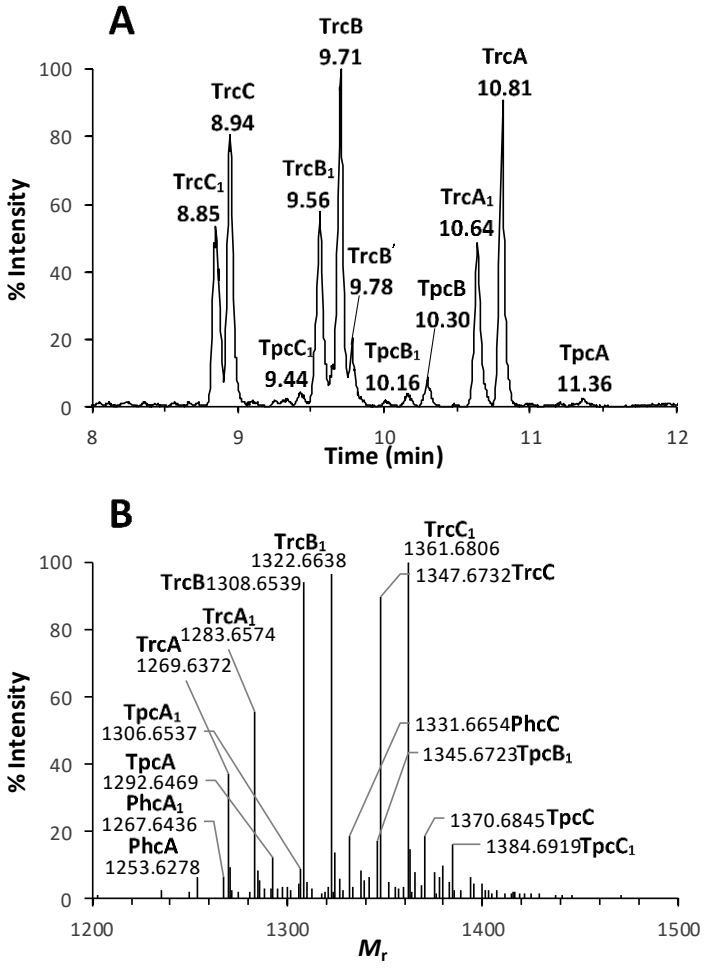

Figure 2.7 The UPLC-MS and ESI-MS analysis of the Trcmix purified from commercial tyrothricin complex. A) The enlarged UPLC chromatogram showing the retention times of the six major tyrocidines above their representative peaks in minutes. B) The enlarged ESI-MS spectrum of the monomeric peptides present in Trcmix.

The purified Trcmix was then subjected to semi-preparative RP-HPLC to purify TrcC. The HPLC chromatogram revealed three major peaks with the first peak having a front shoulder. A total of five fractions were collected between 9 and 15 minutes

Stellenbosch University https://scholar.sun.ac.za

(Figure 2.8). A summary of the peptide composition and ESI-MS spectra of the five fractions collected are shown in Table 2.10. The UPLC-MS analysis (data not shown) indicated that fraction two and three contained the highest purity of TrcC and these fractions were pooled. The purity of the TrcC after pooling of fractions two and three was determined with UPLC-MS analysis and was calculated as 96.4 % pure (Figure 2.9 A-B). A second preparation of pure TrcC was achieved in a similar manner and the UPLC-MS analysis is shown in Figure 2.9 C-D. The analytical weights of the two preparations of pure TrcC (96.4 % pure and 99.5 % pure) was determined as 3.05 mg and 3.36 mg, respectively.

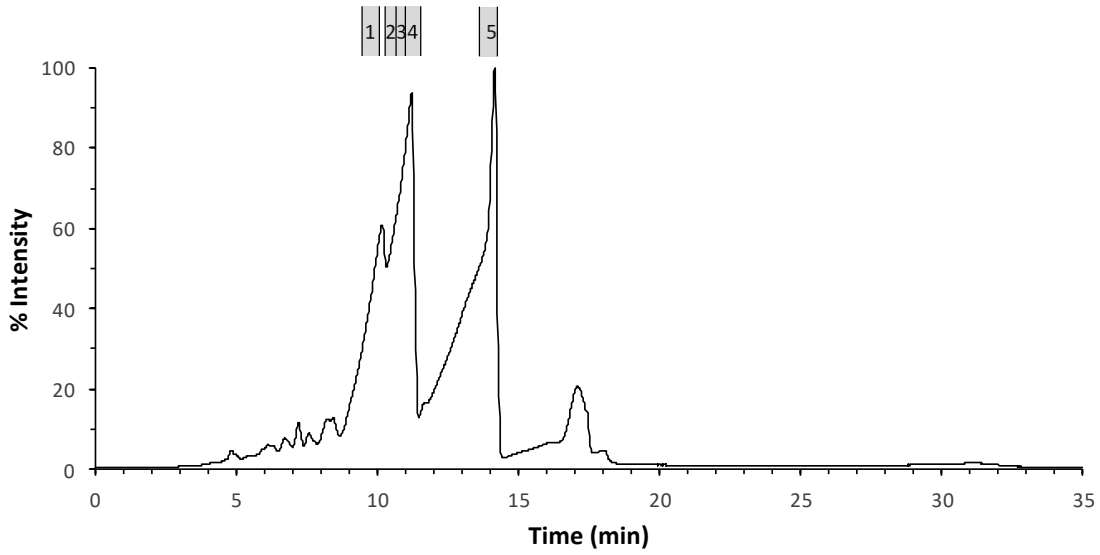

Figure 2.8 The semi-preparative RP-HPLC chromatogram of Trcmix. The five fractions that were collected between 9 and 15 minutes are shown above the chromatogram.

Stellenbosch University https://scholar.sun.ac.za

Table 2.10 Summary of the peptide composition of each fraction collected during RP-HPLC of the purified commercial Trcmix extract. The enlarged ESI-MS spectrum of each fraction is shown, indicating the monoisotopic M_r for each peptide present.

HPLC Fraction	Peptide identity	Experimental M_r[b] (Theoretical M_r[a], ppm error)	Enlarged ESI-MS Spectrum
1	Not determined*	Not determined*	Not determined*
2	TrcC	1347.6734 (1347.6764, -2.2)	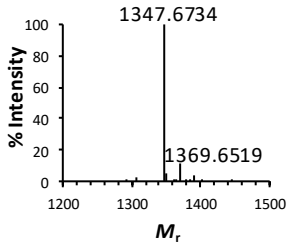
	TrcC Na^+ adduct	1369.6519 (1369.6586, -4.9)	
3	TrcC	1347.6735 (1347.6764, -2.2)	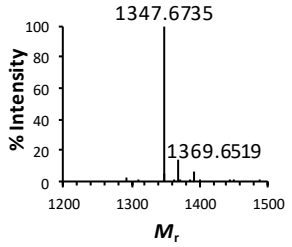
	TrcC Na^+ adduct	1369.6519 (1369.6586, -4.9)	
4	TrcC	1347.6735 (1347.6764, -2.2)	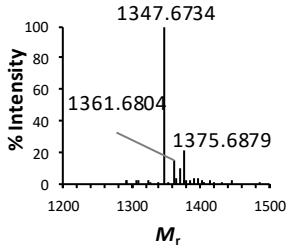
	$TrcC_1$	1361.6804 (1361.6921, -8.6)	
5	TrcB	1308.6539 (1308.6655, -8.9)	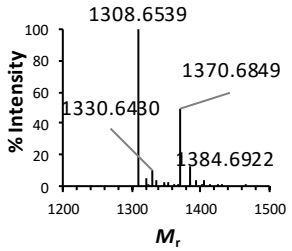
	TrcB Na^+ adduct	1330.6480 (1330.6477, 0.2)	
	TpcC	1370.6849 (1370.6924, -5.5)	
	$TpcC_1$	1384.6922 (1384.7080, -11.4)	

[a] Monoisotopic M_r as determined from the individual ESI-MS spectra.
[b] Theoretical monoisotopic M*r* calculated as the sum of the molecular weights of amino acid residues of each peptide.
*Not useful to determine purity of samples with low amount of peptide in fraction.

Stellenbosch University https://scholar.sun.ac.za

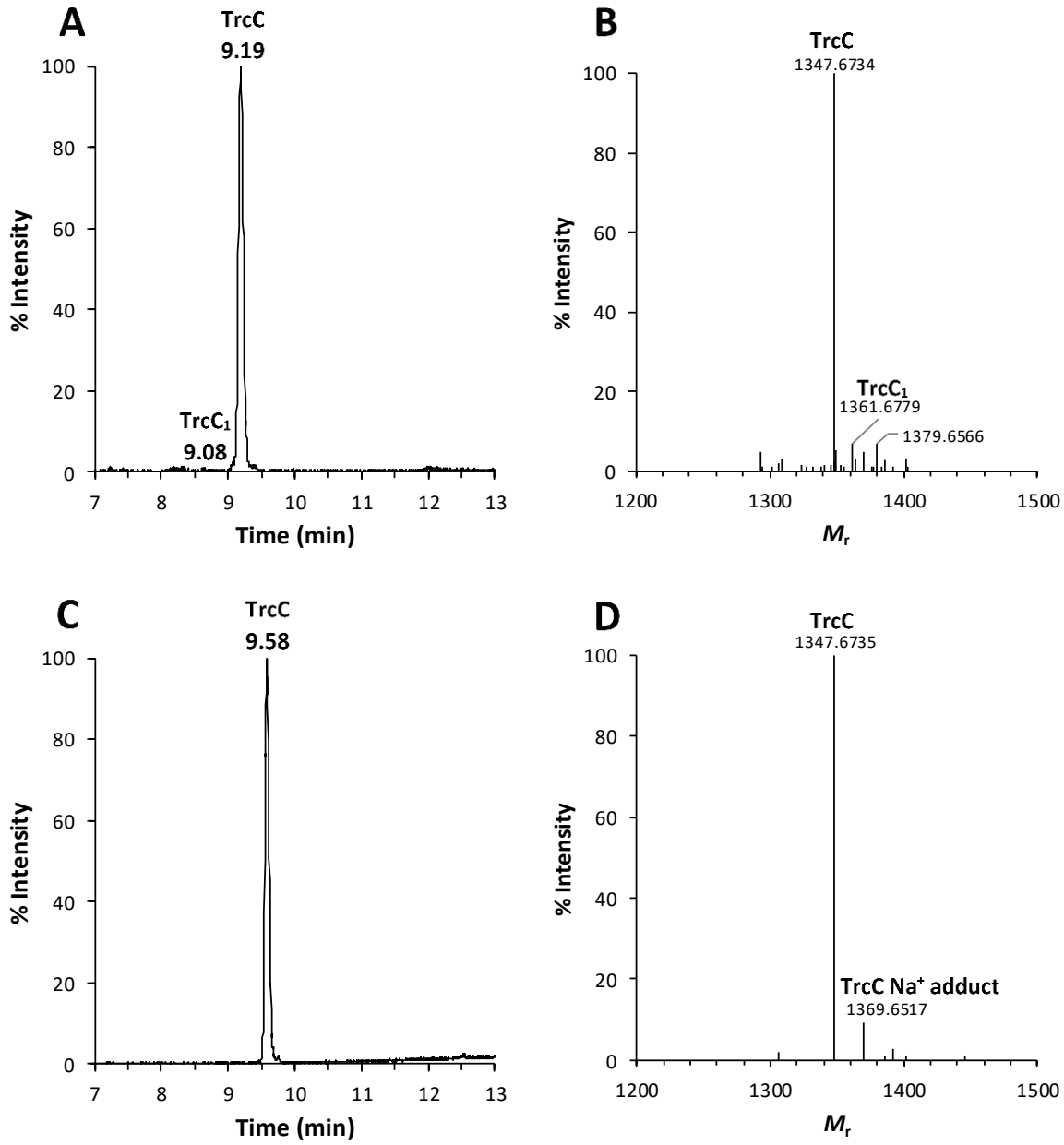

Figure 2.9 The UPLC and ESI-MS analysis of the two preparation of pure TrcC. A) The UPLC chromatogram of the first preparation of purified TrcC (96.4 % pure) (250 µg/mL) showing the retention time in min. B) The ESI-MS spectrum of the first preparation of purified TrcC showing the M_r of the monomeric species and $TrcC_1$ contamination present in the pooled fraction. C) The UPLC chromatogram of the second preparation of purified TrcC (99.5 % pure) (250 µg/mL) showing the retention time in minutes. The retention time of TrcC differs slightly from the first preparation because a newer UPLC column was used. D) The ESI-MS spectrum of the second preparation of purified TrcC showing the M_r of the monomeric species and the Na^+ adduct present in the pooled fraction.

The purification of four peptides was successful and all the peptides were more than 93 % pure. A summary of the peptides purified with the standard C_{18} HPLC protocol from culture and commercial extracts is given in Table 2.11. It is clear from the

Stellenbosch University https://scholar.sun.ac.za

percentage yield of each peptide from extracts that the purification of TrcB is the least time and cost efficient. The separation of TrcB from TrcB' is nearly impossible with C_{18} HPLC column because the two peptides consists of the same amino acid composition and sequence except that the amino acid residues in aromatic dipeptide unit are switched around (Wf to Fw). The inability of the C_{18} HPLC column to separate TrcB' from TrcB is the reason that it is more difficult to purify TrcB than TrcA or TrcC.

Table 2.11 A summary of the selected and purified peptides for the present study. The determined purities and total amount and percentage yield of each peptide from the extract are tabulated.

Peptide	Abbr.	Origen	Purity (%)	Amount (mg)	Yield from extract[c] (%)
Tyrocidine A	TrcA	Phe supplemented crude extract	93.7[a]	8.96	14.0
Tyrocidine B	TrcB	Phe supplemented crude extract	94.0[a]	4.51	7.05
Tyrocidine B	TrcB	Phe supplemented crude extract	95.7[b]	0.90	3.00
Tyrocidine C	TrcC	Commercial Trcmix extract	96.4[a]	3.05	7.63
Tyrocidine C	TrcC	Commercial Trcmix extract	99.5[b]	3.36	13.4
Tryptocidine C	TpcC	Trp supplemented crude extract	94.3[a]	5.54	13.9
Tryptocidine C	TpcC	Trp supplemented crude extract	93.1[b]	5.78	19.3

[a] The purity of the specific peptide achieved with the first preparation.
[b] The purity of the specific peptide achieved with the second preparation.
[c] The % mass yield determined from crude culture extract.

2.4.3 A C_8 HPLC purification method development

The six major tyrocidines found in the tyrothricin complex all differ from each other with only one amino acid residue. Subsequently the isolation of these peptides is difficult from such a complex mixture, especially separating Lys and Orn analogues differing only from each other in CH_2 group, for example TrcA/A_1 and TrcC/C_1, combined with the problem in the group of B-analogues, TrcB/B'/B_1/B_1', where the aromatic dipeptide can be either Wf or Fw. The purification is further complicated by the high propensity of the tyrocidines to form homo- and hetero-oligomers leading to fronting peak shapes as can been seen in Figure 2.2, 2.5 and 2.8. The current purification method consists of RP-HPLC using a C_{18} semi-preparative column and

Stellenbosch University https://scholar.sun.ac.za

the previously described non-linear gradient program which has been optimised by Rautenbach *et al.* [24] and Eyéghé-Bickong [20] for the purification of the tyrocidines and analogues. It was shown by Eyéghé-Bickong [20] by simply adapting the non-linear gradient program did not result in vastly improved peak shapes and separation of $TrcA_1$, $TrcB_1$ and $TrcC_1$ from TrcA, TrcB and TrcC, respectively. However, application of this optimised non-linear gradient program (protocol A, Table 2.4) to an alternative RP-HPLC column could potentially improve the separation of the tyrocidines. Subsequently, Trcmix was subjected to RP-HPLC on an analytical C_{18} and C_8 column while elution was achieved with program A at 35 °C and 25 °C (Figure 2.10 A-C). It is evident from the number of peaks present in the C_8 HPLC chromatogram (Figure 2.10 B) that more tyrocidine peptides (specifically the $TrcB_1$, $TrcB_1$', TrcB and TrcB') were separated to purer fractions than with the C_{18} column (Figure 2.10 A). However, the retention times of the major peaks (TrcC species, TrcB species and TrcA species) were increased with 10 minutes (compare Figure 2.10 A and B) with the C_8 column. The decrease of temperature from 35 °C to 25 °C resulted in a further ±1.0 minute peak retention time increase, however, the peak shapes of the TrcB and TrcA species were slightly improved (Figure 2.10 C). The peak resolution between TrcC and $TrcC_1$, $TrcB_1$ and TrcB, and TrcB and TrcB' produced by the different columns, temperatures and elution programs are summarised in Table 2.12. The C_8 column improved the resolution between TrcC and $TrcC_1$ from 0.5 to 1.19 with elution program A and a column temperature set at 25 °C. The effect of different solvent flow rates and solvent composition on the peak retention times and resolution using the C_8 column at 25 °C was investigated. Program D, which is the combination of a higher flow rate (1.5 mL/min) and a solvent composition of 40 % A to 60 % B, resulted in the lowest peak retention times with

Stellenbosch University https://scholar.sun.ac.za

elution of all peaks before 21 minutes. The resolution between TrcC and $TrcC_1$ was not significantly affected by the alternative solvent ratios (program B) and higher flow rate (program C). However, the combined change (program D) increased the resolution from 1.19 to 1.28. The alternative solvent ratios (program B) and higher flow rate (program C) both increased the resolution of $TrcB_1$ and TrcB significantly (from 0.86 to 0.96 and 1.00, respectively), whereas the combined change (program D) had no marked influence. The resolution between TrcB and TrcB' was not significantly affected by any of the different elution programs (program B-D) with resolution differences of less than 0.05. The total resolution (sum of the resolutions of TrcC and $TrcC_1$, $TrcB_1$ and TrcB, and TrcB and TrcB') was improved most by the combination of higher flow rate and alternative solvent composition (program D), with the higher flow rate contributing the most to this total resolution improvement. Taken together, elution program D produces the best separation and lowest retention times of the major peaks. The purification of the tyrocidines with a C_8 column and elution program D at 25 °C was validated by subjecting both the commercial Trcmix and Phe supplemented crude peptide extract to RP-HPLC (Figure 2.11 A and Figure 2.12 A). The peak resolution of the major peaks of the Phe supplemented crude peptide extract was also determined (Table 2.12). The differences observed in the peak resolution between $TrcC_1$ and TrcC (R_s = 1.63), $TrcB_1$ and TrcB (R_s = 1.39) and TrcB and TrcB' (R_s = 0.32) may be due to the differences in the amounts of the peptides present in the crude peptide extract compared to commercial Trcmix (Table 2.12). The total resolution on the C_8 column for the Phe-supplemented extract was determined as 3.34 which is 0.57 units higher than that of the total resolution determined for Trcmix (Table 2.12). A total of 10 fractions were manually collected

Stellenbosch University https://scholar.sun.ac.za

between 8-21 minutes and 7-28 minutes for commercial Trcmix (Figure 2.11 A) and Phe supplemented crude peptide extract (Figure 2.12*Figure 2.12* A), respectively.

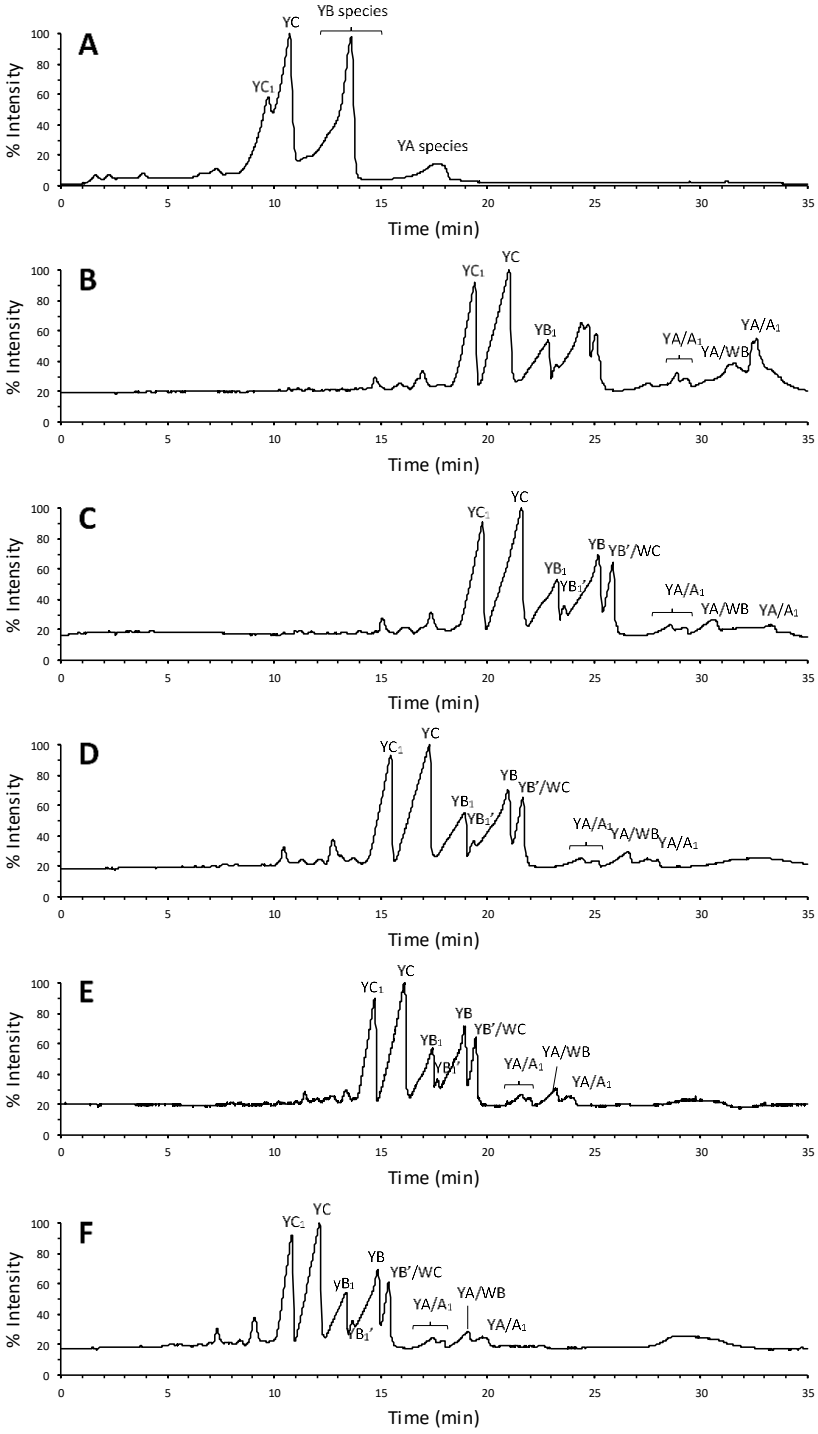

Figure 2.10 The RP-HPLC chromatograms of Trcmix (160 µg) developed on different columns, temperatures and elution programs: A) program A, C_{18} column at 35 °C; B) program A, C_8 column at 35 °C; C) program A, C_8 column at 25 °C. D) HPLC chromatogram achieved with program B, C_8 column at 25 °C; E) program C, C_8 column at 25 °C; F) HPLC chromatogram achieved with program D, C_8 column at 25 °C. For simplicity the letters 'y' and 'w' were used in the place of Trc and Tpc, respectively, to label the peaks, e.g. TrcC labelled as YC and TpcC labelled as wC.

Stellenbosch University https://scholar.sun.ac.za

The UPLC-MS analysis of these fractions collected revealed that all of the major tyrocidines ($TrcC_1$, TrcC, $TrcB_1$, TrcB, $TrcA_1$ and TrcA) were isolated from the commercial Trcmix (Figure 2.11 B), whereas only five ($TrcC_1$, TrcC, $TrcB_1$, TrcB and TrcA) of the six major tyrocidines were isolated from the Phe supplemented crude peptide extract (Figure 2.12 B). The failure to isolate $TrcA_1$ from the Phe supplemented crude extract may be due to the supplementation only promoting increased production of TrcA and not $TrcA_1$. Interestingly, different peptides were isolated in fraction six for Trcmix (isolation of TpcC, Figure 2.11 B) and Phe supplemented crude extract (isolation of TrcB', Figure 2.12 B), even though fraction 6 represents the same RP-HPLC peak collected for both peptide extracts (Figure 2.11 A and Figure 2.12 A)

Table 2.12 A summary of the resolutions achieved with the different elution programs, HPLC columns and temperatures between TrcC and $TrcC_1$, $TrcB_1$ and TrcB, and TrcB and TrcB'.

Program	**HPLC Column**	**Temp. (C°)**	**R_s**			**Total R_s[b]**
			$TrcC_1$ and TrcC	**$TrcB_1$ and TrcB**	**TrcB and TrcB'**	
A	C_{18}	35	0.5	0	0	0.5
A	C_8	35	1.06	-[a]	-[a]	-
A	C_8	25	1.19	0.86	0.47	2.52
B	C_8	25	1.20	0.96	0.42	2.56
C	C_8	25	1.21	1.00	0.44	2.66
D	C_8	25	1.28	1.03	0.46	2.77
D[c]	C_8	25	1.63	1.39	0.32	3.34

[a] Peak shapes prevented R_s determination.
[b] The total resolution is the sum of the resolutions achieved between $TrcC_1$ and TrcC, $TrcB_1$ and TrcB, and TrcB and TrcB'.
[c] Resolution determined from the C_8 HPLC chromatogram produced by elution program D at 25 °C of the tyrocidines present in Phe supplemented crude extract

Stellenbosch University https://scholar.sun.ac.za

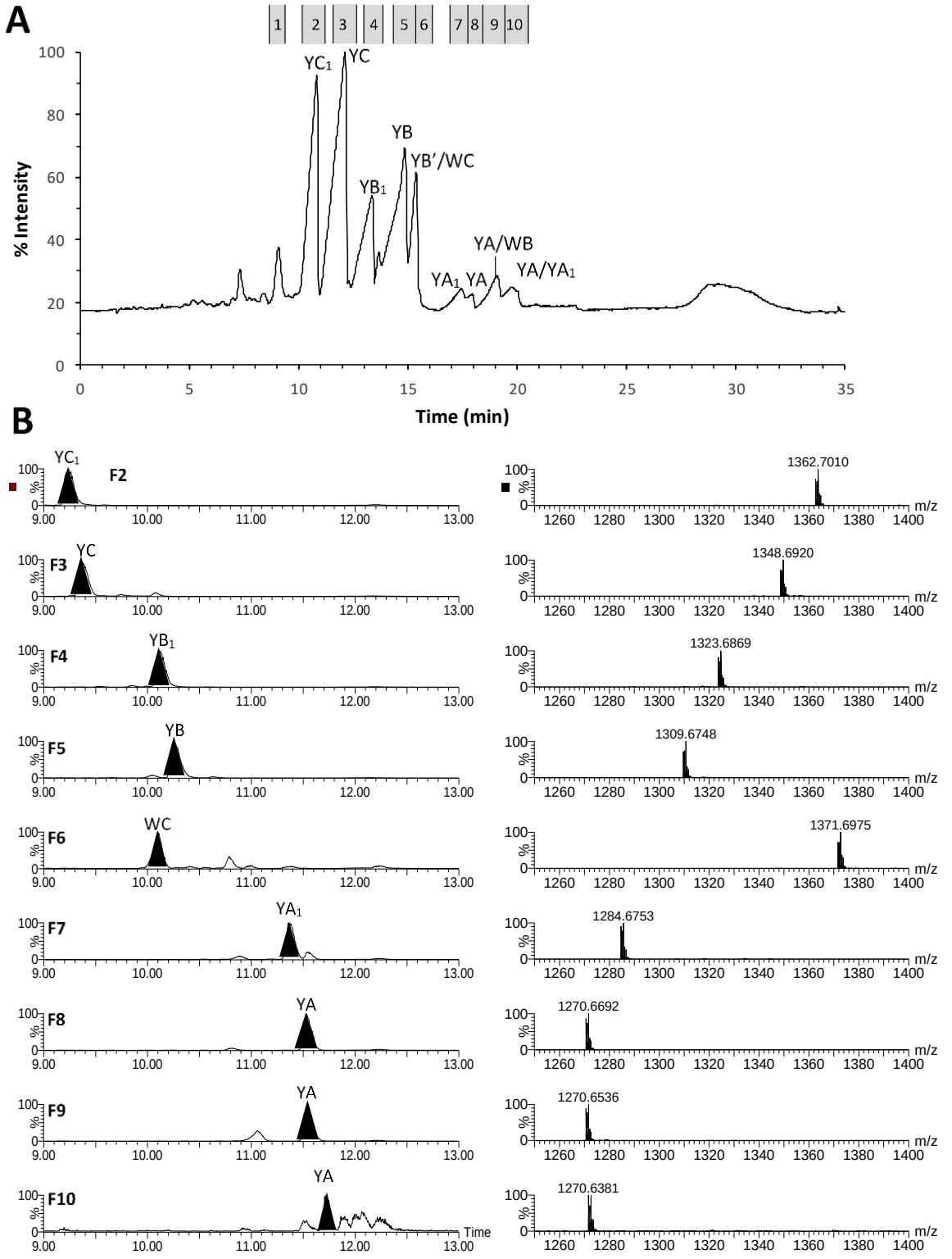

Figure 2.11 The analytical C_8 RP-HPLC chromatogram of the commercial Trcmix extract (160 µg) and UPLC-MS analysis of the fractions (F1-10) collected. A) The analytical C_8 RP-HPLC separation of the major tyrocidines showing the fractions collected above the chromatogram. B) Left: The UPLC chromatogram of each fraction (F1-10) showing the major peaks in black, labelled with the respective peptides. Right: The ESI-MS spectra showing the singly charged monomeric species $[M+H]^+$ of the peptide present in the major peak (in black) of UPLC chromatogram.

Stellenbosch University https://scholar.sun.ac.za

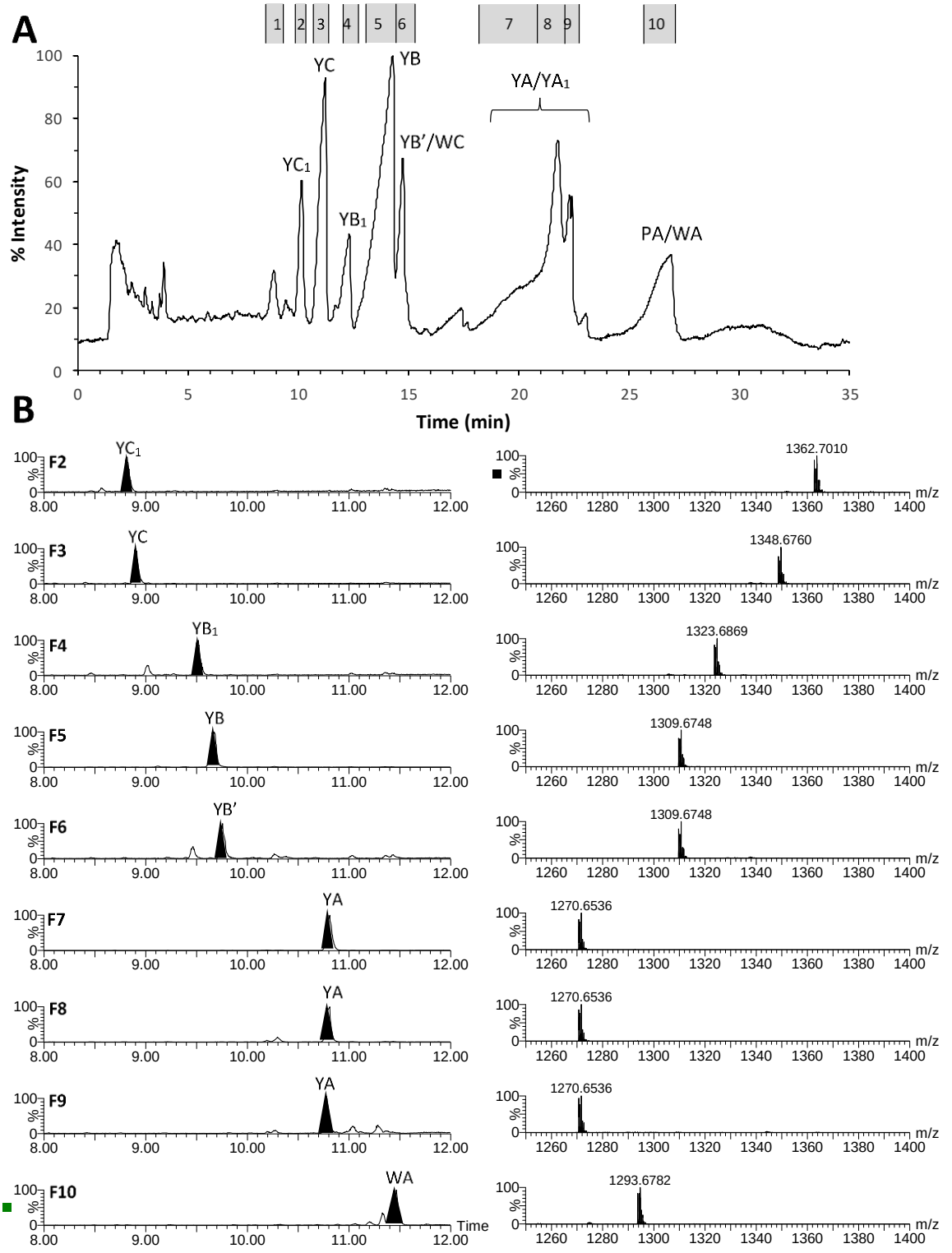

Figure 2.12 The analytical C_8 RP-HPLC chromatogram of the Phe supplemented crude peptide extract (160 µg) and UPLC-MS analysis of the fractions (F1-10) collected. A) The analytical C_8 RP-HPLC separation of the major tyrocidines showing the fractions collected above the chromatogram. B) Left: The UPLC chromatogram of each fraction (F1-10) showing the major peaks in black, labelled with the respective peptides. Right: The enlarged ESI-MS spectra showing the singly charged monomeric species $[M+H]^+$ of the peptide present in the major peak (in black) of UPLC chromatogram.

Stellenbosch University https://scholar.sun.ac.za

A summary the peptides detected in each C_8 HPLC fraction of the commercial Trcmix and Phe supplemented crude peptide extract are given in Table 2.13 and 2.14, respectively.

Table 2.13 Summary of the peptides detected in the C_8 HPLC fractions that were collected from commercial Trcmix. The fraction numbers, peptide identities, retention times, theoretical monoisotopic M_r and high resolution experimental monoisotopic M_r and ppm error are given.

HPLC fraction	Peptide Identity	R_t (min)	Theoretical monoisotopic M_r[a]	Experimental monoisotopic M_r[b]	ppm error in M_r determination
2	$TrcC_1$*	9.24	1361.6921	1361.6788	-9.8
	TpcA	9.57	1292.6706	1292.6351	-27.5
3	TrcC*	9.37	1347.6764	1347.6713	-3.8
	Unknown	9.75	-	1375.6893	-
	$TrcB_1$	10.08	1322.6812	1322.6658	-11.6
4	$TrcC_1$	9.85	1361.6921	1361.6790	-9.6
	PhcA	9.99	1253.6597	1253.6234	-29.0
	$TrcB_1$*	10.12	1322.6812	1322.6654	-11.9
	$PhcA_1$	10.48	1267.6753	1267.6388	-28.8
5	$TpcC_1$	10.05	1384.7080	1384.6898	-13.1
	TrcB*	10.25	1308.6655	1308.6521	-10.2
	unknown	10.64	-	1336.6846	-
6	TpcC*	10.10	1370.6924	1370.6827	-7.1
	TrcB'	10.41	1308.6655	1308.6517	-10.5
	$TrcB_1$	10.79	1322.6812	1322.6676	-10.3
	Unknown	11.00	-	1249.6791	-
	$TrcA_1$	11.38	1283.6703	1283.6591	-8.7
7	$TpcB_1$	10.88	1345.6971	1345.6859	-8.3
	$TrcA_1$*	11.36	1283.6703	1283.6637	-5.1
	TrcA	11.55	1269.6546	1269.6428	-9.3
8	$TpcB_1$	10.82	1345.6971	1345.6860	-8.2
	TrcA*	11.53	1269.6546	1269.6429	-9.2
9	TpcB	11.06	1331.6815	1331.6644	-12.8
	TrcA*	11.55	1269.6546	1269.6412	-10.6
10	TpcB	10.92	1331.6815	1331.6687	-9.6
	TrcA	11.53	1269.6546	1269.6483	-5.0
	Oxidised TrcA*	11.72	1270.6624	1270.6328	-23.3
	Unknown	11.90	-	1297.6825	-
	$TpcA_1$	12.01	1306.6862	1306.6820	-3.2
	$TrcA_1$	12.06	1283.6703	1283.6697	-0.5

[a]The peak retention times as determined from the UPLC chromatograms
[b]Theoretical monoisotopic M*r* calculated as the sum of the molecular weights of amino acid residues of each peptide.
[c]Monoisotopic M_r as determined from the individual ESI-MS spectra.
*The peptide contributing to the major peak in the UPLC chromatogram.

Stellenbosch University https://scholar.sun.ac.za

Astonishingly, 15 of the 19 tyrocidine peptides and analogues were detected (some in very small amounts) with the new optimised C_8 HPLC method (Table 2.13 and 2.14). Most of the high-resolution M_r values had <10 ppm compared to the theoretical value. Only the peptide fractions with very low concentrations exhibited ppm errors of >15 ppm.

Table 2.14 Summary of the peptides detected in the C_8 HPLC fractions that were collected from Phe supplemented crude peptide extract. The fraction numbers, peptide identities, retention times, theoretical monoisotopic M_r and high resolution experimental monoisotopic M_r and ppm error are given.

HPLC fraction	Peptide Identity	R_t (min)	Theoretical monoisotopic M_r[a]	Experimental monoisotopic M_r[b]	ppm error in M_r determination
2	Unknown	8.57	-	1340.6527	-
	$TrcC_1$*	8.81	1361.6921	1361.6805	-8.5
3	Unknown	8.41	-	1351.6731	-
	Unknown	8.80	-	1324.6586	-
	TrcC*	8.90	1347.6764	1347.6713	-3.8
4	Unknown	8.47	-	1354.6658	-
	Unknown	9.02	-	1326.6608	-
	$TrcB_1$*	9.52	1322.6812	1322.6658	-11.6
5	$TpcC_1$	9.38	1384.7080	1384.6898	-13.1
	TrcB*	9.67	1308.6655	1308.6519	-10.4
6	TpcC	9.47	1370.6924	1370.6827	-7.1
	TrcB'*	9.76	1308.6655	1308.6520	-10.3
7	TpcA	10.19	1292.6706	1292.6595	-8.6
	TpcB	10.33	1331.6815	1331.6633	-13.7
	TrcA*	10.81	1269.6546	1269.6400	-11.5
8	TpcA	10.19	1292.6706	1292.6639	-5.2
	TpcB	10.30	1331.6815	1331.6649	-12.5
	TrcA*	10.81	1269.6546	1269.6427	-9.4
9	TpcA	10.19	1292.6706	1292.6566	-10.8
	TpcB	10.27	1331.6815	1331.6687	-9.6
	TrcA*	10.78	1269.6546	1269.6384	-12.8
	Oxidised TrcA	11.04	1270.6624	1270.6328	-23.3
	$TrcA_1$	11.28	1283.6703	1283.6644	-4.6
10	Unknown	10.20	-	1296.6496	-
	PhcA	11.33	1253.6597	1253.6534	-5.0
	TpcA*	11.47	1292.6707	1292.6577	-10.1

[a]The peak retention times as determined from the UPLC chromatograms
[b]Theoretical monoisotopic M*r* calculated as the sum of the molecular weights of amino acid residues of each peptide.
[c]Monoisotopic M_r as determined from the individual ESI-MS spectra.
*The peptide contributing to the major peak in the UPLC chromatogram.

Stellenbosch University https://scholar.sun.ac.za

The four peptides that were not detected are very rare namely TrcAv, $TrcB_1$', TpcB' and $TpcB_1$'. This means that all tyrocidine C analogues were detected and almost all the tyrocidine A analogues were detected, with the rare TrcAv being the only exception. Furthermore, the new optimised C_8 HPLC method allows for the separation of degraded TrcA (oxidised TrcA) from non-degraded TrcA, as determined from the UPLC-MS of HPLC fractions 9 and 10 of Phe supplemented crude extract (Table 2.14) and commercial Trcmix (Table 2.13), respectively. The peptides that were isolated with purities more than 70 % during the validation of the new C_8 HPLC method are summarised in Table 2.15.

From the Trcmix, all the major tyrocidine peptides were isolated with purities more than 70 %. TrcA and $TrcC_1$ and $TrcB_1$ had the highest purities and all were purified to > 90 %. From the Phe supplemented crude peptide extract only five of the six major tyrocidines were purified to > 70 %, however, TpcA was also isolated with a purity of > 70 %. TrcA and TrcB were both purified to >90 %. It is important to note that an entire peak was collected for each of the ten HPLC fractions of both Trcmix and the Phe supplemented crude peptide extract. Therefore, higher purities can be expected if each HPLC peak is fractionated into two or more fractions. This will make it possible to purify all major tyrocidines during the same HPLC run from Trcmix, and to purify five of the major tyrocidines from Phe supplemented crude peptide extract during the same HPLC run. Evidently the new C_8 HPLC protocol has great potential to make the future semi-preparative purification of the tyrocidines and analogues from crude peptide extracts more time and cost efficient, especially TrcB.

Stellenbosch University https://scholar.sun.ac.za

Table 2.15 Summary of the tyrocidines and analogues isolated from both commercial Trcmix and Phe supplemented crude peptide extract (crude) using the optimised C_8 HPLC purification method.

Peptide Identity	**Origen**	**HPLC Fraction**	**UPLC**	**Experimental monoisotopic M_r[a] (Theoretical monoisotopic M_r ppm error)[b]**	**R_t[c] (min)**	**Purity[d] %**
UPLC Column A[e]						
$TrcC_1$	crude	2	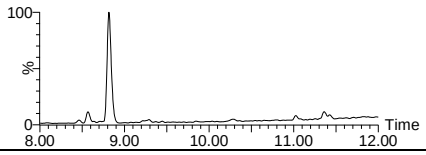	1361.6805 (1361.6921, -8.5)	8.82	85.8
TrcC	crude	3	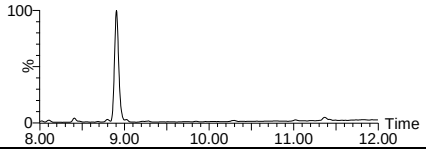	1347.6713 (1347.6764, -3.8)	8.90	85.5
$TrcB_1$	crude	4	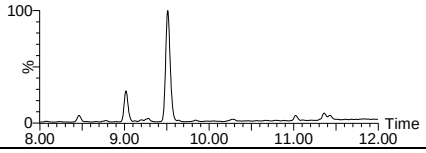	1322.6658 (1322.6812, -11.6)	9.51	72.2
TrcB	crude	5	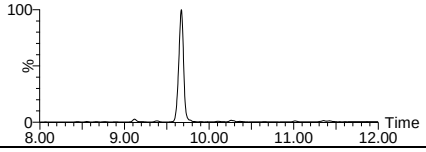	1308.6519 (1308.6655, -10.4)	9.67	93.7
TrcA	crude	7	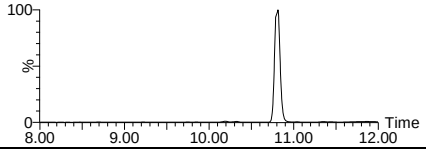	1269.6400 (1269.6546, -11.5)	10.81	95.5
TrcA	crude	8	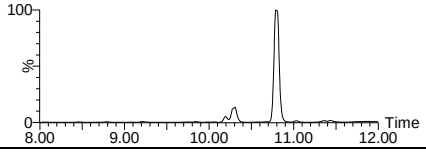	1269.6427 (1269.6546, -9.4)	10.79	83.3
TpcA	crude	10	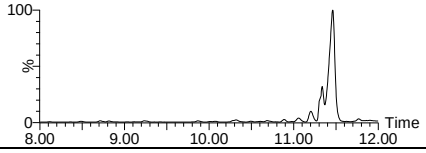	1292.6577 (1292.6707, -10.1)	11.47	72.3
UPLC Column B[e]						
$TrcC_1$	Trcmix	2	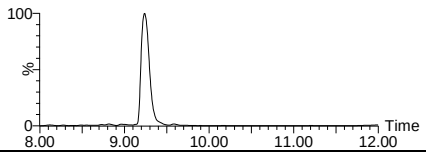	1361.6788 (1361.6921, 9.8)	9.24	90.8

Stellenbosch University https://scholar.sun.ac.za

Peptide Identity	Origen	HPLC Fraction	UPLC	Experimental monoisotopic M_r[a] (Theoretical monoisotopic M_r ppm error)[b]	R_t[c] (min)	Purity[d] %
TrcC	Trcmix	3	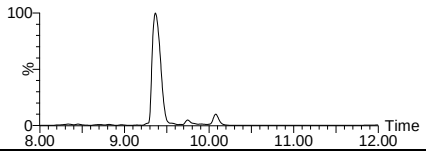	1347.6713 (1347.6764, -3.8)	9.36	84.6
$TrcB_1$	Trcmix	4	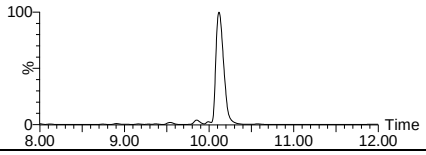	1322.6654 (1322.6812, -11.9)	10.12	90.2
TrcB	Trcmix	5	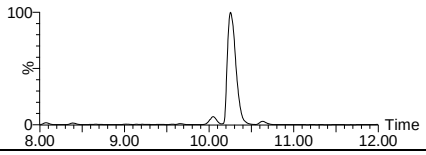	1308.6521 (1308.6655, -10.2)	10.25	88.0
$TrcA_1$	Trcmix	7	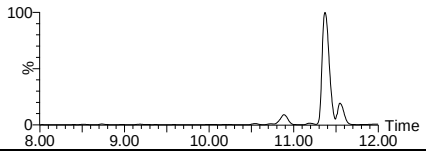	1283.6637 (1283.6703, -5.1)	11.36	74.4
TrcA	Trcmix	8	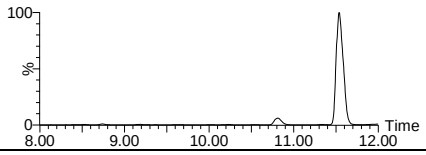	1269.6429 (1269.6546, -9.2)	11.53	91.4

[a]Experimental monoisotopic M_r was determined from UPLC-MS analysis.
[b]The theoretical monoisotopic M_r calculated as the sum of the molecular weights of the amino acid residues of each peptide.
[c]The retention times were determined from the UPLC-MS chromatograms.
[d]The purity of each peptide was calculated from the peak areas of the individual UPLC-MS chromatograms.
[e]Tyrocidines purified from crude or commercial Trcmix and analised using UPLC column A an older column, or B newer column, respectively

Furthermore, TrcC can currently only be purified from the commercial tyrothricin mixture which is not manufactured anymore for commercial use. The discontinuation of commercial tyrothricin mixture poses a problem for the future purification of TrcC. Therefore, it was important to find an alternative way to purify TrcC from crude peptide extract and the new C_8 HPLC protocol resolves this problem.

Stellenbosch University https://scholar.sun.ac.za

2.5 CONCLUSION

The methodologies developed by the BIOPEP group to produce and extract the tyrocidines and analogues proved to be very successful. Supplementation of the *Br. parabrevis* culture broths with Phe and Trp elevated the production of TrcA and TpcC (Figure 2.1 A-F), respectively, which in turn made the purification process more effective. Three peptides, TrcA (Figure 2.3 A-B) , TrcB (Figure 2.4 A-D) and TpcC (Figure 2.6 A-D), were successfully purified from crude *Br. parabrevis* peptide extracts, all having purities of 90 % or higher. Any minor contamination of the pure peptides was due to other tyrocidine peptides.

The removal of the linear gramicidins from commercial tyrothricin with organic extraction was effective. The purity of the subsequent Trcmix was determined as >90 %, with all six major tyrocidines (TrcA, $TrcA_1$, TrcB, $TrcB_1$, TrcC and $TrcC_1$) present (Figure 2.7 A-B). The purification of TrcC was only possible from commercial tyrothricin and a final purity was determined as >90 % (Figure 2.9 A-D). The purities and amount of the peptides isolated, of which biophysical and biological activity will be investigated, are summarised in Table 2.11.

The optimised C_8 HPLC purification method (program D at 25 °C) improved the separation of the tyrocidines (Figure 2.10 A-F). The separation of the $TrcC_1$ and TrcC, $TrcB_1$ and TrcB, and TrcB and TrcB'/TpcC was notable, with increased resolutions from 0.50 to 1.28, 0 to 1.03, and 0 to 0.46, respectively (Table 2.12). All six (TrcA, $TrcA_1$, TrcB, $TrcB_1$, TrcC, and $TrcC_1$) of the major tyrocidines were isolated with the optimised C_8 HPLC purification method (Table 2.15). Purities of 74.4 %, 95.5 %, 90.2 %, 93.7 %, 90.8 % and 85.5 % were achieved for TrcA, $TrcA_1$, TrcB, $TrcB_1$, TrcC, and $TrcC_1$, respectively. This result is significant, considering the

Stellenbosch University https://scholar.sun.ac.za

representative peaks for each peptide were not fractionated and the entire peak was collected in all instances. The lack of a C_8 semi-preparative HPLC column prevented the use of the optimised C_8 HPLC purification method to purify the peptides of interest needed for the subsequent Chapters of the present study. However, because of the success of the purification method developed in this chapter the C_8 HPLC method will be used in the future as the primary method for purification of the tyrocidines and analogues as a C_8 semi-preparative column will be acquired by the BIOPEP Peptide Group.

2.6 REFERENCES

(1) Kontoyiannis, D. P., and Lewis, R. E. (2002) Antifungal drug resistance of pathogenic fungi. *Lancet (London, England) 359*, 1135–44.

(2) Fardel, O., Lecureur, V., and Guillouzo, A. (1996) The P-glycoprotein multidrug transporter. *Gen. Pharmacol. 27*, 1283–1291.

(3) Luqmani, Y. A. (2005) Mechanisms of drug resistance in cancer chemotherapy. *Med. Princ. Pract. 14*, 35–48.

(4) Hoskin, D. W., and Ramamoorthy, A. (2008) Studies on anticancer activities of antimicrobial peptides. *Biochim. Biophys. Acta - Biomembr. 1778*, 357–375.

(5) Hancock, R. E. (2000) Cationic antimicrobial peptides: towards clinical applications. *Expert Opin. Investig. Drugs 9*, 1723–1729.

(6) Shai, Y. (1999) Mechanism of the binding, insertion and destabilization of phospholipid bilayer membranes by α-helical antimicrobial and cell non-selective membrane-lytic peptides. *Biochim. Biophys. Acta - Biomembr. 1462*, 55–70.

(7) Ludtke, S. J., He, K., Heller, W. T., Harroun, T. A., Yang, L., and Huang, H. W. (1996) Membrane pores induced by Magainin. *Biochemistry 35*, 13723–13728.

(8) Gazit, E., Boman, A., Boman, H. G., and Shai, Y. (1995) Interaction of the mammalian antibacterial peptide cecropin PI with phospholipid vesicles. *Biochemistry 34*, 11479–11488.

(9) Ehrenstein, G., and Lecar, H. (1977) Electrically gated ionic channels in lipid bilayers. *Q. Rev. Biophys. 10*, 1–34.

(10) Matsuzaki, K., Murase, O., Fujii, N., and Miyajima, K. (1995) Translocation of a channel-forming antimicrobial peptide, Magainin 2, across lipid bilayers by forming a pore. *Biochemistry 34*, 6521–6526.

(11) Matsuzaki, K., Murase, O., Fujii, N., and Miyajima, K. (1996) An antimicrobial peptide, magainin 2, induced rapid flip-flop of phospholipids coupled with pore formation and peptide translocation. *Biochemistry 35*, 11361–11368.

Stellenbosch University https://scholar.sun.ac.za

(12) Bechinger, B., and Lohner, K. (2006) Detergent-like actions of linear amphipathic cationic antimicrobial peptides. *Biochim. Biophys. Acta - Biomembr. 1758*, 1529–1539.

(13) Kim, S., Kim, S. S., Bang, Y. J., Kim, S. J., and Lee, B. J. (2003) In vitro activities of native and designed peptide antibiotics against drug sensitive and resistant tumor cell lines. *Peptides 24*, 945–953.

(14) Mader, J. S., and Hoskin, D. W. (2006) Cationic antimicrobial peptides as novel cytotoxic agents for cancer treatment. *Expert Opin. Investig. Drugs 15*, 933–946.

(15) Dubos, R. J., and Hotchkiss, R. D. (1941) The production of bactericidal substances by aerobic sporulating Bacilli. *J. Exp. Med. 141*, 155–162.

(16) Dubos, R., and Cattaneo, C. (1939) Studies on a bactericidal agent extracted from a soil Bacillus: III Preparation and activity of a protein-free fraction. *J. Exp. Med. 70*, 249–256.

(17) Tang, X. J., Thibault, P., and Boyd, R. K. (1992) Characterisation of the tyrocidine and gramicidin fractions of the tyrothricin complex from *Bacillus brevis* using liquid chromatography and mass spectrometry. *Int. J. Mass Spectrom. Ion Process. 122*, 153–179.

(18) Ruttenberg, M. A., and Mach, B. (1966) Studies on amino acid substitution in the biosynthesis of the antibiotic polypeptide Tyrocidine. *Biochemistry 5*, 2864–2869.

(19) Vosloo, J. A., Stander, M. A., Leussa, A. N. N., Spathelf, B. M., and Rautenbach, M. (2013) Manipulation of the tyrothricin production profile of *Bacillus aneurinolyticus*. *Microbiol. (United Kingdom) 159*, 2200–2211.

(20) Eyéghé-bickong, H. A. (2011) Role of surfactin from *Bacillus subtilis* in protection against antimicrobial peptides produced by Bacillus species. PhD Thesis, Department of Biochemistry, University of Stellenbosch, http://hdl.handle.net/10019.1/6773.

(21) Vosloo, J. A. (2016) Optimised bacterial production and characterisation of natural antimicrobial peptides with potential application in agriculture. PhD Thesis, Department of Biochemistry, University of Stellenbosch. http://hdl.handle.net/10019.1/98411

(22) Troskie, A. M. (2014) Tyrocidines , cyclic decapeptides produced by soil *bacilli* , as potent inhibitors of fungal pathogens. PhD Thesis, Department of Biochemistry, University of Stellenbosch http://hdl.handle.net/ 10019.1/86162.

(23) Spathelf, B. M. (2010) Qualitative structure-actvity relationships of the major tyrocidines, cyclic decapeptides from *Bacillus aneurinolyticus*. PhD Thesis, Department of Biochemistry, University of Stellenbosch, http://scholar.sun.ac.za/handle/10019.1/4001.

(24) Rautenbach, M., Vlok, N. M., Stander, M., and Hoppe, H. C. (2007) Inhibition of malaria parasite blood stages by tyrocidines, membrane-active cyclic peptide antibiotics from *Bacillus brevis*. *Biochim. Biophys. Acta - Biomembr. 1768*, 1488–1497.

(25) Sneyder, L. R., Kirkland, J. J., and Glajch, J. L. (1992) Practical HPLC method development 2nd ed. Wiley, New York.

Stellenbosch University https://scholar.sun.ac.za

Chapter 3

THE INFLUENCE OF FORMULANTS ON THE BIOPHYSICAL CHARACTER OF THE TYROCIDINES AND ANALOGUES

3.1 INTRODUCTION

The rise of MDR towards chemotherapeutic drugs has forced researchers to find and develop new chemotherapeutic drugs for the treatment of cancer[1, 2]. The decreased risk of resistance development observed towards antimicrobial peptides due to their rapid membranolytic activity has sparked a lot of interest in these peptides[1, 3]. To investigate the factors that modulate the bioactivity of peptides, it is necessary to gain insight into their chemical character and behaviour in different formulations and solvents. The amino acid sequence and side chains in the primary structure of the cyclic cationic decapeptides from tyrothricin dictates their conformation and amphipathicity, which in turn influences their self-assembly in oligomers and larger polymeric structures [4-9]. In addition, the chemical environment (polarity/ionic strength of solvent or the presence of other biomolecules) also influences the secondary structure and/or self-assembly of cyclic decapeptides [4, 5, 10, 11]. The X-ray crystallography and nuclear magnetic resonance spectroscopy revealed that TrcA and TrcC monomers adopt an amphipathic type I β-turn and type II β-turn/β-pleated sheet which is stabilised by four intramolecular hydrogen bonds[12-16]. These peptides have been shown to induce ion conducting pores in model membranes which is directly implicated in the antimicrobial activity of the tyrocidines [17]. Furthermore, the dimers of TrcA and TrcC in an aqueous environment are hypothesised to be the antimicrobial moieties and is the proposed membrane active conformation of the tyrocidines and analogues [12, 13]. On the other hand, overt aggregation/oligomerisation at Trc concentrations >100 μM have been observed [4-9]

Stellenbosch University https://scholar.sun.ac.za

and such preparations have been found to be less active against a variety of microbes by our group (unpublished data). We observed good indications that there is a relationship between the state of oligomerisation/self-assembly structures and the bioactivity of the tyrocidines and analogues. Although the Trcs have potential as a chemotherapeutic lead for drug development, major drawbacks exist due to their haemolytic and cytotoxic activity[18-20]. Extensive research has been done on the formulation of AMP's with different lipid-based molecules with the aim to improve stability, delivery and to decrease the toxicity of the peptides [21, 22]. Refer to Chapter 1 for more detail on peptide formulations.

Many toxic compounds have been successfully formulated, for example the nephrotoxicity of Amphotericin B (AmB), a last resort antifungal drug, is significantly reduced when formulated with detergent-based (sodium deoxycholate, DOC) and lipid-based (cholesterol sulphate, CS) nanocarriers [23]. These nanocarriers ensure effective transport of the drug to target sites, thereby reducing levels of free AmB in the blood and minimising toxicity of AmB [23].

In this chapter, four cyclodecapeptides of interest (TrcA, TrcB, TrcC and TpcC) were formulated with three lipid-based molecules, cholesterol sulphate (CS), lyso-phosphatidylcholine (LPC) and palmitic acid (C16), with the aim to improve stability and reduce toxicity of the peptides while retaining their bioactivity. The investigation on oligomerisation and biophysical properties of the four peptides, alone and in formulation with CS, LPC and C16, are reported in this chapter. The four cyclodecapeptides share a highly conserved primary structure (cyclo(D-Phe^{1}-L-Pro^{2}-L-X^{3}-D-X^{4}-L-Asn^{5}-L-Gln^{6}-L-X^{7}-L-Val^{8}-L-Orn^{9}-L-Leu^{10}) with four amino acid residue variations (denoted by X in sequence) [24]. Variation at position three and four, known as the aromatic dipeptide unit, gives rise to the A (consisting of L-Phe^{3}-D-Phe^{4}), B

Stellenbosch University https://scholar.sun.ac.za

(consisting of L-Trp^3-D-Phe^4) and C (consisting of L-Trp^3-D-Trp^4) analogues [24]. Whereas, variation at position seven gives rise to the tyrocidines (L-Tyr^7), phenycidines (L-Phe^7) and tryptocidines (L-Trp^7) [25]. It has been shown that the variation in peptide sequence, especially at the aromatic dipeptide unit (L-X^3, D-X^4), plays a very important role in the structure-activity relationship of the tyrocidines [26, 27]. Therefore, the interactions of the different formulants with the dipeptide unit is of interest.

Circular dichroism, ion-mobility spectrometry linked to mass spectrometry (IM-MS) and fluorescence spectroscopy (FS) are established techniques to decipher the factors implicated in the oligomerisation and interactions of biomolecules [28-34]. Unfortunately, the formulation of the peptides with CS and C16 results in opaque solutions which prevents the use of CD for the investigation of oligomerisation of the Trcs and TpcC in this study. However, both IM-MS and FS are suitable to analyse solutions of opaque nature. IM-MS is a highly sensitive gas phase separation technique that allows the separation of ionic species with the same or similar mass or *m/z* ratio based on differences in their collision cross-sections (CCS), shape or conformation and charged states by monitoring the mobility of an ion through an opposing gaseous flow in the presence of a weak electrical field [35]. This technique can be applied to analyse the size and shape a wide variety of molecules and mixtures which include pharmaceutical compounds [36, 32], polymers [37, 38], metabolites [39], carbohydrates [40], phospholipids [41], proteins [30, 42] and peptides [28, 29]. As analysis in ESI-MS mode leads to the removal of all water and solvent molecules, the hydrophobic effect is diminished and polar interactions (eg. hydrogen bonds, dipolar interactions and ionic interactions) will be enhanced [43-45]. With the high temperatures, sheering and collisional forces and the high potential in the

Stellenbosch University https://scholar.sun.ac.za

instrument, only the most stable non-covalent complexes and oligomers will be stable in the mass spectrometer [43-47]. Munyuki *et al*. [12] and our group [48-51] illustrated that the dimers and larger oligomers of the Trcs and TpcC are stable during ESI-MS. Therefore, IM-MS will be used to determine the proportions of ionic species (monomers, dimers and larger oligomers) present in each of the four cyclodecapeptides alone and in formulation.

To complement the results of the IM-MS, fluorescence emission maxima and quantum yield will be utilised to further elucidate the conformations and intra- and intermolecular interactions of the Trcs alone and in formulation. The three amino acids that are responsible for the intrinsic fluorescence of the Trcs are phenylalanine (Phe, F), tyrosine (Tyr, Y) and tryptophan (Trp, W)[33, 34]. Phe absorbs at the shortest wavelength (λ_{ex} = 256 nm) of the three fluorescent amino acids and has a highly structured emission spectrum with a maximum at 282 nm [33]. The general wavelength chosen for peptide/protein fluorescence is at 280 nm or higher which excludes the excitation wavelength of phenylalanine. Therefore, Phe fluorescence is usually disregarded during fluorescence studies of peptides/proteins [33, 34]. The most extensively used intrinsic fluorophores are Tyr (λ_{ex} = 276 nm) and Trp (λ_{ex} = 282 nm) which are both excited at a wavelength of 280 nm and emits at wavelengths with maxima at 303 nm and 357 nm, respectively [52-56]. Tyr has a low extinction coefficient and is less sensitive to solvent polarity compared to Trp and therefore the emission of Trp dominates that of Tyr [3334]. Furthermore, the fluorescence of Tyr and Phe is complicated when a peptide contains all three of the intrinsic fluorophores due to resonance energy transfer (RET) from Tyr or/and Phe (photon donors) to Trp (photon acceptor) residues in the same peptide[33, 57]. RET can only occur when there is an overlap of donor emission spectrum and acceptor absorption spectrum [57]. The

Stellenbosch University https://scholar.sun.ac.za

indole group of Trp is highly sensitive to the chemical nature (polarity/hydrophobicity) of the local environment with occurrence of a spectral shift of emission maximum towards a lower wavelength (blue shift or hypsochromic shift) or higher wavelength (red shift or bathochromic shift) when located in a more nonpolar or polar environment, respectively[33, 34, 54, 58]. These spectral shifts are due to interaction of the solvent with the indole group via hydrogen bonding and general solvent effects [33]. Another indication of changes in peptide aggregation, conformation or interactions is the total fluorescence quantum yields of Tyr and Trp. The fluorescence quantum yields of Tyr and Trp can be decreased (quenched) or increased (de-quenched) via different molecular mechanisms such as collisional quenching in an aqueous environment, ground-state complex formation and excited state reactions with local polar groups[33, 54, 58].

3.2 RESEARCH MATERIALS

The cholesterol sulphate (CS), palmitic acid (C16), commercial tyrothricin extract, and methanol (MeOH) were supplied by Sigma-Aldrich (St Louis, USA). Avanti® polar lipids (Alabama, USA) supplied the soy lyso-phosphatidyl choline (LPC). Acetonitrile (ACN, HPLC-grade, far UV cut-off) was purchased from Romil Ltd (Cambridge, United Kingdom) and ethanol (EtOH) was obtained from Merck (Darmstadt, Germany). Analytical grade water was prepared by filtering water from a reverse osmosis plant through a Millipore-Q® water purification system (Milford, USA). The nitrogen (N_2) gas was purchased from AFROX (Johannesburg, South Africa). The 96-well black flat bottom plates were supplied by Thermo Fisher Scientific (Denmark).

Stellenbosch University https://scholar.sun.ac.za

3.3 METHODS

3.3.1 The preparation of peptide formulations

The pure peptides (TrcA, TrcB, TrcC and TpcC) and formulants (CS, LPC and C16) were suspended in 90 % MeOH in water (*v/v*) to concentrations of 1.00 mM. Equimolar amounts of the peptide and the formulant were added together to produce 15 different peptide formulations (Table 3.1). Subsequently, the 90 % MeOH in water (*v/v*) was evaporated under N_2 gas flow. The dried formulations were stored at room temperature until used. It is important to note that only pyrolised glassware and ultra-high purity solvents were utilised in the preparation of the peptides and formulations. This is a necessary measure to limit the influence of residual contaminants such as detergents and pyrogens on the formulation and on the activity of the peptides and their formulations.

Table 3.1 A summary of the peptide formulations that were prepared with cholesterol sulphate (CS), lyso-phosphatidyl choline (LPC) and palmitic acid (C16).

Peptide	**Formulations in 1:1 molar ratio**		
	CS	LPC	C16
TrcA	TrcA:CS	TrcA:LPC	TrcA:C16
TrcB	TrcB:CS	TrcB:LPC	TrcB:C16
TrcC	TrcC:CS	TrcC:LPC	TrcC:C16
TpcC	TpcC:CS	TpcC:LPC	TpcC:C16
Trcmix	Trcmix:CS	Trcmix:LPC	Trcmix:C16

3.3.2 Scanning electron microscopy

The dried pure TpcC were dissolved at 1.00 mg/mL in 50 % EtOH in water *(v/v)* or 500 µM in 15 % EtOH in water (*v/v*). The dried peptide formulations were diluted to 500 µM peptide concentration in analytical grade water. Dissolved samples were sonicated for 1-2 minutes and incubated at room temperature for at least one hour before 5 µL aliquots were dried under vacuum at room temperature on cleaved

Stellenbosch University https://scholar.sun.ac.za

muscovite mica surfaces. Prior to imaging, the samples were mounted on aluminium stubs with double sided carbon tape followed by coating with a layer of gold (± 10 nm thickness). The scanning electron microscope images of the TpcC (1.00 mg/mL) in 50 % EtOH in water (*v/v)* and CS and LPC formulations (500 μM, 15 % EtOH in water (*v/*v)) were recorded by Jai Singh at the Sophisticated Instrument Centre (SIC) at the Dr. Harisingh Gour University in Sagar, India. The images were recorded in high vacuum mode using high resolution scanning electron microscope dual beam system (NOVA 450 NANOLAB, FEI) operating at a working distance (WD) of 4.9 to 5.8 mm and 20 kV.

The scanning electron microscope images of the TpcC (500 μM) in 15 % EtOH in water (*v/*) and C16 formulations (500 μM, 15 % EtOH in water (*v/v*)) were recorded with the assistance of senior analyst Madelaine Frazenburg at the University of Stellenbosch Central Analytical Facilities (CAF). The images were recorded in high vacuum mode using Zeiss MERLIN field emission scanning electron microscope operating at a working distance (WD) of 4.5 to 4.6 mm and 1 to 3 kV. The WD and voltage used to capture each SEM image of the samples are given at the bottom of each image in the results section.

3.3.3 Travelling wave ion mobility mass spectrometric analysis

Pure peptides and the peptide formulations were resuspended in 1.5 % EtOH in water (*v/v*) and analytical grade water to concentration of 50 μM. A doubling dilution series of each pure peptide solution was prepared. The samples were subsequently centrifuged at 10 600 *xg* for 10 minutes to remove any particulate material. Volumes of 3 μL of the samples were injected into the electrospray ionisation mass spectrometry (ESI-MS) system via a Waters Acquity® UPLC allowing direct infusion at a flow rate of 0.3 mL/min. The ESI-MS solvent that was used was 0.1 % formic

Stellenbosch University https://scholar.sun.ac.za

acid in 60 % ACN in water (*v/v/v*). The source temperature and cone voltage were set at 120 °C and 15 V, respectively. The ESI-MS system consisted of a Waters Synapt G2 quadrupole time-of-flight (Q-TOF) mass spectrometer equipped with a Z-spray electrospray ionisation source and a photo diode array detector. The ion mobility spectrometry linked ESMS (IM-MS) analysis was achieved by enabling the traveling-wave ion mobility cell in the ESI-MS system. The travelling wave ion mobility experimental parameters were set as follows: Extraction cone at 4V, Helium cell gas flow at 180 mL/min, ion mobility buffer (N_2) gas at 90 mL/min, trap collision energy at 15 V, trapping release period of 200 µs, mobility trap and extract height at 15 and 0 V, respectively, wave height ramp (100 %) from 8 to 20 V, wave height linear velocity ramp (20 %) from 1000 to 650 m/s at 200 m/s. Poly-Alanine (Poly-Ala) was used as the calibration standard to calibrate to travelling wave ion mobility cell's drift time. Data was collected in positive mode scanning from 350-2000 (*m/z*) at a rate of 0.2 scans per second. Waters MassLynx V4.1 software (Milford, USA) and Driftscope v2.9 software (Milford, MA, USA) were used for the data analysis. The calibration curve used for the collision cross-section (CCS) calculations were constructed as described by Michaelevski *et al*. [30] and Rautenbach *et al.*[29]. The CCS calculation for each of the peptides were determined as described by Ruotolo *et al*. [28]. Total signal for each molecular ion in the TWIM-MS profile were used to compare the contribution of monomers and dimers in a peptide preparation and formulation. The $[M+H]^+$ contribution to the total signal of TrcC and TpcC was corrected from the ratio between $[M+H]^+$ and $[M+2H]^{2+}$ using the signals in the resolved direct injection (determined in the same run), as the $[M+H]^+$ signal not fully resolved in their TWIM-MS profile. Dr. Marietjie Stander at the Central Analytical Facility (CAF) of the

Stellenbosch University https://scholar.sun.ac.za

University of Stellenbosch assisted with the setup and running of the IM-MS analyses on the Synapt G2.

3.3.4 Fluorescence spectroscopy

The pure peptide aliquots were prepared as previously described in 15 % EtOH (*v/v*) in water to final concentrations of 50 µM. Similarly, the dried peptide formulations were resuspended in water to concentrations of 50 µM. Doubling dilution series of the peptide solutions and peptide formulation solutions were prepared in triplicate in black 96 well microtiter plates. The fluorescence was performed on a Varioskan 3.01.15 instrument and data collected with SkanIT Software 2.4.3. Excitation was performed at 280 nm and emission collected from 300 nm to 400 nm at 10 ms intervals. All data was analysed with Graphpad Prism® V 5.0.

3.4 RESULTS AND DISCUSSION

The aim of this study is to formulate and reduce the toxic effects of the Trcs [19] on normal healthy cells of humans and drug formulations is one of the strategies employed to achieve this aim by acting as a carrier system for the drug to the target cells [21].

3.4.1 Scanning electron microscopy of TpcC and formulations

It is well established that peptides undergo self-assembly which is described as a spontaneous organisation of individual molecules into ordered structures (such as nanofibers, nanotubes and nanovesicles) by means of weak non-covalent interactions [59-61]. These non-covalent interactions may include hydrogen bonds, ionic, hydrophobic and van der Waals interactions [59]. Scanning electron microscopy (SEM) is widely used to visualise the self-assembly of compounds [62] and was utilised to investigate the self-assembly and formulation with CS, LPC and C16 of

Stellenbosch University https://scholar.sun.ac.za

one of the peptides, TpcC, in this study. TpcC was chosen because it is a Trp-rich peptide as it contains L-Trp^{7}and the aromatic dipeptide unit consisting of L-Trp^{3}-D-Trp^{4} [24]. Therefore, the role the Trp residues play in the self-assembly/aggregation of the TpcC alone and in formulation can be elucidated. The SEM analysis revealed that TpcC (1.00 mg/mL) form well-defined spheres of different sizes (159 nm to 349 nm in diameter with high dispersity) when dissolved in 50 % ethanol and allowed to self-assemble while slow drying under vacuum (Figure 3.1 A). The preparation procedure seems to influence the size of the nano-spheres, in particular the rate of drying, initial concentration and type and percentage of organic solvent. Under conditions in which 500 μM TpcC in 15 % EtOH:water (*v/v*) was dried under vacuum, uniform TpcC spheres of 13 nm to 25 nm were obtained with a few larger spheres of 63 nm to 88 nm (Figure 3.1 B and D). These larger spheres consisted of multiple smaller uniform spheres in a quasicrystal (Insert in Figure 3.1 B). It is evident that the TpcC, containing three Trp residues, easily forms large spherical quasicrystals.

The LPC had a notable effect on the self-assembly of TpcC into large spherical structures showing disruption/prevention of these well-defined nano-assemblies (Figure 3.1 C). This is reasonable because phospholipids such as lysoPC have been shown to have detergent like actions and is a well-known agent used to solubilise membranes [63, 64]. Therefore, LPC probably act as a detergent on the spheres formed by the Trcs and may prevent and retard the formation of ordered structures. However, some spherical structures were still observed, and the preparation showed polydispersity, which could be related to the preparation of the formulation and will need further optimisation in future studies.

The CS formulation had a similar effect to that of LPC, leading to disruption of the spherical nano-assemblies (Figure 3.1 E). However, although fewer well-defined

Stellenbosch University https://scholar.sun.ac.za

nano-structures were observed, significantly larger spheres were observed in the TpcC:CS formulation, with sphere sizes of between 94 nm and 133 nm (Figure 3.1 E). It is possible that some of the structures are maintained and CS could lead to merging of some of the smaller spherical structures into larger assemblies (Figure 3.1 E). This could likely be due to both electrostatic interactions between the cationic L-Orn^{9} residue and the negative charge on sulfoxide of CS, and hydrophobic interaction between the highly non-polar groups CS (carbon rings and aliphatic tail) and the Trp residues of TpcC. Faure *et al.* [65] have shown that the hydration of dimyristoylphosphatidylcholine (DMPC) membranes incorporated with CS increases compared to DMPC membranes incorporated with cholesterol, which is likely due to more hydrogen binding sites on the sulphate group of CS. Therefore, it is possible that the sulphate group of CS orientates to the aqueous environment to form hydrogen bonds with water molecules and/or interacts with the L-Orn^{9} residues, whereas the non-polar carbon ring/carbon tail end of CS associates with the peptides thereby shielding them from the aqueous environment.

Stellenbosch University https://scholar.sun.ac.za

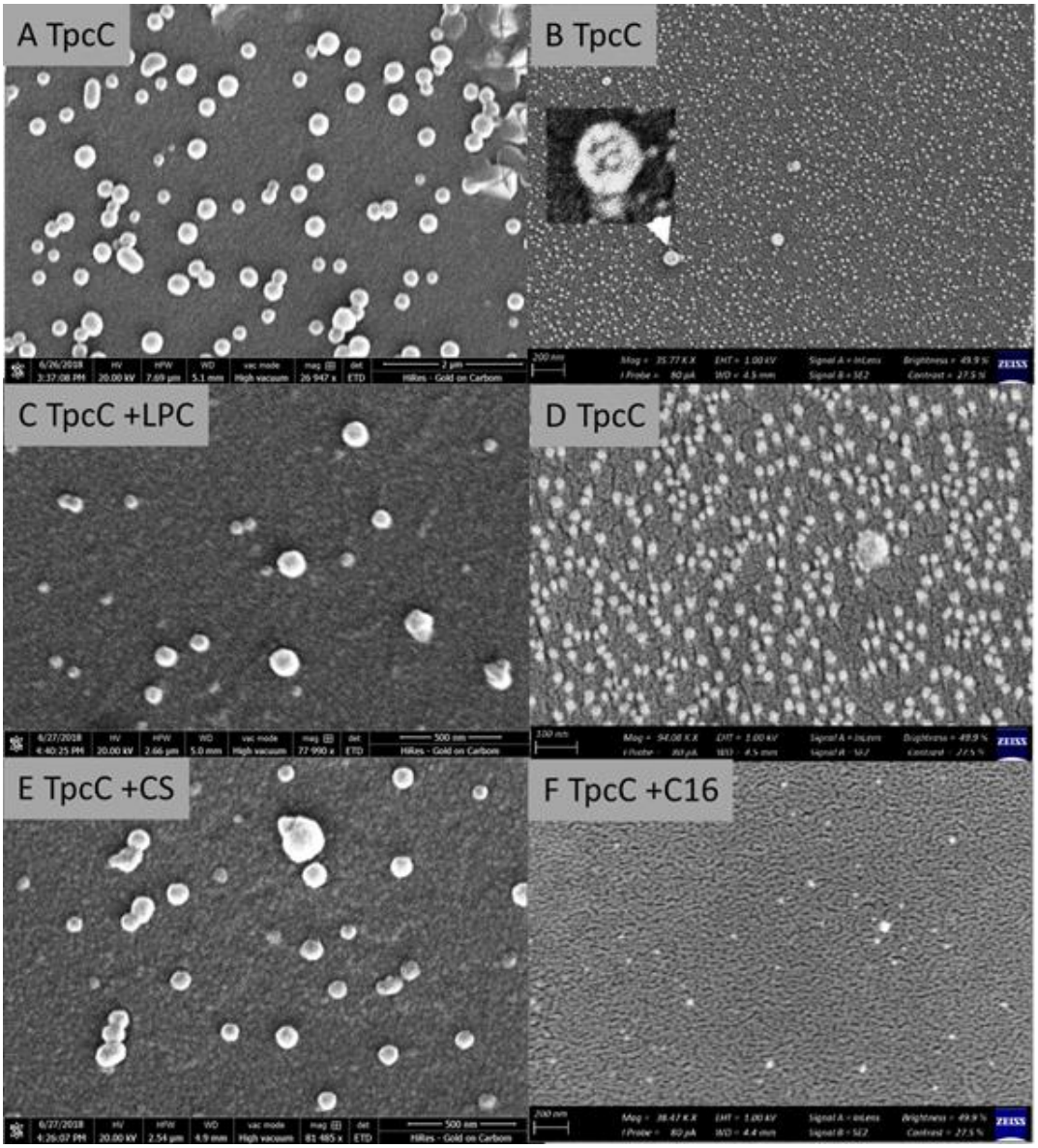

Figure 3.1 The scanning electron microscope micrographs of TpcC alone and in formulation with CS, LPC and C16. A) SEM micrograph of TpcC (1.00 mg/mL) in 50 % EtOH in water (*v/v*). B) and D) SEM micrograph of TpcC (500 µM) in 15 % EtOH (*v/v*) in water. C) SEM micrograph of TpcC:LPC (500 µM) in water. E) SEM micrograph of TpcC:CS (500 µM) in in water (*v/v*). F) SEM micrograph of TpcC:C16 (500 µM) in water. The micrographs in A, C and E were recorded on a NOVA 450 NANOLAB dual beam SEM and those in B, D and F, with a Zeiss MERLIN field emission SEM.

Aggregation of nearby spherical structures was observed (Figure 3.1 E) which confirmed some self-assembly into larger ordered structures of the CS formulated peptides. This polydispersity may also be the result of preparation of the formulation and will need further optimisation in future studies. In contrast to the results observed for CS and LPC formulations, the TpcC:C16 led to almost complete disruption of the

Stellenbosch University https://scholar.sun.ac.za

TpcC nano-spheres (Figure 3.1 F). The disruption of the nano-structures indicates that the C16 probably has a more pronounced detergent effect than CS and LPC. The reduction of the larger nano-assemblies and the smaller spheres of the TpcC by C16 is probably due to the formation of small micellular structures between TpcC and C16.

Taken together, each of the formulants have different influences on the self-assembly of the cyclodecapeptides as interpreted from the size and shape of spheres formed. The formation and disruption of the cyclodecapeptide nano-structures would be dictated, for the most part, by the chemical properties of each of the formulants and the peptide character in the formulation. Future studies will focus on the optimisation of peptide formulation and preparation, as well as including more Trc analogues to assess the role of primary structure in the formation and disruption of nano-structures.

3.4.2 TWIM-MS of the peptides and formulations

Conventional ion mobility spectrometry (IMS) has become a popular method used to rapidly analyse the structures and conformations of a wide variety of molecules [28, 29, 32, 36, 38-42]. IMS is a gas-phase separation technique that separates ions based on structure and size by measuring the time (drift time) it takes an ion to travel through a pressurised tube (drift tube) filled with an inert gas under the influence of a weak uniform electrical field. Larger ions will traverse the drift cell at a slower speed than smaller ions due to the greater number of collisions experienced with the opposing buffer gas which correlates directly with the collisional cross-sections (CCS) and that shape of the molecular ions [41, 42]. IMS can also be coupled to MS (IM-MS) which enables further separation of heterogenous mixtures with similar masses or mass to charge ratios according to differences in their drift times and CCS values [66]. An

Stellenbosch University https://scholar.sun.ac.za

alternative to the conventional IMS techniques is the traveling wave ion mobility spectrometry linked to mass spectrometry (TWIM-MS) where electrical wave pulses are applied rather than a uniform electrical field [35, 67]. In TWIM-MS systems the CCS areas are determined from a calibration curve obtained from the drift times and CCS values (as determined from conventional IMS experiments) of a suitable internal calibrant, whereas the drift time values are directly related to CCS areas in conventional IMS systems[35, 67]. In this study the Trcs were analysed using a TWIM-MS system and poly-alanine (poly-Ala) was used as an internal calibrant in order to obtain a calibration curve from which the CCS areas of the Trcs were calculated. The drift times (t_D) of poly-Ala were determined under exactly the same TWIM-MS instrument conditions (N_2 gas as buffer) used for the Trcs and the CCS areas (Ω) of poly-Ala were obtained from literature [68]. The standard curve was obtained by correcting the drift times (t_D') and CCS areas (Ω') of poly-Ala using Equations 3.1 and 3.2 and subsequently plotting lnΩ' against lnt_D'[30]. The t_D' and Ω' equations are as follows:

$$t_D' = t_D - \frac{c\sqrt{\frac{m}{z}}}{1000} \quad 3.1$$

Where t_D is the observed poly-Ala drift time in milliseconds (ms), *m/z* is the mass to charge ratio of the poly-Ala ion observed and c is the Enhanced Duty Cycle (EDC) delay coefficient which is an instrument dependent parameter [30].

$$\Omega' = \frac{\Omega}{z\sqrt{\frac{1}{m} + \frac{1}{M_G}}} \quad 3.2$$

Where Ω is the literature CCS area of the observed poly-Ala ion, z is the ion charge, m is the molecular weight of observed poly-Ala ion, and M_G is the molecular mass of N_2 gas [30].

Stellenbosch University https://scholar.sun.ac.za

A linear trendline was fitted to the lnΩ' versus lnt_D' plot (Figure 3.2) and the slope (X) which represent the exponential proportion factor and the fit-determined constant (A) was extracted from the linear fit equation ($ln(\Omega') = Xln(t'_D) + A$) (Figure 3.2).

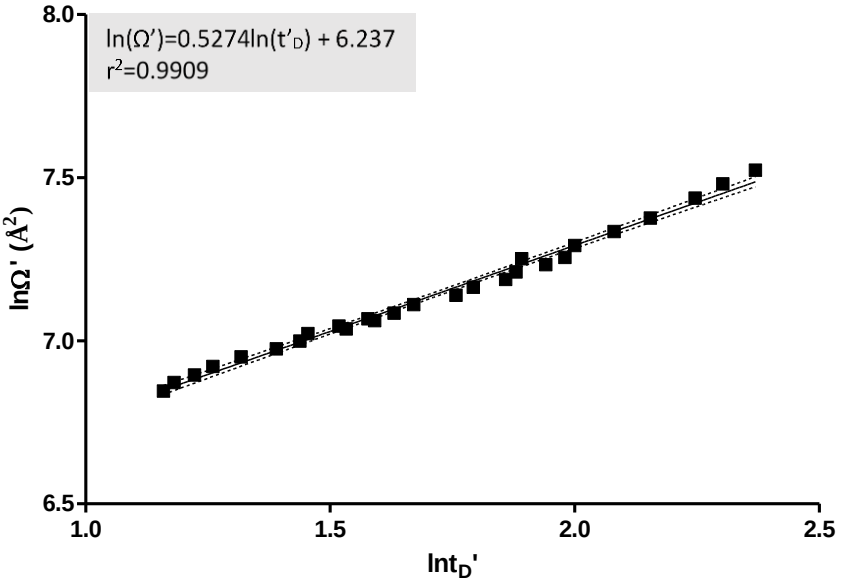

Figure 3.2 The corrected CCS areas versus corrected drift time values of internal calibrant poly-Ala from which the exponential proportion factor (slope) and fit-determined constant was extracted. The equation of the linear fit and correlation coefficient (r^2) are shown on the graph. The dotted lines indicate the 95 % confidence interval.

The exponential proportion factor(X) was used to determine the doubly corrected drift times (t"$_D$) of the poly-Ala ions using the following equation [30]:

$$t"_D = zt'_D{}^X \sqrt{\frac{1}{m} + \frac{1}{M_G}} \qquad 3.3$$

Subsequently, the calibration curve was constructed by plotting literature CCS values of poly-Ala against t"$_D$ (Figure 3.3). The CCS values of the individual Trcs (TrcA, TrcB, TrcC and TpcC) were determined from the poly-Ala calibration curve (Figure 3.3) as described by Ruotolo *et al*. [28]. TrcA was chosen as representative peptide to illustrate the TWIMS-MS drift profiles generated (Figure 3.4 A-E) for each of the Trc peptides and the peptide formulations. The peptide ion drift times and

Stellenbosch University https://scholar.sun.ac.za

percentage ionic species contribution were determined from the generated TWIM-MS drift profiles.

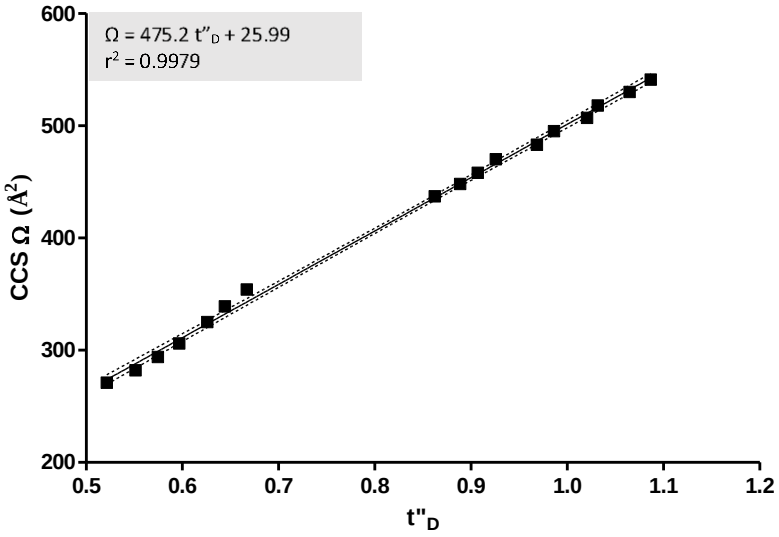

Figure 3.3 The calibration curve constructed by plotting the CCS areas (Ω) of poly-Ala ions obtained from literature [68] versus doubly corrected drift time ($t"_D$) values of the observed poly-Ala ions. The equation of the linear fit and correlation coefficient (r^2) are shown on the graph. The dotted lines indicate the 95 % confidence interval. The missing data-points on the graph are due to the absence of either CCS values or failure to detect the molecular ion in the poly-Ala preparation during the TWIM-MS analysis.

Previous studies by our group (Rautenbach *et al*., unpublished data) showed that higher order structures of the Trcs up to hexamers were detected using TWIMS-MS. From the TWIMS-MS drift profiles of all the peptides in this study it was evident that the signals of trimers, tetramers and other oligomeric species ($[nYA+nH]^{n+}$) are very low when analysing the peptides at 50 μM rather than 200-250 μM, as with previous studies. In this study the signal to noise ratio were insufficient making the determination of accurate drift times and subsequently the oligomeric ionic species signal contribution very difficult (results not shown). The focus was therefore directed on to the monomeric and dimeric ionic species for all the peptides, as well as their formulations. Regardless of all the precautions to avoid contaminants in our samples, a contamination by a general plasticiser (bis(2-ethylhexyl) phthalate, detected *m/z* =413.2679, theoretical *m/z*= 413.2662) from micropipette tips, used in

Stellenbosch University https://scholar.sun.ac.za

the final sample preparation, was observed at drift time 4.55 ms in the TWIM-MS profile of TrcA (Figure 3.4 A). This contaminant was present in all the peptide preparations but did not seem to interfere with the analysis. It was in fact used as internal standard to monitor that the ion signal remains consistent from run to run (results not shown). The CCS parameter of selected ionic species of the peptides (TrcA, TrcB, TrcC and TpcC) were determined, except for the singly charged monomers $[WC+H]^+$ of TpcC due to partial detection of the IM-MS peak of this ionic species, and are summarised in Table 3.2

Table 3.2 Summary of the average CCS areas of the Trc ionic species as determined from their drift times and Poly-Ala calibration curve. Each CCS area was determined from three repeats and standard deviation (SD) given.

Identity	**Abbr.**[a]	**Variable amino acid residues**[b]	**CCS Ω (Å²) ± SD**		
			$[M+H]^+$	$[M+2H]^{2+}$	$[2M+2H]^{2+}$
TrcA	YA	F^3-f^4-Y^7	366.7 ± 0.00	386.3 ± 0.00	552.1 ± 0.00
TrcB	YB	W^3-f^4-Y^7	373.2 ± 0.58	389.7 ± 0.00	561.8 ± 0.00
TrcC	YC	W^3-w^4-Y^7	379.0 ± 1.14	396.7 ± 0.00	571.7 ± 0.00
TpcC	WC	W^3-w^4-W^7	ND*	396.7 ± 0.00	573.2 ± 1.44

[a]The first letter in the abbreviation represent the residue at position 7 in the structure of the Trcs.
[b] D- and L-amino acids are represented by lower case and upper-case letters, respectively.
*Unknown drift time which prevented CCS area calculation.

The CCS areas of the singly charged monomers $[M+H]^+$ of the Trcs increase in the following order, TrcA<TrcB<TrcC with CCS areas determined as 366.7, 373.2 and 379.0 Å², respectively. The larger Trc peptides have a larger CCS area which is an expected result and correlates well with previous result from our group. The same trend is observed for the doubly charged monomers [M+2H]2+ of the cyclodecapeptides with CCS areas increasing in the following order, TrcA<TrcB<TpcC=TrcC with CCS areas determined as 386.3, 389.7, 396.7 and 396.7 Å2, respectively.

Stellenbosch University https://scholar.sun.ac.za

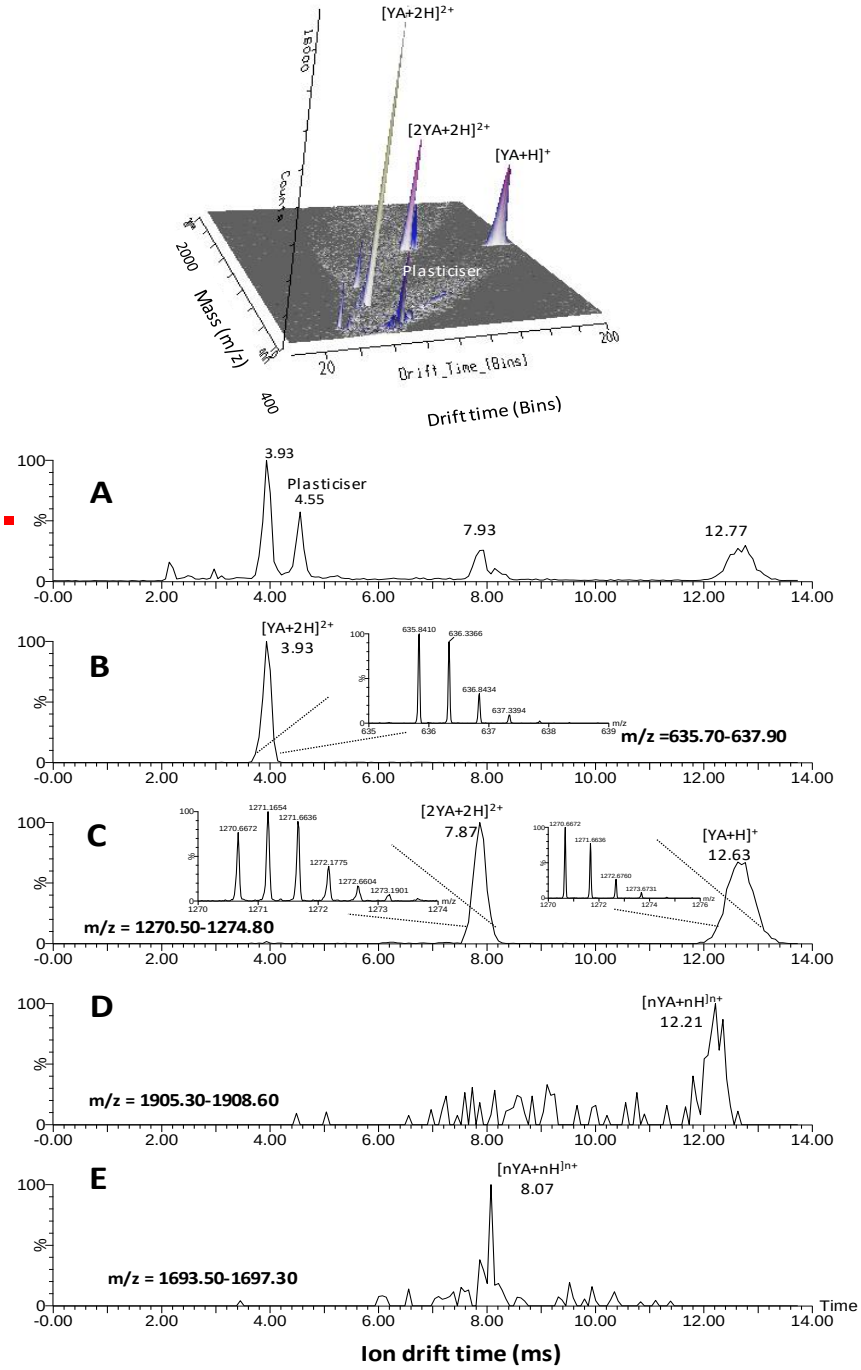

Figure 3.4 The TWIM-MS drift profiles generated for representative peptide, TrcA. The top graph is a 3D chromatogram showing the drift time (Bins) on the x-axis, total signal counts on the y-axis and the *m/z* ratio on the z-axis. A) The 2D chromatogram of all the ionic species of TrcA (50 µM) separated by TWIMS-MS showing plasticiser contamination at 4.55 ms drift time. The drift times of B) doubly charged monomeric $[YA+2H]^{2+}$ species, C) doubly charged dimeric $[2YA+2H]^{2+}$ species and singly charged monomeric $[YA+H]^{+}$ species, and D-E) oligomeric species $[nYA+nH]^{n+}$ are shown. The m/z ratio range of each ionic specie are given on the individual drift profiles. The enlarged MS spectra of the monomeric and dimeric species are also shown next to the representative ionic specie peak.

Stellenbosch University https://scholar.sun.ac.za

The CCS areas of the monomeric species are directly related to the molar mass of the peptide, which is indicative that the cyclodecapeptides have similar conformations *in vacuo*.

The CCS of doubly charged monomers $[M+2H]^{2+}$ of all the peptides were found to be larger (± 20 Å^2) than the singly charged monomers $[M+H]^+$. This difference is probably due to a more "relaxed or open" peptide conformation to accommodate the extra positive charge.

The doubly charged dimers $[2M+2H]^{2+}$ of the Trcs and TpcC also increased as the molar mass of the peptide in the dimer increased from TrcA<TrcB<TrcC<TpcC with CCS areas determined as 552.1, 561.8, 571.7 and 573.2 Å^2, respectively (Table 3.2). It was expected that the CCS areas of the doubly charged peptide dimers will be about twice the size of the singly and doubly charged monomers. However, less than a 2-fold increase in the CCS areas were observed for the doubly charged dimers $[2M+2H]^{2+}$ of the cyclodecapeptides. This indicated that the packing of the dimers is denser possibly due to specific hydrogen bonding and electrostatic interactions between peptide molecules thereby decreasing the overall size/surface area of the dimeric species. The overall decrease of the CCS area of all the peptide dimers confirms the previous work by Munyuki *et al*. [12] and Loll *et al.* [13] that the Trc dimers are the result of strong specific interactions.

The influence of the peptide concentration on the oligomerisation of the Trcs and TpcC were assessed by determining the percentage signal contribution of the ionic species at four different concentrations 50, 25, 12.5 and 6.13 µM (Figure 3.5 A-D). Similar mirror sigmoidal dose response trends are observed for TrcA, TrcB, TrcC and TpcC where the doubly charged monomers $[M+2H]^{2+}$ decreases and both the singly charged monomers $[M+H]^+$ and doubly charged dimers $[2M+2H]^{2+}$ increase as

Stellenbosch University https://scholar.sun.ac.za

the concentration of peptide increases (Figure 3.5 A2-D2). The increase of dimeric species with increase in concentration is an expected result, but the fact that the singly charged monomeric species follows a similar trend (Figure 3.5 A-D) is very interesting and indicate this specie could be derived from dissociation of dimers and larger oligomers. A decrease in doubly charged monomeric ions directly correlates with an increase in doubly charged dimers for all the peptides (Figure 3.5 A-D), which indicates that the doubly charged monomers are the monomeric species in solution that decreases with concentration dependent oligomerisation.

The total signal contribution of each of the ionic species of the peptides alone and in formulations at 50 μM were investigated to gain insight into the influence of the formulants (CS, LPC and C16) on the contribution of monomers versus dimers. A relationship exists between the hydrophobicity of the peptides and the degree of oligomerisation with the observation of a higher dimer contribution for the more hydrophobic TrcA and TrcB (Figure 3.6 A and B) than the more polar TrcC and TpcC (Figure 3.6 C and D). Similarly, the doubly charged signal of the monomers also followed the same trend with TpcC>TrcC>TrcB>TrcA (Figure 3.6 A-D).

For all the peptides in formulation with CS, LPC and C16 an increase in the % doubly charged monomers were observed, indicating a release of monomeric species from the formulations. Conversely, a decrease in the % doubly charged dimers were observed for all the LPC and C16 formulations, indicating that there may be less dimers (and higher oligomers) in the formulation. This correlated with the disruption of nanostructures by the formulants as observed by SEM. The CS influence on the % doubly charged dimers of the cyclodecapeptide depended on the

Stellenbosch University https://scholar.sun.ac.za

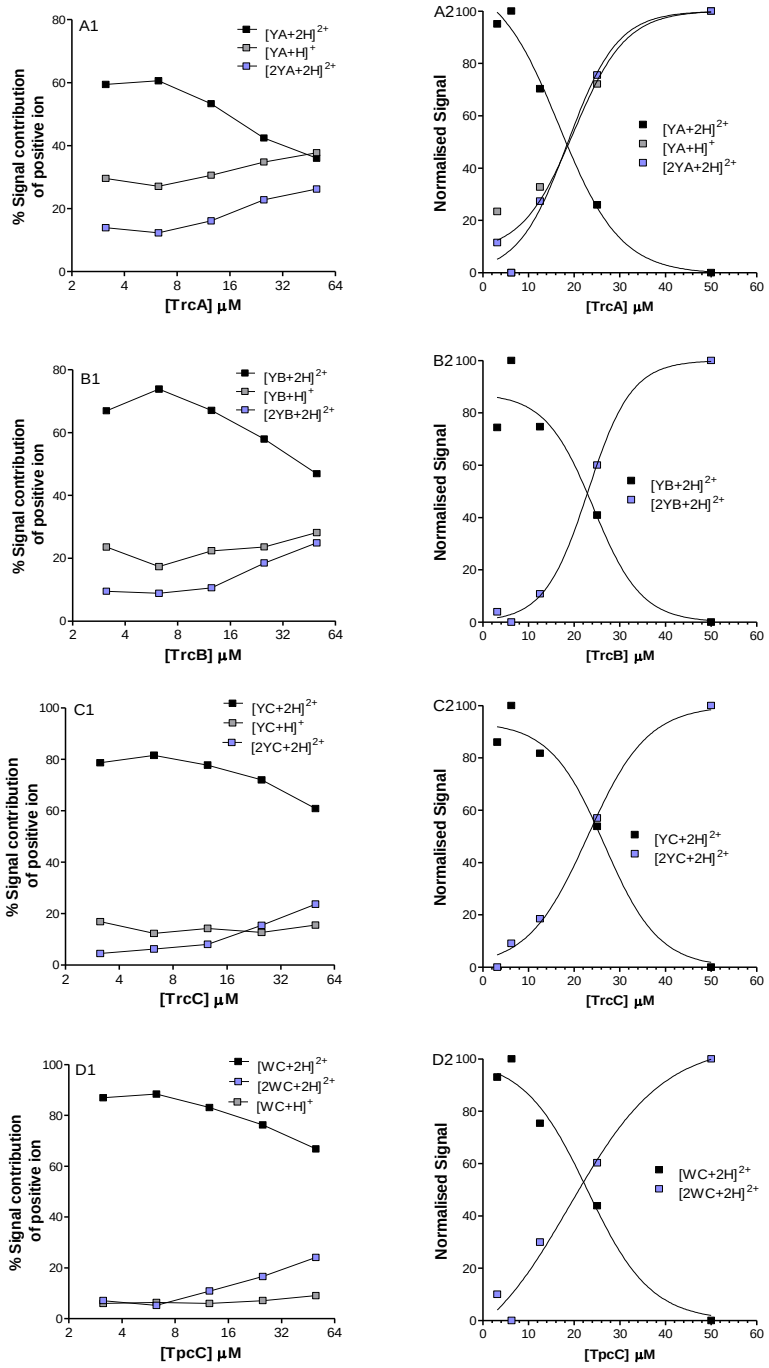

Figure 3.5 The concentration dependence of the oligomerisation of the Trcs. A1) The percentage contribution of TrcA ionic species versus peptide concentration and A2) normalised signal contribution of TrcA ionic species versus peptide concentration fitted with Boltzman sigmoidal curve B1) The percentage contribution of TrcB ionic species versus peptide concentration and B2) normalised signal contribution of TrcB ionic species versus peptide concentration fitted with Boltzman sigmoidal curve. C1) The percentage contribution of TrcC ionic species versus peptide concentration and C2) normalised signal contribution of TrcC ionic species versus peptide concentration fitted with Boltzman sigmoidal curve. D1) The percentage contribution of TpcC ionic species versus peptide concentration and D2) normalised signal contribution of TpcC ionic species versus peptide concentration fitted with Boltzman sigmoidal curve.

Stellenbosch University https://scholar.sun.ac.za

peptide identity (Figure 3.6 A-D). In general, the % of singly charged monomers did not show major changes induced by the formulants (Figure 3.6 A-D).

However, as the differences are minor in the latter two, further investigation must be done in order to determine if the changes are statistically relevant.

There was a general decrease in dimers, corresponding with the increase in doubly charged monomers of the Trcs and TpcC when formulated with LPC and C16 (Figure 3.6 A-D). This could be the disruption of electrostatic/ionic/hydrogen bonding by formulant and peptide polar group interaction or an induced conformational change which changes location of peptide polar groups which play a role in the oligomerisation of peptides. The formulants which decreased the proportion of dimeric species to the largest extent were LPC and C16, which correlates well with the SEM results (Figure 3.1 C and F). LPC possibly acts as a detergent (disrupting oligomerisation) and that C16 forms small micelles possibly leading to entrapment of peptide monomers preventing formation of oligomers. On the other hand, it seems as if CS had no marked influence on the dimer formation (Figure 3.6 A-D). However, the doubly charged monomers were increased and singly charged monomers decreased, which does indicate some changes in the oligomerisation, correlating with the SEM results. It must be noted that total TWIM-MS signal is decreased when formulated with LPC and C16 compared to the peptide controls (Figure 3.7), indicating that the ionic peptide species are not completely released from the LPC and C16 formulation which probably skews the results discussed above. This result also indicated that a significant amount of peptide molecules was trapped in stable neutral lipid complexes in the formulation. This result could indicate ionic interactions between the negative lipid group and the positive L-Orn^{9} in the cyclodecapeptides.

Stellenbosch University https://scholar.sun.ac.za

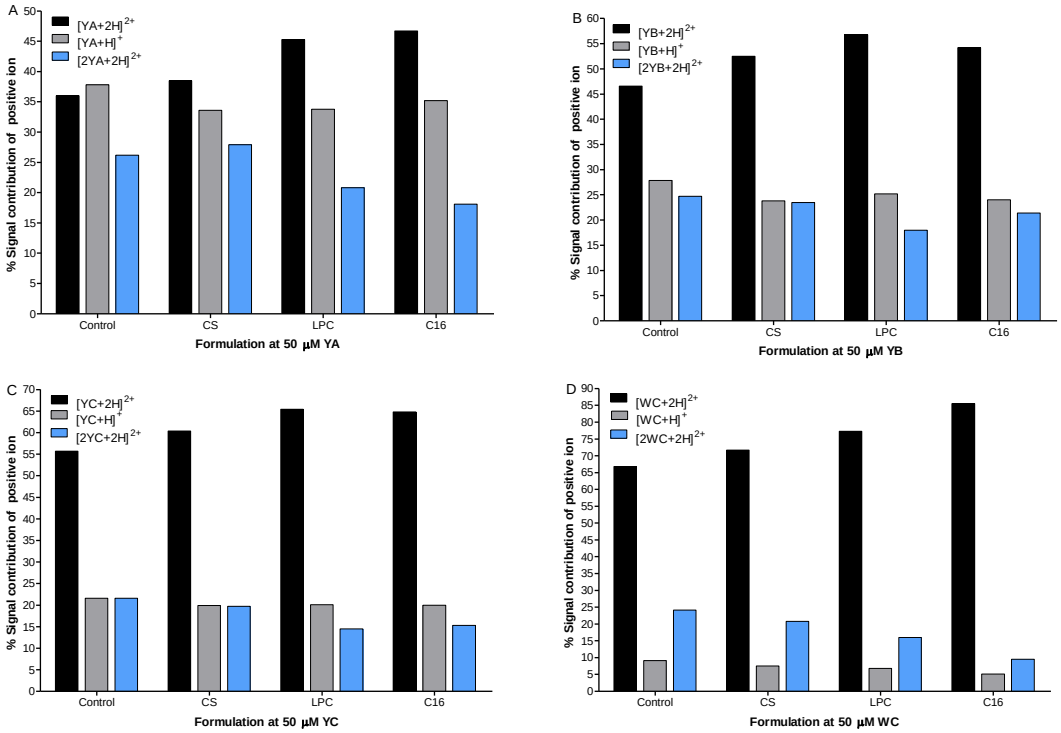

Figure 3.6 The percentage contribution of positive peptide ions of the Trcs alone and in formulation with CS, LPC and C16 at fixed concentration of 50 µM. A) Percentage contribution of monomeric and dimeric ionic species of TrcA and formulations. B) Percentage contribution of monomeric and dimeric ionic species of TrcB and formulations C) Percentage contribution of monomeric and dimeric ionic species of TrcC and formulations. D) Percentage contribution of monomeric and dimeric ionic species of TpcC and formulations

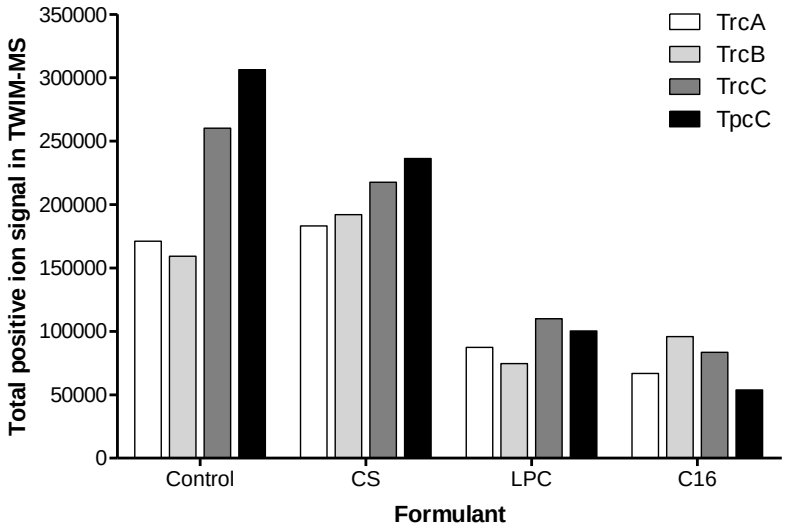

Figure 3.7 Total TWIM-MS signal of the TrcA, TrcB, TrcC and TpcC and their respective formulations at a specific concentration of 50 µM.

Stellenbosch University https://scholar.sun.ac.za

Comparison of the TWIM-MS signals from the unformulated peptides with those formulated with CS, the role of hydrophobicity is again highlighted with both TrcA and TrcB signal increasing, indicating release from oligomeric structure, while the inverse is true for the Trp-rich TrcC and TpcC indicating trapping of more molecules in the formulation (Figure 3.7). This result on the CS formulations may also indicate that this formulation is less ESI-MS stable than the LPC and C16 formulations, because of more hydrophobic interactions that are removed in the mass spectrometer (MS).

3.4.3 Fluorescence spectroscopy of the peptides and formulations

The Trcs contain three intrinsic fluorophores i.e. Phe, Tyr and Trp. However, the emission maximum of Phe is at 282 nm, which is similar to the excitation wavelengths of Trp (λ_{ex} 282 nm) and Tyr (λ_{ex} 276 nm) [33, 34]. To prevent spectral overlap of Phe emission and excitation of Tyr and Trp, Phe is usually not used during fluorescence studies [33, 34]. In addition, the fluorescence of Tyr is overshadowed by that of Trp due to the low extinction coefficient and sensitivity to polar solvent/environment of Tyr and the high sensitivity of the Trp indole group to its local environment [33, 34, 54, 57, 58]. Therefore, Trp was the major fluorophore used to investigate the self-assembled states of the Trcs and TpcC alone and in formulation during the present study. The peptides containing at least one Trp residues, TrcB, TrcC and TpcC, had emission maxima that were blue shifted (shorter wavelengths) from the expected 357 nm [33, 56] to 344 ± 2 nm (TrcB), 340 ± 2 nm (TrcC) and 340 ± 0 nm (TpcC).

These results correlate well with the findings by Vosloo [48] who observed that the Trp residues are located in a more hydrophobic environment possibly as a result of

Stellenbosch University https://scholar.sun.ac.za

oligomerisation of the Trcs when in an aqueous environment [33, 54, 55, 58]. The spectral shift, if any, of TrcA could not be determined due to the lack of Trp residues in the structure. The fluorescence of TrcA is solely due to the Tyr residue at position seven which is expected to emit at 303 nm [33, 55]. If a blue shift does occur (shifted to shorter wavelengths than 303 nm) in the spectrum of TrcA, it would not be observed because the fluorescence was scanned from 300 nm onwards. Therefore, quenching and quantum yield are the only parameters that were used to gain info on the aggregated states of TrcA. Vosloo [48] found that the fluorescence of TrcB, TrcC and TpcC are quenched when placed in a membrane mimicking environment, therefore the same trend is expected for the peptides when in formulation with the three different lipid-based formulants used in the study. Indeed, this was the result with all peptides formulations having quenched fluorescence including Trcmix (Figure 3.8 A-E). Interestingly, the quenched fluorescence of the peptides and Trcmix by CS was accompanied by a blue shift of the spectrum, with the exception of TrcA (Figure 3.8 B-E).

Quenching of fluorescence can be the consequence of various reasons including the molecular mechanisms such as collisional quenching via an aqueous environment, ground-state complex formation and excited state reactions with local polar groups present in the peptide backbone (amide groups) or side chains (amide groups of Asn and Gln, amino group of Orn and hydroxyl group of Tyr) [33, 54, 58] or even the polar groups of the formulants (sulfoxide group of CS, carboxyl group of C16 and amino- or phosphate group of LPC) [69, 70]. In general, the quenching of the Trcs by LPC and C16 was similar except for TpcC where LPC resulted in less quenching compared to C16 (Figure 3.8 A-E). The quenching of the Trcs fluorescence by the formulants can be caused by three scenarios: 1) Exposure of Trp residues to aqueous environments

Stellenbosch University https://scholar.sun.ac.za

leading to collisional quenching [33, 54, 58], 2) excited state reactions with the polar groups of peptide backbone and residue side chains [70] and 3) excited state reactions with polar groups of the formulants [69, 70].

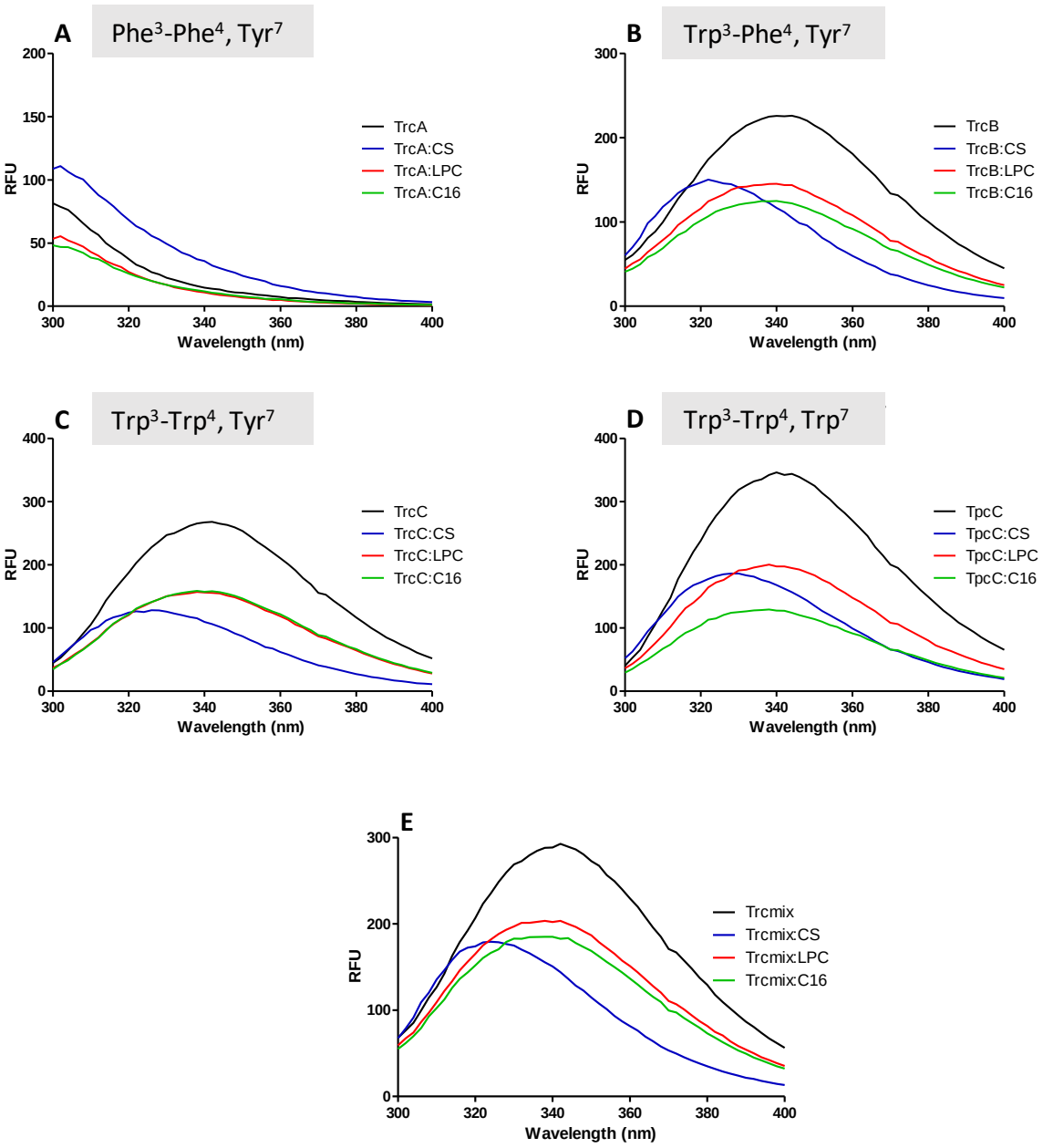

Figure 3.8 The fluorescence emission spectra of the Trcs alone and in formulation with lipid-based molecules, CS, LPC and C16 in an aqueous environment at 1-hour maturation. The solutions were excited at 280 nm to and emission scanned from 300 nm to 400 nm to produce fluorescence spectra of A) TrcA and its formulations, B) TrcB and its formulations, C) TrcC and its formulations, D) TpcC and its formulations and E) Trcmix and its formulations. The fluorescence quantum yield is given in relative fluorescent units (RFU). The variable residues at positions three, four and seven are given on each spectrum except for Trcmix which consists of the mixture of Trc analogues.

Stellenbosch University https://scholar.sun.ac.za

Considering the SEM and TWIM-MS results for LPC and C16 formulations, we hypothesise that small micellular structures were formed with a decreased Trc dimer content (Figure 3.1 and Figure 3.6). With this it is most likely that the quenching is collisional due to exposure of Trp residues to water molecules and/or quenching via excited state reactions of Trp with the polar groups of LPC and C16. Alternatively, the L-Orn^{9} residue could be in close proximity to the aromatic rings as a hydrogen bond partner in leading to quenching.

On the other hand, SEM revealed that CS may cause the cyclodecapeptides to form some larger structures (Figure 3.1). TWIM-MS results indicated that hydrophobic interaction may be important in these structures and that the formulation retained a significant proportion of dimers (Figures 3.6 and 3.7). This would point to fluorescence quenching by CS as the consequence of excited state reactions of the Trp residues with the polar sulphate group of CS, the peptide backbone and/or the side chains of peptides residues. The blue shift of emission spectra observed for the CS formulations (Figure 3.8) suggests that the Trp residues are in a more hydrophobic environment [33, 34].

Trp generally has a higher fluorescence when blue shifted [33, 71] but with the Trp-rich peptides in this study CS leads to quenching. The quenching is possibly due to the aromatic ring stacking of aromatic residues as proposed by Munyuki et al.[12]. The blue shifts observed for CS formulations were as follows: for TrcB from 344 nm to 322 nm, for TrcC from 340 nm to 327 nm, TpcC from 340 nm to 328 nm and for Trcmix from 342 nm to 323 nm. Note that this is a 22-32 nm blue shift from the 357 nm maximum of Trp [56] which is highly significant, and could be explained by a combinatorial effect of aromatic ring stacking of Trp residues and a highly non-polar local environment [12, 33, 34, 70, 71].

Stellenbosch University https://scholar.sun.ac.za

The fact that the same trend was seen for each of the peptides formulated with CS suggests that the CS (non-polar and polar groups of CS) does not have preference for any of the different variations of the aromatic dipeptide unit. Considering the blue shift and quenching caused by CS it is more likely that the CS probably interacts with other group/groups of the Trcs and TpcC inducing hydrophobic aromatic ring stacking (causing the blue shift) and quenching via excited state reactions between the dipeptide unit and polar groups within the peptide structures and the sulphate group in CS. Neither LPC nor C16 caused spectral shifts of the maxima (Figure 3.8) indicating hydrophobic Trp ring stacking are not involved further strengthening the theory that the fluorescence quenching observed for the LPC and C16 formulations are due to collisional quenching of fluorophores by water molecules or polar groups of the formulants. TWIM-MS also indicated that neutral complexes may exist in the C16 and LPC formulations, correlating with this result.

The stability of the Trcs and TpcC alone and in formulation was investigated by allowing 24-hour maturation before measuring the fluorescence (Table 3.3). Overall, similar trends were observed for all the peptides at 1-hour and 24-hour maturation with regards to the quenching of the fluorescence by CS, LPC and C16 and a blue shift observable for the CS formulations. However, the total quantum yields of all the peptides and their formulations revealed either less or more quenching at 24-hour maturation compared to 1-hour maturation depending on the peptide and formulation (Table 3.3). For TrcA and its CS and C16 formulations, even more quenching of FS is observed at 24-hour maturation compared to 1-hour maturation whereas LPC had similar total quantum yields between the two maturation periods. This indicates over time the oligomeric states of TrcA within the CS and C16 formulation changes. It is possible that TrcA within the CS formulation requires more time to form new nano-

Stellenbosch University https://scholar.sun.ac.za

structures leading to increased quenching, whereas the Tyr residues within the TrcA:C16 formulation becomes more exposed to the aqueous environment and/or carboxyl group of C16 as time progresses leading to increased collisional quenching. Both TrcB and TrcA experienced quenching by CS, which could indicate a role of Tyr^{7} in the maturation. Conversely TrcC, TpcC and the Trcmix were dequenched over time in the CS formulation. This could be due to the D-Trp^{4} residue that is contained in all three peptide preparations mowing into a more hydrophobic environment. LPC led to dequenching in all the preparations containing Trp^{3}, namely TrcB, TrcC and TpcC which could point to a role in maturation of the residue in the aromatic dipeptide unit. In comparison with TrcA, TrcC, TpcC and Trcmix and their formulations, dequenching was observed at 24-hour compared to 1-hour maturation, for the most part, with the exception Trcmix which had more quenching at 24 hours. TrcB, which is an intermediate peptide between the A and C analogues, were the least influenced, except for the CS formulation, after 24 hours.

The decrease in quenching for the CS, LPC and C16 formulations may indicate that as time progresses that one or both the Trp residues in the aromatic dipeptide unit become less exposed to aqueous environment/polar groups in the formulant. The changes in the total quantum yield of the peptides and their formulations when allowed different maturation time periods cannot be fully explained, however, it is certain that minor conformational changes do occur within the peptides and formulation, but the major differences between the formulations are stable over time.

If the FS and TWIM-MS results are compared there is an exponential relationship (R^{2}=0.8), with the exception of the CS formulations of the three peptides with Trp residues (Figure 3.9). A number of conclusions on the role of certain residues and molecular interactions can be derived from this interesting correlation.

Stellenbosch University https://scholar.sun.ac.za

Table 3.3 Comparison of fluorescence spectra of the Trc alone and in formulation at 1-hour and 24-hour maturation period. The total fluorescence quantum yield and the emission maxima of the Trcs and their formulations at 1 hour and 24 maturation period are given. The maxima of TrcA and TrcA formulations could not be determined.

Identity	Total quantum yield comparison	Influence on total quantum yield	Maximum wavelength ± SD (nm)	
			1 hour	24 hours
TrcA	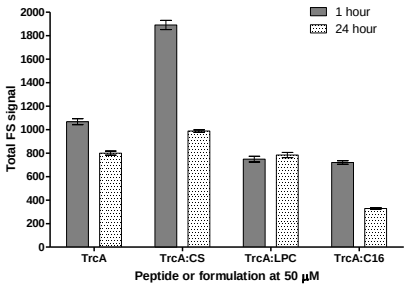	Quenched	N.A.	N.A.
TrcA:CS		Quenched	N.A.	N.A.
TrcA:LPC		No influence	N.A.	N.A.
TrcA:C16		Quenched	N.A.	N.A.
TrcB	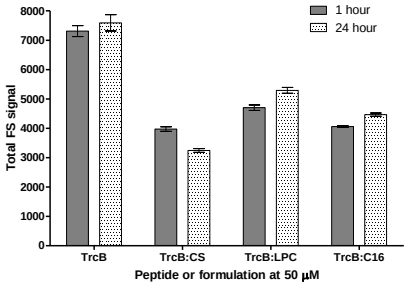	No Influence	344 ± 2	342 ± 0
TrcB:CS		Quenched	322 ± 0	322 ± 2
TrcB:LPC		Slightly Dequenched	339 ± 1	338 ± 0
TrcB:C16		Slightly Dequenched	339 ± 2	338 ± 0
TrcC	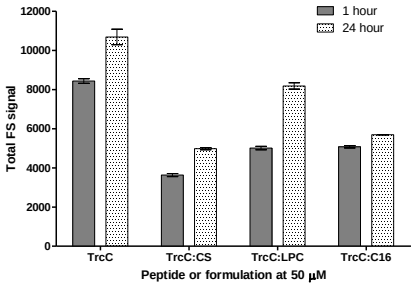	Dequenched	340 ± 2	341 ± 1
TrcC:CS		Dequenched	327 ± 1	328 ± 0
TrcC:LPC		Dequenched	339 ± 2	339 ± 1
TrcC:C16		Slightly Dequenched	340 ± 2	339 ± 1
TpcC	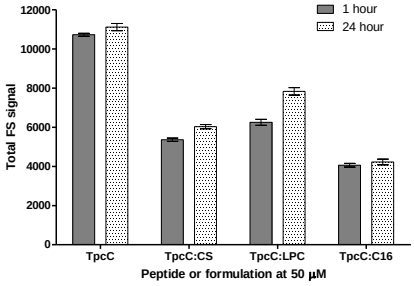	No Influence	340 ± 0	341 ± 1
TpcC:CS		Slightly Dequenched	328 ± 2	329 ± 1
TpcC:LPC		Dequenched	338 ± 0	336 ± 2
TpcC:C16		No influence	337 ± 2	339 ± 2
Trcmix	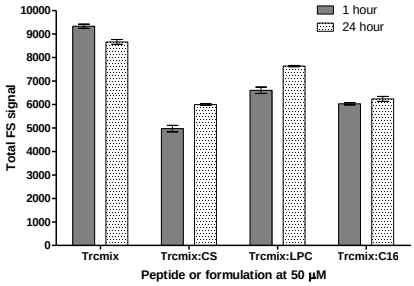	Quenched	342 ± 0	341 ± 1
Trcmix:CS		Dequenched	323 ± 1	326 ± 0
Trcmix:LPC		Dequenched	339 ± 2	337 ± 3
Trcmix:C16		No influence	339 ± 4	338 ± 0

Stellenbosch University https://scholar.sun.ac.za

The C16 formulant led to decreased total TWIM-MS and FS signals of the peptides (Figure 3.9, Table 3.3). This indicates that the side chains of the Trp and Tyr residues are moved to a polar environment (FS quenching) and do not form part of assemblies with aromatic stacking which would lead to better TWIM-MS signal (because of loss of such interactions in the MS instrument).

The C16 carboxylate group probably associates with L-Orn^9 leading to neutral complexes which explains the low MS signal intensities. LPC led to moderate loss in total FS signals, but low TWIM-MS signals. Similar to C16, the phosphate group may associate with L-Orn^9 leading to neutral complexes. However, only few of the Trp and Tyr residues may be exposed to polar environment, leading to some quenching in FS signals (Table 3.3). CS led to pronounced quenching in all the peptides with Trp (Table 3.3, Figure 3.9), which indicates that one or more of the residues in the aromatic dipeptide moiety are part of aromatic stacking, as the MS signal is only moderately influenced. The Tyr on the other hand is placed in a hydrophobic environment in the CS formulation highlighted by the increased total FS signal of TrcA:CS. The sulphate group of CS does not seem to have such a strong association with the L-Orn^9 of the peptides as the negative groups in C16 and LPS, as the TWIM-MS signal is still maintained.

Stellenbosch University https://scholar.sun.ac.za

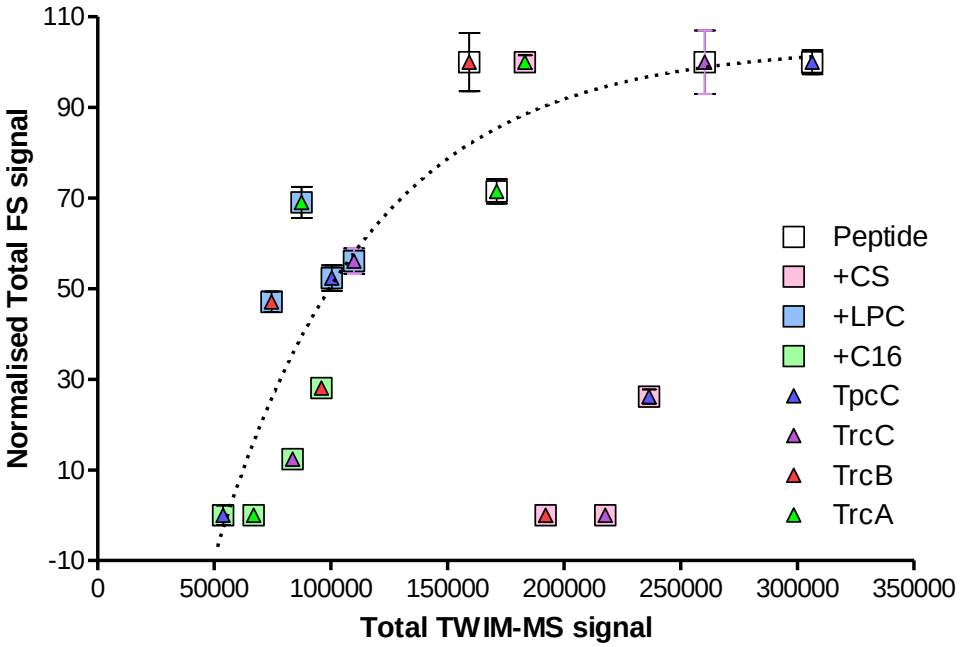

Figure 3.9 The relationship between the normalised total FS signals and the total TWIM-MS signals of the peptides and peptide formulations. The dotted line shows the exponential curve fitted to data points (R^2=0.80), with exclusion on the CS formulations of TrcB, TrcC and TpcC.

3.5 CONCLUSION

Clear correlation between CCS areas of ionic species and molecular mass of all the peptides were observed indicative of similar peptide conformation adoption *in vacuo.* Higher dimer contribution was observed for the more hydrophobic TrcA and TrcB than the more polar TrcC and TpcC peptides, with an expected concentration dependant increase in dimerisation observed for all the peptides.

In correlation with the SEM results where the detergent-like effects of LPC and C16 led to disruption of the self-assembly of TpcC into uniform spheres, the dimer contribution of all the peptides were decreased within these formulations. In addition, the LPC and C16 formulants led to loss in total TWIM-MS signal compared to controls, indicating entrapment of peptide within stable neutral lipid complexes possibly due to ionic interaction between anionic lipid group and cationic L-Orn[9] of

Stellenbosch University https://scholar.sun.ac.za

the peptides. There is a direct relationship between the quenching of total FS signal and loss of ionic species TWIM-MS signal of the peptides in formulation with C16 and LPC. With these results, as well as the SEM and other TWIM-MS results, we hypothesise that formulation with LPC and C16 induces stable neutral lipid-complexes which entraps peptides (via ionic interaction between the anionic lipid headgroup and cationic L-Orn[9]), decreases dimer formation and exposes the aromatic peptide unit to a polar environment which could be the aqueous environment (collisional FS quenching) and/or the polar groups of the LPC and C16 (FS quenching via excited state reactions).

The dimer contribution of the CS formulations was not markedly influenced compared to the controls and depended on the peptide identity. Furthermore, the total TWIM-MS signal of the CS formulations were largely maintained, indicating less stable formulation due to loss of hydrophobic interactions in the TWIM-MS instrument. This result agrees with the significant blue shifts and quenching observed in the FS spectra of the peptides when formulated with CS, indicative of a combinatorial effect of hydrophobic aromatic ring stacking and excited state reactions between dipeptide unit and the polar groups within peptide conformations.

It is evident that both the dipeptide unit and peptide characteristics have an influence on the self-assembly of the peptides into higher order structures and that these higher order structures can be further influenced by solvent systems, peptide concentration and formulants. As the oligomerisation of the Trcs have been shown to dictate their antimicrobial activity, it is expected that the formulations will have influences on the biological activity of the peptides which will be investigated in Chapter 4.

Stellenbosch University https://scholar.sun.ac.za

3.6 REFERENCES

(1) Mader, J. S., and Hoskin, D. W. (2006) Cationic antimicrobial peptides as novel cytotoxic agents for cancer treatment. *Expert Opin. Investig. Drugs 15*, 933–946.

(2) Hancock, R. E. (2000) Cationic antimicrobial peptides: towards clinical applications. *Expert Opin. Investig. Drugs 9*, 1723–1729.

(3) Kim, S., Kim, S. S., Bang, Y. J., Kim, S. J., and Lee, B. J. (2003) In vitro activities of native and designed peptide antibiotics against drug sensitive and resistant tumor cell lines. *Peptides 24*, 945–953.

(4) Ruttenberg, M. A., King, T. P., and Craig, L. C. (1966) The chemistry of tyrocidine. VII. Studies on association behavior and implications regarding conformation. *Biochemistry 5*, 2857–2864.

(5) Ruttenberg, M. A., King, T. P., and Craig, L. C. (1965) The use of the tyrocidines for the study of conformation and aggregation behavior. *J. Am. Chem. Soc. 87*, 4196–4198.

(6) Stern, A., Gibbons, W. A., and Craig, L. C. (1969) The effect of association on the nuclear magnetic resonance spectra of tyrocidine B. *J. Am. Chem. Soc. 91*, 2794–2796.

(7) Eyéghé-bickong, H. A. (2011) Role of surfactin from Bacillus subtilis in protection against antimicrobial peptides produced by Bacillus species, PhD Thesis, Department of Biochemistry, University of Stellenbosch, http://hdl.handle.net/10019.1/6773. Stellenbosch.

(8) Paradies, H. H. (1979) Aggregation of tyrocidine in aqueous solutions. *Biochem. Biophys. Res. Commun. 88*, 810–817.

(9) Williams, R. C., Yphantis, D. A., and Craig, L. C. (1972) Noncovalent association of tyrocidine B. *Biochemistry 11*, 70–77.

(10) Jelokhani-Niaraki, M., Prenner, E. J., Kay, C. M., McElhaney, R. N., Hodges, R. S., and Kondejewski, L. H. (2001) Conformation and other biophysical properties of cyclic antimicrobial peptides in aqueous solutions. *J. Pept. Res. 58*, 293–306.

(11) Laiken, S., Printz, M., and Craig, L. C. (1969) Circular dichroism of the tyrocidines and gramicidin S-A. *J. Biol. Chem. 244*, 4454–4457.

(12) Munyuki, G., Jackson, G. E., Venter, G. A., Kövér, K. E., Szilágyi, L., Rautenbach, M., Spathelf, B. M., Bhattacharya, B., and Van Der Spoel, D. (2013) β-sheet structures and dimer models of the two major tyrocidines, antimicrobial peptides from *Bacillus aneurinolyticus* . *Biochemistry 52*, 7798–7806.

(13) Loll, P. J., Upton, E. C., Nahoum, V., Economou, N. J., and Cocklin, S. (2014) The high resolution structure of tyrocidine A reveals an amphipathic dimer. *Biochim. Biophys. Acta - Biomembr. 1838*, 1199–1207.

(14) Gibbons, W. A., Beyer, C. F., Dadok, J., Sprecher, R. F., and Wyssbrod, H. R. (1975) Studies of individual amino acid residues of the decapeptide tyrocidine A by proton double-resonance difference spectroscopy in the correlation mode. *Biochemistry 14*, 420–429.

(15) Kuo, M. C., and Gibbons, W. A. (1979) Determination of individual side-chain

Stellenbosch University https://scholar.sun.ac.za

conformations, tertiary conformations, and molecular topography of tyrocidine A from scalar coupling constants and chemical shifts†. *Biochemistry 18*, 5855–5867.

(16) Kuo, M. C., and Gibbons, W. A. (1980) Nuclear overhauser effect and cross-relaxation rate determinations of dihedral and transannular interproton distances in the decapeptide tyrocidine A. *Biophys. J. 32*, 807–836.

(17) Wenzel, M., Rautenbach, M., Vosloo, J. A., Siersma, T., Aisenbrey, C. H. M., Zaitseva, E., Laubscher, W. E., van Rensburg, W., Behrends, J. C., Bechinger, B., and Hamoen, L. W. (2018) The multifaceted antibacterial mechanisms of the pioneering peptide antibiotics tyrocidine and gramicidin S. *MBio 9*, 1–20.

(18) Dimick, K. P. (1951) Hemolytic action of gramicidin and tyrocidin. *Exp. Biol. Med. 78*, 782–784.

(19) Rammelkamp, Charles H. Weinstein, L. (1942) Toxic effects of tyrothricin , gramicidin and tyrocidine. *J. Infect. Dis. 71*, 166–173.

(20) Rautenbach, M., Vlok, N. M., Stander, M., and Hoppe, H. C. (2007) Inhibition of malaria parasite blood stages by tyrocidines, membrane-active cyclic peptide antibiotics from *Bacillus brevis*. *Biochim. Biophys. Acta - Biomembr. 1768*, 1488–1497.

(21) Carmona-Ribeiro, A. M., and Carrasco, L. D. de M. (2014) Novel formulations for antimicrobial peptides. *Int. J. Mol. Sci. 15*, 18040–18083.

(22) Faya, M., Kalhapure, R. S., Kumalo, H. M., Waddad, A. Y., Omolo, C., and Govender, T. (2018) Conjugates and nano-delivery of antimicrobial peptides for enhancing therapeutic activity. *J. Drug Deliv. Sci. Technol. 44*, 153–171.

(23) Lemke, A., Kiderlen, A. F., and Kayser, O. (2005) Amphotericin B. *Appl. Microbiol. Biotechnol. 68*, 151–162.

(24) Tang, X. J., Thibault, P., and Boyd, R. K. (1992) Characterisation of the tyrocidine and gramicidin fractions of the tyrothricin complex from *Bacillus brevis* using liquid chromatography and mass spectrometry. *Int. J. Mass Spectrom. Ion Process. 122*, 153–179.

(25) Vosloo, J. A., Stander, M. A., Leussa, A. N. N., Spathelf, B. M., and Rautenbach, M. (2013) Manipulation of the tyrothricin production profile of *Bacillus aneurinolyticus*. *Microbiol. (United Kingdom) 159*, 2200–2211.

(26) Spathelf, B. M. (2010) Qualitative structure-actvity relationships of the major tyrocidines, cyclic decapeptides from *Bacillus aneurinolyticus*. PhD Thesis, Department of Biochemistry, University of Stellenbosch, http://scholar.sun.ac.za/handle/10019.1/4001. Stellenbosch.

(27) Leussa, A. N. yang. N., and Rautenbach, M. (2014) Detailed SAR and PCA of the tyrocidines and analogues towards leucocin A-sensitive and leucocin A-resistant *Listeria monocytogenes*. *Chem. Biol. Drug Des. 84*, 543–557.

(28) Ruotolo, B. T., Tate, C. C., and Russell, D. H. (2004) Ion mobility-mass spectrometry applied to cyclic peptide analysis: Conformational preferences of gramicidin S and linear analogs in the gas phase. *J. Am. Soc. Mass Spectrom. 15*, 870–878.

(29) Rautenbach, M., Vlok, N. M., Eyéghé-Bickong, H. A., van der Merwe, M. J., and Stander, M. A. (2017) An Electrospray Ionization Mass Spectrometry Study on the

Stellenbosch University https://scholar.sun.ac.za

"In Vacuo" Hetero-Oligomers Formed by the Antimicrobial Peptides, Surfactin and Gramicidin S. *J. Am. Soc. Mass Spectrom. 28*, 1623–1637.

(30) Michaelevski, I., Kirshenbaum, N., and Sharon, M. (2010) T-wave ion mobility-mass spectrometry: basic experimental procedures for protein complex analysis. *J. Vis. Exp.* 1–8.

(31) Chen Hua, D. J. and H. Q. (2008) Biomolecule analysis by ion mobility spectrometry. *Annu. Rev. Anal. Chem. 1*, 293–327.

(32) Weston, D. J., Bateman, R., Wilson, I. D., Wood, T. R., and Creaser, C. S. (2005) Direct analysis of pharmaceutical drug formulations using ion mobility spectrometry/quadrupole-time-of-flight mass spectrometry combined with desorption electrospray ionization. *Anal. Chem. 77*, 7572–7580.

(33) Lakowicz, J. R. (2013) Principles of Fluorescence Spectroscopy. Springer Science & Bussiness Media.

(34) Chattopadhyay, A., and Raghuraman, H. (2004) Application of fluorescence spectroscopy to membrane protein structure and dynamics. *Curr. Sci.*

(35) Smith, D., Knapman, T., Campuzano, I., Malham, R., Berryman, J., Radford, S., and Ashcroft, A. (2009) Deciphering drift time measurements from travelling wave ion mobility spectrometry-mass spectrometry studies. *Eur. J. Mass Spectrom. 15*, 113.

(36) Chan, E. C. Y., New, L. S., Yap, C. W., and Goh, L. T. (2009) Pharmaceutical metabolite profiling using quadrupole/ion mobility spectrometry/time-of-flight mass spectrometry. *Rapid Commun. Mass Spectrom. 23*, 384–394.

(37) Bagal, D., Zhang, H., and Schnier, P. D. (2008) Gas-phase proton-transfer chemistry coupled with TOF mass spectrometry and ion mobility-MS for facile analysis of poly(ethylene glycols) and PEGylated polypeptide conjugates. *Anal. Chem. 80*, 2408–2418.

(38) Trimpin, S., and Clemmer, D. E. (2008) Ion mobility spectrometry/mass spectrometry snapshots for assessing the molecular compositions of complex polymeric systems. *Anal. Chem. 80*, 9073–9083.

(39) Dwivedi, P., Schultz, A. J., and Hill, H. H. J. (2010) Metabolic profiling of human blood by high resolution ion mobility mas spectrometry (IM-MS). *Int. J. Mass Spectrom. Ion Process. 298*, 78–90.

(40) Dwivedi, P., Bendiak, B., Clowers, B. H., and Hill, H. H. J. (2007) Rapid Resolution of carbohydrate isomers by electrospray ionization ambient pressure ion mobility spectrometry-time-of-flight mass spectrometry (ESI-APIMS-TOFMS). *J. Am. Soc. Mass Spectrom. 18*, 1163–1175.

(41) Ridenour, W. B., Kliman, M., Mclean, J. A., and Caprioli, R. M. (2010) Structural characterization of phospholipids and peptides directly from tissue sections by MALDI traveling-wave ion mobility-mass spectrometry. *Anal. Chem. 82*, 1881–1889.

(42) Uetrecht, C., Rose, R. J., Van Duijn, E., Lorenzen, K., and Heck, A. J. R. (2010) Ion mobility mass spectrometry of proteins and protein assemblies. *Chem. Soc. Rev. 39*, 1633–1655.

(43) Bich, C., Baer, S., Jecklin, M. C., and Zenobi, R. (2010) Probing the hydrophobic effect of noncovalent complexes by mass spectrometry. *J. Am. Soc.*

Stellenbosch University https://scholar.sun.ac.za

Mass Spectrom. 21, 286–289.

(44) Daniel, J. M., Friess, S. D., Rajagopalan, S., Wendt, S., and Zenobi, R. (2002) Quantitative determination of noncovalent binding interactions using soft ionization mass spectrometry. *Int. J. Mass Spectrom. 216*, 1–27.

(45) Robinson, C. V, Chung, E. W., Kragelund, B. B., Knudsen, J., Aplin, R. T., Poulsen, F. M., and Dobson, C. M. (1996) Probing the nature of noncovalent interactions by mass spectrometry. A study of protein-CoA ligand binding and assembly. *J. Am. Chem. Soc. 118*, 8646–8653.

(46) Hilton, G. R., and Benesch, J. L. P. (2012) Two decades of studying non-covalent biomolecular assemblies by means of electrospray ionization mass spectrometry. *J. R. Soc. Interface 9*, 801–816.

(47) Liu, J., and Konermann, L. (2011) Protein-protein binding affinities in solution determined by electrospray mass spectrometry. *J. Am. Soc. Mass Spectrom. 22*, 408–417.

(48) Vosloo, J. A. (2016) Optimised bacterial production and characterisation of natural antimicrobial peptides with potential application in agriculture. PhD Thesis, Department of Biochemistry, University of Stellenbosch, Stellenbosch, South Africa, http://hdl.handle.net/10019.1/98411

(49) Troskie, A. M. (2014) Tyrocidines , cyclic decapeptides produced by soil bacilli , as potent inhibitors of fungal pathogens. PhD Thesis, Department of Biochemistry, University of Stellenbosch, Stellenbosch, South Africa, http://hdl.handle.net/10019.1/86162.

(50) Laubscher, W. E. (2016) Production , characterisation and activity of selected and novel antibiotic peptides from soil bacteria. MSc Thesis, Department of Biochemistry, University of Stellenbosch, Stellenbosch, South Africa.

(51) Berge, S. N. (2017) Production and characterisation of analogues of the antimicrobial tyrocidine peptides with modified aromatic amino acid residues. MSc Thesis, Department of Biochemistry, University of Stellenbosch, Stellenbosch, South Africa, http://hdl.handle.net/10019.1/103710

(52) Bent, D. V., and Hayon, E. (1975) Excited state chemistry of aromatic amino acids and related peptides. II. tyrosine. *J. Am. Chem. Soc. 97*, 2599–2606.

(53) Bent, D. V., and Hayon, E. (1975) Excited state chemistry of aromatic amino acids and related peptides. II. phenylalanine. *J. Am. Chem. Soc. 97*, 2606–2612.

(54) Bent, D. V., and Hayon, E. (1975) Excited state chemistry of aromatic amino acids and related peptides. III. tryptophan. *J. Am. Chem. Soc. 97*, 2612–2619.

(55) Teale, F. W. J., and Weber, G. (1957) Ultraviolet fluorescence of the aromatic amino acids. *Biochem. J. 65*, 476–482.

(56) Creed, D. (1984) The photophysics and photochemistry of the near-UV absorbing amino acids-I. Tryptophan and its simple derivatives. *Photochem. Photobiol. 39*, 537–562.

(57) Andrews, D. L. (1989) A unified theory of radiative and radiationless molecular energy transfer. *Chem. Phys. 135*, 195–201.

Stellenbosch University https://scholar.sun.ac.za

(58) Lakey, J. H., and Raggett, E. M. (1998) Measuring protein – protein interactions. *Curr. Opin. Struct. Biol. 8*, 119–123.

(59) Zhang, S., Marini, D. M., Hwang, W., and Santoso, S. (2002) Design of nanostructured biological materials through self-assembly of peptides and proteins. *Curr. Opin. Chem. Biol. 6*, 865–871.

(60) Whitesides, G. M., Mathias, J. P., and Seto, C. T. (1991) Molecular self-assembly and nanochemistry: A chemical strategy for the synthesis of nanostructures. *Science (80-.). 254*, 1312–1319.

(61) Vauthey, S., Santoso, S., Gong, H., Watson, N., and Zhang, S. (2002) Molecular self-assembly of surfactant-like peptides to form nanotubes and nanovesicles. *Proc. Natl. Acad. Sci. 99*, 5355–5360.

(62) Goldstein, J., Newbury, D. E., Michael, J. R., Ritchie, N. W. M., and Scot, J. H. J. Scanning electron microscopy and x-ray microanalysis Fourth.

(63) Weltzien, U. (1979) Detergent Properties of Water-soluble Choline Phosphatides Solubilization Analogs. *J. Biol. Chem. 254*, 3652–3657.

(64) Weltzien, H. U. (1979) Cytolytic and membrane-perturbing properties of lysophosphatidylcholine. *Biochim. Biophys. Acta 559*, 259–287.

(65) Faure, C., Tranchant, J. F., and Dufourc, E. J. (1996) Comparative effects of cholesterol and cholesterol sulfate on hydration and ordering of dimyristoylphosphatidylcholine membranes. *Biophys. J. 70*, 1380–1390.

(66) Pringle, S. D., Giles, K., Wildgoose, J. L., Williams, J. P., Slade, S. E., Thalassinos, K., Bateman, R. H., Bowers, M. T., and Scrivens, J. H. (2007) An investigation of the mobility separation of some peptide and protein ions using a new hybrid quadrupole / travelling wave IMS / oa-ToF instrument. *Int. J. Mass Spectrom. Ion Process. 261*, 1–12.

(67) Ridenour, W. B., Kliman, M., Mclean, J. A., and Caprioli, R. M. (2010) Structural characterization of phospholipids and peptides directly from tissue sections by MALDI traveling-wave ion mobility-mass spectrometry *82*, 1881–1889.

(68) Bush, M. F., Campuzano, I. D. G., and Robinson, C. V. (2012) Ion mobility mass spectrometry of peptide ions: effects of drift gas and calibration strategies. *Anal. Chem. 84*, 7124–7130.

(69) Bolen, E. J., and Holloway, P. W. (1990) Quenching of tryptophan fluorescence by brominated phospholipid. *Biochemistry 29*, 9638–9643.

(70) Chen, Y., and Barkley, M. D. (1998) Toward understanding tryptophan fluorescence in proteins. *Biochemistry 37*, 9976–9982.

(71) Gryczynski, I., Wiczk, W., Johnson, M. L., and Lakowicz, J. R. (1988) Lifetime distributions and anisotropy decays of indole fluorescence in cyclohexane/ethanol mixtures by frequency-domain fluorometry. *Biophys. Chem. 32*, 173–185.

Stellenbosch University https://scholar.sun.ac.za

Chapter 4

THE INFLUENCE OF FORMULANTS ON THE BIOLOGICAL ACTIVITY OF THE TYROCIDINES AND ANALOGUES

4.1 INTRODUCTION

The search for alternative chemotherapeutic drugs for the treatment of cancer has been ongoing for many years, yet no drug has been found that is successful in treating cancer without causing severe side effects or resistance development [1]. In this regard, antimicrobial peptides (AMP's) have been at the forefront in the search for alternative chemotherapeutic drugs due to speculation that the rapid membranolytic activity of AMP's, including the tyrocidines from *Brevibacillus parabrevis*, lowers the risk of drug resistance development towards them [2, 3]. Although the activity of the tyrocidines against various microorganisms (the Gram-positive bacteria [4, 5], fungi [6 ,7], malaria parasite *Plasmodium falciparum*[2]) and human erythrocytes (haemolytic activity) [8] are well established, little information is available about the anticancer activity of the tyrocidines. Results by Rautenbach *et al.*[2] revealed that the tyrocidines do not possess selectivity between cervical cancer cells (HeLa cells) and an immortal cell line namely human pulmonary epithelial (A549 cells). It is proposed that the cationic nature of the tyrocidines will allow interaction with negatively charged cell membranes of cancer cells [9] and not with the neutral cell membranes of healthy human tissue [10]. The low selectivity of many potential chemotherapeutic compounds prevents their use in the medical industry and strategies have been employed to eliminate the problem [11]. One such strategy is the formulation of drugs with lipid-based molecules which act as carrier systems for the drugs to the desirable target cell or area [12, 13]. Therefore, the tyrocidines will be formulated with three different lipid-based molecules (cholesterol, a

Stellenbosch University https://scholar.sun.ac.za

fatty acid and phospholipids) with the aim of reducing haemolytic activity and toxicity of the peptides while retaining their anticancer activity. It has been shown that the dipeptide unit plays an important part in the oligomerisation of the tyrocidines with dimers being the proposed active conformation for antimicrobial activity[14-18]. It is expected that the formulants will have influences on the aggregation/self-assembly of the peptides [19] and therefore insight into the structure-activity relationship of the peptides alone and in formulation will help to develop these peptides into successful chemotherapeutic agents. In this chapter, selected purified cyclodecapeptides, TrcA, TrcB, TrcC and TpcC, as well as the Trcmix were formulated with cholesterol sulphate (CS), palmitic acid (C16), and lysophosphatidylcholine (LPC) and a combination of CS and C16 (denoted as CSC16) and the activity towards human erythrocytes (haemolytic activity), three cancer cell lines (anticancer activity) and healthy human immortal cell lines (toxicity) was determined. Selectivity indexes were calculated from the HC_{50}, IC_{50} and LC_{50} values which eluded the peptide formulation with the greatest potential as chemotherapeutic formulation lead. Relationships between the structural characteristics of the peptides and the activity of the peptides alone and in formulation were also determined to give insight into possible mode of action of the peptides and how the formulations influence their mode of action.

4.2 MATERIALS

4.2.1 General materials

The cholesterol sulphate (CS), palmitic acid (C16), commercial tyrothricin extract, gramicidin S (GS), methanol (MeOH), Roswell Park Memorial Institute media (RPMI-1640), hydroxyethyl piperazineethanesulfonic acid (HEPES), hypoxanthine, gentamicin, sodium bicarbonate and Resazurin sodium salt were supplied by Sigma-Aldrich (St Louis, USA). Avanti® polar lipids (Alabama, USA) supplied the soy

Stellenbosch University https://scholar.sun.ac.za

lysophosphatidylcholine (LPC). The acetonitrile (ACN, HPLC-grade, far UV cut-off) was from Romil Ltd (Cambridge, United Kingdom). The ethanol (EtOH), chloroform and D-glucose was obtained from Merck (Darmstadt, Germany). Analytical grade water was prepared by filtering water from a reverse osmosis plant through a Millipore-Q® water purification system (Milford, USA). Mixed cellulose syringe filters (0.22 μm) were purchased from Merck-Millipore (Massachusetts, USA). Becton Dickson Labware (Lincoln Park, USA) supplied Falcon® tubes and Lasec (Cape Town, South Africa) supplied microfuge tubes and petri dishes. The nitrogen (N_2) gas was from AFROX (Johannesburg, South Africa). The 96-well flat bottom polypropylene microtiter plates were supplied by Thermo Fisher Scientific (Denmark). The phosphate buffered saline (PBS) ingredients (NaCl, KCl, Na_2HPO_4 and KH_2PO_4 were from Merck (Darmstadt, Germany). Packed erythrocytes (A^+) from anonymous donors were supplied by the Western Cape Blood services (National Health Laboratory, South Africa) as a 300 mL enriched erythrocyte fraction containing 100 mL saline-adenine-glucose mannitol preservative and 63 mL citrate-phosphate-dextrose anticoagulant.

4.2.2 Materials for cell culture

The European Collection of Cell Cultures (ECACC) (England, UK) and the American Type Culture Collections (ATCC) (Manassa, VA, USA) supplied the human prostatic adenocarcinoma (LNCaP) and human embryonic kidney (HEK293) cells, respectively. The human prostatic carcinoma (C4-2B) cells and human colorectal adenocarcinoma (HT-29) cells were given by Professor D Neal from Oxford University (UK) and Dr Stefan Abels from Cape Peninsula University of Technology (CPUT, Cape Town, South Africa) as generous gifts, respectively. Dulbecco's modified Eagles medium (DMEM) and RPMI-1640 media were supplied by Sigma Aldrich (St Louis, USA). The foetal calf serum (FCS), foetal bovine serum (FBS), sodium pyruvate and

Stellenbosch University https://scholar.sun.ac.za

HEPES were from Biochrom (Cambourne, UK). Gibco® (Gaithersburg, MD,USA) supplied the Penicillin-Streptomycin.

4.3 METHODS

4.3.1 The preparation of peptide formulations

The preparation of peptide formulations has been previously described in Chapter 3, section 3.3.1. A fourth formulant (mixture of CS and C16 in equimolar amounts, 1:1) was used to prepare five more peptide formulations (TrcA:CSC16, TrcB:CSC16, TrcC:CSC16, TpcC:CSC16 and Trcmix:CSC16) in a similar manner.

4.3.2 Cell culturing

The LNCaP, C4-2B and HEK 293 cells were obtained from various post-graduate students in the group of Dr. Karl Storbeck and Prof Amanda Swart in the Biochemistry department (University of Stellenbosch, Stellenbosch, South Africa). The cells were cultured by using standard cell culturing methodologies. For details about the cell culturing methodologies, refer to MSc thesis of Monique Barnard [20]. The HT-29 cells were cultured and obtained from Dr. Tanja Davis from the Physiology department (University of Stellenbosch, Stellenbosch, South Africa). All cells were grown in 90 % humidity and 5 % CO_2 at 37 °C. A summary of each cell line and the culture media supplementation is given in Table 4.1

Table 4.1-Summary of the cell culture conditions for each of the different cell lines.

Cell line	Culture media	Supplementation
LNCaP	RPMI-1640	10 % FBS, 1.5 g/L NaHCO3, 2.5 g/L D-(+)-Glucose, 1 % HEPES, 1 % sodium pyruvate and 1 % penicillin-streptomycin.
C4-2B	RPMI-1640	10 % FBS, 1.5g/L NaHCO3, 2.5 g/L D-(+)-Glucose and 1 % penicillin-streptomycin
HT-29	DMEM	10 % FBS and 1 % penicillin-streptomycin
HEK293	DMEM	10 % FCS, 1.5 g/L NaHCO3, 1 % sodium pyruvate and 1 % penicillin-streptomycin

Stellenbosch University https://scholar.sun.ac.za

4.3.3 Haemolytic dose response assay

The haemolytic activity of the peptides and the peptide formulations towards human erythrocytes was analysed by a haemolysis assay adapted from Rautenbach *et al.*[2]. Erythrocytes (A^+) from anonymous donors was washed twice with modified RPMI 1640 media (10.4 g/L RPMI 1640, 4 g/L glucose, 6 g/L HEPES, 5 g/L Albumax ^{TM} II, 2.1 g/L sodium bicarbonate and 50 mg/L gentamycin). During each washing step, the supernatant was removed after centrifugation at 1200x*g* for 3 minutes. The washed red blood cells were subsequently diluted to 2 % in PBS media (8 g/L NaCl, 0.2 g/L KCl, 1.44 g/L Na_2HPO_4 , 0.24 g/L KH_2PO_4) and stored at 4 °C. The dried pure peptides and peptide formulations were sterilised by using two methods: 1) resuspension in 50 % ACN in water (*v/v*) followed by lyophilisation; 2) placement in a glass desiccator saturated with chloroform vapour for 20 minutes. The sterilised pure peptides and peptide formulations were then made up to 1.00 mM in filter sterilised 15 % EtOH in analytical quality water (*v/v*) and analytical quality water, respectively. The sample solutions were then sonicated for ± 5 minutes and allowed to stand for either one hour or 24 hours before used in the assay. A doubling dilution series of the pure peptide and peptide formulation solutions were prepared in a sterile 96-well microtiter plate (dilution plate). Subsequently, 10 µL of peptide and peptide formulation were transferred from the dilution plate to a 96-well microtiter plate (assay plate) containing 90 µL of 2 % blood in PBS in each well, resulting in 10X dilution of the peptides and peptide formulation in the assay plate (concentrations ranging from 100 µM to 1.56 µM). The positive control (100 % haemolysis) was gramicidin S (100 µM in water) and the negative controls (0 % haemolysis) were water and 1.5 % EtOH in water. The assay plates were incubated for two hours at 37 °C, followed by centrifugation at 900x*g* for 10 min. The supernatants (10 µL of each well) were transferred to a 96-well

Stellenbosch University https://scholar.sun.ac.za

microtiter plate containing 90 µL of PBS in each well. The absorbance of the wells was measured at 415 nm with a Biotek PowerWave 340 spectrometer. The measured absorbance converted to percentage haemolysis as described by Equation 4.1

$$\%\ \text{haemolysis} = \left(\frac{A_{415nm}\ \text{of well} - \text{Average}\ A_{415nm}\ \text{of}\ 0\ \%\ \text{haemolysis}}{\text{Average}\ A_{415nm}\ \text{of}\ 100\ \%\ \text{haemolysis} - \text{Average}\ A_{415nm}\ \text{of}\ 0\ \%\ \text{haemolysis}}\right) \quad 4.1$$

4.3.4 Cell viability dose response assay

The dried pure peptides and peptide formulations were sterilised by using method 2 as described in Section 4.3.2. The sterilised pure peptides and peptide formulations were then made up to 0.50 mM in filter sterilised 15 % EtOH in water (*v/v*) and water, respectively. The sample solutions were then sonicated for ± 5 minutes and allowed to stand for either 1 hour or 24 hours before used in the assay. A doubling dilution series of the pure peptide and peptide formulation solutions were prepared in a 96-well microtiter plate (dilution plate). Subsequently, 10 µL of peptide and peptide formulation solution was transferred from the dilution plate to a 96-well microtiter plate (assay plate) containing 90 µL of target cells (LNCaP/HT-29/HEK293) at concentrations of $1x10^5$ cells/mL (for LNCaP and HEK293) and $1x10^4$ cells/mL (for HT-29), resulting in 10X dilution of the peptides and peptide formulation in the assay plate (concentrations ranging from 50 µM to 0.39 µM). The positive control (100 % proliferation inhibition) was gramicidin S (50 µM in water) and the negative controls (100 % proliferation) were water and 1.5 % EtOH in water *(v/v).* The assay plates were incubation for 20 hours in 90 % humidity and 5 % CO_2 at 37 °C, followed by addition of 10 µL resazurin reagent (0.30 mg/mL) to each well. The assay plates were incubated for another four hours (in 90 % humidity and 5 % CO_2 at 37 °C) except for the HT-29 assay plates which were incubated for another 24 hours. For C4-2B ($1x10^5$ cells/mL) the activity of the peptides and peptide formulations were only tested at a single concentration of 50 µM. The absorbance of each well was measured at 570 nm

Stellenbosch University https://scholar.sun.ac.za

and 600 nm with a Biotek PowerWave 340 spectrometer. The measured absorbance ratio of 570nm/600nm was converted to % proliferation inhibition as described by Equation 4.2

$$\%\ \text{proliferation inhibition} = \left(\frac{\frac{A_{570nm}}{600nm}\text{of well} - \text{Average}\ \frac{A_{570nm}}{600nm}\ \text{of 100 \% proliferation}}{\text{Average}\ \frac{A_{570nm}}{600nm}\ \text{of 100 \% proliferation inhibition} - \text{Average}\ \frac{A_{570nm}}{600nm}\ \text{of 100 \% proliferation}}\right) \quad 4.2$$

4.3.5 Activity data analysis

Duplicate dose response assays with two repeats were performed for each peptide and its formulations against each target cell. All data analysis was performed by using GraphPad Prism® V 5.0 software (San Diego, CA, USA). Non-linear regressions were performed and a sigmoidal curve with variable slope (Hill slope less than 7) were fitted to the dose response data. The sigmoidal curves were fitted using equation 4.3 [21].

$$Y = \frac{bottom + (top - bottom)}{1 + 10^{logIC_{50}X\ activity\ slope}} \quad 4.3$$

The top and bottom represent the percentage haemolysis/proliferation inhibition at high and low peptide and peptide formulation concentrations, respectively. The 50 % haemolytic activity (HC_{50}), 50 % LNCaP/HT-29 proliferation inhibitory concentrations (IC_{50}) and 50 % lethal concentration (LC_{50}) for HEK293 cells were determined as described by Rautenbach *et al*. [21]. The selectivity was determined by ratios of HC_{50}/IC_{50} or LC_{50}/IC_{50} and was defined as selectivity indexes. Statistical analyses were performed by determining Row totals/means with standard deviation (SD) followed by One-way analysis of variance (ANOVA) with Bonferroni multiple/selected comparison post test.

Stellenbosch University https://scholar.sun.ac.za

4.4 RESULTS AND DISCUSSION

4.4.1 Haemolytic activity of the peptides and peptide formulations

The tyrocidines have been shown to possess haemolytic activity in the micromolar (µM) range[8] which ultimately prevents their use as drugs for the systemic treatment of bacterial and fungal infections as well as for cancer. It has been shown that the formulation of such toxic peptides with various molecules (including lipids, polymers and steroids) can significantly reduce the toxic activity of AMPs by acting as delivery systems for the peptides to the target cells[11-13].Therefore, the tyrocidines (TrcA, TrcB, TrcC and TpcC) were formulated with three lipid-based molecules CS, LPC and C16 and the haemolytic activity of each determined. To ensure sterility of the peptides and peptide formulations, two different methods were tested : in method 1 the peptides and peptide formulations were incubated in a glass vessel saturated with chloroform vapour; and in method 2 the peptides and peptide formulations were resuspended in 50 % ACN in water (*v/v*) and lyophilised. The haemolytic activity of the peptides and peptide formulations were first determined by using sterilisation method 1. The samples were then resuspended in 15 % EtOH in water (for pure peptides) and in water (for the formulations) and allowed to stand for 24 hours before performing the haemolytic dose responses. The haemolytic dose responses revealed that the HC_{50} values increases in the following order (TrcB,TrcA,TpcC) <TrcC, with peptides in brackets having statistically similar HC_{50} values (Table 4.2). TrcA, TrcB and Trcmix all had HC_{50} values of less than 15 µM (Table 4.2). These values correlate well with previously determined HC_{50} values for these Trcs in the range of 2-11 µM [2, 22], especially TrcB which was also found by Rautenbach *et al*. [2] to be the most haemolytic. On the other hand, the HC_{50} values for TrcC and TpcC were much higher than reported by other studies [2, 23] (making them the peptides with the lowest haemolytic activity in

Stellenbosch University https://scholar.sun.ac.za

this study), possibly due to the effects of the peptide and peptide formulations preparation which entails the suspension in 90 % MeOH in water (*v/v*) followed by evaporation with N_2 gas (refer to methods, Section 4.3.1). Another possible explanation could be peptide self-assembly during the 24-hour maturation period, which would allow the peptides to form different self-assembly structures, especially for the C analogues that contain at least two Trp residues (unpublished data from a member of our group, V. Kumar and M. Rautenbach). It has also been shown that Phe allows deeper penetration into the cell membrane of target cells than Trp residues[2, 24-26], therefore it makes sense that the peptides with the most Trp residues (TrcC and TpcC) will have less haemolytic activity (higher HC_{50} values) than their Phe (TrcA and TrcB) counterparts. The L-Lys^9/Orn^9 has been proposed to insert into the negatively charged membranes of target cells via the so called “snorkelling effect” thereby causing cell lysis [2, 27]. The fact that the C analogues present the lowest haemolytic activity suggests that self-assembly of the C analogues with the bulkier Trp residues may place the L-Orn^9 in a position that sterically prevents it from readily associating and inserting into the cell membrane of red blood cells which may then also lower the haemolytic activity of the peptides in an additional way. Of the formulations, the CS and C16 had the largest influence on all the peptides, with significant increases in HC_{50} seen for TrcA:CS/C16, TrcB:CS/C16, TrcC:CS/C16, TpcC:CS/C16 and Trcmix:CS (Table 4.2). It is proposed that the anionic sulphate group of CS interacts with the cationic amino group of L-Orn^9, thereby shielding it and preventing red blood cell membrane interaction, whereas the hydrophobic ring/carbon tail of CS in turn associates with the aromatic dipeptide unit preventing their membrane interaction.

Stellenbosch University https://scholar.sun.ac.za

Table 4.2 A summary of the haemolytic activities (HC_{50} in µM) of the peptides and peptide formulations. The dose response curves for each of the peptides with the respective formulations are given. Each HC_{50} is represented by two biological assays, each with two technical repeats.

Identity	Abbr.	Dose response curve	HC_{50} ± SD (n) (µM)
Tyrocidine A formulations (Cyclo-(fP**Ff**NQYVOL)			
Tyrocidine A	TrcA	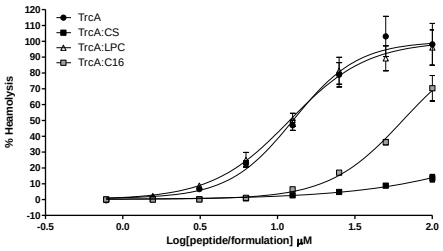	12.8 ± 1.3 (2)
Formulated with CS	TrcA:CS		**851 ± 210 (2)*
Formulated with LPC	TrcA:LPC		12.2 ± 0.5 (2)
Formulated with C16	TrcA:C16		65.7 ± 5.5 (2)
Tyrocidine B formulations Cyclo-(fP**Wf**NQYVOL)			
Tyrocidine B	TrcB	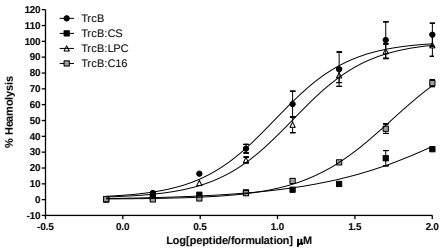	9.63 ± 0.9 (2)
Formulated with CS	TrcB:CS		**211± 9.4* (2)
Formulated with LPC	TrcB:LPC		12.6 ± 1.0 (2)
Formulated with C16	TrcB:C16		54.7 ± 0.3 (2)
Tyrocidine C formulations Cyclo-(fP**WW**NQYVOL)			
Tyrocidine C	TrcC	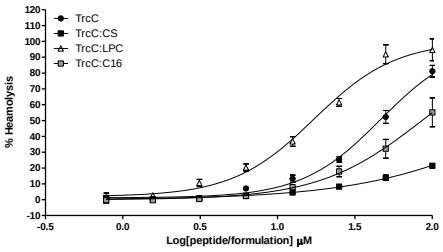	46.3 ± 1.4 (2)
Formulated with CS	Trcc:CS		**419 ±4.5* (2)
Formulated with LPC	TrcC:LPC		17.3 ± 1.4 (2)
Formulated with C16	TrcC:C16		90.1 ± 28 (2)
Tryptocidine C formulations Cyclo-(fP**WW**NQWVOL)			
Tryptocidine C	TpcC	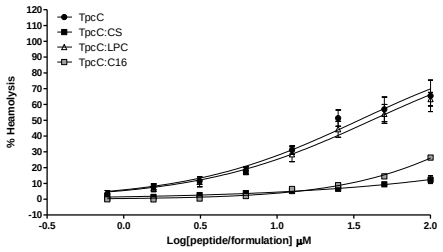	35.9 ± 12 (2)
Formulated with CS	Tpcc:CS		**4690 ± 1020* (2)
Formulated with LPC	TpcC:LPC		42.1 ± 12 (2)
Formulated with C16	TpcC:C16		**300 ± 4.0* (2)
Tyrocidine mixture formulations			
Tyrocidine mixture	Trcmix	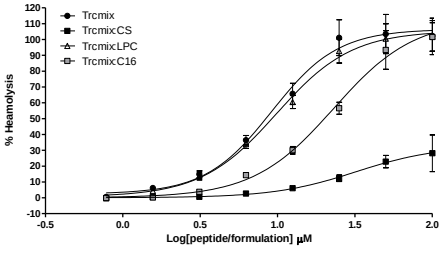	8.59 ± 0.5 (2)
Formulated with CS	Trcmix:CS		**287 ±110* (2)
Formulated with LPC	Trcmix:LPC		9.33 ± 0.9 (2)
Formulated with C16	Trcmix:C16		20.0 ± 1.4 (2)

The number of repeats is represented by n; * Predicted HC_{50} values from dose-response; Refer to addendum Table 4.8 for statistical analysis of the haemolysis data.

Stellenbosch University https://scholar.sun.ac.za

The TpcC:CS resulted in the largest increase in HC_{50}, possibly due to the lack of L-Tyr^7 which implicates this residue in the facilitation of haemolytic activity. LPC as formulant did not have a significant influence on the haemolytic activity of TrcA, TrcB, TrcC, TpcC and Trcmix (Table 4.2).

Interestingly, LPC increased the haemolytic activity of TrcC (not significantly), which may indicate that the interaction of LPC with L-Trp^4 in the dipeptide unit places the L-Tyr^7 residue in a position which facilitates increased haemolytic activity.

The fact that LPC did not have the same effect on TpcC, which also contains L-Trp^4 but not L-Tyr^7, further strengthens the hypothesis that the position of L-Tyr^7 is important to elicit haemolytic activity. The C16, similarly to CS, increased HC_{50} values of TrcA, TrcB and TrcC, with the greatest effect on TpcC. However, TrcB was the only peptide formulated with C16 which had significantly higher HC_{50} value compared to peptide alone. This increase in HC_{50} by C16 as formulant indicates that the anionic carboxyl group and hydrophobic carbon tail of C16 possibly interacts with the L-Orn^9 and the aromatic dipeptide unit thereby preventing membrane insertion and changing the position/exposure of L-Tyr^7.

The haemolytic activity of the peptides and peptide formulations were tested using sterilisation method 2 which entails the resuspension in 50 % ACN in water (*v/v*) followed by lyophilisation. Subsequently, the peptides and peptide formulations were resuspended in 15 % EtOH in water and water, respectively, and the dose responses were performed. The HC_{50} values were expected to remain constant, however, the opposite was observed. Almost all the HC_{50} values decreased (increased haemolytic activity), with significant decreases observed for all the CS formulations and C16 formulations of TrcB and TrcC, by using the sterilisation method 2 (Table 4.3). This indicates the effect that solvent systems and preparation methods have on the self-

Stellenbosch University https://scholar.sun.ac.za

assembly of the peptides alone or in formulations. It has been shown that solvent does affect the aggregation of the peptides [19] , therefore it is proposed that the acetonitrile combined with the lyophilisation step in method 2 is responsible for the disruption of interaction of the formulants with the peptides which eliminates the suppression of the haemolytic activity. It was therefore decided that sterilisation method 1 will be used to decontaminate all peptide and peptide formulation samples used in the rest of the activity assays.

To assess whether the haemolytic activity will be influenced if the peptides and peptide formulations were allowed less time to mature, the % haemolytic activity at one peptide concentration (50 μM) were determined after samples were one hour old (Figure 4.1 A-E). In general, no significant changes were observed in the haemolytic activity of the peptides alone and in formulation with LPC between 1-hour and the 24-hour maturation period. However, the haemolytic activity of TrcC decreased when allowed to mature for 24 hours which may be due to formation of more compact aggregates leading to less exposure of the polar groups of L-Orn^{9}and L-Tyr^{7}, hypothesised in this study to be responsible for elicitation of haemolytic activity (Figure 4.1 C). For TrcA, TrcC and TpcC (Figure 4.1 A, C and D) opposite effects were observed for the CS and C16 formulations. The % haemolytic activity at 50 μM of the TrcA, TrcC and TpcC CS formulations did not significantly increase when allowed 24-hour maturation, whereas that of the C16 formulations were decreased significantly, except for TpcC:C16 (Figure 4.1 A, C and D). It is likely that the assembly and disassembly induced by the CS doesn't reach an equilibrium at one hour, therefore polar groups and the side chains of the dipeptide unit may become more exposed in the peptides after 24-hour time period. Conversely, the C16 possibly increases shielding of the peptides over time leading to less exposure of the polar groups and dipeptide unit. TrcB (Figure 4.1 B)

Stellenbosch University https://scholar.sun.ac.za

follows the same trend as the other peptides (% haemolysis of TrcB:CS significantly increased) except that the haemolytic activity of the C16 formulation did not increase significantly over time.

Table 4.3-Summary of the haemolytic activity (HC_{50} in µM) of the peptides and peptide formulations observed between two different sterilisation methods. The HC_{50} values were all determined from 2 biological repeats each with duplicate technical repeats.

Identity	HC_{50} ± SD		Influence [a]
	Sterility method 1	Sterility method 2	
TrcA	12.8 ± 1.2	7.23 ± 0.1	slight
TrcA:CS	851 ± 210*	26.7 ± 3.3	negative
TrcA:LPC	12.2 ± 0.5	9.20 ± 2.8	no influence
TrcA:C16	65.7 ± 5.5	18.9 ± 5.6	negative
TrcB	9.63 ± 0.9	9.97 ± 0.4	no influence
TrcB:CS	211 ± 9.4*	56.7 ± 1.8	negative
TrcB:LPC	12.6 ± 1.0	10.9 ± 0.4	no influence
TrcB:C16	54.7 ± 0.3	18.0 ± 1.8	negative
TrcC	46.3± 1.4	10.7 ± 1.2	negative
TrcC:CS	419 ± 4.5*	20.6 ± 1.0	negative
TrcC:LPC	17.3 ± 1.4	11.3 ± 0.2	slight
TrcC:C16	90.1 ± 28	13.9 ± 0.2	negative
TpcC	35.9 ± 12	15.1 ± 1.8	negative
Tpcc:CS	4691 ± 1018*	46.1 ± 0.3	negative
TpcC:LPC	42.1 ± 12	14.4 ± 3.0	negative
TpcC:C16	300 ± 4.0*	24.5 ± 7.4	negative
Trcmix	8.59 ± 0.5	8.30 ± 1.0	no influence
Trcmix:CS	287 ± 112*	71.9 ± 4.6	negative
Trcmix:LPC	9.33 ± 0.9	9.83 ± 0.7	no influence
Trcmix:C16	20.0 ± 1.4	10.8 ± 0.7	negative

[a]A >2fold decrease of HC_{50} value by using sterilisation method 2 is deemed negative. * Predicted HC_{50} values from dose-response. Refer to addendum Table 4.9 for statistical analysis of the haemolysis data.

Stellenbosch University https://scholar.sun.ac.za

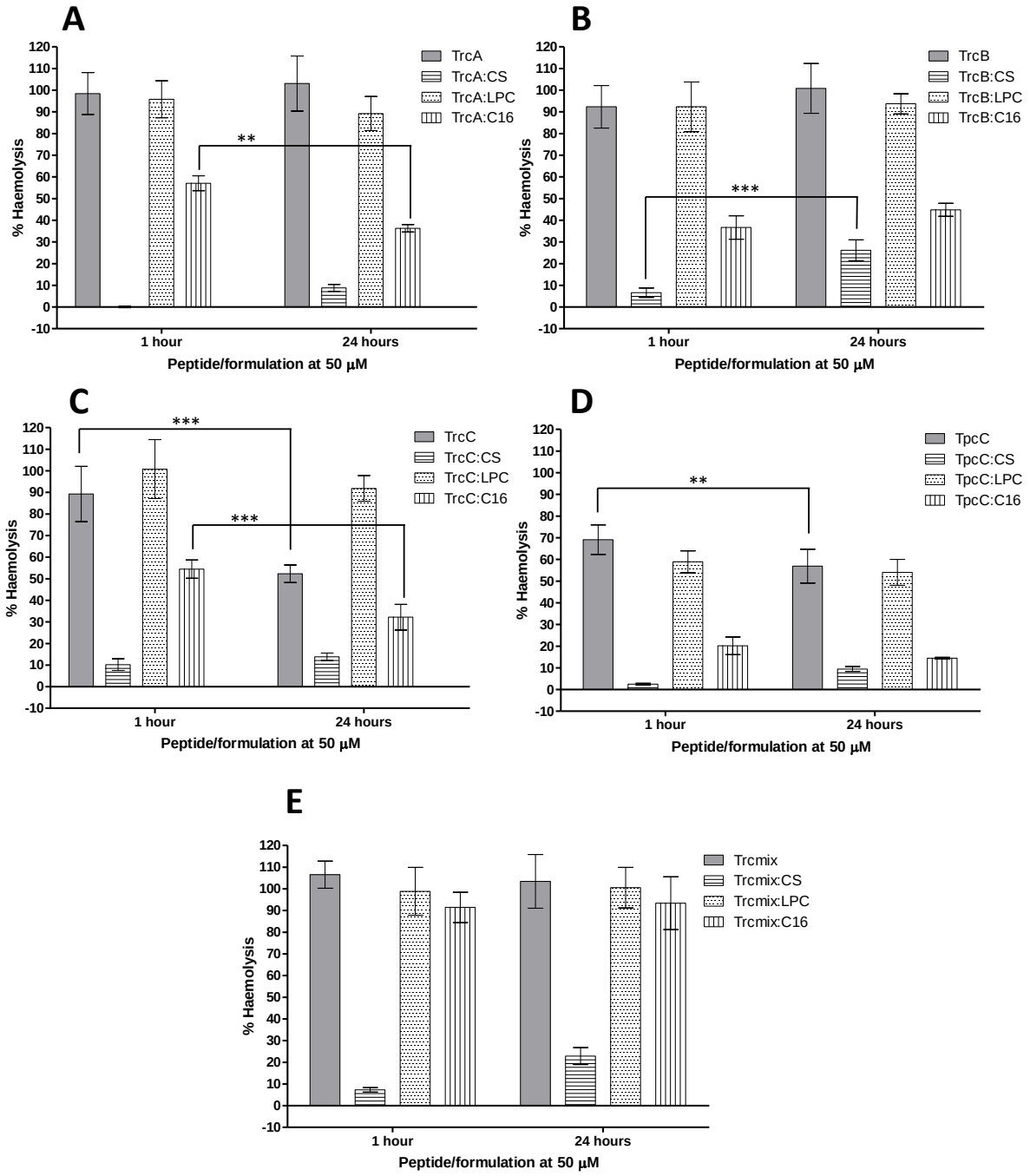

Figure 4.1 The haemolytic activity of the peptides and peptide formulations at 50 µM when allowed a 1 hour versus a 24-hour maturation period. Haemolytic activity for the A) TrcA with formulations, B) TrcB with formulations, C) TrcC with formulations, D) TpcC with formulations and E) Trcmix with formulations. Each bar represents the average of 4 repeats from two biological repeats, each with two technical repeats. Refer to addendum Table 4.10 for statistical analysis of the haemolysis data. P-values > 0.05 ns (not shown on graph), P-values < 0.05 = *, P-values < 0.01 = **, P-values < 0.001 = ***.

The haemolytic activity for Trcmix formulation with LPC and C16 did not change over time, however, the haemolytic activity of the CS formulations increases similarly to the

Stellenbosch University https://scholar.sun.ac.za

rest of the peptides (Figure 4.1 E). It is clear that the self-assembled states and exposure of certain groups of these peptides are everchanging and can be influenced by many different factors including preparation method (Table 4.3) and time (Figure 4.1 A-E) which in turn dictates their activity. Taken together, the CS formulation influenced the toxicity of the peptides to the largest extent and lower haemolytic activities for the CS formulations were observed at 1-hour maturation period compared to 24-hour maturation for all the peptides.

Therefore, one hour of maturation was allowed for all the samples for the rest of the biological activity studies done in this chapter. Because C16 also lowered the haemolytic activity of the peptides substantially for all the peptides (excluding Trcmix), it was decided to test the combination of CS and C16 on the haemolytic activity of the peptides. The combination revealed TpcC:CSC16 had the lowest % haemolytic activity at 50 µM (Figure 4.2) which agrees with the hypothesis that substitution of L-Tyr^{7} with Trp results in less insertion of residue 7 which may play a role in haemolytic activity. Overall, the CSC16 formulation decreased the haemolytic activity of all the peptides significantly, with an increase in % haemolysis observed in the following order TrcA<TrcB<TrcC (Figure 4.2). This gradual increase indicates that the dipeptide unit is implicated in the haemolytic activity of the combinatorial formulation with an addition of Trp residue each time leading to an increase in % haemolysis.

Stellenbosch University https://scholar.sun.ac.za

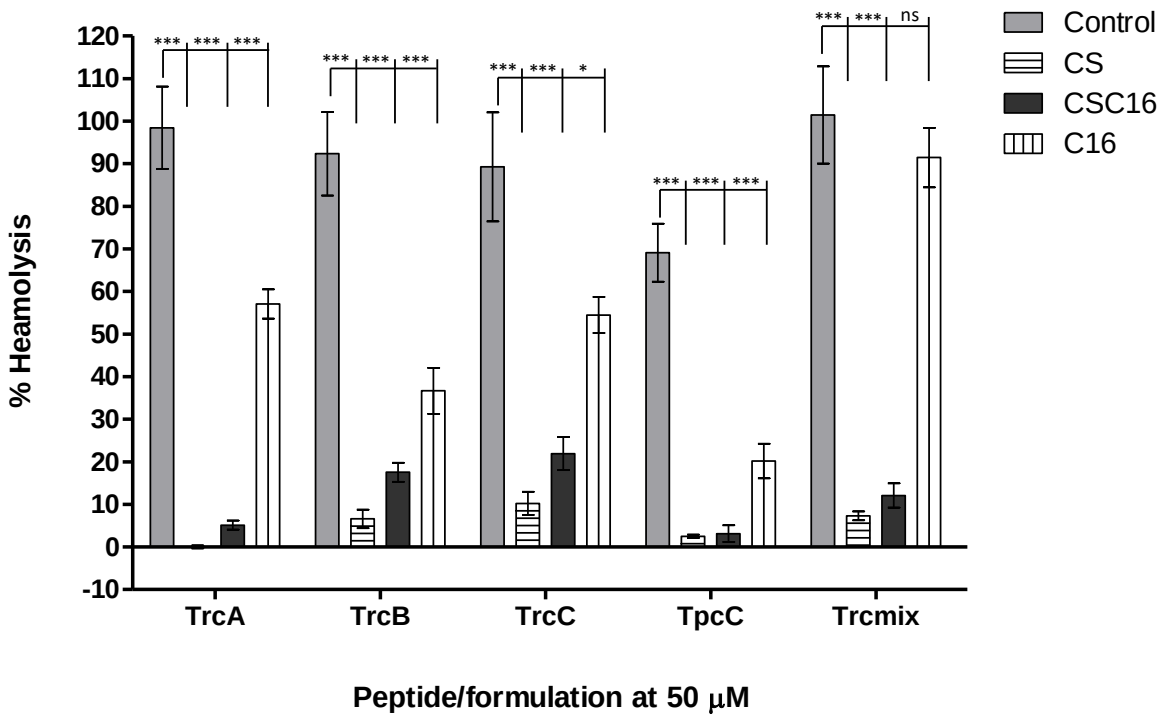

Figure 4.2 Comparison of the % haemolysis induced by the peptides alone and the peptides in formulation with CS, C16 and a combination of CS and C16 (CSC16). The percentage haemolysis was determined at peptide or peptide formulation concentration of 50 μM and 1-hour sample maturation period. Each bar represents the average of 4 repeats. Refer to addendum Table 4.8 for statistical analysis of the haemolysis data. P-values > 0.05 ns, P-values < 0.05 = *, P-values < 0.01 = **, P-values < 0.001 = ***.

This is likely due to larger aggregates forming when there are more Trp residues thereby hampering both the shielding of cationic L-Orn[9] by CSC16 and the exposure of L-Tyr[7]. An increase in haemolytic activity is also observed for the CS formulations of TrcA, TrcB and TrcC in the order of TrcA>TrcB>TrcC (Figure 4.2), similar to the CSC16 formulations. This is not the case for the C16 formulations alone, indicating that the influence of C16 on the peptide aggregation/self-assembly is overpowered by the CS in the CSC16 formulations. It is likely that the sulphate group and/or the hydrophobic ring/tail structure of CS forms a stronger interaction with the polar residues and dipeptide unit compared to C16.

Stellenbosch University https://scholar.sun.ac.za

4.4.2 Biological activity of the peptides and peptide formulations

The Trcs possess activity against a broad spectrum of different microorganisms including Gram-positive bacteria such as *Listeria monocytogenes* and *Micrococcus luteus* [4, 5, 23], fungi such as *Candida albicans* [7], *Botrytis cinereal* and *Fusarium* spp [6], and the malaria parasite *Plasmodium falciparum* [2]. The activity of the Trcs doesn't stop at microorganisms, as results from Rautenbach *et al*. [2] showed activity against HeLa cervical cancer cells with IC_{50} values ranging from 13 to 28 µM for the six major Trcs. These results sparked an interest in the activity of the Trcs against other types of cancer. Therefore, the anticancer activity of the Trcs and the formulations against three different cancer cell lines (LNCaP, C4-2B and HT-29), two of which are prostate cancer cell lines (LNCaP, C4-2B) were investigated. It is also important that the toxicity of these peptides and their formulations are tested against mammalian non-cancerous cells, as to evaluate selectivity of the peptide formulations. The Trcs and formulations were therefore also tested against human embryonic kidney cells (HEK293) an immortal cell line.

Full dose responses were only performed on LNCaP, HT-29 and HEK293 cells with all the peptide and formulations, but the CSC16 formulations could only be tested towards HT-29 and HEK293 cells due limited amount of the pure and fully characterised peptides. As a result, the activity of the Trcs and formulations could only be tested at one concentration against the C4-2B cancer cells. A representative peptide, TrcA, was chosen to display the dose response data acquired for each of the peptides and their formulations against each of the cancer cell lines (Figure 4.3). The IC_{50} values (for LNCaP and HT-29) and LC_{50} values (for HEK293) are summarised in Table 4.4. The HT-29 IC_{50} values for the peptides alone (including Trcmix) ranged from 6.86 to 8.49 µM and in formulation with CS, LPC, C16 and CSC16 ranged

Stellenbosch University https://scholar.sun.ac.za

between 6.87 to 27.6 µM (Table 4.4). The LNCaP IC_{50} values were in similar ranges as observed for HT-29, with IC_{50} values for the peptides alone (including Trcmix) ranging from 6.62-13.2 µM, and in formulation with CS, LPC and C16 ranging between 6.09-44.1 µM (Table 4.4). From the IC_{50} values of the peptides alone and in formulation, no clear trend could be observed indicating that the primary structure does not dictate the anticancer activity of the peptides and that membranolytic activity is likely not the sole mechanism of action of the peptides towards cancer cells. It is probable that the peptides may be translocated/internalised into the cancer cells, considering that multiple internal targets have been proposed for AMPs such as the enzymes of the electron transport chain, RNA and DNA, and nucleic acid and protein synthesis. Furthermore, it was observed that CS, C16 and CSC16 lower the activity of all the peptides (with a few significant increases in IC_{50} values) towards HT-29 and LNCaP to some extent (less than observed for haemolytic activity), whereas LPC has no marked influence on the activity of the peptides. This indicates and further strengthens the theory that the mechanism of action of the Trcs towards red blood cells and cancer cells are different.

Stellenbosch University https://scholar.sun.ac.za

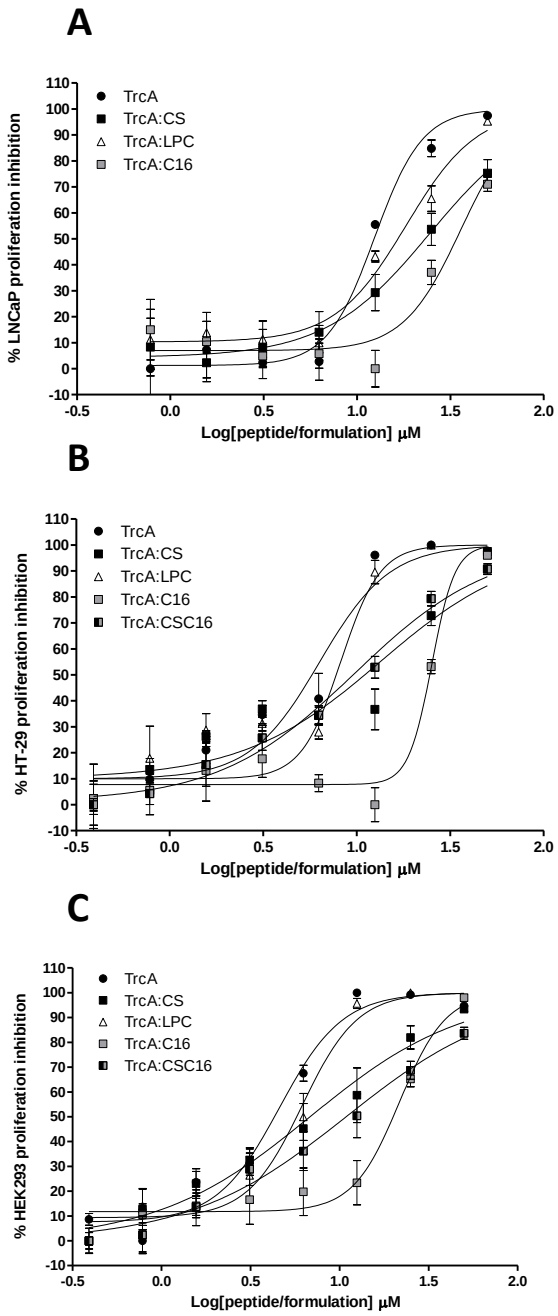

Figure 4.3 Representative dose response assays to determine the activity of TrcA and TrcA peptide formulations against A) LNCaP, B) HT-29 and C) HEK293 cells. Each data point is represented by two technical repeats from duplicate biological repeats, with error bar indicating the SD.

Considering the internalisation and targeting of internal targets, it is reasonable that the CS and C16 hamper the internalisation of the peptides or the release of the peptides once internalised into cancer cells leading to decrease in anticancer activity.

Stellenbosch University https://scholar.sun.ac.za

Unfortunately, the formulation of peptides did not decrease the toxicity of the peptides to a large extent towards non-cancerous (HEK293) cells for most of the peptides. The LC_{50} values against HEK293 cells for the peptides alone (including Trcmix) ranged from 3.47-7.81 µM, and in formulation with CS, LPC, C16 and CSC16 ranged between 5.03-57.4 µM (Table 4.4). Similar to the observed results for HT-29 and LNCaP, no clear relationship was observed between the primary structures of the peptides and the activity towards HEK293 cells. However, a decrease in toxicity of the peptides is also observed when formulated with CS (significant decreases seen for TrcB and Trcmix) and C16 (significant decreases seen for all of the peptides). The fact that the activity (IC_{50} and LC_{50} values) of the peptides towards the cancer cells and the non-cancerous cells are similar, indicates that neither the overall negative charge of the target cell nor the cationic L-Lys/L-Orn^9 of the Trcs is necessary for activity and that alternative targets exist.

The % haemolysis/proliferation inhibition of the peptides alone and in formulation with CS, C16 and CSC16 (where applicable) are displayed at 50 and 25 µM (Figure 4.4 A-H) to assess which peptide and formulation had the lowest activity towards human erythrocytes (RBC) and HEK293 cells, while retaining activity towards cancer cells (HT-29, LNCaP and C4-2B where applicable). At 50 µM, the CSC16 formulation decreased the % toxicity of TrcA, TrcB and TrcC (Figure 4.4 A, B, C) the most, whereas the C16 formulation decreased the toxicity of TpcC (Figure 4.4 D) the most.

Although the toxicity of TrcA, TrcB, and TrcC was decreased with the CSC16 formulation, the activity towards HT-29 and C4-2B were also decreased. However, for TrcA:CSC16 and TrcB:CSC16 the activity towards HT-29 and C4-2B was ± 10% higher than towards HEK293 cells, indicating decreased toxicity (Figure 4.4 A and B).

Stellenbosch University https://scholar.sun.ac.za

Table 4.4 The activity of the peptides and peptide formulations towards HT-29, LNCaP and HEK293 cells. The IC_{50} and LC_{50} values were determined from duplicate biological assays each consisting of two technical repeats.

Identity	IC_{50} ± SD (µM)		LC_{50} ± SD (µM)
	Towards HT-29	Towards LNCaP	Towards HEK293
TrcA	6.86 ± 2.3	13.2 ± 2.8	4.46 ± 0.7
TrcA:CS	20.5 ± 5.3	26.3 ± 7.9	10.6 ± 5.7
TrcA:LPC	9.39 ± 1.8	19.0 ± 4.6	6.31 ± 1.4
TrcA:C16	25.1 ± 1.7	36.1 ± 3.7	20.6 ± 4.5
TrcA:CSC16	10.9 ± 0.5	N.A.[a]	10.8 ± 3.8
TrcB	8.49 ± 1.3	8.71 ± 1.2	7.81 ± 0.6
TrcB:CS	8.64 ± 1.5	15.3 ± 1.0	11.2 ± 0.1
TrcB:LPC	7.93 ± 0.2	11.0 ± 0.1	8.51 ± 0.3
TrcB:C16	26.6 ± 0.2	44.1 ± 3.7	29.8 ± 1.5
TrcB:CSC16	11.2 ± 2.0	N.A.[a]	N.A.[a]
TrcC	6.96 ± 1.8	12.3 ± 2.1	6.65 ± 1.0
Trcc:CS	6.87 ± 1.8	18.7 ± 2.6	10.9 ± 1.2
TrcC:LPC	6.95 ± 1.2	8.82 ± 1.7	8.58 ± 0.2
TrcC:C16	17.0 ± 0.8	27.4 ± 3.7	18.5 ± 6.1
TrcC:CSC16	8.49 ± 4.1	N.A.[a]	5.40 ± 0.7
TpcC	7.23 ± 2.1	6.94 ± 0.1	3.47 ± 1.6
Tpcc:CS	7.44 ± 3.2	13.7 ± 0.9	5.03 ± 1.7
TpcC:LPC	8.08 ± 0.2	11.4 ± 3.6	8.01 ± 0.2
TpcC:C16	N.A.[a]	36.2 ± 5.9	57.4 ± 3.5
TpcC:CSC16	8.49 ± 4.1	N.A.[a]	6.90 ± 3.2
Trcmix	7.10 ± 0.3	6.62 ± 0.5	5.00 ± 0.4
Trcmix:CS	27.6 ± 3.9	27.0 ± 3.2	13.5 ± 4.0
Trcmix:LPC	7.55 ± 0.4	6.09 ± 0.3	6.04 ± 0.1
Trcmix:C16	15.4 ± 0.1	10.4 ± 0.5	13.3 ± 0.4
Trcmix:CSC16	12.0 ± 5.2	N.A.[a]	8.50 ± 0.1

[a] Data not feasible for determination of IC_{50} or LC_{50} values. Refer to addendum Table 4.11 and 4.12 for statistical analysis of the anticancer and toxicity data.

The toxicity of TpcC:C16 towards HEK293 cells was decreased to below 55 % at 50 µM concentration, while still retaining more than 80 % and 65% activity towards C4-2B and LNCaP, respectively (Figure 4.4 D). At 25 µM, the C16 formulation decreased the % toxicity of TrcB and TpcC the most, whereas the CSC16 and C16 formulations both decreased the toxicity of TrcA and TrcC the most (Figure 4.4 E-H).

Stellenbosch University https://scholar.sun.ac.za

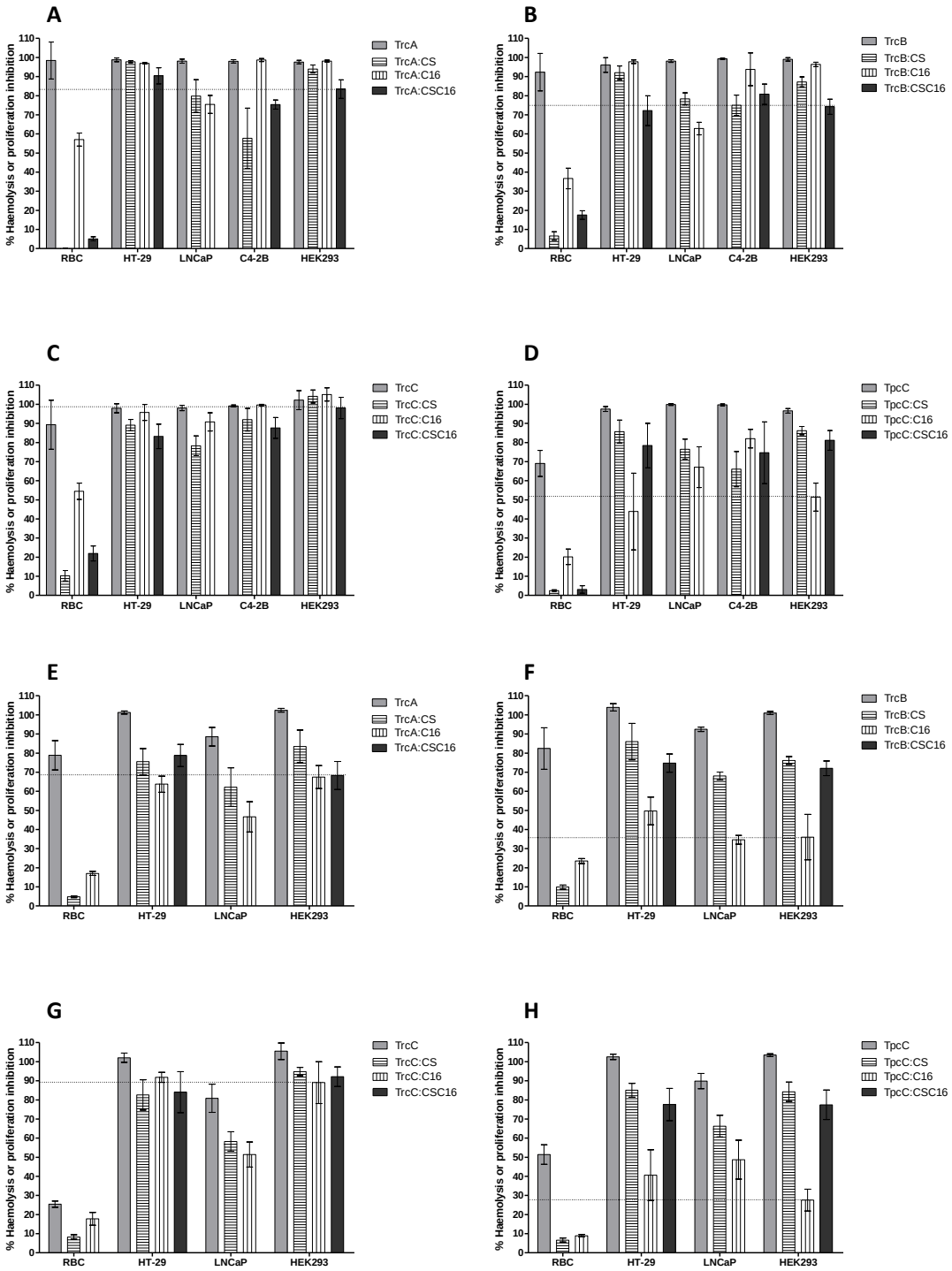

Figure 4.4 Comparison of the activities of the Trcs and Trc formulations toward human red blood cells (RBC), HEK293, HT-29, LNCaP and C4-2B cells at a specific concentration of 50µM (A-D) and 25 µM (E-H) with A and E) TrcA alone and in formulation; B and F) TrcB alone and in formulation C and G) TrcC alone and in formulation D and H) TpcC alone and in formulation. Note that the CSC16 formulation was not evaluated against the LNCaP cells. The dotted line in each graph indicates which peptide formulation has the lowest activity toward HEK293 cells. Refer to addendum table 4.13 for statistical analysis of the anticancer and toxicity data.

Stellenbosch University https://scholar.sun.ac.za

Their activity towards HT-29 and LNCaP of TpcC:C16 is 10-20 % higher than towards HEK293 cells (Figure 4.4 E-H). Therefore, at both 50 µM and 25 µM the TpcC:C16 formulation has the lowest toxicity toward RBC and HEK293 cells, while retaining more than 50 % activity toward at least one of the cancer cell lines.

4.4.3 Selectivity and structure-activity analysis of the peptides and peptide formulations

From the biological activity analysis, it was evident that CS and C16 were the formulations that worked the best. To gain insight into structure-activity relationships of the Trcs (TrcA, TrcB, TrcC and TpcC) alone and in formulation with CS and C16, two physicochemical parameters were correlated with biological activity (HC_{50}, IC_{50} and LC_{50}) and *in vitro* selectivity (HC_{50}/IC_{50} and LC_{50}/IC_{50}). The retention time (R_t) and the Σ side chain surface area (SCSA) were the two physicochemical parameters chosen to represent the apparent hydrophobicity and peptide size/volume, respectively. The retention times were determined from the C_{18} UPLC chromatograms (refer to Chapter 2) of the pure peptides and the side chain surface areas were taken from Frecer [28], as calculated from Connolly surfaces [29]. A summary of al the physicochemical descriptors of the peptides are given in Table 4.5.

Table 4.5 Summary of the physicochemical descriptors of the tyrocidines with the variable amino acid residues at position 3, 4, 7, and 9 are given where Phe, Trp, Tyr and Orn depicted by F, W, Y and O, respectively.

Identity	Variable Residues[a]	UPLC R_t[b] (min)	Σ side chain surface area[c] (Å)
TrcA	F^3-f^4-Y^7-O^9	10.78	796.7
TrcB	W^3-f^4-Y^7-O^9	9.68	825.6
TrcC	W^3-w^4-Y^7-O^9	9.19	854.5
TpcC	W^3-w^4-W^7-O^9	9.49	873.6

[a] D-amino acids and L-amino acids are represented by lower case and upper-case letters, respectively.
[b] Retention times were determined from C_{18} UPLC chromatograms of the purified peptides
[c] The sum of the side chain surface areas of the constituent amino acids of the peptides were determined from [28] as calculated from Connolly surfaces [29]

Stellenbosch University https://scholar.sun.ac.za

The physicochemical parameters were correlated with the biological activity and selectivity of the non-formulated peptides first, as to establish any structure-activity relationship that may exist before investigating the influence of the formulations on these relationships. No direct relationship could be observed between the IC_{50} or LC_{50} values and the retention times (hydrophobicity) and SCSA of the Trcs (Figure 4.5 A and B). However, the haemolytic activity of the peptides is influenced by both the hydrophobicity and peptide size/volume (Figure 4.5 A and B). The above-mentioned results agree with the theory mentioned previously that the mechanism of action toward RBC and cancerous/non-cancerous cells are different. As hydrophobicity increases (TrcC<TpcC<TrcB<TrcA) the haemolytic activity increases indicating that Phe containing peptides are more haemolytic, possibly due to deeper penetration into cell membrane by Phe residue side chains [25, 26]. The opposite trend is observed for the SCSA, with decreasing haemolytic activity observed as SCSA increases (TrcA<TrcB<TrcC<TpcC), suggesting that larger sized peptides (containing more than one Trp residue) cannot penetrate the cell membrane as deep as the Phe residues leading to decreased red blood cell membrane disruption [24]. Taken together, smaller more hydrophobic peptides (TrcA and TrcB) are more haemolytic, possibly due to deeper insertion of Phe residues into the cell membrane and stronger interaction with hydrophobic phospholipid tails of the cell membrane lipid bilayer.

Stellenbosch University https://scholar.sun.ac.za

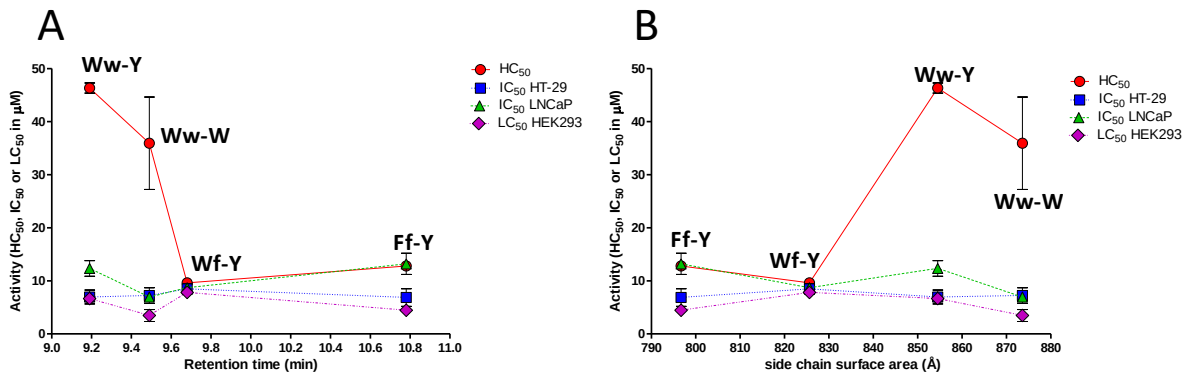

Figure 4.5 The relationship between the tyrocidine activity and peptide hydrophobicity or Σ side chain surface area. A) The peptide activity towards erythrocytes (HC_{50}), HT-29 and LNCaP cancer cells (IC_{50}) and HEK293 mammalian cells (LC_{50}) plotted against the C_{18} UPLC retention time of the tyrocidines. B) The peptide activity towards erythrocytes (HC_{50}), HT-29 and LNCaP cancer cells (IC_{50}) and HEK293 mammalian cells (LC_{50}) plotted against the Σ side chain surface area of the tyrocidines.

Now that it has been established that there is no trend between the peptide size or apparent hydrophobicity and the activity of the peptides towards cancer and mammalian immortal cell lines, the effect of the C16 and CS formulations on the activity of the peptides can be determined. Opposing or mirror trends are seen between the activity of both CS and C16 formulations and the SCSA and hydrophobicity of the peptides indicating that CS and C16 have opposite effects on the anticancer activity of the peptides (Figure 4.6 A-B). These opposite effects seem to be more pronounced for TpcC (Ww-W) and TrcB (Wf-Y), indicating interaction of the formulants with the dipeptide unit leading to decreased or increased anticancer activity. Assuming internalisation and attack of internal targets of cancer cells by the tyrocidines, it is probable that the hydrophobic parts of the formulants (C16 carbon tail and CS carbon ring/tail structure) associate differently with the smaller more hydrophobic peptide dipeptide unit, leading to either entrapment (stronger C16-peptide interaction) or release (weaker CS-peptide interaction) of the peptides once internalised.

Stellenbosch University https://scholar.sun.ac.za

Considering the SEM and TWIM-MS data from Chapter 3, where C16 causes increased disruption of self-assembled spheres and loss of ionic specie signal compared to CS stabilising the spheres and maintained ionic signal, it is possible that less peptide molecules are internalised in an interacting lipid-peptide "bolus" and released from the C16 formulation compared to CS formulation due to stronger C16-peptide interaction.

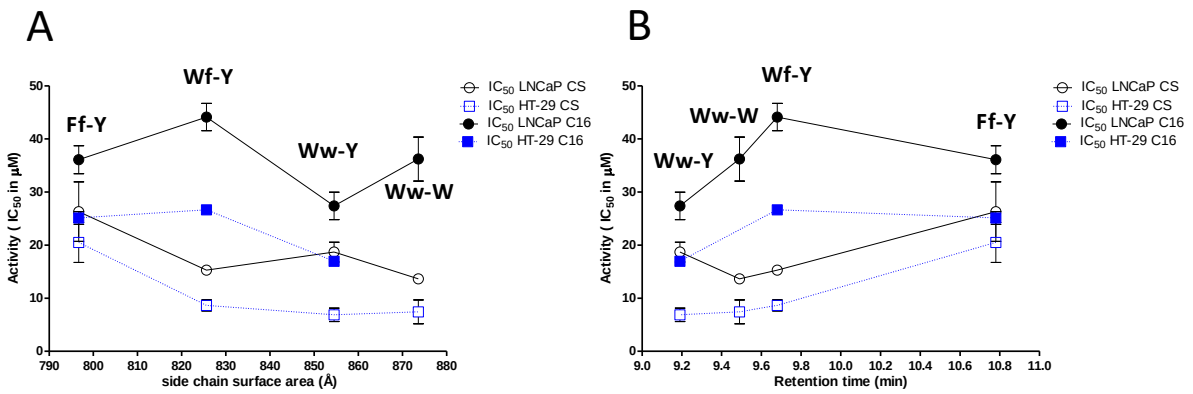

Figure 4.6 The relationship between the activity of the peptide formulations (CS and C16) and peptide hydrophobicity or Σ side chain surface area. A) The activity of the peptide formulations towards HT-29 and LNCaP cancer cells (IC_{50}) plotted against the Σ side chain surface area of the tyrocidines. B) The activity of the peptide formulations towards HT-29 and LNCaP cancer cells (IC_{50}) plotted against the C_{18} UPLC retention time of the tyrocidines.

To elucidate which formulation has the most potential as an alternative chemotherapeutic drug with minimised toxicity towards human erythrocytes and mammalian cells while retaining anticancer activity, the selectivity of the CS and C16 formulations were determined. The selectivity parameters for the CS and C16 peptide formulations are summarised in Table 4.6. Similar trends are seen between the selectivity of the CS and C16 formulations and the SCSA of the peptides (Figure 4.7 A, C). From the correlation between selectivity of the formulated peptides (formulated with CS and C16) and the Σ side chain surface areas, it is evident that TpcC:C16 has the highest selectivity between erythrocytes and LNCaP cancer cells (HC_{50}/IC_{50}) and between LNCaP cancer cells and HEK 293 mammalian cells (LC_{50}/IC_{50}) (Figure 4.7)

Stellenbosch University https://scholar.sun.ac.za

Table 4.6 A summary of the selectivity of the peptides formulated with CS and C16 determined from the ratios of the HC_{50} (from red blood cells), IC_{50} (from HT-29 and LNCaP cells) and LC_{50} (from HEK293 cells) values.

Formulation	HC_{50}/IC_{50}[a] ± SD		LC_{50}/IC_{50}[a] ± SD	
	HT-29	LNCaP	HT-29	LNCaP
TrcA:CS	44.3 ± 22	35.1 ± 19	0.50 ± 0.2	0.40 ± 0.1
TrcB:CS	24.9 ± 5.3	13.9 ± 1.5	1.31 ± 0.2	0.73 ± 0.0
TrcC:CS	63.2 ± 17	22.7 ± 3.4	1.67 ± 0.6	0.60 ± 0.2
TpcC:CS	662 ± 146	342 ± 53	0.70 ± 0.1	0.40 ± 0.1
TrcA:C16	2.61 ± 0.1	1.82 ± 0.0	0.82 ± 0.1	0.60 ± 0.1
TrcB:C16	2.05 ± 0.0	1.24 ± 0.1	1.12 ± 0.1	0.70 ± 0.1
TrcC:C16	5.36 ± 1.9	3.25 ± 0.6	1.08 ± 0.3	0.70 ± 0.3
TpcC:C16	N.A.	8.41 ± 1.5	N.A.	1.61 ± 0.4

[a] IC_{50} values of HT-29 or LNCaP used to calculate selectivity indexes.

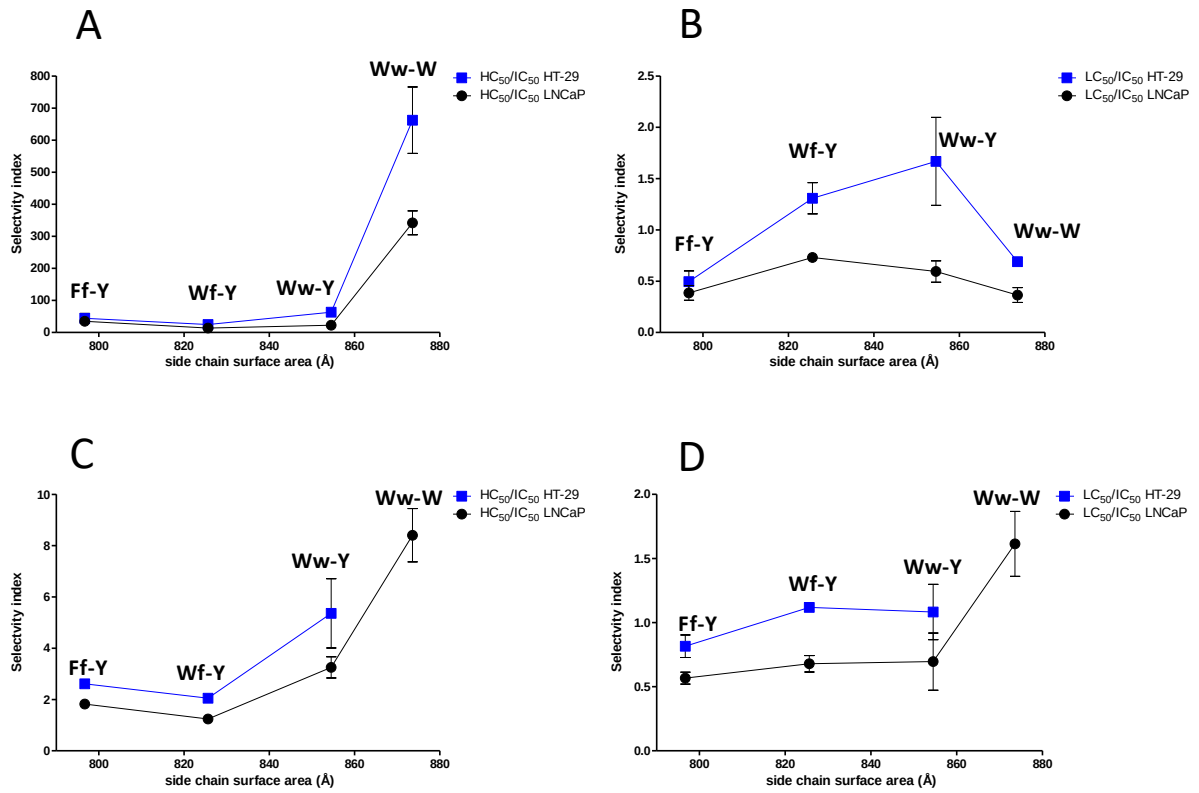

Figure 4.7 The relationship between the selectivity of the peptide formulations (CS and C16) and peptide Σ side chain surface area. A) The selectivity (HC_{50}/IC_{50}) of the CS peptide formulations between erythrocytes (HC_{50}) and cancer cells (HT-29 and LNCaP cells)(IC_{50}) plotted against the Σ side chain surface area of the tyrocidines. B) The selectivity (LC_{50}/IC_{50}) of the CS peptide formulations between HEK293 mammalian cells (LC_{50}) and cancer cells (HT-29 and LNCaP cells)(IC_{50}) plotted against the Σ side chain surface area of the tyrocidines. C) The selectivity (HC_{50}/IC_{50}) of the C16 peptide formulations between erythrocytes (HC_{50}) and cancer cells (HT-29 and LNCaP cells)(IC_{50}) plotted against the Σ side chain surface area of the tyrocidines. D) The selectivity (LC_{50}/IC_{50}) of the C16 peptide formulations between HEK293 mammalian cells (LC_{50}) and cancer cells (HT-29 and LNCaP cells)(IC_{50}) plotted against the Σ side chain surface area of the tyrocidines.

Stellenbosch University https://scholar.sun.ac.za

Unfortunately, due to material and time-constraints, the IC_{50} of TpcC:C16 for HT-29 cells could not be determined. However, it is likely that the selectivity between erythrocytes (HC_{50}/IC_{50}) or HEK 293 mammalian cells (LC_{50}/IC_{50}) and HT-29 cells would be high, if it follows the trend of the LNCaP selectivity. For the CS formulation, the selectivity of TpcC:CS is highest between erythrocytes and HT-29 cells (HC_{50}/IC_{50}) whereas, TrcC:CS has the highest selectivity between HEK293 mammalian cells and HT-29 cancer cells (LC_{50}/IC_{50}). Taken together, the TpcC:C16 formulation has the greatest potential as alternative chemotherapeutic lead formulation for cancer treatment.

4.5 CONCLUSIONS

A relationship was observed between the hydrophobicity as well as the size of dipeptide unit and the haemolytic activity of the peptides, with the smaller and more hydrophobic peptides, TrcA and TrcB, being more haemolytic. The CS and C16 formulations led to a decrease of haemolytic activity (except for Trcmix:C16), with the largest influence induced by CS. The LPC had no marked effect on the haemolytic activity of the peptides.

It was found that sample preparation may influence the self-assembled states of the peptides in formulation, as different sterility methods caused significant differences in the haemolytic activity of the CS formulations and some of the C16 formulations. Maturation periods influenced the haemolytic activities of some of the formulations, with significant differences only observed for three of the 15 peptide formulations.

The structure-activity analysis of the peptides revealed no apparent relationships between the activity towards HT-29, LNCaP and HEK293 cells and the physical properties of the peptides (hydrophobicity and size), indicating an additional mode of

Stellenbosch University https://scholar.sun.ac.za

action(s) such as internalisation followed by attack of internal targets. However, the CS and C16 formulations seem to have opposite/mirror effects on the anticancer activity of the peptides which appear to be more pronounced for TrcB and TpcC. The C16 formulation have lower anticancer activity compared to CS formulations which may indicate stronger C16-peptide interaction possibly leading to entrapment of peptides. Although the C16 formulations have lower anticancer activity compared to CS, it is the TpcC:C16 formulation that presents the highest combined selectivity indexes (HC_{50}/IC_{50} and LC_{50}/IC_{50}) making TpcC:C16 the formulation with the greatest potential as lead formulation for alternative chemotherapeutic drug for the treatment of cancer.

4.6 REFERENCES

(1) Holohan, C., Van Schaeybroeck, S., Longley, D. B., and Johnston, P. G. (2013) Cancer drug resistance: An evolving paradigm. *Nat. Rev. Cancer 13*, 714–726.

(2) Rautenbach, M., Vlok, N. M., Stander, M., and Hoppe, H. C. (2007) Inhibition of malaria parasite blood stages by tyrocidines, membrane-active cyclic peptide antibiotics from *Bacillus brevis*. *Biochim. Biophys. Acta - Biomembr. 1768*, 1488–1497.

(3) Yount, N. Y., and Yeaman, M. R. (2005) Immunocontinuum: perspectives in antimicrobial peptide mechanisms of action and resistance. *Protein Pept. Lett. 12*, 49–67.

(4) Spathelf, B. M., and Rautenbach, M. (2009) Anti-listerial activity and structure-activity relationships of the six major tyrocidines, cyclic decapeptides from *Bacillus aneurinolyticus*. *Bioorganic Med. Chem. 17*, 5541–5548.

(5) Leussa, A. N. yang. N., and Rautenbach, M. (2014) Detailed SAR and PCA of the tyrocidines and analogues towards leucocin A-sensitive and leucocin A-resistant *Listeria monocytogenes*. *Chem. Biol. Drug Des. 84*, 543–557.

(6) Troskie, A. M., de Beer, A., Vosloo, J. A., Jacobs, K., and Rautenbach, M. (2014) Inhibition of agronomically relevant fungal phytopathogens by tyrocidines, cyclic antimicrobial peptides isolated from *Bacillus aneurinolyticus*. *Microbiol. (United Kingdom) 160*, 2089–2101.

(7) Troskie, A. M., Rautenbach, M., Delattin, N., Vosloo, J. A., Dathe, M., Cammue, B. P. A., and Thevissen, K. (2014) Synergistic activity of the tyrocidines, antimicrobial cyclodecapeptides from *Bacillus aneurinolyticus*, with amphotericin B and caspofungin against *Candida albicans* biofilms. *Antimicrob. Agents Chemother. 58*, 3697–3707.

(8) Rammelkamp, Charles H. Weinstein, L. (1942) Toxic effects of tyrothricin ,

Stellenbosch University https://scholar.sun.ac.za

gramicidin and tyrocidine. *J. Infect. Dis. 71*, 166–173.

(9) Fidler, I. J., Schroit, A. J., Connor, J., Bucana, C. D., and Fidler, I. J. (1991) Elevated expression of phosphatidylserine in the outer membrane leaflet of human tumor cells and recognition by activated human blood monocytes. *Cancer Res. 51*, 3062–3066.

(10) Connor, J., Bucana, C., Fidler, I. J., and Schroit, A. J. (1989) Differentiation-dependent expression of phosphatidylserine in mammalian plasma membranes: quantitative assessment of outer-leaflet lipid by prothrombinase complex formation. *Proc. Natl. Acad. Sci. 86*, 3184–3188.

(11) Carmona-Ribeiro, A. M., and Carrasco, L. D. de M. (2014) Novel formulations for antimicrobial peptides. *Int. J. Mol. Sci. 15*, 18040–18083.

(12) Rawat, M., Singh, D., Saraf, S., and Saraf, S. (2008) Lipid carriers: a versatile delivery vehicle for proteins and peptides. *Pharm. Soc. Japan 128*, 269–280.

(13) Lemke, A., Kiderlen, A. F., and Kayser, O. (2005) Amphotericin B. *Appl. Microbiol. Biotechnol. 68*, 151–162.

(14) Munyuki, G., Jackson, G. E., Venter, G. A., Kövér, K. E., Szilágyi, L., Rautenbach, M., Spathelf, B. M., Bhattacharya, B., and Van Der Spoel, D. (2013) β-sheet structures and dimer models of the two major tyrocidines, antimicrobial peptides from *Bacillus aneurinolyticus* . *Biochemistry 52*, 7798–7806.

(15) Loll, P. J., Upton, E. C., Nahoum, V., Economou, N. J., and Cocklin, S. (2014) The high resolution structure of tyrocidine A reveals an amphipathic dimer. *Biochim. Biophys. Acta - Biomembr. 1838*, 1199–1207.

(16) Ruttenberg, M. A., King, T. P., and Craig, L. C. (1966) The chemistry of tyrocidine. VII. Studies on association behavior and implications regarding conformation. *Biochemistry 5*, 2857–2864.

(17) Paradies, H. H. (1979) Aggregation of tyrocidine in aqueous solutions. *Biochem. Biophys. Res. Commun. 88*, 810–817.

(18) Ruttenberg, M. A., King, T. P., and Craig, L. C. (1965) The use of the tyrocidines for the study of conformation and aggregation behavior. *J. Am. Chem. Soc. 87*, 4196–4198.

(19) Vosloo, J. A. (2016) Optimised bacterial production and characterisation of natural antimicrobial peptides with potential application in agriculture. PhD Thesis, Department of Biochemistry, University of Stellenbosch, Stellenbosch, South Africa, http://hdl.handle.net/10019.1/98411

(20) Barnard, M. (2017) The characterization of 17β - hydroxysteroid dehydrogenase type 2 (17βHSD2) activity towards novel C19. MSc Thesis, Department of Biochemistry, University of Stellenbosch, Stellenbosch, South Africa, http://hdl.handle.net/10019.1/101459

(21) Rautenbach, M., Gerstner, G. D., Vlok, N. M., Kulenkampff, J., and Westerhoff, H. V. (2006) Analyses of dose-response curves to compare the antimicrobial activity of model cationic α-helical peptides highlights the necessity for a minimum of two activity parameters. *Anal. Biochem. 350*, 81–90.

Stellenbosch University https://scholar.sun.ac.za

(22) Leussa, N.-N. A. (2014) Characterisation of small cyclic peptides with antilisterial and antimalarial activity. PhD Thesis, Department of Biochemistry, University of Stellenbosch,Stellenbosch, South Africa, http://hdl.handle.net/100191/86161.

(23) Laubscher, W. E. (2016) Production , characterisation and activity of selected and novel antibiotic peptides from soil bacteria. MSc Thesis, Department of Biochemistry, University of Stellenbosch.

(24) Norman, K. E., and Nymeyer, H. (2006) Indole localization in lipid membranes revealed by molecular simulation. *Biophys. J. 91*, 2046–2054.

(25) Kelkar, D. A., and Chattopadhyay, A. (2006) Membrane interfacial localization of aromatic amino acids and membrane protein function. *J. Biosci. 31*, 297–302.

(26) Wymore, T., and Wong, T. C. (1999) Molecular dynamics study of substance P peptides in a biphasic membrane mimic. *Biophys. J. 76*, 1199–1212.

(27) Segrest, J. P., De Loof, H., Dohlman, J. G., Brouillette, C. G., and Anantharamaiah, G. M. (1990) Amphipathic helix motif: Classes and properties. *Proteins Struct. Funct. Bioinforma. 8*, 103–117.

(28) Frecer, V. (2006) QSAR analysis of antimicrobial and haemolytic effects of cyclic cationic antimicrobial peptides derived from protegrin-1. *Bioorganic Med. Chem. 14*, 6065–6074.

(29) Connolly, M. L. (1983) Analytical molecular surface calculation. *J. Appl. Crystallogr. 16*, 548–558.

Stellenbosch University https://scholar.sun.ac.za

4.7 ADDENDUM

Table 4.7 Summary P-values from Bonferroni multiple comparison test of the HC_{50} values and % haemolysis at 50 µM for the pure peptides. The HC_{50} values and % haemolysis was determined from haemolytic dose responses performed and haemolysis assays, respectively, after different sterility methods and formulation maturation periods were used. The exact P-values are less than the limit shown in the table with P-values > 0.05 denoted as "ns".

					HC_{50}					
	Sterility method 1; 24-hour maturation					Sterility method 2; 1-hour maturation				
	TrcA	**TrcB**	**TrcC**	**TpcC**	**Trcmix**	**TrcA**	**TrcB**	**TrcC**	**TpcC**	**Trcmix**
TrcA	-	ns	0.05	ns	ns	-	ns	ns	0.01	ns
TrcB		-	0.05	ns	ns		-	ns	0.05	ns
TrcC			-	ns	0.05			-	ns	ns
TpcC				-	0.05				-	0.05
					% Haemolysis at 50 µM peptide/formulation					
	Sterility method 1; 24-hour maturation					Sterility method 1; 1-hour maturation				
	TrcA	**TrcB**	**TrcC**	**TpcC**	**Trcmix**	**TrcA**	**TrcB**	**TrcC**	**TpcC**	**Trcmix**
TrcA	-	ns	0.001	0.001	ns	-	ns	ns	0.05	ns
TrcB		-	0.001	0.001	ns		-	ns	ns	ns
TrcC			-	ns	0.001			-	ns	ns
TpcC				-	0.001				-	0.01

Table 4.8 Summary P-values from Bonferroni selected pair comparison test of the HC_{50} values and % haemolysis at 50 µM for the peptide formulations with CS, LPC and C16. The HC_{50} values and % haemolysis was determined from haemolytic dose responses performed and haemolysis assays, respectively, after different sterility methods and formulation maturation periods were used. The X represents the peptide in each row, for instance the cell in column one row one represents TrcA:CS. The exact P-values are less than the limit shown in the table with P-values > 0.05 denoted as "ns".

				HC_{50}				
	Sterility method 1; 24-hour maturation			Sterility method 2; 1-hour maturation				
	XCS	**XLPC**	**XC16**	**XCS**	**XLPC**	**XC16**		
TrcA	0.01	ns	0.01	0.05	ns	ns		
TrcB	0.001	ns	0.05	0.001	ns	0.05		
TrcC	0.001	ns	0.05	0.01	ns	ns		
TpcC	0.01	ns	0.001	0.01	ns	ns		
Trcmix	0.05	ns	ns	0.001	ns	ns		
				% Haemolysis at 50 µM peptide/formulation				
	Sterility method 1; 24-hour maturation			Sterility method 1; 1-hour maturation				
	XCS	**XLPC**	**XC16**	**XCS**	**XLPC**	**XC16**	**XCSC16**	
TrcA	0.001	ns	0.001	0.001	ns	0.001	0.001	
TrcB	0.001	ns	0.001	0.001	ns	0.001	0.001	
TrcC	0.001	0.001	0.001	0.001	ns	0.05	0.001	
TpcC	0.001	ns	0.001	0.001	ns	0.001	0.001	
Trcmix	0.001	ns	ns	0.001	ns	ns	0.001	

Stellenbosch University https://scholar.sun.ac.za

Table 4.9 Summary P-values from Bonferroni selected pair comparison test of the HC_{50} values for the pure peptides and peptide formulations. The HC_{50} values was determined from haemolytic dose responses performed after different sterility methods and formulation maturation periods were used. Only the same peptide and peptide formulation were compared to elucidate any significant effects caused by sample preparation. The exact P-values are less than the limit shown in the table with P-values > 0.05 denoted as "ns".

HC_{50} STERILITY METHOD 2; 1-HOUR MATURATION

HC_{50} STERILITY METHOD 1; 24-HOUR MATURATION

	TrcA	TrcA:CS	TrcA:LPC	TrcA:C16	TrcB	TrcB:CS	TrcB:LPC	TrcB:C16
TrcA	ns							
TrcA:CS		0.001						
TrcA:LPC			ns					
TrcA:C16				ns				
TrcB					ns			
TrcB:CS						0.001		
TrcB:LPC							ns	
TrcB:C16								0.001
	TrcC	TrcC:CS	TrcC:LPC	TrcC:C16	TpcC	TpcC:CS	TpcC:LPC	TpcC:C16
TrcC	ns							
TrcC:CS		0.001						
TrcC:LPC			ns					
TrcC:C16				0.001				
TpcC					ns			
TpcC:CS						0.001		
TpcC:LPC							ns	
TpcC:C16								ns
	Trcmix		Trcmix:CS		Trcmix:LPC		Trcmix:C16	
Trcmix	ns							
Trcmix:CS			0.01					
Trcmix:LPC						ns		
Trcmix:C16							ns	

Stellenbosch University https://scholar.sun.ac.za

Table 4.10 Summary P-values from Bonferroni selected pair comparison test of the % haemolysis using 24-hour versus 1-hour maturation periods for the pure peptides and peptide formulations at 50 µM. The % haemolysis was determined from haemolysis assays performed after sterility method 1 and different maturation periods were used. Only the same peptide and peptide formulation were compared to elucidate any significant effects caused by maturation time. The exact P-values are less than the limit shown in the table with P-values > 0.05 denoted as "ns".

% HAEMOLYSIS; 1-HOUR MATURATION

% HAEMOLYSIS; 24-HOUR MATURATION	TrcA	TrcA:CS	TrcA:LPC	TrcA:C16	TrcB	TrcB:CS	TrcB:LPC	TrcB:C16
TrcA	ns	-	-	-	-	-	-	-
TrcA:CS	-	ns	-	-	-	-	-	-
TrcA:LPC	-	-	ns	-	-	-	-	-
TrcA:C16	-	-	-	0.01	-	-	-	-
TrcB	-	-	-	-	ns	-	-	-
TrcB:CS	-	-	-	-	-	0.001	-	-
TrcB:LPC	-	-	-	-	-	-	ns	-
TrcB:C16	-	-	-	-	-	-	-	ns
	TrcC	TrcC:CS	TrcC:LPC	TrcC:C16	TpcC	TpcC:CS	TpcC:LPC	TpcC:C16
TrcC	0.001	-	-	-	-	-	-	-
TrcC:CS	-	ns	-	-	-	-	-	-
TrcC:LPC	-	-	ns	-	-	-	-	-
TrcC:C16	-	-	-	0.001	-	-	-	-
TpcC	-	-	-	-	0.01	-	-	-
TpcC:CS	-	-	-	-	-	ns	-	-
TpcC:LPC	-	-	-	-	-	-	ns	-
TpcC:C16	-	-	-	-	-	-	-	ns
	Trcmix		Trcmix:CS		Trcmix:LPC		Trcmix:C16	
Trcmix	ns		-		-		-	
Trcmix:CS	-		ns		-		-	
Trcmix:LPC	-		-		ns		-	
Trcmix:C16	-		-		-		ns	

Table 4.11 Summary P-values from Bonferroni selected pair comparison test of the IC50 or LC50 values of the peptide formulations towards LNCaP, HT-29 and HEK293 cells. The IC_{50} and LC_{50} values were determined from cell viability dose responses performed after using sterility method 1 and a 1-hour maturation period. The X represents the peptide in each row, for instance the cell in column one row one represents TrcA:CS. The exact P-values are less than the limit shown in the table with P-values > 0.05 denoted as "ns". P-values that could not be determined due to insufficient data are denoted by "N.A".

IC_{50} or LC_{50}

	LNCaP			HT-29				HEK293			
	XCS	**XLPC**	**XC16**	**XCS**	**XLPC**	**XC16**	**XCSC16**	**XCS**	**XLPC**	**XC16**	**XCSC16**
TrcA	ns	ns	ns	0.05	ns	0.01	ns	ns	ns	0.05	ns
TrcB	ns	ns	0.001	ns	ns	0.001	ns	0.05	ns	0.001	N.A
TrcC	ns	ns	0.05	ns	ns	0.05	ns	ns	ns	0.05	ns
TpcC	ns	ns	0.05	ns	ns	N.A.	ns	ns	ns	0.001	ns
Trcmix	0.01	ns	ns	0.01	ns	ns	ns	0.05	ns	0.05	ns

Stellenbosch University https://scholar.sun.ac.za

Table 4.12 Summary P-values from Bonferroni multiple comparison test of the IC_{50} or LC_{50} values of the pure peptides and peptide formulations towards LNCaP, HT-29 and HEK293 cells. The IC_{50} and LC_{50} values were determined from cell viability dose responses performed after using sterility method 1 and a 1-hour maturation period. The X represents the peptide in each row, for instance the cell in column one row one represents TrcA:CS. The exact P-values are less than the limit shown in the table with P-values > 0.05 denoted as "ns". P-values that could not be determined due to insufficient data are denoted by "N.A".

IC_{50} or LC_{50}

Pure peptides

	LNCap					HT-29					HEK293				
	TrcA	**TrcB**	**TrcC**	**TpcC**	**Trcmix**	**TrcA**	**TrcB**	**TrcC**	**TpcC**	**Trcmix**	**TrcA**	**TrcB**	**TrcC**	**TpcC**	**Trcmix**
TrcA	-	ns	ns	ns	ns	-	ns	ns	ns	ns	-	ns	ns	ns	ns
TrcB		-	ns	ns	ns		-	ns	ns	ns		-	ns	ns	ns
TrcC			-	ns	ns			-	ns	ns			-	ns	ns
TpcC				-	ns				-	ns				-	ns

CS formulations

	TrcA	**TrcB**	**TrcC**	**TpcC**	**Trcmix**	**TrcA**	**TrcB**	**TrcC**	**TpcC**	**Trcmix**	**TrcA**	**TrcB**	**TrcC**	**TpcC**	**Trcmix**
TrcA	-	ns	ns	ns	ns	-	ns	ns	ns	ns	-	ns	ns	ns	ns
TrcB		-	ns	ns	ns		-	ns	ns	0.05		-	ns	ns	ns
TrcC			-	ns	ns			-	ns	0.05			-	ns	ns
TpcC				-	ns				-	0.05				-	ns

LPC formulations

	TrcA	**TrcB**	**TrcC**	**TpcC**	**Trcmix**	**TrcA**	**TrcB**	**TrcC**	**TpcC**	**Trcmix**	**TrcA**	**TrcB**	**TrcC**	**TpcC**	**Trcmix**
TrcA	-	ns	ns	ns	ns	-	ns	ns	ns	ns	-	ns	ns	ns	ns
TrcB		-	ns	ns	ns		-	ns	ns	ns		-	ns	ns	ns
TrcC			-	ns	ns			-	ns	ns			-	ns	ns
TpcC				-	ns				-	ns				-	ns

C16 formulations

	TrcA	**TrcB**	**TrcC**	**TpcC**	**Trcmix**	**TrcA**	**TrcB**	**TrcC**	**TpcC**	**Trcmix**	**TrcA**	**TrcB**	**TrcC**	**TpcC**	**Trcmix**
TrcA	-	ns	ns	ns	0.05	-	ns	0.01	N.A.	0.01	-	ns	ns	0.01	ns
TrcB		-	ns	ns	0.01		-	0.01	N.A.	0.01		-	ns	0.01	ns
TrcC			-	ns	ns			-	N.A.	ns			-	0.01	ns
TpcC				-	0.05				-	N.A.				-	0.001

CSC16 formulations

	TrcA	**TrcB**	**TrcC**	**TpcC**	**Trcmix**	**TrcA**	**TrcB**	**TrcC**	**TpcC**	**Trcmix**	**TrcA**	**TrcB**	**TrcC**	**TpcC**	**Trcmix**
TrcA	-.	N.A.	N.A.	N.A.	N.A.	-	ns	ns	ns	ns	-	N.A.	ns	ns	ns
TrcB		-.	N.A.	N.A.	N.A.		-	ns	ns	ns		-	N.A.	N.A.	N.A.
TrcC			-	N.A.	N.A.			-	ns	ns			-	ns	ns
TpcC				-	N.A.				-	ns				-	ns

Stellenbosch University https://scholar.sun.ac.za

Table 4.13 Summary of P-values from Bonferroni selected pair comparison test of the % haemolysis and % proliferation inhibition of peptides and formulations towards RBC, LNCaP, HT-29, C4-2B and HEK293 cells at 50 µM and 25 µM. The exact P-values are less than the limit shown in the table. P-values > 0.05 denoted as "ns". P-values that could not be determined due to insufficient data are denoted by "N.A". The P-values in brackets were determined from data obtained at peptide and peptide formulation concentrations of 25 µM.

	TrcA			**TrcB**		
	HT-29	LNCaP	C4-2B	HT-29	LNCaP	C4-2B
RBC	ns (0.001)	ns (ns)	ns	ns (0.001)	ns (ns)	ns
HEK293	ns (ns)	ns (0.05)	ns	ns (ns)	ns (ns)	ns
	TrcC			**TpcC**		
	HT-29	LNCaP	C4-2B	HT-29	LNCaP	C4-2B
RBC	ns (0.001)	ns (0.001)	ns	0.001 (0.001)	0.001 (0.001)	0.001
HEK293	ns (ns)	ns (0.001)	ns	ns (ns)	ns (ns)	ns
	TrcA:CS			**TrcB:CS**		
	HT-29	LNCaP	C4-2B	HT-29	LNCaP	C4-2B
RBC	0.001 (0.001)	0.001 (0.001)	0.001	0.001 (0.001)	0.001 (0.001)	0.001
HEK293	ns (ns)	0.01 (0.001)	0.001	ns (ns)	ns (ns)	0.01
	TrcC:CS			**TpcC:CS**		
	HT-29	LNCaP	C4-2B	HT-29	LNCaP	C4-2B
RBC	0.001 (0.001)	0.001 (0.001)	0.001	0.001 (0.001)	0.001 (0.001)	0.001
HEK293	0.01 (ns)	0.001 (0.001)	0.05	ns (ns)	ns (ns)	0.05
	TrcA:C16			**TrcB:C16**		
	HT-29	LNCaP	C4-2B	HT-29	LNCaP	C4-2B
RBC	0.001 (0.001)	0.001 (0.001)	0.001	0.001 (0.001)	0.001 (ns)	0.001
HEK293	ns (ns)	0.001 (0.001)	ns	ns (0.05)	0.001 (ns)	ns
	TrcC:C16			**TpcC:C16**		
	HT-29	LNCaP	C4-2B	HT-29	LNCaP	C4-2B
RBC	0.001 (0.001)	0.001 (0.001)	0.001	0.01 (0.001)	0.001 (0.001)	0.001
HEK293	ns (ns)	0.01 (0.001)	ns	ns (ns)	ns (0.01)	0.001
	TrcA:CSC16			**TrcB:CSC16**		
	HT-29	C4-2B		HT-29	C4-2B	
RBC	0.001	0.001		0.001	0.001	
HEK293	ns (ns)	0.05		ns (ns)	ns	
	TrcC:CSC16			**TpcC:CSC16**		
	HT-29	C4-2B		HT-29	C4-2B	
RBC	0.001	0.001		0.001	0.001	
HEK293	0.01 (ns)	ns		ns (ns)	ns	

Stellenbosch University https://scholar.sun.ac.za

Chapter 5
SUMMARY, CONCLUSIONS AND FUTURE STUDIES

5.1 INTRODUCTION

The ultimate goal of this study was to develop a formulation of the Trcs and analogues that reduces the toxicity of these cyclodecapeptides towards human red blood cells (erythrocytes)[1-3] and non-cancerous mammalian cells [2, 3], while simultaneously retaining activity towards cancer cells. Before any experiment could be performed, the tyrocidines had to be produced and purified from crude *Brevibacillus parabrevis* culture extracts supplemented with amino acids. Subsequently, peptide formulations with different lipid-based molecules had to be prepared followed by determination of biophysical properties induced by the different formulants. After establishing the possible influence formulants have on the biophysical properties of the peptides, the activity towards human red blood cells (haemolytic activity), non-cancerous human immortal cells (HEK293 cells) and different cancer cells (LNCaP, C4-2B and HT-29) were investigated to elucidate potential peptide formulation(s) as alternative anticancer agent.

5.2 EXPERIMENTAL CONCLUSIONS AND FUTURE STUDIES

5.2.1 Production and purification of tyrocidine A, B, C and tryptocidine C

Determination of the biophysical and biological activity of different tyrocidines and analogues required sufficient amounts of highly pure (>90 %) peptide. The supplementation of *Br. parabrevis* culture media with amino acids, as described by Vosloo *et al.* [4], successfully increased amount of the peptides of interest (TrcA, B and TpcC). Supplementation with Phe resulted in increased production of TrcA and B, whereas supplementation with Trp increased TpcC and TpcB amounts. Three

Stellenbosch University https://scholar.sun.ac.za

peptides, TrcA, TrcB and TpcC, were subsequently isolated from crude culture extracts and the fourth (TrcC) isolated from commercial Trc mixture (Trcmix) by means of established C_{18} semi-preparative reverse-phase HPLC (RP-HPLC) methodology [2, 5]. With UPLC analysis of the manually isolated peptides the identities and purities of all the peptides were determined. All the isolated peptides had purities of 90% or higher.

5.2.2 Development of a C_8 HPLC purification method

The tyrothricin complex consists of a complex mixture of tyrocidines and analogues, all differing from each other with only one amino acid residue which makes their purification difficult especially separating Lys and Orn analogues (example TrcA/A1 TrcB/TrcB1 and TrcC/C1) differing only from each other in CH_2 group. Separation of the B-analogues (TrcB/B'/B1/ B1') are further complicated where the aromatic dipeptide can be either Wf or Fw. Therefore a new purification method was developed by applying the current optimised C_{18} HPLC program2, 5 to an alternative column, a C_8 column, to make purification of these peptides in the future more cost and time efficient. The optimised C_8 HPLC purification method (program D at 25 °C, Chapter 2) improved the separation of the tyrocidines significantly with notable separation of the $TrcC_1$ and TrcC, $TrcB_1$ and TrcB, and TrcB and TrcB'/TpcC. Purities of 74.4 %, 95.5 %, 90.2 %, 93.7 %, 90.8 % and 85.5 % were achieved for TrcA, $TrcA_1$, TrcB, $TrcB_1$, TrcC, and $TrcC_1$. Isolation of all six major tyrocidines is a very significant result, however, manual collection of peaks remains time consuming. Collection of the peaks was attempted by using a fraction collector but was less successful than manual collection due to the delay between the signal of the HPLC detector and the fraction collector, as well as the aggregation/oligomerisation of these peptides over time leading to retention time drifts. This delay and retention time drift have a significant

Stellenbosch University https://scholar.sun.ac.za

effect due to close proximity of each peptide peak to one another resulting in the wrong/overlapping collection of peak fractions. Future studies should focus on correcting the time delay between the fraction collector and HPLC detector, as well as directed fraction collection via absorption and/or molecular mass (mass-directed fraction collection using a mass spectrometer as detector). Due to the success of the C_8 HPLC purification method developed in Chapter 2, the method will be used in the future as the primary method for purification of the tyrocidines and analogues as soon as a C_8 semi-preparative column is acquired in the BIOPEP Peptide Group.

5.2.3 The influence of formulants on the peptide biophysical character

The aim of Chapter 3 of this study was to elucidate the biophysical properties of four chosen Trcs (TrcA, TrcB, TrcC and TpcC) alone and in formulation with lipid-based molecules (CS, LPC and C16). The techniques chosen to do this were scanning electron microscopy (SEM), traveling wave ion mobility mass spectrometry (TWIM-MS) and fluorescence spectroscopy (FS).

Oligomerisation of TrcA, TrcB, TrcC and TpcC: It has been shown that the cyclodecapeptides from tyrothricin form oligomers which is generally dictated by the variable residues of the aromatic dipeptide unit. The results from the TWIM-MS results of this study correlates well with previous results found by Vosloo [6] in which it was observed that the more hydrophobic Trcs (TrcA and TrcB) have a greater tendency to form dimers. Furthermore, the more hydrophobic and smaller TrcA and TrcB have lower cross-sectional (CCS) areas for both the monomeric ionic species and the dimeric species than that of the TrcC and TpcC. In contrast to what was expected, the CCS areas of the dimeric ionic species were observed be less than 2-fold that of both the singly and doubly charged monomeric species. This indicates that the forces

Stellenbosch University https://scholar.sun.ac.za

(hydrogen bonding, ionic interaction and hydrophobic interaction) that are involved in the dimerisation of the Trcs result in denser conformation of the peptides. Furthermore, an expected concentration dependent increase in dimerisation was observed for all the peptides.

The SEM results revealed that TpcC self-assembles into well-defined spherical structures with high dispersity in the nanometre range, 13 nm to 349 nm, depending on concentration and solvent system used to prepare the samples. Larger spheres were formed with higher peptide concentration (1.00 mg/mL) and a less polar solvent (50 % EtOH in water (*v/v*)) ranging from 159 nm to 349 nm compared to the spheres formed with lower concentration (500 µM) and more polar solvent (15 % EtOH in water (*v/v*)) which ranged from 13 nm to 25 nm. Quasicrystals composed of multiple smaller uniform spheres were also observed to form by TpcC which signifies the ability of these peptides to form larger self-assembled structures. Preliminary studies showed that TrcA, TrcB and TrcC also formed nanospheres, as well as other larger structures. This study will now be taken further in a separate project.

The FS studies revealed that the conformation of the peptides dictates the location of the Trp residues. Blue shifts of the fluorescence maxima observed in the spectra of TrcB, TrcC and TpcC from the expected 357 nm [7] to 344 nm, 340 nm and 340 nm, respectively, are indicative of translocation of Trp residues to a pure hydrophobic environment[7-10]. This signifies the influence peptide self-assembly and conformation have on the location of the aromatic dipeptide unit in oligomeric structures. Considering the SEM results of TpcC, it is likely that the Trp residues are positioned towards hydrophobic pockets of the spherical nano-constructs.

Oligomerisation of the Trcs caused by lipid-based formulants: The proportion of the dimeric ionic species of the Trcs decreases when formulated with LPC and C16, as

Stellenbosch University https://scholar.sun.ac.za

determined by TWIM-MS. The SEM results of TpcC:LPC and TpcC:C16 revealed that LPC and C16 lead to either retardation or the disruption/prevention of the formation of uniform large spheres, which correlates with the decrease in proportion of doubly charged dimers observed by TWIM-MS for the LPC and C16 formulations. Additionally, the LPC and C16 formulants led to loss in total TWIM-MS signal compared to controls, indicating entrapment of peptide within stable neutral lipid complexes. Stable neutral lipid complexes are possibly formed due to ionic interaction between anionic lipid group and cationic amino group of the L-Orn^{9} residues of the peptides. Considering both the SEM and TWIM-MS results, the quenching of the fluorescence of the C16 and LPC formulations is therefore more likely due to exposure of the Trp residues to the aqueous environment or due to excited state reactions between the Trp residues and polar carboxyl group of C16 and the amino and phosphate groups of LPC [8, 9 10, 11].

The direct relationship observed between the quenching of total FS signal and loss of ionic species TWIM-MS signal of the peptides in formulation with C16 and LPC, as well as the SEM and other TWIM-MS results led us to hypothesise the following:

- C16 and LPC formulations with the cationic cyclodecapeptides form stable neutral lipid-complexes which entraps peptides (via ionic interaction between the anionic lipid headgroup and cationic L-Orn^{9});
- C16 and LPC both act as detergents and decreases dimer formation and
- the side-chains of the aromatic dipeptide unit is exposed to a polar environment which could either be the aqueous environment (collisional FS quenching) and/or the polar groups of the LPC and C16 (FS quenching via excited state reactions).

Stellenbosch University https://scholar.sun.ac.za

The SEM of TpcC formulated with CS induced the formation of large non-uniform spheres compared to smaller non-uniform spheres induced by LPC and C16. Some of spheres induced by CS were almost 10X the size (94 nm - 133 nm) of the majority of the spheres formed by TpcC alone (13 nm – 25 nm), indicating that CS may lead to merging of the small spheres into larger structures. The TWIM-MS results revealed that the proportion of dimeric ionic species in the CS formulation is not markedly influenced compared to the control. However, some changes in monomeric species contributions were evident indicating some influence, correlating with the SEM results of TpcC:CS. Furthermore, the maintained total TWIM-MS signal observed for the CS formulations indicates less stable formulation due to loss of hydrophobic interactions (aromatic ring stacking) in the TWIM-MS instrument [12-14]. The FS studies agrees with this result where significant blue shifts accompanied by quenching in the CS formulation spectrums were observed, indicating a combinatorial effect of ring stacking [15] and excited state reactions between the dipeptide unit amino acid side chains and polar groups of the peptide backbones.

5.2.4 Biological activity of the tyrocidines

The aim of Chapter 4 was to minimise the toxicity of the Trcs towards human erythrocytes (RBCs) and human non-cancerous cells such as HEK293 cells. Four of the Trcs, TrcA, TrcB, TrcC and TpcC, as well as the mixture known as Trcmix, were formulated with CS, LPC and C16 (all lipid-based molecules) in an attempt to achieve the goal mentioned above. Decontamination of the formulations was achieved by means of sterility method 1 (which entails the saturation of formulations with chloroform vapour within a glass desiccator) and sterility method 2 (resuspension of samples in 50 % ACN followed by lyophilisation). The latter method resulted in the decrease of almost all the HC_{50} values (increase in toxicity) of the peptides and

Stellenbosch University https://scholar.sun.ac.za

formulations which signified the dependence of peptide aggregation/self-assembly on solvent systems and preparation methods. Therefore, the rest of the biological assays were performed using sterility method 1 for the decontamination of the samples prior to biological activity experiments.

The haemolytic dose responses (24-hour maturation period, sterility method 1) revealed that TrcC and TpcC are less haemolytic than TrcB and TrcA, with TrcB observed as the most haemolytic peptide. The HC_{50} values of TrcA and TrcB correlate well with previous results[2, 16], where TrcB was also found to be the most haemolytic[2]. We hypothesise that the peptides with more than one Trp residue have hampered association with cell membranes of red blood cells because of the shallow insertion of Trp side chain compared to Phe side chain[2, 17-19], as well as adjusted L-Orn[9] orientation (hampered "snorkelling" effect)[20] caused by different induced oligomerisation structures of the C-analogues.

The CS significantly increased the HC_{50} values of all the peptides, including Trcmix, indicating that the peptide structures that caused the haemolytic activity was neutralised in this formulation. It is proposed that CS shields the aromatic groups preventing them from penetrating the phospholipid membrane, as well as possibly competing with the interaction of the tyrocidines with the sterol, cholesterol [21]. However, LPC, a lysophospholipid that is potentially a lipid target for many toxic membrane active peptides, had no significant effect on any of the HC_{50} values of the cyclodecapeptides. Formulation with C16 also significantly increased the HC_{50} values of the peptides and thus this lipid formulation also negated some of the haemolytic toxicity. It is probable that carboxyl group of C16 shields the cationic amino group of L-Orn[9], while the aliphatic tail interacts with some of the hydrophobic groups, thereby hampering dimer formation and cell membrane interaction.

Stellenbosch University https://scholar.sun.ac.za

In general, the time allowed for the peptides and peptide formulations to mature had no marked influences on their haemolytic activities, with significant differences only observed for three of the 15 peptide formulations between two different maturation periods (1-hour vs 24-hours). Comparison of % haemolysis at 1-hour and 24-hour maturation periods (at 50 μM) of the peptides alone and in formulation with LPC revealed no significant changes, except for non-formulated TrcC and TpcC. Similar % haemolysis was observed for CS formulations at 24-hour compared to 1-hour maturations, except for TrcB:CS with significant increase. However, a decrease in % haemolysis for TrcA:C16 and TrcC:C16 were observed for C16 formulations at 24-hour compared to 1-hour maturation period, except for TrcB:C16 where an increase was again observed. The self-assembled states and exposure of certain groups of these peptides change over time, and it is proposed to in turn affect their activity, as well as toxicity. This signifies the influence of different factors, including preparation method, solvent systems and time of maturation, have on the activity of the Trcs and their formulations.

A 1-hour maturation period was allowed for all the samples for the rest of the activity assays in Chapter 4 because the CS formulation influenced the haemolytic activity of the peptides to the largest extent with decreased haemolytic activities observed at 1-hour maturation period.

Similar to the CS formulations, the combinatorial formulation, CSC16, increased the % haemolysis (1-hour maturation) of all the peptides at 50 μM with an increase observed in the following order TrcA<TrcB<TrcC suggesting that effects of C16 on the self-assembly of the peptides are overpowered by CS in the CSC16 formulation. However, CS remains the formulant that lowers haemolytic activity of the peptides the most.

Stellenbosch University https://scholar.sun.ac.za

All peptides and peptide formulations were active against LNCaP, HT-29, HEK293 and C4-2B cells. In general, the CS and C16 formulations showed decreased anticancer and HEK293 activity. However, at both 25 µM and 50 µM the % proliferation inhibition of cancer cells by TpcC:C16 was higher than the % proliferation inhibition of HEK293 cells.

No direct relationship could be observed between the IC_{50} (LNCaP and HT-29) or LC_{50} (HEK293) values and the physicochemical characteristics (retention times and side chain surface area) of the peptides alone and in formulation, which suggest that the primary structure does not dictate their anticancer activity or activity towards non-cancerous human cells. However, the haemolytic activity of the peptides is influenced by both the hydrophobicity and peptide size/volume with increased haemolytic activity observed for the smaller more hydrophobic peptides (TrcA and TrcB) possibly due to deeper insertion of Phe residues into the cell membrane and stronger interaction with hydrophobic phospholipid tails of the cell membrane lipid bilayer. It is therefore suggested that the mechanism of action of the Trcs towards erythrocytes and cancerous/mammalian non-cancerous immortal cell lines are different and that the peptides are likely translocated/internalised into the cancer cells via the lipidic formulations as internal targets have been proposed as alternative mechanism of action for the tyrocidines [2, 16, 22-29]. Furthermore, the fact that the activity of the peptides and peptide formulations are similar towards cancerous and non-cancerous mammalian cells suggests that neither the negative charge of the cancer cell nor the positive charge of the Trcs is necessary for activity and strengthens the theory that alternative targets exists.

Opposite/mirror trends are seen between the anticancer activity and the surface side chain area (SCSA) and hydrophobicity of the peptides for both the CS and C16

Stellenbosch University https://scholar.sun.ac.za

formulations. This indicates that CS and C16 have opposite effects on the anticancer activity of the peptides. The C16 formulations have lower anticancer activity compared to CS formulation counterparts. With this result, and the results seen from the SEM (disruption of spheres by C16) and TWIM-MS data (loss of ionic specie signal by C16) from Chapter 3, it is possible that less peptide molecules are internalised in an interacting lipid-peptide “bolus” and released from the C16 formulation compared to CS formulation due to stronger C16-peptide interaction.

Despite the decreased anticancer activity of the Trcs by the C16 formulation, it is the TpcC:C16 formulation which had the best combined selectivity of HC_{50}/IC_{50} (between erythrocytes and LNCaP) and LC_{50}/IC_{50} (between HEK293 and LNCaP) which makes TpcC:C16 the peptide formulation with the most potential as future cancer chemotherapeutic drug formulation.

5.3 FUTURE STUDIES

This was the first exploratory study on Trc-formulation and must be expanded to test Trcs peptide formulations with different formulant molecules, such as polymer-type nanocarriers, cyclodextran, chitosan and many others. However, future studies on these peptides and their formulations must be undertaken with care, specifically in interpretation of results if methodology is not stringently controlled and standardised. As CS is a highly promising formulant, it is suggested that focus is placed on the optimisation of the CS formulations in terms of peptide:CS ratio, type and time of agitation, solvent systems, as well as utilising other types of amphipathic sterols. As TpcC:C16 formulation showed promise it would be beneficial to assess the influence on the length and saturation of the aliphatic tail of the fatty acid. Different types of headgroups can also be considered for detergent-type formulations. However, the

Stellenbosch University https://scholar.sun.ac.za

toxicity of the formulations is still an issue, therefore mixed-type formulation such as C16:CS type with targeting ligands on CS and/or C16 would improve the selectivity. Targeting ligands can include:

- poly-glutamate or poly-glutamate folates for targeting the PSMA in prostate cancer.
- Molecules such as folic acid (Vitamin B9), transferrin and hyaluronan used as ligand for targeting different receptors expressed in cancer cells.
- CPPs such as transactivator of transcription protein (TATp).

Covalent modification of the tyrocidines with palmitic acid was attempted in this study in order to modulate the toxicity of the peptides. The conjugation of C16 to tyrocidine mixture was successful with double conjugation of C16 also observed from ESI-MS analysis (data not shown). Unfortunately, purification of the conjugates proved to be a difficult task and preliminary activity studies revealed complete loss of activity. However, these constructs can be used as a co-formulants with the Trcs in place of C16 alone or with CS. Focus should also be placed on developing a prodrug-nanoformulation of the tyrocidines, similar to the Trc-PVP nano-formulation to target the malaria parasite, or by implementing pH (N,N'-dimethylaminoethyl methacrylate (DMAEMA)) or enzyme sensitive linkers (glycylphenylalanylleucylglycine (GFLG) tetrapeptide) between the conjugates and the peptides.

This study has proven that the three major tyrocidines (A, B, C) and tryptocidine C have a broad-spectrum activity against cancers and that lipid formulation can modulate the activity of these peptides. From these promising results it is suggested that the search for the ideal nanocarrier system for the delivery of tyrocidines to cancer cells and tumours should be continued.

Stellenbosch University https://scholar.sun.ac.za

5.4 REFERENCES

(1) Dimick, K. P. (1951) Hemolytic action of gramicidin and tyrocidin. *Exp. Biol. Med. 78*, 782–784.

(2) Rautenbach, M., Vlok, N. M., Stander, M., and Hoppe, H. C. (2007) Inhibition of malaria parasite blood stages by tyrocidines, membrane-active cyclic peptide antibiotics from *Bacillus brevis*. *Biochim. Biophys. Acta - Biomembr. 1768*, 1488–1497.

(3) Rammelkamp, C. H., and Weinstein, L. (1942) Toxic effects of tyrothricin, gramicidin and tyrocidine. *J. Infect. Dis. 71*, 166–173.

(4) Vosloo, J. A., Stander, M. A., Leussa, A. N. N., Spathelf, B. M., and Rautenbach, M. (2013) Manipulation of the tyrothricin production profile of *Bacillus aneurinolyticus*. *Microbiol. (United Kingdom) 159*, 2200–2211.

(5) Eyéghé-bickong, H. A. (2011) Role of surfactin from Bacillus subtilis in protection against antimicrobial peptides produced by Bacillus species, PhD Thesis, Department of Biochemistry, University of Stellenbosch, http://hdl.handle.net/10019.1/6773. Stellenbosch.

(6) Vosloo, J. A. (2016) Optimised bacterial production and characterisation of natural antimicrobial peptides with potential application in agriculture. PhD Thesis, Department of Biochemistry, University of Stellenbosch, http://hdl.handle.net/10019.1/98411

(7) Creed, D. (1984) The photophysics and photochemistry of the near-UV absorbing amino acids-I. Tryptophan and its simple derivatives. *Photochem. Photobiol. 39*, 537–562.

(8) Chen, Y., and Barkley, M. D. (1998) Toward understanding tryptophan fluorescence in proteins. *Biochemistry 37*, 9976–9982.

(9) Lakey, J. H., and Raggett, E. M. (1998) Measuring protein – protein interactions. *Curr. Opin. Struct. Biol. 8*, 119–123.

(10) Lakowicz, J. R., and Masters, B. R. (2008) Principles of Fluorescence Spectroscopy, Third Edition. *J. Biomed. Opt. 13*, 029901.

(11) Bent, D. V., and Hayon, E. (1975) Excited state chemistry of aromatic amino acids and related peptides. III. tryptophan. *J. Am. Chem. Soc. 97*, 2612–2619.

(12) Daniel, J. M., Friess, S. D., Rajagopalan, S., Wendt, S., and Zenobi, R. (2002) Quantitative determination of noncovalent binding interactions using soft ionization mass spectrometry. *Int. J. Mass Spectrom. 216*, 1–27.

(13) Robinson, C. V, Chung, E. W., Kragelund, B. B., Knudsen, J., Aplin, R. T., Poulsen, F. M., and Dobson, C. M. (1996) Probing the nature of noncovalent interactions by mass spectrometry. A study of protein-CoA ligand binding and assembly. *J. Am. Chem. Soc. 118*, 8646–8653.

(14) Bich, C., Baer, S., Jecklin, M. C., and Zenobi, R. (2010) Probing the hydrophobic effect of noncovalent complexes by mass spectrometry. *J. Am. Soc. Mass Spectrom. 21*, 286–289.

(15) Munyuki, G., Jackson, G. E., Venter, G. A., Kövér, K. E., Szilágyi, L., Rautenbach, M., Spathelf, B. M., Bhattacharya, B., and Van Der Spoel, D. (2013) β-sheet structures and dimer models of the two major tyrocidines, antimicrobial peptides from *Bacillus*

Stellenbosch University https://scholar.sun.ac.za

aneurinolyticus . *Biochemistry 52*, 7798–7806.

(16) Leussa, A. N.-N. (2014) Characterisation of small cyclic peptides with antimalarial and antilisterial activity. PhD Thesis, Department of Biochemistry, University of Stellenbosch, http://hdl.handle.net/10019.1/86161.

(17) Norman, K. E., and Nymeyer, H. (2006) Indole localization in lipid membranes revealed by molecular simulation. *Biophys. J. 91*, 2046–2054.

(18) Kelkar, D. A., and Chattopadhyay, A. (2006) Membrane interfacial localization of aromatic amino acids and membrane protein function. *J. Biosci. 31*, 297–302.

(19) Wymore, T., and Wong, T. C. (1999) Molecular dynamics study of substance P peptides in a biphasic membrane mimic. *Biophys. J. 76*, 1199–1212.

(20) Segrest, J. P., De Loof, H., Dohlman, J. G., Brouillette, C. G., and Anantharamaiah, G. M. (1990) Amphipathic helix motif: Classes and properties. *Proteins Struct. Funct. Bioinforma. 8*, 103–117.

(21) Rautenbach, M., Troskie, A. M., Vosloo, J. A., and Dathe, M. E. (2016) Antifungal membranolytic activity of the tyrocidines against filamentous plant fungi. *Biochimie 130*, 122–131.

(22) Spathelf, B. M., and Rautenbach, M. (2009) Anti-listerial activity and structure-activity relationships of the six major tyrocidines, cyclic decapeptides from *Bacillus aneurinolyticus*. *Bioorganic Med. Chem. 17*, 5541–5548.

(23) Troskie, A. M., de Beer, A., Vosloo, J. A., Jacobs, K., and Rautenbach, M. (2014) Inhibition of agronomically relevant fungal phytopathogens by tyrocidines, cyclic antimicrobial peptides isolated from Bacillus aneurinolyticus. *Microbiol. (United Kingdom) 160*, 2089–2101.

(24) Dubos, R. J., and Hotchkiss, R. D. (1941) The production of bactericidal substances by aerobic sporulating bacilli. *J. Exp. Med. 73*, 629–640.

(25) Dubos, R. J., Hotchkiss, R. D., and Coburn, A. F. (1942) The effect of gramicidin and tyrocididne on bacterial metabolism. *J. Biol. Chem. 146*, 421–426.

(26) Schazschneider, B., Ristow, H., and Kleinkauf, H. (1974) Interaction between the antibiotic tyrocidine and DNA in vitro. *Nature 249*, 757–759.

(27) Bohg, A., and Ristow, H. (1987) Tyrocidine-induced modulation of the DNA conformation in *Bacillus brevis*. *Eur. J. Biochem. 170*, 253–258.

(28) Ristow, H. (1986) DNA-supercoiling is affected *in vitro* by the peptide antibiotics tyrocidine and gramicidin. *Eur. J. Biochem. 160*, 587–591.

(29) Danders, W., Marahiel, M. A., Krause, M., Kosui, N., Kato, T., Izumiya, N., and Kleinkauf, H. (1982) Antibacterial action of gramicidin S and tyrocidines in relation to active transport, *in vitro* transcription, and spore outgrowth. *Antimicrob. Agents Chemother. 22*, 785–790.